DYNAMIC CORROSION RISK-BASED INTEGRITY ASSESSMENT OF MARINE AND OFFSHORE SYSTEMS

By

©Sidum Adumene

A thesis submitted to the School of Graduate Studies

In partial fulfillment of the requirements for the degree of

Doctor of Philosophy

Faculty of Engineering and Applied Science

Memorial University of Newfoundland

October 2021

St. John's Newfoundland, Canada

This research is dedicated to God Almighty for his provision, favor, and mercy in all ways, and to my late father HRH Mene A. A Deekor, my Mother Ngozi Cecilia Deekor, my wife Barigiasi Adumene and my lovely children – Tegio Adiya Adumene, Giodu Eliana Adumene, and Popka Sidum Adumene

ABSTRACT

Corrosion poses a serious integrity threat to marine and offshore systems. This critical issue leads to high rate of offshore systems degradation, failure, and associated risks. The microbiologically influenced corrosion (microbial corrosion), which is a type of corrosion mechanism, presents inherent complexity due to interactions among influential factors and the bacteria. The stochastic nature of the vital operating parameters and the unstable microbial metabolism affect the prediction of microbial corrosion induced failure and the systems' integrity management strategy. The unstable and dynamic characteristics of the corrosion induced risk factors need to be captured for a robust integrity management strategy for corroding marine and offshore systems.

This thesis proposes dynamic methodology for risk-based integrity assessment of microbially influenced corroding marine and offshore systems. Firstly, a novel probabilistic network based structure is presented to capture the non-linear interactions among the monitoring operating parameters and the bacteria (e.g., sulfate-reducing bacteria) for the microbial corrosion rate predictions. A Markovian stochastic formulation is developed for the corroding offshore system failure probability prediction using the degradation rate as the transition intensity. The analysis results show that the non-linear interactions among the microbial corrosion influential parameters increase the corrosion rate and decrease the corroding system's failure time. Secondly, a dynamic model is introduced to evaluate the offshore system's operational safety under microbial corrosion induced multiple defect interactions. An effective Bayesian network - Markovian mixture structure is integrated with the Monte Carlo algorithm to forecast the effects of defects interactions and the corrosion response parameters' variability on offshore system survivability under multispecies biofilm architecture. The results reveal the impact of defects interaction on the system's

survivability profile under different operational scenarios and suggest the critical intervention time based on the corrosivity index to prevent total failure of the offshore system.

Finally, a probabilistic investigation is carried out to determine the parametric interdependencies' effects on the corroding system reliability using a Copula-based Monte Carlo algorithm. The model simultaneously captures the failure modes and the non-linear correlation effects on the offshore system reliability under multispecies biofilm structure. The research outputs suggest a realistic reliability-based integrity management strategy that is consistent with industry best practices. Furthermore, a dynamic risk-based assessment framework is developed considering the evolving characteristics of the influential microbial corrosion factors. A novel dynamic Bayesian network structure is developed to capture the corrosion's evolving stochastic process and the importance of input parameters based on their temporal interrelationship. The associated loss scenarios due to microbial corrosion induced failures are modeled using a loss aggregation technique. A subsea pipeline is used to demonstrate the model performance. The proposed integrated model provides a risk-based prognostic tool to aid engineers and integrity managers for making effective safety and risk strategies. This work explores the microbial corrosion induced failure mechanisms and develops dynamic risk-based tools under different operational scenarios for systems’ integrity management in the marine and offshore oil and gas industries.

ACKNOWLEDGEMENT

I would like to express my profound gratitude to my supervisor, Dr. Faisal Khan, for his patience, guidance, and love throughout my PhD study at the Memorial University. It is a great pleasure to have worked under his supervision. I sincerely acknowledge my co-supervisor, Dr. Sohrab Zendehboudi, for his valuable contribution. He is always available to provide support whenever needed. I am thankful to my supervisory committee members, Dr. Sunday Adedigba, and Dr. Hodjat Shiri, for their support, encouragement, guidance, and mentorship.

I extend a special appreciation to the Faculty of Engineering and Applied Science, School of Graduate Studies of the Memorial University, Centre for Risk, Integrity and Safety Engineering (CRISE), the organizations which funded this PhD research; Genome Canada, MITACS, and the supporting partners; Husky and Suncor Energy Inc, and Canada Research Chair (CRC) Tier I Program in Offshore Safety and Risk Engineering.

I would like to extend my heartiest appreciation to my lovely wife Barigiasi Adumene and my adorable children, Tegio Adiya Adumene, Giodu Eliana Adumene, and Popka Sidum Adumene. They have been a source of great inspiration and motivation during the PhD program. To the entire Ngozi Cecilia Deekor family; Penedum Adumene, Princess Giobia Johnny, Kile Adumene, HRH Mene Magnus B. Adumene, Leton Adumene, Monale Adumene, Gold Adumene, and all my steps brothers and sisters, nephews, nieces, and in-laws, you have all contributed through your words of encouragements for the period of my study. My sincere appreciation also goes to my late father-in-law, Elder Sunday E. Kabari, Mrs. Esther Adedigba, Dr. Ledibabari Paago, Dr. C. T. Nwaoha, Rev. Blessed Akpojisheri, Rev. Nitonye Samson, Pastor Innocent Owasi, Dr. Victor Akor, Hingis Timiala Michael, Obi Usutu, Pastor James Johnny, members of Deeper Life Bible Church, St. John's NL, and many others for their prayers and moral support.

TABLE OF CONTENTS

LIST OF TABLES

LIST OF FIGURES

NOMENCLATURE

Acronyms

APB	Acid producing bacteria
BN	Bayesian network
CVN	Charpy V-notch impact test
COV(cov)	Coefficient of variation
CPT	Conditional probability table
CL	Chloride ion
DBN	Dynamic Bayesian network
FAD	Failure assessment diagram
IRB	Iron reducing bacteria
LSF	Limit state function
DWTT	Drop-weight tear test
MCS	Monte Carlo simulation
MIC	Microbially influenced corrosion/microbiologically influenced corrosion/ microbial corrosion
rvs	Random variables
SPSS	Statistical package for the social sciences
SO_4	Sulfate ion
SRB	Sulphur reducing bacteria
EVAR1	Total expected loss value with cost incurred on safety barriers test statistics
EVAR2	Total expected loss value without safety barriers incurred cost test statistics

USE	Upper self-energy
WC	Water cut

Variables, Parameters, and Functions

Y_e	Age of the structure
a_l, c_l	Axial corrosion rate
a_f	Accounted for the defect size at the transition to crack
r_b, P_b	Burst capacity
f_s	Combined failure state
$C_{g_1 g_2 \ldots\ldots g_n}$	Copula function for the joint probability distribution of the performance functions
$P(\cup \mid E)$	Conditional probability
$P\left(n_{i,j+1} \middle\| P_a(n_{i,j+1})\right)$	Conditional probability for the dynamic node
$Cov\{L_d, L_{d'}\}$	Covariance between L_d and $L_{d'}$
pCO_2	CO_2 partial pressure
Δa	Ductile crack extension
J_{app} & J_{mat}	Equivalent in J-terminology of the applied load and the material toughness
l_{nm}	Effective length of all combinations of adjacent defects
w_{nm}	Effective width of all combinations of adjacent defects
$\mathbb{E}[\cdot]$	Expectation operator
$\mathrm{E_{Loss}}$	Expected economic loss
C_1 & C_2	Fixed coefficient of the corrosion model

M	Folias factor
$P_f(t)$	Failure probability
G_{n+1}	Future pit depth state of the system
P_i	Failure probability
$\{S_1^{n_i}, \dots \dots S_M^{n_i}\}$	Finite number of states
M	Folias factor
V	Fluid flow rate
K_{mat}	Fracture toughness for opening mode fracture
$C\varphi(u_1 \dots . u_d)$	General Archimedean family copula function
$\varphi(\cdot)$	Generator function
$\varphi^{-1}(\cdot)$	Generator inverse function
Q	Generator matrix
pH_2S	H_2S partial pressure
$P(M = m \mid \mathcal{H}_t^k)$	History-based conditional probabilit
d_i	Individual defect depth
d_o	Initial defect depth
l_o	Initial defect length
$\mathbb{R}_{i,t}$	ith node at time t
$P(\cup)$	Joint probability distribution
T_{cl}, T_c	Life of coating
$L^j_{scenario1}$	Loss scenario
$(L_{ij})_{Lim}$	Limiting criteria for longitudinal spacing

$(W_{ij})_{Lim}$	Limiting criteria for circumferential spacing
Q, Q_{nm}	Length correction factor
$g_1(wt, d, t)$	Limit state function for leak
$g_2(r_b, P_o, t)$	Limit state function for burst
$g_3(J_{app}, J_{mat}, t)$	Limit state function for fracture
$g_4(r_{rp}, P_o, t)$	Limit state function for rupture
L_{ij}	Maximum longitudinal spacing between adjacent defects
W_{ij}	Maximum circumferential spacing between adjacent defects
K_{max}	Maximum stress intensity factor threshold
d_{max}	Maximum defect depth
C & m	Model constants of crack propagation rate model
Z	Mixing variable
J	Number of simulation runs
$\varphi: [0, \infty]$	Non-increasing function
n	Number of simulation cycles when LSF ≤ 0
P_o, P_{op}	Operating pressure
$P_a(\mathbb{R}_{i,t})$	Parent nodes of $\mathbb{R}_{i,t}$
$P_y(Y_i)$	Parent of variable X_i
G_{n-1}	Past pit depth state of the system
pH	pH of the fluid
G_n	Present pit depth state of the system
$P_x(X_i)$	Parent of variable X_i

$\mathbb{P}$, P	Probability
wt	Pipe-wall thickness
D	Pipe outer diameter
$F_i(t)$	Probability of failure for ith failure mode at time t
$F_i(\cdot)$	Probability distribution function of the ith failure mode
$\mathbb{P}(L_d)$	Probability of the loss element/scenario
$y_j^{n_i}$	Probability distribution over node states at time step k
$\mathbb{P}(L_i, t)$	Probability of loss occurrence within [0, t]
a_d, c_d	Radial corrosion rate
$L_{1,\ldots\ldots,}L_d$	Random variable that represents the elements
r_{rp}	Rupture capacity
μ_{ij}	State transition intensity
P_{ij}	State transition probability
S	State space
$\mathbb{R}$	Set of random variables $Y_1, Y_2, \ldots\ldots, Y_n$
K	Stress intensity factor due to the applied load
σ_a	Stress amplitude
K_{ISCC}	Stress intensity factor threshold of the SCC
D	Total number of loss elements
t-step	Time-step transition
$P\left(\mathcal{H}_t^k \middle\| M = m\right)$	Transition probabilities based on the defect's states at inspection
$P_{nm}(t)$	Time-variant residual strength

P_{MSOP}	Time-variant safe operating pressure
$d_{max}(T)$	Time-dependent radial corrosion depth
$L_{eff}(T)$	Time-dependent axial corrosion length
$P_{fsys}(t)$	Time-dependent system failure probability
$d(t)$	Time-dependent radial corrosion growth
$L(t)$	Time-dependent axial corrosion growth
$a(t)$	Time-dependent crack growth
$R_{sys}(t)$	Time-dependent system reliability
N	Total number of simulation cycles
E_{Loss}^{T}	Total expected economic loss
$d(t), f_c, D_{max}(t)$	Time-dependent radial corrosion depth
$L(t)$	Time-dependent axial corrosion length
N	Total number of simulation cycles
t, T	Time of exposure
T_t	Transition between no corrosion and corrosion initiation
d_∞	Thickness loss during the long-term corrosion
$P(\mathbb{R}_t \mid \mathbb{R}_{t-1})$	Temporal interrelationship across time slices
$E[L_i(\mu_t, \sigma_t)]$	Unit expected economic loss value for the loss element i
$Var\{L_d\}$	Variance of each loss element L_d
$i\&j$	Vector notation for state characteristic
L_r	Yielding parameter; abscissa of the FAD
$f(L_r)$	Yielding correction function

Greek Letters

θ	Copula argument
β_C	Crack shape parameter
σ_f	Flow stress
$\lambda^{ij}(t\|\mathcal{H}_t)$	History-based merged defect growth rate
τ	Kendall's tau
γ	Location parameter
ρ	Pearson's correlation coefficient
υ	Poisson ratio
π_i	Prior state probability distribution
β	Scale parameter
α	Shape parameter
σ	Stress load
μ_m^{ij}	Transition intensity (MIC rate)
θ_t	Temperature
σ_u	Ultimate tensile strength
σ_y	Yield stress

Chapter 1

Introduction

1.1. Background

Marine and offshore systems are vital infrastructures that face corrosion-related damages in the ocean environments. They are exposed to harsh operating and environmental conditions. The harshness of the working environments is due to external, operational, and environmental factors. These factors may include but are not limited to biofouling, carbon dioxide concentration, pH, pollutants, temperature, pressure, water velocity, carbonate solubility, salinity, concentration/amount of suspended solids, and bacteria. These external factors result in corrosion induced deterioration of the marine and offshore systems, raising safety and integrity concerns. The interactions between these parameters and their non-linear effects support the stochastic degradation of the corresponding systems such as oil and gas transportation systems (e.g., pipeline). The water-in-oil phase provides a stimulating environment when in contact with the offshore system's internal surface; it leads to CO_2 dissolution and microbial growth. The interactions among these factors with microorganisms initiate microbiologically influenced corrosion (MIC) [1].

Generally, corrosion, including MIC, poses integrity challenges to marine and offshore oil and gas operations. MIC is a stochastic degradation process of engineering systems that is instigated by the presence and metabolic process of microorganisms such as fungi and bacteria [2]. Their formation and metabolic activities produce corrosive substances that alter the corrosion

mechanisms and complicate the offshore systems' failure characteristics. The formation process of the MIC is enhanced by the bio-chemical nutrients and external environmental factors.

Moreover, the microorganisms play a substantial role in the deterioration of the marine and offshore oil and gas systems such as pipeline corrosion [3,4], ship hull fouling and cargo tank leakage [5,6], and reservoir souring [2,7]. Recent research has shown that MIC contributes to over 20% of corrosion-related failures globally, with associated devastating consequences [8]. The complexity of the microbial metabolism and growth process poses difficulty in understanding their characteristics in the corrosion mechanism. Their instability and the co-existence of the multispecies microbes in a biofilm architecture have contributed to several catastrophic failures in onshore, marine, and offshore systems [2–4,9]. In particular, the failure of the transit line at Prudhoe Bay [10] and the rupture failure of a high-pressure natural gas transporting pipeline near Carlsbad, New Mexico [11], are attributed to microbial corrosion. The Prudhoe accident resulted in a failure cost consequence of over $8billion, while the gas transporting line failure claimed twelve lives with associated cost consequences and loss of reputation. This implies the need for continuous research to understand, reliably diagnose, and accurately predict MIC induced failure characteristics and consequences. A proper knowledge of the MIC induced failure phenomenon will aid in the development of a robust risk-based integrity management tool for corroding marine and offshore systems.

To better understand the devastating potency of the MIC, several models have been proposed, including mechanistic models, qualitative risk-based MIC models, experimental models, and probabilistic models [12–16]. Despite the attempt to model the MIC potential and engineering systems' susceptibility, the failure induced characteristics and associated integrity risks are still not fully explored. The impacts of the dependencies between the monitoring corrosion influencing

factors, environmental factors, materials composition, and the microbial activities on the offshore system failure characteristics (failure probability, survivability, and failure time) have not been thoroughly studied. There are limited quantitative risk modeling tools that can capture the complex interactions among failure key factors and the corresponding consequences under MIC.

The existing models are inadequate to capture the non-linear interaction effects of the physio-chemical parameters on the MIC rate and the failure probability prediction simultaneously. The bacteria's co-existence effects on the marine and offshore systems failure characteristics have not been taken into account in the susceptibility models. There are a limited number of dynamic quantitative models to assess the impact of microbial induced multi-failure modes' dependencies on the remaining strength of corroding offshore systems. The multispecies biofilm effects on the strength loss and survival likelihood of the corroding offshore systems need to be addressed appropriately. There is a need to better explore the stochastic and dynamic nature of microbial corrosion induced failures of marine and offshore systems for a risk-based integrity management.

1.2. Motivation and objectives

Microbial corrosion creates severe integrity risks in the marine and offshore oil and gas industries. This is highlighted in its contribution to the overall failure due to corrosion and the associated consequences [8,17,18]. MIC is enhanced under a multispecies biofilm, in which the bacteria mutualistic relationship serves as a source of energy among the bacteria types. The biofilm is a complex structure formed by fusing the extracellular polymeric substances and the bacteria cells. Such a complex mutualistic microbial community presents a dynamic and diverse failure influencing potentials to marine and offshore systems. Thus, the mechanistic approach is inadequate to capture the complex non-linearity in the MIC mechanism modeling.

Moreover, the bacteria metabolic process and their degradation pathway are enhanced by the available nutrients and monitoring operating (physio-chemical) parameters. For instance, the physio-chemical parameters play a vital role in the microbes' survivability and growth. The interplay among the multiphase fluids in the oil and gas production/transportation systems can create a sustainable mode for bacteria growth when in contact with the system wall. This exposure leads to an interactive tendency among the corrosion dominant parameters and bacteria for the MIC formation, considerably affecting total system failures. There is no comprehensive knowledge of the interaction effects among these factors on the propagation of the MIC upon initiation. The time of the system's complete collapse in terms of the system's failure rate, failure likelihood, future pits distribution, and survivability needs to be explored in a systematic manner.

The material response to the dynamic interactions among the influential corrosion factors in terms of the failure rates and the associated consequences has not been fully understood. There are a few dynamic quantitative risk-based frameworks that characterize the MIC induced failure modes considering complex interaction among corrosion key factors and multispecies biofilm. Hence, a better understanding of these complex interactions among the corrosion influencing parameters and the bacteria and their impacts on the failure characteristics is essential to develop a proper dynamic corrosion risk-based integrity assessment tool for the corroding marine and offshore systems.

This research is aimed at developing a dynamic risk-based integrity assessment tool for marine and offshore systems affected by MIC. The model captures the complex, non-linear and unstable dependencies among the various corrosion vital factors (pH, temperature, water cut, fluid velocity,

CO_2 partial pressure) and the bacteria for the marine and offshore systems failure analysis. The research goal is achieved through the following objectives. Each of these research objectives are translated into a research task presented in Figure 1.1.

i. To develop a novel probabilistic model for system failure characteristics analysis by predicting the MIC rate, failure probability, and future pit depths distribution.
ii. To model the system survivability (safety) considering the non-linear dependencies among corrosion influential factors and multiple defects interaction under a complex multispecies biofilm.
iii. To introduce a dynamic model for system reliability analysis considering multi-failures modes dependencies under complex multispecies microbial biofilms.
iv. To develop an integrity assessment model considering material and parametric uncertainty.
v. To develop a dynamic risk model capable of analyzing the microbial corrosion risk under multiple failure mechanisms and complex multispecies biofilms.

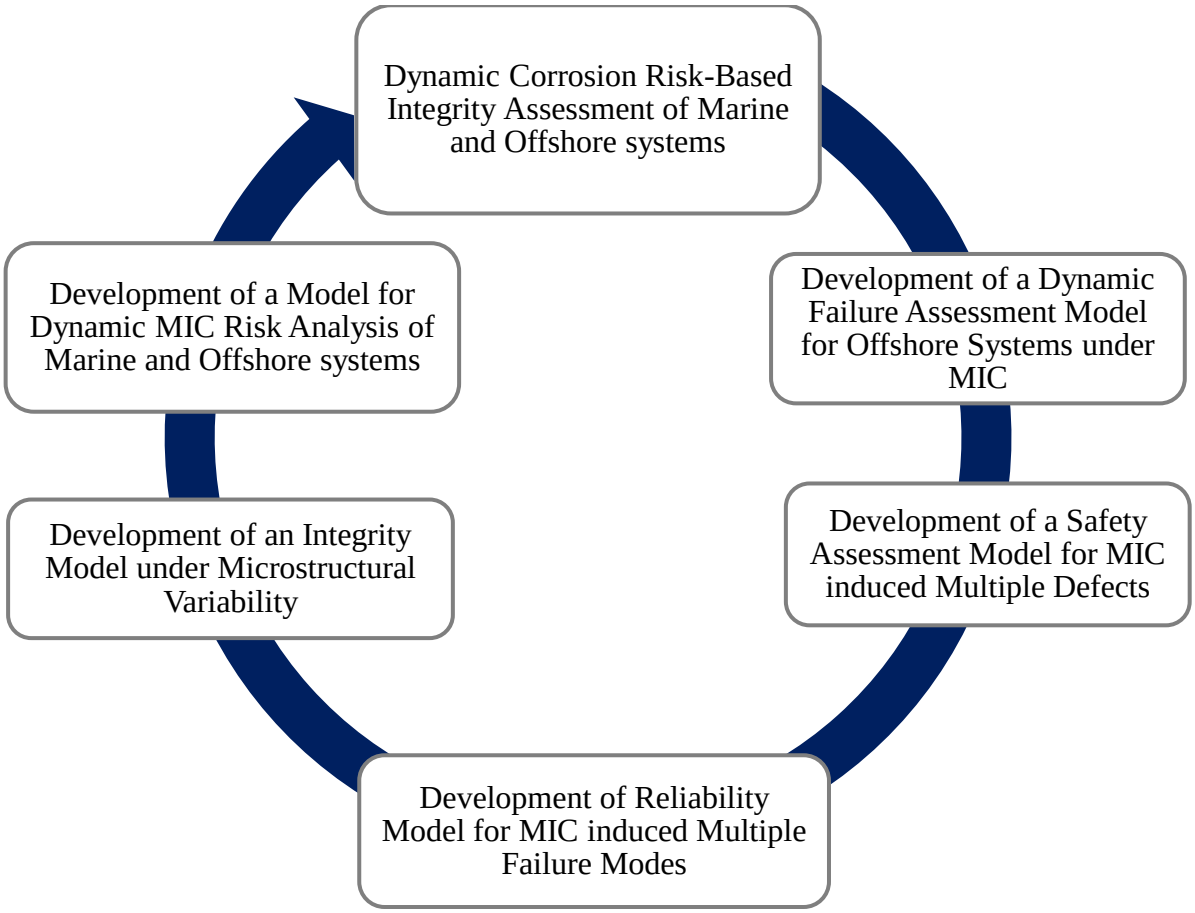

Figure 1.1. Research objectives

1.3. Scope and limitations

This study is developed specifically for marine and offshore oil and gas operations. The research focuses mainly on dynamic risk-based integrity assessment of marine and offshore systems suffering microbiologically influenced corrosion. Microbiologically influenced corrosion is a complex degradation process in offshore operations. It poses critical challenges in its prediction and management because of its stochastic nature. To analyze the safety and reliability of these critical offshore systems suffering MIC, we need robust and dynamic models to capture the associated complexity, stochasticity, and uncertainties. There are several uncertainties with the formation, key corrosion influential parameters' data processing, and deteriorating mechanisms

due to sparse data availability that may introduce subjectivity in the proposed models. The current study is not an attempt to address all research gaps associated with dynamic risk-based integrity assessment of marine and offshore systems suffering MIC but an attempt to address some of the research gaps related to offshore operations considering microbial corrosion.

1.4. Contributions and novelty

This doctoral research's main contributions and novelties are in the area of dynamic risk-based integrity assessment of marine and offshore systems suffering microbiologically influenced corrosion. The highlights of the contributions are listed below:

- A novel probabilistic failure model is introduced to assess the corrosion rate, failure probability, and critical failure time of offshore pipelines suffering MIC. This work proposes the integration of the Bayesian network with the Markovian stochastic process to captures the non-linear interactions among the MIC influential factors for probability of failure prediction. This will serve as a useful tool to facilitate integrity risk assessment and management of corroding offshore systems. This contribution is presented in chapter 3.
- An innovative and dynamic operational safety model is proposed. The model is used to assess the effects of the multiple MIC defects interaction and multispecies biofilms characteristics on offshore systems' safety. This novel approach provides a useful operational monitoring tool for MIC management and ensuring safety in offshore operations. This contribution is presented in chapter 4.
- A new reliability model is introduced to consider the complex non-linear interactions among corrosion influencing parameters and multiple failure modes’ interdependencies.

This work focuses on the hybridization of the Bayesian network with a Copula-based Monte Carlo algorithm for offshore system reliability prediction. This model effectively captures the unstable dependencies among the physio-chemical parameters and the multi-failure modes impacts on the system reliability under multispecies microbial biofilms. This contribution is presented in chapter 5.

- An innovative integrity model is suggested to assess failure behavior of different offshore steel pipelines. The model accounts for the microstructural and parametric variability of the steel for failure probability prediction in a mixed corrosive environment. This probabilistic approach is effective for material selection and risk-based integrity management strategy under uncertainty. This contribution is presented in chapter 6.
- An innovative and dynamic risk assessment model is proposed. The model captures the link between MIC induced failures and potential consequences. The dynamic Bayesian network is integrated with the loss function technique to model the evolving stochastic process by capturing the temporal interactions among the random corrosion parameters for failure probability and the associated economic loss prediction. This novel approach provides a risk-based prognostic tool for marine and offshore systems suffering from MIC. This promising contribution is presented in chapter 7.

1.5. Co-authorship statement

The contributions of Sidum Adumene, Dr. Faisal Khan, Dr. Sohrab Zendehboudi, Dr. Sunday Adedigba, and Dr. Hodjat Shiri towards the research work and the thesis [the structure as outlined in Figure 1.2] are discussed here.

Sidum Adumene: Conceptualization and idea formulation, development of methodology, corrosion risk model development, performing data analysis, and model testing; writing original draft of the manuscript along with all supporting documents for submission to journals; Reviewing and editing the manuscripts based on feedback from co-authors and journal reviewers.

Faisal Khan: Idea formulation of research, development of the methodology, development of corrosion and risk model algorithm, guidance in data analysis, and re-organizing and review of the manuscripts and thesis.

Sohrab Zendehboudi: Idea formulation of research, guidance in data analysis, and re-organizing and review of the manuscripts and thesis.

Sunday Adedigba: Guidance in development of BN model, and reviewing the manuscripts.

Hodjat Shiri: Guidance in data analysis, and re-organizing and review of the manuscripts and thesis.

1.6. Organization of the Thesis

This thesis is written in a manuscript-based format. The overall outcomes of this thesis are represented in five peer-reviewed journal chapters. Figure 1.2 shows the organizational structure of this thesis. Chapter 1, 2, and 5 are the introduction, literature review, and conclusions, respectively. Chapters 3 to 7 of this thesis are developed based on the chapter submissions to peer-reviewed journals.

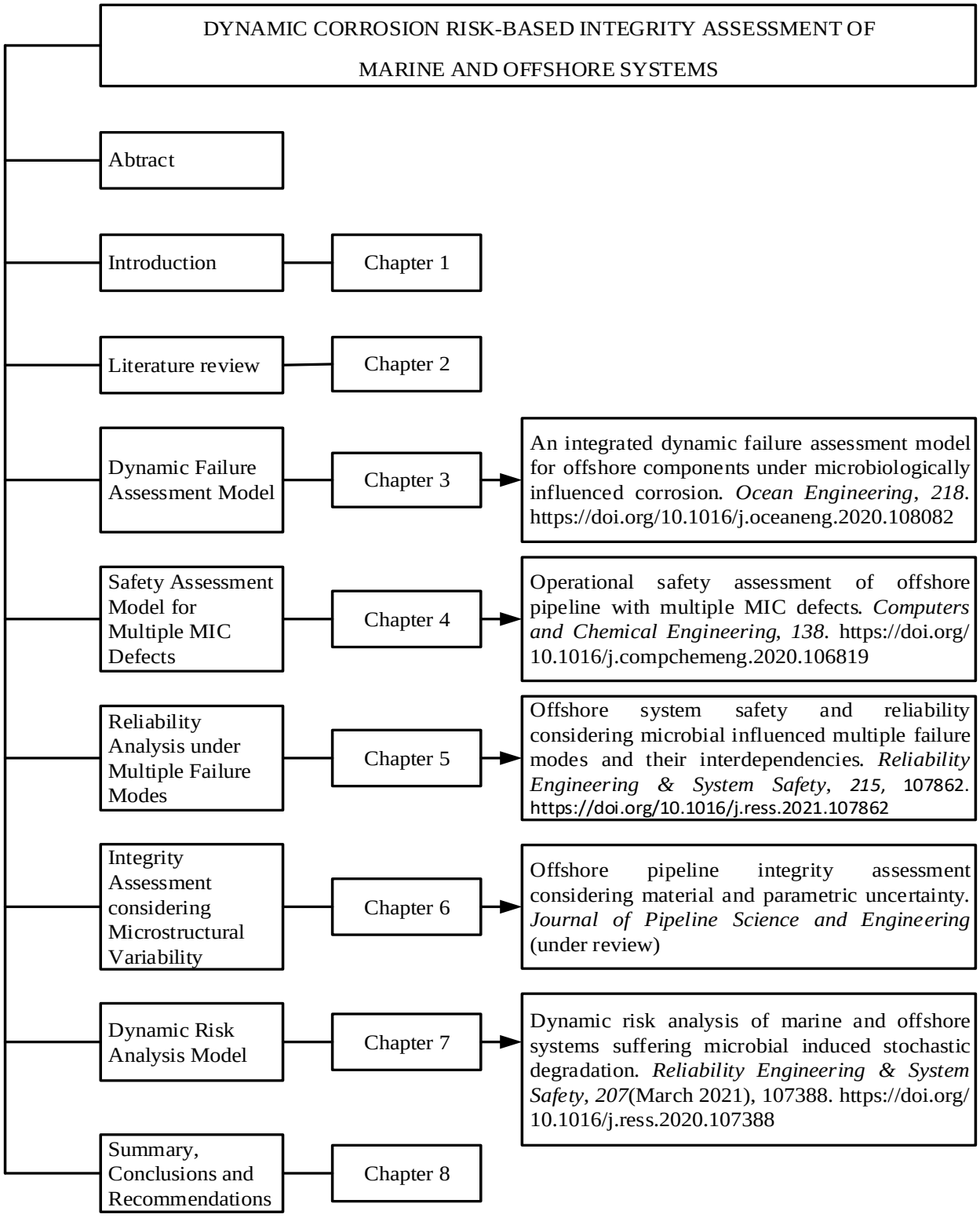

Figure 1.2. Structure of the Ph.D. thesis and related publications

Chapter 2 covers a systematic literature review relevant to the research. This includes MIC susceptibility analysis and risk analysis due to MIC induced failures of offshore systems.

Chapter 3 introduces an innovative and dynamic probabilistic model to assess the failure characteristics of subsea pipelines under MIC. This chapter is published in *Ocean Engineering 2020; 218: 108082.*

Chapter 4 includes an operational safety analysis based on an integrated BN-Markov mixture technique with the Monte Carlo algorithm. This chapter is published in *Computers and Chemical Engineering 2020; 138: 106819.*

Chapter 5 presents an integrated reliability analysis approach considering microbial induced multiple failure modes and their interdependencies. This chapter is submitted to *Reliability Engineering and System Safety 2021; 215: 107862.*

Chapter 6 presents a probabilistic approach for the integrity assessment of corroding offshore pipelines. The approach integrates the semi-empirical susceptibility models with the Monte Carlo algorithm for failure behavior prediction in a mixed corrosive environment. This chapter is submitted to the *Journal of Pipeline Science and Engineering*.

Chapter 7 presents an innovative and dynamic risk assessment approach for MIC induced failures using an integrated dynamic Bayesian network and loss function technique. This chapter is published in *Reliability Engineering and System Safety 2021; 207: 107388.*

References

[1] Papavinasam S, Doiron A, Revie RW. Model to Predict Internal Pitting Corrosion of Oil and Gas Pipelines. Corrosion 2010;66:1–11.

[2] Beech IB, Gaylarde CC. Recent Advances in the Study of Biocorrosion - An Overview. Rev Microbiol 1999;30:177–90.

[3] Eckert R. Field Guide for Investigating Internal Corrosion of Pipelines. NACE International, Houston USA; 2003.

[4] Paik JK, Kim DK. Advanced method for the development of an empirical model to predict time-dependent corrosion wastage. Corros Sci 2012;63:51–8. https://doi.org/10.1016/j.corsci.2012.05.015.

[5] Alasvand K, Ravishankar Z V. Identification of the traditional and non-traditional sulfate-reducing bacteria associated with corroded ship hull. 3 Biotech 2016;6:1–8. https://doi.org/10.1007/s13205-016-0507-6.

[6] Huang RT, McFarland BL, Hodgman RZ. Microbial Influenced Corrosion in Cargo Oil Tanks of Crude Oil Tankers. NACE Int. Corros. Conf., 1997.

[7] Gieg LM, Jack TR, Foght JM. Biological souring and mitigation in oil reservoirs. Appl Microbiol Biotechnol 2011;92:263–82. https://doi.org/10.1007/s00253-011-3542-6.

[8] Little BJ, Lee JS. Microbiologivally Influenced Corrosion. John Wiley & Sons, Houston, New Jersey; 2007.

[9] Al-jaroudi S, Ul-hamid A, Al-Gahtani MM. Failure of crude oil pipeline due to microbiologically induced corrosion. Corros Eng Sci Technol 2011;46:568–79. https://doi.org/10.1179/147842210X12695149033819.

[10] Bailey A. BP:Learning from oil spill lessons. Pet News 2006.

[11] Kotu SP, Eckert RB. A framework for conducting analysis of microbiologically influenced corrosion failures. Insp J 2019.

[12] Gu T, Zhao K, Nesic S. A new mechanistic model for MIC based on a biocatalytic cathodic

sulfate reduction theory. Corrosion 2009:1–12.

[13] Liu H, Cheng YF. Mechanistic aspects of microbiologically influenced corrosion of X52 pipeline steel in a thin layer of soil solution containing sulphate-reducing bacteria under various gassing conditions. Corros Sci 2018;133:178–89. https://doi.org/10.1016/j.corsci.2018.01.029.

[14] Pots BFM, John RC, Rippon IJ, Thomas MJJS, Kapusta SD, Girgis M., et al. Improvements of De Waard-Milliams Corrosion Prediction and Applications to Corrosion Managment. NACE Int. Corros. Conf. No. 02235, 2002, p. 1–19.

[15] Taleb-berrouane M, Khan F, Hawboldt K, Eckert R, Skovhus TL. Model for microbiologically influenced corrosion potential assessment for the oil and gas industry. Corros Eng Sci Technol 2018:1–15. https://doi.org/10.1080/1478422X.2018.1483221.

[16] Marciales A, Peralta Y, Haile T, Crosby T, Wolodko J. Mechanistic microbiologically influenced corrosion modeling — A review. Corros Sci 2019;146:99–111. https://doi.org/10.1016/j.corsci.2018.10.004.

[17] Kotu SP, Erbay C, Sobahi N, Han A, Mannan S, Jayaraman A. Integration of electrochemical impedance spectroscopy and microfluidics for investigating microbiologically influenced corrosion using co-culture biofilms. NACE - Int Corros Conf Ser 2016;6:4312–25.

[18] Adesina AY, Aliyu IK, Al-Abbas FM. Microbiologically influenced corrosion (MIC) challenges in unconventional gas fields. NACE - Int Corros Conf Ser 2015;2015-Janua.

Chapter 2

Literature Review

2.1. Microbiologically influenced corrosion

Microbiologically influenced corrosion or microbial corrosion (MIC) is a stochastic degradation process that is influenced and instigated by the microorganisms such as microalgae, fungi, and bacteria. They alter the corrosion mechanisms in various processes by a complex biofilm structure that is attached to the surface of the systems [1]. The microbes' participation in the corrosion process influences the deterioration process through an electrochemical shifting in the corrosion mechanisms [2,3]. The microorganism degree of influence is dependent on the available nutrient and the complex interactions among the physio-chemical parameters. These parameters sustain the growth and metabolic process of the bacteria. According to the literature, such interactions could displace the corrosion potential and render the engineering systems susceptible to localized corrosion or pitting [4]. Also, the metabolite from the microorganism interacts with the material structure and environment to form Fe_2S, resulting in hydrogen and sulfide induced crack related degradation of the system [5,6].

The preferential mode of survival of the bacteria, even in the most aggressive environment, is sustained by the biofilm architecture that is produced by the bacteria cells in an extracellular polymeric substance (EPS) matrix for protection [7]. The biofilm houses mixed bacteria communities with different deteriorating potentials. For instance, the sulfate-reducing bacteria (SRB), iron-oxidizing bacteria (IOB), manganese-oxidizing bacteria (MOB), sulfur-oxidizing bacteria (SOB), iron reducing bacteria (IRB), and acid-producing bacteria (APB) co-exist with the exopolymers in a biofilm. The IOB have been identified as acidophilic/aerobic group of

microorganisms that enhance corrosion of steel. They are metal-depositing bacteria that oxidize soluble ferrous (Fe^{2+}) to ferric (Fe^{3+}) as energy source. Such oxides promote cathodic reduction leading to corrosion. However, for the current study, consideration is given to understand the failure characteristics of offshore systems subjected to long term corrosive (SRB, IRB, APB) environment. This mutualistic consortium actively alters and complicates the electrochemical process, resulting in a severe degradation rate. The offshore system under the mixed microbial biofilm may experience complex and unpredictable failure mechanisms in long-term exposure. A better knowledge of the failure propagation mechanisms through a robust risk-based prediction of microbial corrosion induced failure is essential.

2.2. Microbial corrosion propagation/susceptibility analysis

The microorganism metabolism is dependent on the availability of nutrients, such as energy source, carbon source, and water for propagation [1]. The heterogeneous material surfaces in the presence of water and carbon sources enhance the formation and propagation of microbial corrosion on offshore systems. The microbial corrosion propagation rate is further influenced by several other factors, including physio-chemical parameters, environmental factors, material microstructural composition, and biofilm characteristics.

Several researchers have studied the microbial corrosion propagation characteristics and proposed models to predict the propagation/susceptibility rate [8–16]. For instance, Gu et al. [9] proposed a MIC susceptibility model based on biocatalytic cathodic sulphate reduction theory (BCSR). Their model considered the effect of the charge transfer resistance and mass movement of the sessile SRB at the biofilm-metal surface interface for estimation of pitting corrosion rate. The concept

was based on the Butler Volmer and the mass balance equations. In their phenomenological model, Melchers and Wells [16] introduced a two-phase approach for MIC susceptibility modeling. The first phase captures the transition corrosion behavior, while the second (anaerobic) phase explores the long-term corrosion loss due to the SRB in the marine environment. The authors adopted the Fickian diffusion model to evaluate the SRB depleting activities based on a uniform diffusion process on the metal surface. The MIC rate was proportional to the nutrient flux based on the Fickian diffusion criteria.

Haile et al. [17] proposed a mechanistic model to incorporate the SRB concentration, SRB growth, and biofilm thickness and density to predict the microbial corrosion propagation rate and the biomass detachment rate. The model applied the Monod kinetics framework to obtain an equation for the pitting corrosion rate prediction. The characterized MIC rate is defined as the ratio of the corrosion rate of the iron to the rate of the sulphate depletion based on the SRB characteristics and the Monod half velocity coefficient. The researchers concluded that the interactions among the aforementioned parameters affect the corroding system's degradation and failure. Xu et al. [15] applied the anodic current density-based oxidation model for a mechanistic prediction of the MIC susceptibility rate of iron in a bacteria-infested environment. They forecasted the corrosion rate based on the cathodic SRB reduction and the proton reduction by the APB formulation. It was found that the MIC susceptibility (pitting) rate decreases as the time of exposure increases due to the increase in the microbial biofilm thickness and temperature effect. The models captures the impacts of the inferential parameters on the susceptibility rate of the corroding system. Nevertheless, they are deterministically structured and are not able to capture the dynamic non-linear interaction of the corrosion parameters influencing the MIC rate. Also, the stochastic natures

of the MIC and the instability and variability of the various physio-chemical parameters require a dynamic quantitative model.

Pots et al. [13] proposed a quantitative predictive model for MIC susceptibility analysis based on the water chemistry and the pipeline operating parameters to improve the De Waard-Milliams corrosion model. The researchers identified water presence, fluid flow, water wetting, pH, salinity, and temperature as the critical influencing parameters for MIC susceptibility in the presence of microbial activities. However, due to the MIC formation's stochastic nature, the predicted corrosion rate by the proposed model is not adequate enough. It was observed that the predictive model is limited due to the complex interactions among the biotic and the abiotic MIC influencing factors. Recently, Taleb-berrouane et al. [18] proposed a probabilistic approach for MIC susceptibility modeling. The method was intended to capture the complex interaction among the multivariate MIC influential factors for susceptibility analysis. They used a network-based Object-Oriented Bayesian Network to capture the multidimensional interactions among sixty MIC influencing parameters. Although the model explores the interdependencies among the corrosion vital factors to establish their degree of influence on the MIC susceptibility, it is limited to quantitatively predict the MIC propagation/susceptibility rate for the suffering engineering systems.

2.3. Microbial corrosion induced failure characteristics

Microbial corrosion induced failures pose severe/devastating issues in the marine and offshore oil and gas operations. Several systems that suffered MIC have resulted in catastrophic failures (pipeline and cargo tank leakage) [19,20]. Limited knowledge and literature on the system failure

characteristics (i.e., likely failure probability and failure time) upon MIC formation are available in the open sources. Moreover, the stochastic and unstable nature of the MIC formation and propagation complicate the failure probability prediction. The characterized multidimensional influencing parameters also play a role in the MIC induced failure prediction complexity. The failure characteristic of a system suffering MIC is a function of the degradation rate, failure probability, and the complex interactions among the influential parameters.

In recent years, researchers have proposed experimental and analytical models for system failure analysis under MIC [11,21–24]. For example, Liu & Cheng [11] investigated the failure characteristics of X52 pipeline steel in a thin simulated soil solution layer in the presence of microbial activities, subjected to diverse gassing conditions. This study explored the impact of the corrosion influencing parameters on the corrosion rate under microbial corrosion. The failure tendency was confirmed by the weight loss and polarization curve measurement for different days of exposure. Similarly, Al-jaroudi et al. [22] experimentally studied a crude oil pipeline that failed in the 3rd year of operation due to MIC. Samples from the pipeline and the pipe surface were analyzed, and the results showed a high presence of SRB, Iron oxide (Fe_2O_4 and FeO(OH)), high corrosivity of the water, and presence of H_2S. It was observed that the combined effects of the bacteria and the physio-chemical parameters increase the corrosion rate to about 2.5 mm/year, which leads to the premature leak failure of the pipeline.

Melchers [21] investigated the failure characteristics of marine systems exposed to the prolonged bacteria-infested environment. The author proposed an extreme value probabilistic model for the estimation of the maximum pit depth distribution over time. The researcher concluded that the

system failure exhibits non-linear characteristics for long term exposure to microbial activities. Although, the model reasonably predicts the external pitting corrosion propagation, the integration of the physio-chemical parameters and the microbial activities for failure probability and prediction of critical failure year upon the formation of MIC was not investigated. Moreover, the reviewed models are mostly post failure-based and are limited to dynamically capture the effects of the unstable corrosion influential parameters on the failure probability of internally corroding marine and offshore systems.

2.4. Microbial corrosion risk assessment

Microbial corrosion is characterized by the degradation of engineering systems instigated by the microorganisms. The deterioration of the systems results in failure with associated consequences, which describe the risk induced by MIC. Risk is measured in terms of human injury, environmental damage, or economic loss as a function of the failure probability and the consequence of failure [25]. Dynamic risk assessment employs a method capable of updating the estimated risks with respect to the system's deteriorating state changes in terms of performance, safety, and maintenance activities [26]. Dynamic risk-based integrity assessment of systems suffering MIC utilizes the understanding of the stochastic behavior and unstable failure characteristics and propagation for integrity management strategy in offshore operations. This captures the dynamics of the probability of failure and the associated consequences of failure. Risk-based models, particularly for MIC induced failures, are rarely found in open sources. For integrity management, a comprehensive understanding of the risk level associated with systems suffering MIC is needed for critical decision-making. This will provide a well-informed guideline for both design and operational risk reduction strategies in offshore operations.

A few models for MIC risk analysis are presented in the literature [24,27–30]. For instance, Maxwell & Campbell [28] proposed a risk-based mitigation model for predicting biocide performance and MIC monitoring in field operations. They adopted the Monod kinetics framework to model the biofilm development under inhibitor application and integrate it into the Pots et al. [13] model. The researchers scaled the MIC risk level based on the amount of Sulphide production in the microbial biofilm. The model only gives a diagnostic risk-based monitoring capacity via key performance indicators without quantitatively predicting the risk of MIC induced system failure under diverse operational scenarios. Sørensen et al. [27] developed a semi-quantitative MIC risk assessment model based on the sulfate-reducing prokaryotes (SRP) and the methanogens (MET) counts. The model includes the sulfate reduction rate and CO_2 reduction rate to formulate an Integrated MIC risk factor (IMRF) for the estimation of the MIC initiation time and the potential pit generation rate (PPGR) under biofilm. The model can quantify the risk in term of the microbial counts and the pit generation rate for long term exposure by an integrated molecular microbiological methods. The proposed approach is inadequate to capture the dynamic interactions among corrosion vital factors for MIC risk modelling.

Furthermore, Skovhus et al. [30] proposed a quantitative model for estimation of the probability of failure (PoF) for an offshore facility under MIC. They introduced screening assessment criteria for credible threat likelihood prediction on the system integrity upon inspection. The chosen criteria ranked the PoF by integrating the settlement potential, oxygen ingress, rate of metal dissolution, availability, and MIC mitigation effectiveness. However, the proposed approach captures the screening parameters' effects to establish the PoF indicators/levels (very high, high, medium, low, and very low). The risk indicators were qualitatively structured and represented by

a logic diagram with a characterized path number. The model did not capture the effect of non-linear interactions among MIC influential factors for quantitative risk prediction.

2.5. Current state of knowledge and gaps

The reviewed literature reveals the state of knowledge for MIC risk assessment. Risk-based integrity assessment due to MIC induced failure requires a better understanding of the stochastic behavior exhibited by the MIC and its influential parameters. The stochastic effects complicate the likely consequences of failure prediction. For a robust risk-based integrity assessment, a dynamic model formulation is needed. The dynamic framework will capture the time-dependent behavior of the MIC and its influential parameters to predict the complex failure mechanisms, the likelihood of failure, and its consequences.

A comprehensive review of the existing MIC susceptibility, failure, and risk-based models reveals the following weaknesses:

i. The models are not dynamically structured to estimate the MIC rate, considering the non-linear interactions among corrosion influencing parameters.
ii. The models could not predict the failure probability and the future pit depth distribution given the monitoring operating parameters and the bacteria characteristics
iii. The models do not consider the effect of the mutualistic co-existence of the bacteria under the multispecies biofilm architecture on the remaining strength and survivability of the corroding systems
iv. The models are limited to predict the impact of microbiologically influenced multiple defects interaction on the strength loss and safe operating pressure of corroding systems

v. The models could not explore the dynamic effects of random corrosion parameters and multiple failure modes' interdependencies on the marine and offshore systems' safety and reliability during operation.

vi. There are no microbial corrosion cost models for offshore systems considering multi-failure mechanisms under multispecies biofilm structure

vii. There are inadequate dynamic quantitative risk-based models to explore the effect of the time-dependent corrosion vital parameters on the failure likelihood and their consequences for risk profiling under multiple failure modes and multispecies biofilms.

References

[1] Little BJ, Lee JS. Microbiologically Influenced Corrosion. John Wiley & Sons, Houston, New Jersey; 2007.

[2] Gu T, Jia R, Unsal T, Xu D. Toward a better understanding of microbiologically influenced corrosion caused by sulfate reducing bacteria. J Mater Sci Technol 2019;35:631–6. https://doi.org/10.1016/j.jmst.2018.10.026.

[3] Javaherdashti R. Microbiologically Influenced Corrosion. 2nd Editio. Springer International Publishing Switzerland; 2017.

[4] Eckert R. Field Guide for Investigating Internal Corrosion of Pipelines. NACE International, Houston USA; 2003.

[5] Raja VS, Shoji T. Stress corrosion cracking, Theory and practice. 1st Editio. Woodhead Publishing Limited; 2011.

[6] Mohtadi-Bonab MA, Eskandari M. A focus on different factors affecting hydrogen induced cracking in oil and natural gas pipeline steel. Eng Fail Anal 2017;79:351–60. https://doi.org/10.1016/j.engfailanal.2017.05.022.

[7] de Carvalho CCCR. Marine Biofilms : A Successful Microbial Strategy With Economic Implications. Front Mar Sci 2018;5:1–11. https://doi.org/10.3389/fmars.2018.00126.

[8] Al-Darbi MM, Agha K, Islam MR. Comprehensive Modelling of the Pitting Biocorrosion of Steel. Can J Chem Eng 2005;83:872–81. https://doi.org/10.1002/cjce.5450830509.

[9] Gu T, Zhao K, Nesic S. A new mechanistic model for MIC based on a biocatalytic cathodic sulfate reduction theory. Corrosion 2009:1–12.

[10] Li Y, Xu D, Chen C, Li X, Jia R, Zhang D, et al. Anaerobic microbiologically influenced corrosion mechanisms interpreted using bioenergetics and bioelectrochemistry: A review. J Mater Sci Technol 2018;34:1713–8. https://doi.org/10.1016/j.jmst.2018.02.023.

[11] Liu H, Cheng YF. Mechanistic aspects of microbiologically influenced corrosion of X52 pipeline steel in a thin layer of soil solution containing sulphate-reducing bacteria under various gassing conditions. Corros Sci 2018;133:178–89. https://doi.org/10.1016/j.corsci.2018.01.029.

[12] Marciales A, Peralta Y, Haile T, Crosby T, Wolodko J. Mechanistic microbiologically influenced corrosion modeling — A review. Corros Sci 2019;146:99–111. https://doi.org/10.1016/j.corsci.2018.10.004.

[13] Pots BFM, John RC, Rippon IJ, Thomas MJJS, Kapusta SD, Girgis M., et al. Improvements of De Waard-Milliams Corrosion Prediction and Applications to Corrosion Management. NACE Int. Corros. Conf. No. 02235, 2002, p. 1–19.

[14] Melchers RE, Jeffrey R. The critical involvement of anaerobic bacterial activity in modelling the corrosion behaviour of mild steel in marine environments. Electrochim Acta 2008;54:80–5. https://doi.org/10.1016/j.electacta.2008.02.107.

[15] Xu D, Li Y, Gu T. Mechanistic modeling of biocorrosion caused by biofilms of sulfate reducing bacteria and acid producing bacteria. Bioelectrochemistry 2016;110:52–8. https://doi.org/10.1016/j.bioelechem.2016.03.003.

[16] Melchers RE, Wells T. Models for the anaerobic phases of marine immersion corrosion. Corros Sci 2006;48:1791–811. https://doi.org/10.1016/j.corsci.2005.05.039.

[17] Haile T, Teevens P, Zhu Z. Sulphate-reducing bacteria growth kinetics-based microbiologically influenced corrosion predictive models. J Pipeline Eng 2015;14:259–67.

[18] Taleb-berrouane M, Khan F, Hawboldt K, Eckert R, Skovhus TL. Model for microbiologically influenced corrosion potential assessment for the oil and gas industry. Corros Eng Sci Technol 2018:1–15. https://doi.org/10.1080/1478422X.2018.1483221.

[19] Bailey A. BP:Learning from oil spill lessons. Pet News 2006.

[20] Kotu SP, Eckert RB. A framework for conducting analysis of microbiologically influenced corrosion failures. Insp J 2019.

[21] Melchers RE. Extreme value statistics and long-term marine pitting corrosion of steel. Probabilistic Eng Mech 2008;23:482–8. https://doi.org/10.1016/j.probengmech.2007.09.003.

[22] Al-jaroudi S, Ul-hamid A, Al-Gahtani MM. Failure of crude oil pipeline due to microbiologically induced corrosion. Corros Eng Sci Technol 2011;46:568–79. https://doi.org/10.1179/147842210X12695149033819.

[23] Mokhtari M, Melchers RE. A new approach to assess the remaining strength of corroded steel pipes. Eng Fail Anal 2018;93:144–56. https://doi.org/10.1016/j.engfailanal.2018.07.011.

[24] Kaduková J, Škvareková E, Mikloš V, Marcinčáková R. Assessment of microbiologically influenced corrosion risk in slovak pipeline transmission network. J Fail Anal Prev 2014;14:191–6. https://doi.org/10.1007/s11668-014-9782-x.

[25] CPQRA. Guidelines for Chemical Process Quantitative Risk Analysis. 2nd Editio. New York: American Institute of Chenical Engineers; 1999.

[26] Khan F, Hashemi SJ, Paltrinieri N, Amyotte P, Cozzani V, Reniers G. Dynamic risk management: a contemporary approach to process safety management. Curr Opin Chem Eng 2016;14:9–17. https://doi.org/10.1016/j.coche.2016.07.006.

[27] Sørensen KB, Thomsen US, Juhler S, Larsen J. Cost Efficient MIC Management System based on Molecular Microbiological Methods. NACE Int. Conf. expo, 2012, p. 1–15.

[28] Maxwell S, Campbell S. Monitoring the Mitigaation of MIC Risk in Pipelines. Corros. NACExpo; 61st Annu. Conf. &E Expo., 2006, p. 1–10.

[29] Vigneron A, Head IM, Tsesmetzis N. Damage to offshore production facilities by corrosive microbial biofilms. Appl Microbiol Biotechnol 2018. https://doi.org/https://doi.org/10.1007/s00253-018-8808-9.

[30] Skovhus TL, Andersen ES, Hillier E. Management of Microbiologically Influenced Corrosion in Risk-Based Inspection Analysis. SPE Annu. Tech. Conf. Exhib., 2018, p. 122–30.

Chapter 3

An integrated dynamic failure assessment model for offshore components under microbiologically influenced corrosion

Preface

A version of this chapter has been published in the ***Ocean Engineering 2020; 218: 108082.*** *I am the primary author along with the Co-authors, Sundady Adedigba, Faisal Khan, and Sohrab Zendehboudi. I developed the conceptual framework for the failure assessment model and carried out the literature review. I prepared the first draft of the manuscript and subsequently revised the manuscript based on the co-authors' and peer review feedback. Co-author Sunday Adedigba provided support in implementing the concept and testing the model. Co-author Faisal Khan helped in the concept development, design of methodology, reviewing, and revising the manuscript. Co-author Sohrab Zendehboudi provided fundamental assistance in validating, reviewing, and correcting the model and results. The co-authors also contributed to the review and revision of the manuscript.*

Abstract

The microbiologically influenced corrosion (MIC) is a serious issue that should be considered for effective risk-based integrity management of offshore systems under MIC. This chapter presents a proper methodology by using a hybrid Bayesian network (BN) and Markov process to predict the MIC rate, failure probability, and critical failure year of an internally corroded subsea pipeline. The BN model is developed to probabilistically obtain the MIC rate, considering the dynamic non-linearity and interdependency among vital input factors. The effects of the nonlinear interactions of various prominent factors are evaluated, and their degree of influence is explored. The Markov process is employed to predict the failure probability, critical failure year, and the time evolution

MIC pit depth distribution using the predicted MIC rate as a transition intensity. The developed model is adaptive and captures the evolving impact of microbiologically influenced corrosion. The proposed integrated methodology is tested on a case study, and the most critical parameters that influence the MIC rate and system failure are identified. The proposed approach would provide an early warning guide for a timely intervention to prevent total failure of corroded subsea pipelines and associated consequences.

Keywords: Failure assessment; Bayesian network; Markov process; Pipeline failure probability; Pit depth; Microbiologically influenced corrosion

3.1. Introduction

Corrosion plays a critical role in the failure of infrastructures in the oil and gas industry. Several catastrophic steel failure events in marine and offshore environments have been attributed to undesirable corrosion phenomenon [1]. The complexity of the corrosion mechanisms in the petroleum industry depends on numerous operational, environmental, and material related factors [2–4]. These factors may include biofouling, presence of carbon dioxide, pH, pollutants, temperature, pressure, water velocity, carbonate solubility, salinity, amount of suspended solids, presence of bacteria, material composition, and surface roughness. In petroleum production processes, oil, gas, and water exist under various flow regimes and process conditions; due to the ionic nature of oil and gas, the emulsion is formed at a low concentration of water. The emulsions may exist in the form of either water-in-oil or oil-in-water [5,6]. The oil-in-water emulsions, having contact with the pipe wall, provide a stimulating environment that may favor microbial growth and carbonic acid formation due to CO_2 dissolution [5,7]. The resulting carbonic acid may

initiate different types of internal corrosion, and the bacteria enhance their growth, especially in carbon steel pipelines [8].

Several corrosion induced failures occur in vertical and/or deviated subsea oil pipelines as a result of water hang-up, which provides a stimulating environment that activates corrosion influencing factors such as bacteria, dissolved salts, and volatile fatty acids [9]. The water hang-up builds sufficient pressure that causes periodic spasms of slugging [10]. At high slug formation frequencies of 50-90 per minute, the corrosion rate may linearly increase with slug frequency [11]. The slug frequency depends on the inclination of the pipeline, and the corrosion rate increases by 50% when the slug frequency is doubled [11]. In addition, steel composition and microstructural configuration, as well as the micro-organisms in the area of corrosion initiation, play vital roles in the corrosion growth rate. This is shown in the high rate of material degradation in the dynamic and bacteria-infested environment [12]. According to the literature, the failure of the marine and offshore oil and gas infrastructures due to corrosion defects significantly depends on the depth of the defect and the corrosion growth rate. Therefore, a proper understanding of corrosive environmental dynamics and the material response is crucial in failure prediction and corrosion management in the oil and gas industry. Moreover, the associated dynamics in corrosion mechanisms under the microbial influence need to be adequately understood to predict and also inhibit the risks of failure of critical infrastructures in the marine and offshore industry.

Microbiologically influenced corrosion (MIC) describes the degradation process of various systems instigated by the presence and metabolic activities of micro-organisms such as bacteria and fungi [13]. The formation of metabolites (organic and inorganic acids) by the bacteria influences the electrochemical mechanisms and complicates the corrosion process. Previous research studies have shown that microbiologically influenced internal corrosion contributes to

several onshore and offshore systems' failure with catastrophic consequences [14–16]. The microbial growth is promoted by the availability of the supporting nutrients in the environment. These nutrients synergize with the metallic surface and abiotic corrosion product to provide a sustainable growing environment for the bacteria.

Heterogeneous material surfaces in the presence of water accelerate the formation of bacteria colonies called biofilms. The fused microbial cells and extracellular polymeric substances (EPS) form the biofilm, which provides a favorable mode of subsistence for the microorganisms, even in a hostile environment. The biofilm also promotes a more sustainable environment that enhances reproduction and growth of metabolisms, greatly influencing the corrosion mechanisms [13,17]. The polymeric substances within the multispecies bacteria colony produce a mixed complex array of dynamic corrosive microenvironments that boost the steel material deterioration. This complexity poses difficulty in the understanding of the microbial process and addressing the subsequent challenges [17].

The marine and offshore infrastructures under the microbial biofilm complexity continue to experience severe degradation, especially in micro-organism communities where the sulphate-reducing bacteria, iron-oxidizing bacteria, manganese-oxidizing, sulphate-oxidizing bacteria, acid-producing bacteria, and the exopolymers coexist in the same colony or biofilm [13]. This synergistic consortium alters the electrochemical processes, resulting in microbiologically influenced localized pitting corrosion that reduces the integrity of the structure. The byproduct of the bacteria metabolism cracks the corrosion protection layer, thereby exposes the steel material to severe degradation [3]. The loss of structural integrity occurs when the structure becomes susceptible owing to the breakdown of the thin passive oxide film that resists corrosion. The breakdown is due to the formation of organic and inorganic deposits on the structure surfaces that

compromise the stability of the oxide film [13]. Further growth of the micro-organisms sustains the growth of pit formation and pit density across the length of the pipeline, resulting in MIC induced failures of offshore, shipping, and process systems, for example, pipeline leakages and ruptures, ballast tank, and cargo tank leakages [1,13,14]. These MIC induced failures lead to direct and indirect consequences with associated economic losses/risks.

To model the MIC potential and its propagation, several researchers have proposed mechanistic models [12]. For instance, Gu et al. [18] proposed a bioenergetic-based theory to describe the thermodynamic mechanism for Type I MIC formation by sulphate-reducing bacteria (SRB). The Type 1 MIC formation occurs due to the process of microbes' respiration on exogenous oxidants. This process involves an extracellular electron transfer by the sulphate or nitrate ions into the microbial cytoplasm. This is mostly involved in electrogenic biofilms' formation. The authors emphasized the possibility of alteration in the electrochemical corrosion mechanisms during this phenomenon. They argued that the process of thermodynamic equilibrium-based potential analysis only determines the potential of MIC formation but does not alter the rate of corrosion wastage. They also concluded that an integrated mechanistic model through involvement of microbial growth kinetics, mass transfer, and various chemical, biochemical, and electrochemical reactions would provide a more reliable tool for prediction of MIC potential.

Sørensen et al. [19] proposed a risk-based MIC model for the worst-case pitting corrosion rate and risk factors based on sulphate reducing archasa (SRA), sulphate reducing bacteria (SRB) and methanogens (MET). The authors showed that in the combined colony of the bacteria, the rate of wastage increases; they suggested a proactive plan for the potentially high pit generation rate due to the exponential growth of microbial cells. Al-Darbi et al. [20] developed a mathematically and/or numerically based polarization model. They described the cathodic SRB mediated

polarization as it affects the corrosion rate overtime at different pit depth increments. The developed anaerobic model in the SRB environment was based on cathodic depolarization, which describes the corrosion rate dependency on the consumption rate of sulphate by the SRB and the change in pit depth. More details on the mechanistic models for MIC potential and rate prediction and their limitations are presented in [12]. Generally, these models are not dynamically structured to reflect the complexity and nonlinear interdependency among MIC influencing factors for real-time application and failure probability prediction.

In recent years, advanced models/approaches that better predict the microbial potential based on the screening and operating parameters, and their influence on corrosion wastage of oil and gas infrastructures have been introduced. These include experimental, regression, quantitative, and probabilistic tools [21–25]. Papavinasam et al. [6] experimentally analyzed effects of physical pipeline parameters and fluid characteristics on internal pitting corrosion. The researchers identified the pipe diameter, thickness, inclination angle, production rate, CO_2 partial pressure, and concentration of bicarbonates, sulphate, H_2S, and chloride as pit corrosion contributing factors. Pots et al. [26] proposed a quantitative methodology to assess critical parameters contributing to the corrosion rate in a microbial infested environment. Six factors, such as water presence, pH, salinity, water wetting, dissolved solids, and temperature exhibited the key roles. However, the complex nature of the interactions of the biotic and abiotic parameters poses a challenge in the application of this model. Further models that correlate the operating parameters, metallurgical properties, pit formation, and its propagation over time are found in the open sources [27–29].

The stochastic nature of MIC pit formation and growth requires dynamic models, such as the Markov, Poisson, Petri nets, and Bayesian network approaches for pit depth distribution prediction. For example, Hong [30] used the combined inhomogeneous Poisson and Markov

strategies to model pit generation and its depth growth. It was found that the point of surface wetting and coating breakdown play key roles in pit generation; the Kolmogorov forward equation through a time transformation condensation method was used. Similarly, other researchers [31–33] proposed a nonhomogeneous and continuous-time linear growth pure birth Markov procedure for pit depth distribution. They made efforts to predict pit growth characteristics and the corroded pipeline failure time under the influence of the pipeline's operating parameters.

Although the probabilistic models provide a better representation of the randomness in corrosion pit nucleation and growth, compared to deterministic tools [34–38], the reviewed probabilistic models do not consider the microbial influence on corrosion rate and failure probability. Some of them are also empirically formulated with multiple inspection data fitted for a comparative framework that have limitations due to sparse data availability and an associated high degree of uncertainties.

Generally, MIC significantly contributes to the failures of offshore systems, and the associated risks. Pipeline deterioration progressively increases the risk of failure over time. The safety of a pipeline is dependent on the management of the remaining useful life and the reliability estimation, which determine the intervention measures over time [29,39–41]. These can only be forecasted if the failure probability of the defective pipeline is known. The recent improvements in inspection techniques such as acoustic emission, guided waves ultrasonic testing (GWUT), visual imaging and photography, autonomous underwater vehicles (AUVs), remotely operating vehicles (ROVs), and marine inspection robotic assistant (MIRA) systems have enhanced the capacity for marine/offshore assets integrity assessment for failure-based prediction [42–45].

Despite considerable attempts to understand, predict, and manage MIC in the oil and gas industry, one critical aspect of offshore systems integrity management under MIC that remains unsolved is

how to dynamically predict the MIC rate, failure probability, and future MIC pit depth distribution of a corroding offshore system from single inspection data and by monitoring operating parameters. The existing models are not adequate for the precise prediction of the corrosion rate and failure probability in a dynamic and complex microbial infested environment. There are a limited number of dynamic quantitative models to evaluate the MIC rate and failure probability, considering dynamic nonlinear interdependency among contributory factors.

The main objective of this research is to develop an integrated BN-Markov process model for predicting the MIC rate, failure probability, and future pit depth distribution under microbiologically influenced internal corrosion and its effects on offshore system structural integrity. The MIC influential factors are represented using BN to capture their dynamics, nonlinear dependency, and interdependency. The system failure characteristics based on the critical pit depth state and the future MIC pit depth distribution are estimated using a Markovian process for an offshore system.

The remaining of the chapter is structured as follows: Section 3.2 presents the failure assessment due to MIC. Section 3.3 briefly describes the proposed research methodology. Section 3.4 includes and illustrates the application of the methodology using a case study. Section 3.5 provides the research results and discussion, and Section 3.6 highlights the most important findings of this study.

3.2. Failure assessment due to microbiologically influenced corrosion

Several probabilistic approaches have demonstrated high potential for assessing the failure of offshore systems with corrosion defects, especially pitting corrosion [31–33]. The integrated BN-

Markov process provides a better multi-dimensional dependency modeling capability for the prediction of the MIC rate and corroding offshore systems failure probability [32]. The main elements of the integrated model are briefly illustrated in the following subsections.

3.2.1 Bayesian network

Several modeling (and deterministic) methodologies have shown limitations for modeling of complex and dynamic dependencies among the contributory parameters [46–51]. The application of a Bayesian network (BN) tool for probability modeling can capture the interaction of the multivariate influential factors and their dynamic dependency nature and predict their nonlinear relationships [24,52,53]. The BN is a strong approach for complex system modeling, especially in stochastically formulated scenarios where deterministic or mathematical models have shown limited applications; in fact, BN provides a better dependency framework for both multi-state and multi-dimensional configurations [54,55]. Some of the recent studies focusing on the use of BN for MIC potential prediction can be found in the literature [24,56,57].

The BN technique is a probabilistic inference tool for reasoning and prediction under uncertainties [4,58]. It is represented by a specific graphical model called a directed acyclic graph, which demonstrates the logical relationship between random variables in terms of their conditional probabilities. The nodes are characterized by directed arcs that depict causal conditional dependencies among parent and child nodes, and an assigned conditional probability table is used to model the dependencies among the nodes [53,59]. Using BN modeling, the process of dependency representation can be vertically and horizontally framed. The former describes where the intermediate nodes depend on the root cause nodes, while the latter describes the dependency of root cause nodes on each other [24]. This configuration exhibits both the qualitative and quantitative capability of BN. For a random set of operating variables $\mathrm{U} = \{X_1, \ldots\ldots, \mathrm{X_n}\}$, the

chain rule and joint probability distribution P(U) based on conditional independence is mathematically represented by the following Eqs. [60]:

$$P(U) = \prod_{i=1}^{n} P(X_i | P_x(X_i)) \tag{3.1}$$

where $P_x(X_i)$ introduces the parent of variable X_i and P(U) refers to the joint probability distribution of the variables. The probability of X_i is calculated as follows:

$$P(X_i) = \sum_{U \setminus X_i} P(U) \tag{3.2}$$

where the summation is taken over all the variables except X_i.

The BN updates the prior probability of events upon the availability of new information (called evidence E) using Bayes' theorem to produce the consequence probability (called posterior). Eq. (3.3) is used to estimate the posterior probability. Also, in BN, canonical probabilistic models are utilized to signify the canonical interactions between nodes and provide techniques for statistical dependencies and nonlinear modeling [59].

$$P(U|E) = \frac{P(U,E)}{P(E)} = \frac{P(U,E)}{\sum_U P(U,E)} \tag{3.3}$$

In the recent research works [24,56,61], the BN model technique has exhibited good potential for MIC susceptibility and defect growth prediction in the dynamic marine environment. Hence, the current work builds on the technique practicality to determine the MIC rate, considering the dynamics of the monitoring operating parameters and the environmental factors.

3.2.2 Markov chain approach

The Markov chain tool stochastically uses random variables to model the probability of future events on the basis of the present events in sequence. The Markov model assumes a memoryless principle, where, given the likelihood of the present event, the probability of the future event is independent of the past event but relies on the present [62]. For a Markov chain of N states designated by $1, 2 \dots \dots, N$, the random variable X_N represents the state of the process at any specified time-step. The indexed sequence of the random variables, $\{X_0, X_1, X_2, \cdots\cdots\}$, is observed at different time-steps over the system life cycle. If this sequence $\{X_0, X_1, X_2, \cdots\cdots\}$ satisfies the Markov property, its mathematical formulation gives the following expression [63]:

$$\mathbb{P}(X_{t+1} = s|X_t = s_t,\ X_{t-1} = s_{t-1}, \cdots\cdots, X_0 = s_0) = \mathbb{P}(X_{t+1} = s|X_t = s_t) \tag{3.4}$$

for all $t = 1, 2, 3, \dots \dots \dots$ and for all states $s_0, s_1, \cdots\cdots\ s_t, s$.

The Markov chain is formulated, given the system states and the transitions between different states. The transition intensity/rate (μ_{ij}) and the transition probability(P_{ij}), characterize the Markov approach. These transition probabilities are estimated by a set of Kolmogorov's forward equation (KFE), and for the multi-state Markov process, the Laplace -Stieltjes transform and its inverse are used to estimate the states' transition probabilities [64]. The generated transition probability matrix is represented by a vector notation as P_{ij}, where (i, j) represents the conditional probability that the system will next be in state j, given that it is now in state i. The state-dependent transition probability from state i to state j provides $P_{ij} = \mathbb{P}(X_{t+1} = j|X_t = i)$. Therefore, for t-step transition probabilities, $(P^t)_{ij} = \mathbb{P}(X_t = j|X_0 = i) = \mathbb{P}(X_{n+t} = j|X_n = i)$ for any n.

Several researchers have demonstrated the practicality of Markovian models in various engineering applications [65–67]. This work builds on its usefulness, by adopting the technique,

and integrates it with the partition theorem for probability distribution prediction of the states in any given *t*-step transition. The probability function is mathematically expressed by Eq. (3.5). Therefore, the row vector $(\pi^T P^t)$, as shown below, gives the probability distribution of X_t; for all $(t = 1,2,3 \ \ldots\ldots)$. In this work, the Markov model is treated to have a finite number of states, as N designates.

$$\mathbb{P}(X_t = j) = \sum_{i=1}^{N} \mathbb{P}(X_t = j | X_{t-1} = i)\mathbb{P}(X_{t-1} = i) = \sum_{i=1}^{N} (P^t)_{ij}\pi_i = (\pi^T P^t)_j \quad (3.5)$$

3.3. BN-Markov method for MIC rate and failure assessment

This section presents the developmental stages of an integrated BN-Markov methodology for prediction of MIC rate, failure probability, and future pit wastage propagation of a corroding offshore system under the microbial influence, as shown in Fig. 1. The modeling approach begins with assessing the contributory factors to microbial growth and their probabilities, microbial counts, and sets of inspection data, followed by the use of the BN model to forecast the MIC rate and then integrate it into the Markov approach to estimate the failure probability. The following subsections describe the hybridized modeling strategy.

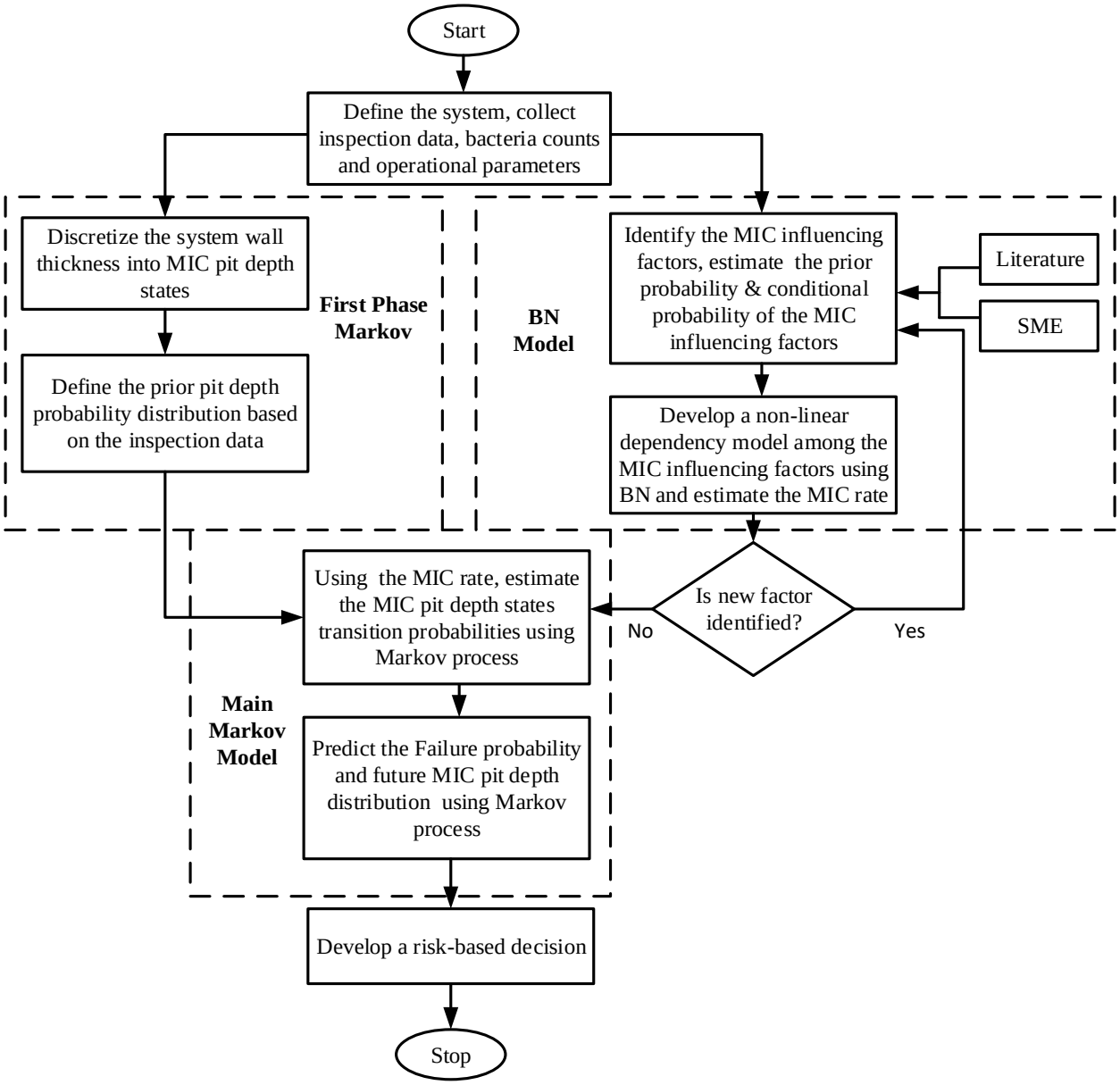

Figure 3.1. Flowchart of the proposed methodology

3.3.1 Collection of relevant information and data

Information regarding the offshore system is collected by inspection, measurements, and fluid analysis (see Fig. 3.1). This information/data may include but not limited to, the operating characteristics and parameters (e.g., temperature, salinity, pH, velocity, exposure time, alloy

composition, sulphate ions, chloride ions, CO_2 partial pressure, water cut), microbial count, mechanical properties, design characteristics, extent of corrosion flaws, and their geometry.

3.3.2 Estimation of MIC rate using Bayesian network

According to several research studies [6,26,29,33,68], there are different degrees of correlations among the monitoring operating parameters ($e.g., CO_2$ partial pressure, bicarbonates concentration, sulphate concentration, H_2S content, chloride concentration, water cut, pH, salinity, temperature) with the corrosion rate and the maximum defect depth. In particular, Ossai et al. [29] used the regression model to analyze the linear dependencies among the operating parameters and defect growth. Although the approach is able to determine the corrosion rate under the prevailing environmental conditions, it is limited to analyze the non-linearity and dynamic interdependencies among the operating parameters and their effects on the microbial corrosion defect rate. For complex relationships between the operating parameters (corrosion influencing parameters) and the microbial corrosion defect rate, BN provides a reliable modeling capacity. It captures the multi-dimensional interactions and influences of the operating parameters and the SRB on the microbial corrosion rate simultaneously at any given operating condition. BN also offers a practical probabilistic network-based model for prediction of MIC defect rate where a single set of inspection data is available with a historical data log for the monitoring operating variables, environmental factors, and micro-organisms [58].

To implement the BN model (see Fig. 3.1), the probabilities of the MIC influencing factors are estimated (prior probabilities) from the available monitoring operating parameters and environmental factors' data set/information by data partitioning. The operating parameters, metallurgical parameters, and environmental factors are used as the input parameters to simulate the process based on their prior estimated probabilities. The cause-consequences relationships are

then modeled using the BN framework. The conditional probabilities define the dependency among the corrosion influencing parameters. The conditional probabilities for the intermediate (SRB) node and the child (MIC rate) node are created by exploring the dynamic relationships among different microbial corrosion influencing factors in long-term exposure. Also, a part of the information is derived from theoretical and experimental corrosion model proposed by the researchers [6,69] and available field data. By inputting the prior probabilities of these MIC vital factors and the conditional probabilities, the MIC rate is predicted. For this research, some of the BN nodes are categorized into high, moderate, and low states, depending on the range of the available operational data. In contrast, others are expressed in two states: "Present" and "Absent" or "Yes" and "No", which describe a state of the positive assertion of a cause of a specific variable and their interacting effect on the MIC rate.

It is important to note that upon the availability of new information/data, the model is dynamically updated, and the evidence can be set on the various MIC rate categories to predict the posterior probabilities of the contributory factors for different scenarios. All the BNs in this work are simulated in the GeNIe™ software environment.

3.3.3 MIC pit states and pipe wall discretization

The pipeline wall thickness is discretized into MIC pit states, as shown in Fig. 3.2. The discretized states, given by $i = 1,2 \dots \dots \dots N$, represent the different degrees of corrosion wastage on the internal surface of the offshore pipeline. The initial state and subsequent states are bounded by a given interval to define different MIC pit depths of the pipeline. The critical depth, N, is the corrosion penetration depth of the pipe wall that results in total failure over time (i.e., over 80% corrosion wastage). The continuous growth of the MIC pit is depth and time-dependent; the greater the depth of the pit, the higher the corrosion rate with time.

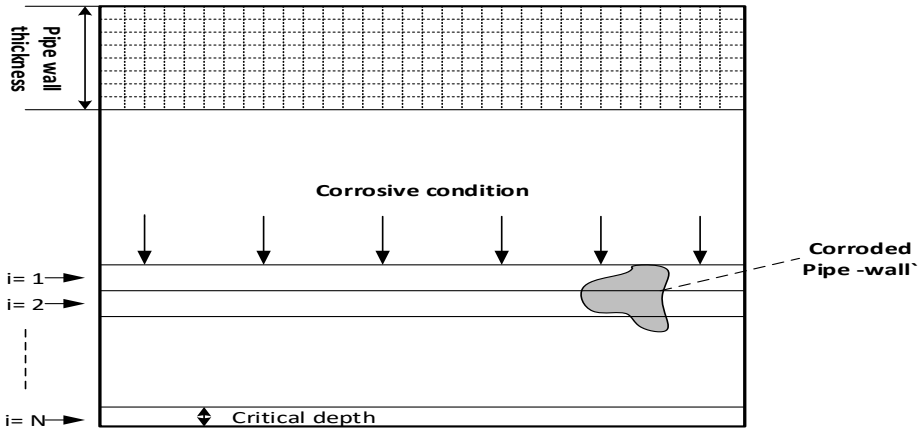

Figure 3.2. Discretization of a corroded pipe wall thickness

3.3.4 Estimation of MIC pit depth states transition probabilities

Given the present pit depth state (G_n) at time n, the pipeline future pit depth state after time n can be described by $\{G_{n+1}, G_{n+2}, \dots \dots \dots \dots\}$, while the past state is $\{G_0, \dots \dots . . G_{n-1}\}$. If the value $G_n = i$ is known, the future pit depth evolution of the chain can be predicted, which depends only on i; it is stochastically independent of the past values or states $\{G_{n-1} \dots \dots ., \ G_0\}$. Therefore, given the present state of the MIC pit depth with characterized MIC rate (μ_{ij}) across the state over time, the transition probability function of the MIC pit depth states, as shown in Fig. 3.1, can be defined by the Kolmogorov forward equations, as follows:

$$\begin{cases} \frac{dP_{G11}(t)}{dt} = -\mu_{12}(t)P_{G11}(t) \\ \frac{dP_{G12}(t)}{dt} = \mu_{12}(t)P_{G11}(t) - \mu_{23}(t)P_{G12}(t) \\ \frac{dP_{G13}(t)}{dt} = \mu_{23}(t)P_{G12}(t) - \mu_{34}(t)P_{G13}(t) \\ \vdots \quad = \quad \vdots \quad \cdots \quad \vdots \\ \frac{dP_{GN}(t)}{dt} = \mu_N(t)P_{GN}(t) \end{cases} \tag{3.6}$$

where $G_1, \ldots\ldots\ldots\ldots\ldots G_N$ introduce the MIC pit depth states; $P_{G11}(t), \ldots\ldots\ldots\ldots\ldots P_{GN}(t)$ are the probabilities of the pits in the state G_{ij} $(i, j = 1,2, \ldots\ldots\ldots\ldots, N)$, with the sum of the pit depth state transition probability function equal to one, as presented below:

$$\sum_{i=1}^{N} P_G^i(t) = P_{G11}(t) + P_{G12}(t) + \ldots\ldots\ldots\ldots P_{GN}(t) = 1 \tag{3.7}$$

For a pit depth in state 1 after inspection, the prior distribution gives $P_{G11}(t) = 1$. The prior distribution serves as the initial condition for future pit depth propagation prediction over time. Applying the multi-state element approach, Eq. (3.6) is solved for the transition probability across the states using the Laplace-Stieljes transformation and its corresponding inverse transform [64]. The resulting state transition probability matrix and generator matrix are written below:

$$Transition\ matrix\ P = \{p_{ij}\} = \begin{Vmatrix} P_{G11} & P_{G12} & P_{G13} & \cdots & \cdots \\ P_{G21} & P_{G22} & P_{G23} & \cdots & \cdots \\ \vdots & \vdots & \vdots & \vdots & \vdots \\ P_{GN1} & P_{GN2} & P_{GN3} & \cdots & \cdots \\ \vdots & \vdots & \vdots & \vdots & \vdots \end{Vmatrix} \tag{3.8}$$

$$Generator\ matrix = Q = \begin{Vmatrix} -\mu_{12}(t) & \mu_{12}(t) & 0 & 0 & \cdots \\ 0 & -\mu_{23}(t) & \mu_{23}(t) & 0 & \cdots \\ 0 & 0 & -\mu_{34}(t) & \mu_{34}(t) & \cdots \\ \vdots & \vdots & \vdots & \vdots & \cdots \\ \vdots & \vdots & \vdots & \vdots & \ddots \end{Vmatrix} \tag{39}$$

The element in the i^{th}row and j^{th}column, p_{ij}, indicates the probability when going from pit depth state i to pit depth state j in one step. This is referred to as one-step pit depth transition probability, while the square transition matrix $P = (P_{ij}), ij \in S$ is called the one-step pit depth transition matrix.

3.3.5 Prediction of pit depth distribution and failure probability

Having the MIC rate (as evaluated in subsection 3.2) and the MIC state transition probability (see subsection 3.4), the pit depth state failure probability is predicted for the critical pit depth using the Markovian procedure. This is achieved through a probabilistic formulation using Eq. (3.5). The time-dependent failure probability is then evaluated over the life cycle of the offshore pipeline. The failure profile of the system is drawn to estimate the likelihood of exceeding the target (threshold) probability, based on the annual target probability safety class for offshore pipelines [70]. The time of occurrence is also estimated from the failure probability profile for the different defect depths and geometries. Therefore, given the evaluated corrosion rate, the time-dependent linear corrosion growth models presented by [71,72] are adopted for the future pit depth prediction in the research analysis

The decision-making process in offshore system health management is often limited by inadequate knowledge of the operating parameters and the stochastic degradation due to environmental factors. Also, limited data and restricted access to the offshore systems/platform could impair accurate information for decision making. Hence, based on the predicted failure likelihood and future state of the asset, critical decision making against total failure can be inferred by operators and integrity managers.

The outcomes of the nonlinear parametric interactions between the monitoring operating variables using BN provide reliable predictions of MIC rate at various prevailing environmental conditions. The likely failure probability and critical failure year are predicted based on the evaluated corrosion rate. The proposed methodology presents a new application of the BN-Markovian methodology in MIC analysis. The proposed approach offers an efficient operational decision-making strategy under MIC.

The illustrative computational example for the hybrid connectionist methodology is shown in the supplementary material (see page 253).

3.4. Application of methodology: case study

The proposed methodology is demonstrated with a case study using inspection data and operating parameters [14]. Based on the established cause-effect interaction among monitoring operating parameters and the MIC defect rate, the limited available data is used as the mean value for the analysis. It is further used to simulate data set for a period of 5 years. Cases of offshore subsea pipeline failure due to corrosion defects have been reported in the literature [14,73,74]. Three segments of an offshore subsea oil pipeline with different internal MIC pit depths taken from the available data/information are used to assess the methodology. The pipeline segments pit depths for the case study are shown in Table 3.1. For this analysis, the offshore subsea pipeline defect is microbiologically influenced, and the initial single corrosion pit depth is used for the case study. The wall thickness is discretized into four pit depth states to reduce the mathematical complexity (and computational costs) associated with complex multi-state systems. The MIC pits are assumed stable, and there is a sustainable growth over the period under consideration.

Predicting the time-dependent failure likelihood of microbiologically influenced corroded offshore pipeline is paramount in safety and integrity management in the oil and gas industry. As the corrosion defect grows in an in-service pipeline, the pipeline gradually loses its strength and is prone to failure at any time when the residual strength is equal to or less than the operating pressure of the pipeline. Due to the stochastic nature of MIC pit formation and its propagation, the MIC rate is probabilistically predicted; it is used as the transition intensity for the failure probability estimation in this study.

Table 3.1. MIC pits geometry for the pipeline segments

	Segment 1 pit		Segment 2 pit		Segment 3 pit	
	Length (mm)	Depth (mm)	Length (mm)	Depth (mm)	Length (mm)	Depth (mm)
Max.	85	0.3300	110	1.7110	135	3.3261

Assuming at the time of inspection (5.1 years), the operating conditions and the measured parameters are the same for the three segments. The monitoring operating parameters are then partitioned into set bounds (high, moderate, and low) to estimate the parameters' prior probabilities based on the data counts within the range, as shown in Table 3.2, for characterization of the prevalent operating environmental conditions. The estimated prior probability and the conditional probabilities are used as the probabilistic input data for the BN model. For the conditional probabilities, additional information from the theoretical and experimental corrosion model proposed by the previous works [6,69] is obtained. In the case of incomplete information, data from subject matter experts and literature [24,56] is used for the analysis.

The mechanical properties of the API 5L pipeline are listed in Table 3.3. All parameters (see Tables 3.2 and 3.3) are required to predict the critical MIC pit depth probability of failure, critical year of failure, and the time evolution pit depth distribution of the offshore subsea pipeline. Furthermore, the following assumptions are made in this hybrid modeling:

a) The data bounds, as reported in Table 3.2, represent the prevailing environmental conditions for the period under consideration.

b) The future defect growth is predicted based on the MIC defect rate; it is constant for the period under study.

c) The Markovian method is established based on the assumption that the asset is at an initial state with no defects at the commencement of the offshore operation.

d) The MIC defect growth is assumed to linearly propagate.

e) The different pipe segments are subjected to the same environmental conditions.

The computational procedure is found in the supplementary material (see page 253).

Table 3.2. Monitoring operating parameters, environmental parameters, and their probabilities for the analysis.

Variables (Node)	Range	State /Probability	Variables (Node)	Range	State/Probability
pH	2.21 ~ 8.85	Acidic ~ 0.4401 Neutral ~ 0.3125 Basic ~0.2474	Water cut	1~ 9%	High ~ 0.6002 Moderate ~ 0.3265 Low ~ 0.0733
Temp (^oC)	21 ~ 85	High ~ 0.3333 Moderate ~ 0.5191 Low ~ 0.1474	Salinity		Present ~ 0.67 Absent ~ 0.33
Flow rate(m/s)	0.04 ~ 2.05	High ~ 0.0132 Moderate ~ 0.3312 Low ~ 0.6556	Chlorine (mg/l)	66 ~ 8000	High ~ 0.6033 Moderate ~ 0.3037 Low ~ 0.0930
CO_2 partial pressure (MPa)	0.01 ~ 0.61	High ~ 0.6932 Moderate ~ 0.2955 Low ~ 0.0114	Sulfate ion (mg/l)	2 ~ 80	High ~ 0.5938 Moderate ~ 0.3118 Low ~ 0.0943
Steel composition	Present Absent	> 0.5% = 0.612 < 0.5% = 0.388	Exposure period		Max. > 3.5yrs ~ 0.6512 Mean 2.5-3.5yrs ~0.2912
SRB (cfu/ml) $< 10^4$ $10^4 \sim 10^5$ $>10^5$		Low Moderate High			Min < 2.5yrs ~ 0.0576

Table 3.3. Mechanical properties of the pipeline.

Wall Thickness	Inside Diameter	Drift Diameter	Collapse Resistance	Internal Yield Pressure
6.45mm	41mm	38.5mm	65.5Mpa	73.6MPa

3.5. Results and discussion

The primary objective of developing the integrated BN-Markov model is to precisely predict the MIC rate from a single set of inspection data and the operational parameters. The MIC rate is used as the transition intensity for determination of the probability of failure and the critical failure year of an internally corroded subsea pipeline. To model the MIC rate, the BN is built, connecting the intermediate and basic events by arcs, designating the dependency and interdependency among the contributory factors. The vital parameters and their probabilities are given in Table 3.2 (see Section 3.4). They serve as the input parameters and are used to simulate the BN model. The BN is constructed based on a cause-consequences relationship among the operating parameters, environmental factors, material properties, and the MIC rate. The parametric learning of the developed BN uses the prior probabilities and conditional probabilities for the monitoring of operating parameters (as the input data) to predict the MIC rate. Fig. 3.3 demonstrates the developed BN model, which dynamically predicts the MIC rate given the prior probabilities of the monitoring operating parameters, environmental factors, and metallurgical properties. It is found that temperature, water cut, flow velocity, and pH are of importance in the microbial growth and the MIC rate simultaneously.

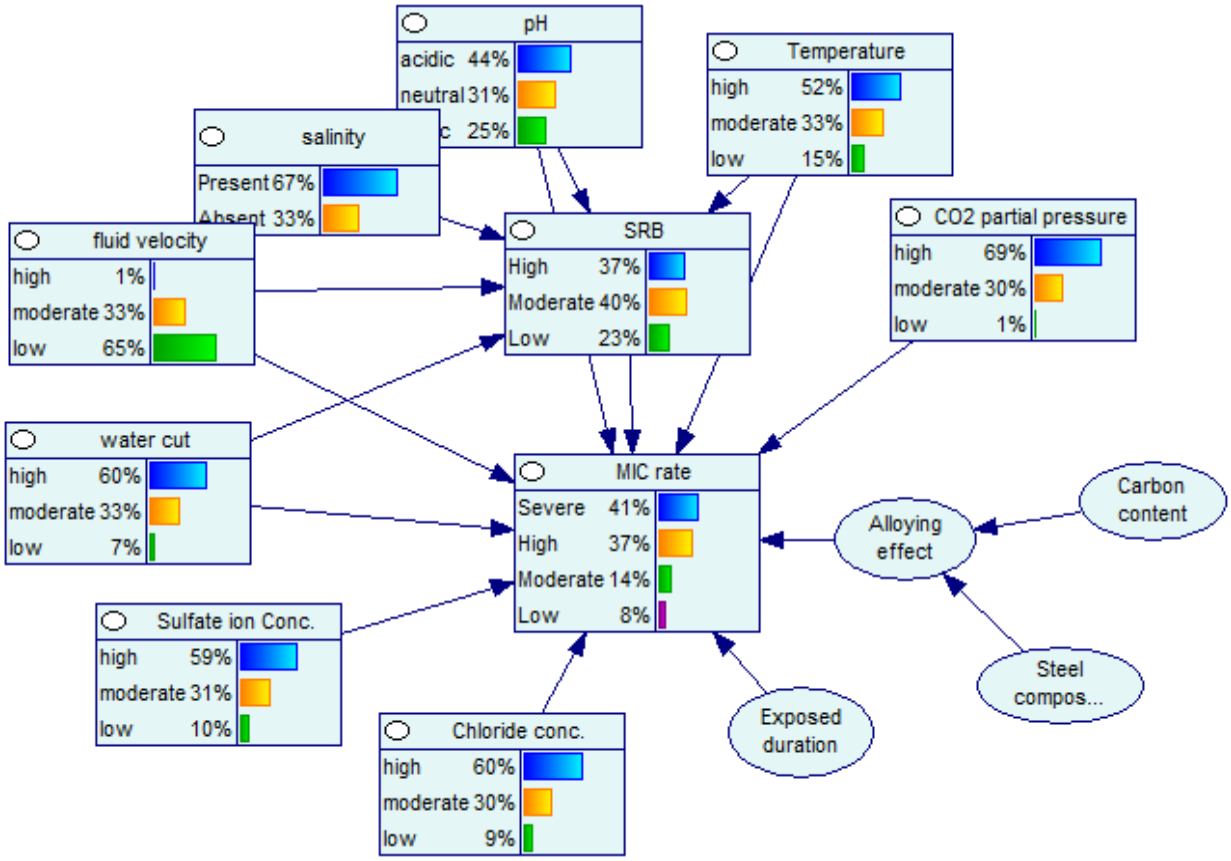

Figure 3.3. Parametric learning of the BN for MIC rate prediction based on the prior probabilities of corrosion influencing factors.

The predicted MIC rates from the parametric simulation of the BN model for the corroding offshore subsea oil pipeline under the prevailing conditions are obtained to be 0.0779mm/year, 0.1423mm/year, 0. 3672mm/year, and 0.4125mm/year, respectively for the low, moderate, high, and severe corrosion categories. The results explore the parameters' interactions; this is in agreement with the findings and data of [33,75]. Furthermore, a sensitivity analysis is performed on the BN model to identify the degree of influence of each operating parameter on the MIC rate. It follows that within the temperature range $21℃ - 45℃$, the MIC rate increases by 4.2%. The BN model analysis shows that temperature is a key factor contributing to the SRB metabolism and

the rate of defect growth under MIC. Further confirmation on the effects of temperature on microbial corrosion in the marine environment is obtained based on the previous studies [56,68,76]. The effect of seawater salinity on the MIC phenomenon(and rate) is crucial especially in seawater environments. According to the sensitivity analysis, the salinity exhibits a moderate support for SRB sustenance for the case study, with an increase in the MIC rate of 1.7%. However, the degree of influence is mainly site-specific.

The effect of alloy composition is premised on its susceptibility due to the breakdown of the passive protective film. At this point, the MIC of identifiable depth is formed. Evaluating the effect of the alloy composition, an increase of 1.9% in the MIC rate is noticed. The sensitivity analysis of the pH based on an overly acidic state indicates that the MIC rate increases by 1.7%. This confirms the important role of the water phase of the multiphase flow systems in the carbonic acid formation and buffering of pH in oil and gas production processes. According to the BN modeling results, pH, which is a dependent variable, is positively correlated with temperature and CO_2 partial pressure. The combined characteristic effects of these parameters promote a high rate of system degradation in a microbial infested environment.

Flowing velocity exhibits different distribution for both internal and external microbial corrosion in the marine environment. The low fluid velocity supports the formation and sustainability of complex microbial biofilms on the internal surface of the pipeline. Hence, it is crucial to dynamically analyze the effect of flow velocity on the SRB metabolism and the corrosion rate. For low fluid speed and high water cut, it is observed that the MIC rate increases by 2.7% and 1.6%, respectively. This reflects the significant effect of these operating parameters on the MIC rate of the corroded subsea oil pipeline. The systematic analysis of the impacts of sulphate ion concentration, chloride concentration, and the CO_2 partial pressure reveals their relative

contribution to the MIC rate. It is found that the MIC rate increases by 2.4%, 2.7%, and 1.6% respectively, due to the sulphate ion concentration, chloride ion concentration, and CO_2 partial pressure effects. At this condition, inorganic acid is formed and can be further metabolized by oxidation to form SO_4^{2-}, which creates sustainable nutrient sources for SRB growth and promotes a severe MIC rate. Upon an increase in the exposure time and the SRB counts, the MIC rate increases by 2.1% and 10.1%, respectively, which is in agreement with the findings of [77]. Based on the parametric sensitivity analysis, the SRB count exhibits a severe effect on the MIC rate, compared to other parameters under the same operating conditions. Hence, the SRB significantly affects the MIC rate and future MIC pit depth distribution for the subsea pipeline. Table 3.4 reports a summary of the percentage effects of the operating parameters on the MIC rate. This phase of the study provides an initial validation of the model. Fig. 3.4 further highlights the impacts of the operating parameters on the SRB enhancement.

Table 3.4. Percentage effect of operating and environmental parameters on the predicted MIC rate.

Operating Parameters	Effects on MIC Rate (%)
Temperature	4.2
Salinity	1.7
Alloy composition	1.9
Fluid velocity	2.7
pH	1.7
Water cut	1.6
Sulphate ion	2.4
Chloride ion	2.7
CO_2 partial pressure	1.6
Exposure time	2.1
SRB counts	10.1

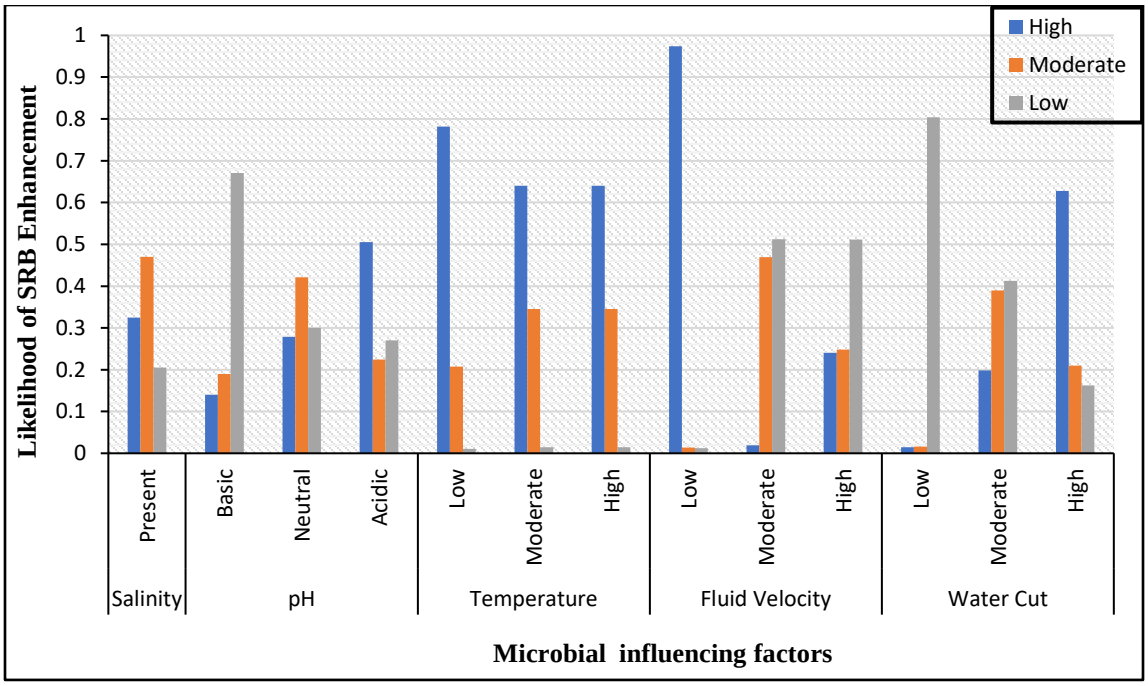

Figure 3.4. Monitoring operating parameters' likelihood of SRB enhancement

More analysis of the contributory factors' lower and upper bound probability effects on the MIC rate is performed. By setting evidence on the bounds of the influential factors, new sets of MIC rates are predicted, as shown in Fig. 3.5 and Fig. 3.6. It is noticed that the MIC rate is increased by 40.4% for the severe corrosion category with evidence on the upper bound probability, compared with the parametric learning result. This confirms the dynamics of the contributory parameters on the MIC rate; the BN framework also shows the capacity to model the dynamic nonlinear dependencies among the key factors. The summary of the results for the different scenarios is given in Table 3.5. A comparative analysis of the lower and upper bounds MIC rates shows an increase of 11.33% and 53.2% for the high and severe corrosion category, respectively. This increase in the MIC rate will promote a rapid failure in offshore systems where water hang-up and slug formation pose critical challenges. It is important to avoid such a sudden system failure through development of a useful and reliable predictive strategy.

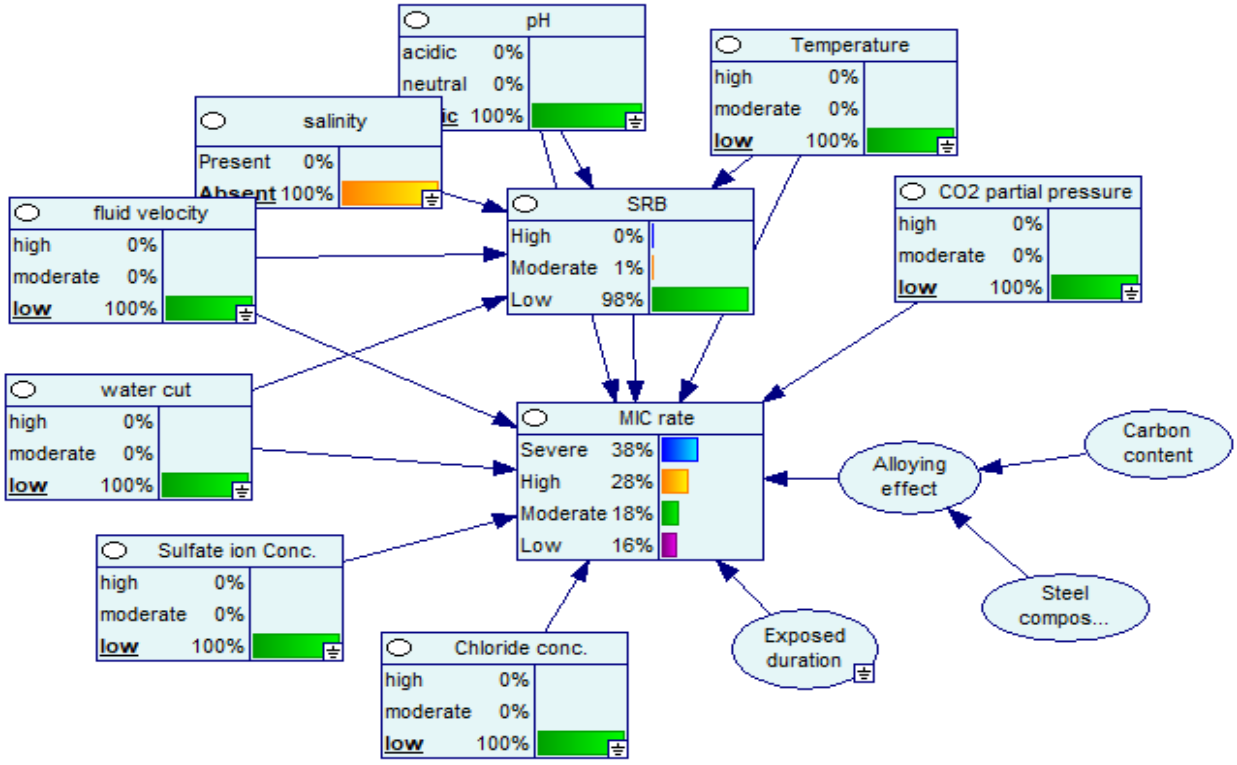

Figure 3.5. Implementation of the BN model for MIC rate prediction with evidence on lower bound probabilities of the corrosion contributory factors

Table 3.5. Categorization of MIC rate for subsea pipeline.

	Maximum Predicted MIC Rate (mm/year)		
Pitting Category	Lower Bound	Normal	Upper Bound
Low	0.1603	0.0779	0.0409
Moderate	0.1812	0.1423	0.0678
High	0.2806	0.3672	0.3124
Severe	0.3779	0.4125	0.5789

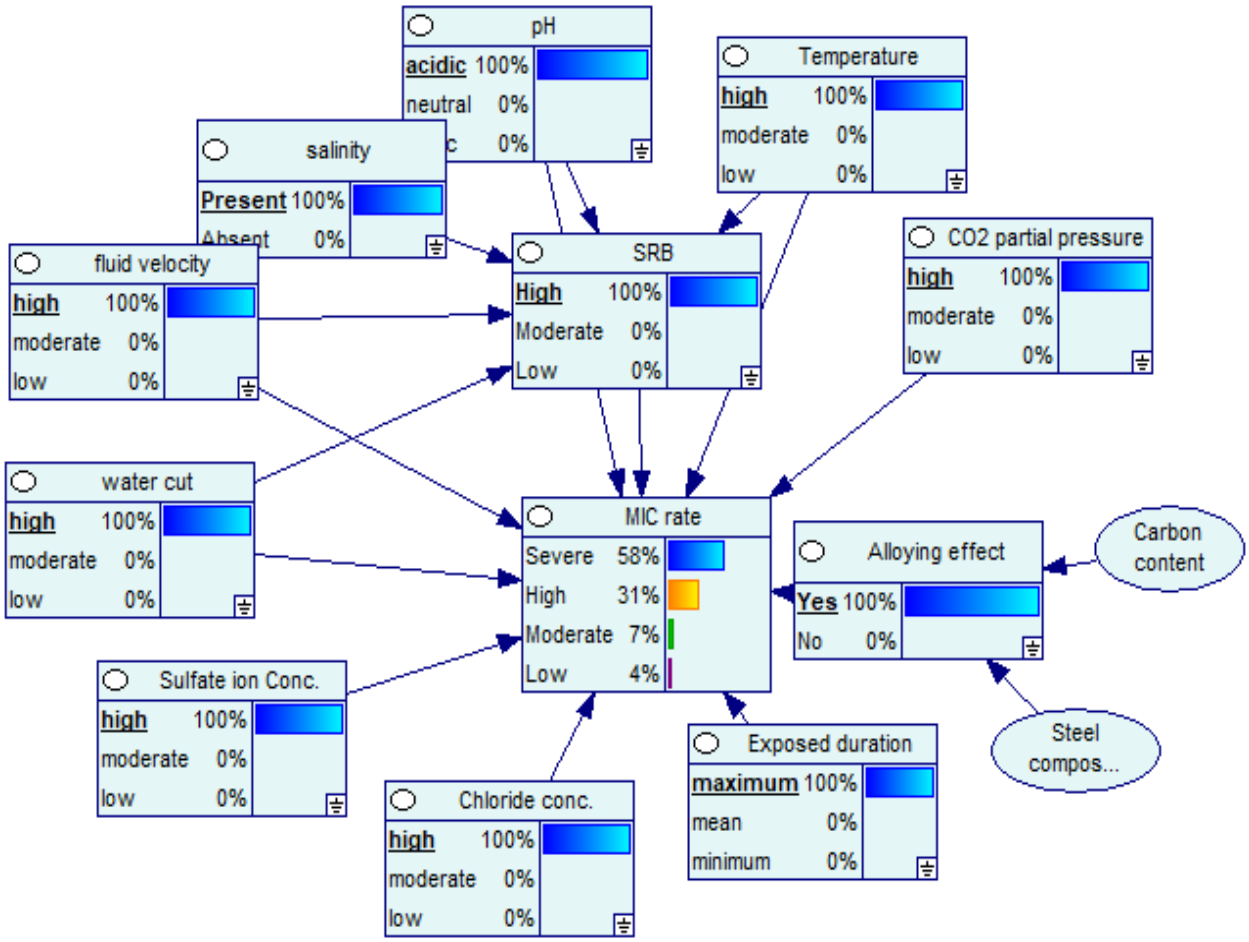

Figure 3.6. Implementation of the BN model for MIC rate prediction with evidence on the upper bound probabilities of corrosion contributory factors

The estimated upper bound MIC rate is integrated into the Markovian stochastic procedure to evaluate the MIC pit depth state transition probabilities. The formulated transition probability function and the defined prior pit depth state distribution are then used to determine the failure probability for the three corroded subsea pipeline segments. At the point of inspection, the corrosion defect for pipe segment 1 is at pit depth state 1, segment 2 at pit depth state 2, and segment 3 at pit depth state 3 based on the pipeline's wall thickness discretization. The results of

the analysis are presented in Fig. 3.7 for the three segments of the subsea pipeline with different MIC pit depths.

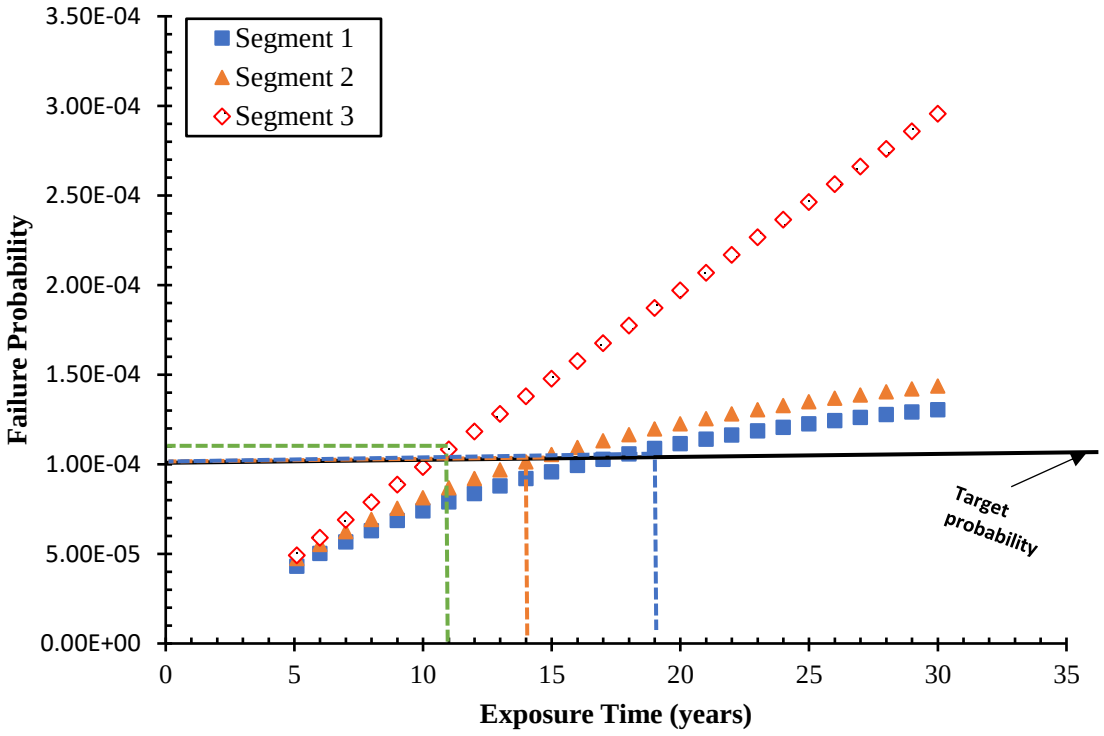

Figure 3.7. Time evolution failure probability of microbiologically influenced corroded subsea pipeline segments

It is found that the time evolution failure probability for the three segments is progressively increased, with a higher magnitude for the third pipeline segment. It is concluded that under the same operating and environmental conditions, components with greater corrosion depth (segment 3) will experience an early failure, compared to the two other components. This finding is in agreement with the previous studies [33,78]; it implies that the critical failure year and risk increase for a severely corroded offshore pipeline. The predicted failure probability for the three segments and the mean first passage time (critical failure year) are provided in Table 3.6. These parameters

are estimated from the failure probability profile of the critical pit depth state exceeding 80% of the pipe wall thickness (as shown in Fig. 3.7) based on the normal safety class annual target probability of failure for corroded offshore pipelines [70].

The results exhibit the time-dependent effect of microorganisms on the degradation process of offshore pipelines. The stochastic natures of the operating parameters affect the residual strength of the corroding subsea pipeline. It follows that as the MIC rate increases, the residual strength continues to decline, limiting the structural resistance to the internal pressure loading. Most importantly, the residual strength is exponentially reduced when the microbial biofilm results in a sustainable growth and a protective environment. The biofilm lowers the effect of corrosion inhibitors (biocides) and continues to influence the development of the MIC pit at multiple growth rates. A sudden failure is inevitable under this condition in the absence of a proactive monitoring framework and model for failure probability prediction.

Table 3.6. Failure probability for offshore subsea pipeline using the predicted upper bound MIC rate.

Subsea Pipeline Segment	Critical Failure Probability	Critical Failure Year
Segment 1	1.059E-04	18
Segment 2	1.013E-04	14
Segment 3	1.085E-04	11

The impacts of MIC rate on failure probability and critical failure time are illustrated in Fig. 3.8 and Table 3.7. According to the results if the MIC rate is increased, the failure probability increases while the critical failure year decreases. Thus, an early failure of the pipeline is anticipated by increasing the MIC rate. A comparative analysis of Fig. 3.7 and Fig. 3.8 reveals a backward shift

in the critical failure year, which reflects the dynamics of the MIC rate on the system failure time and probability.

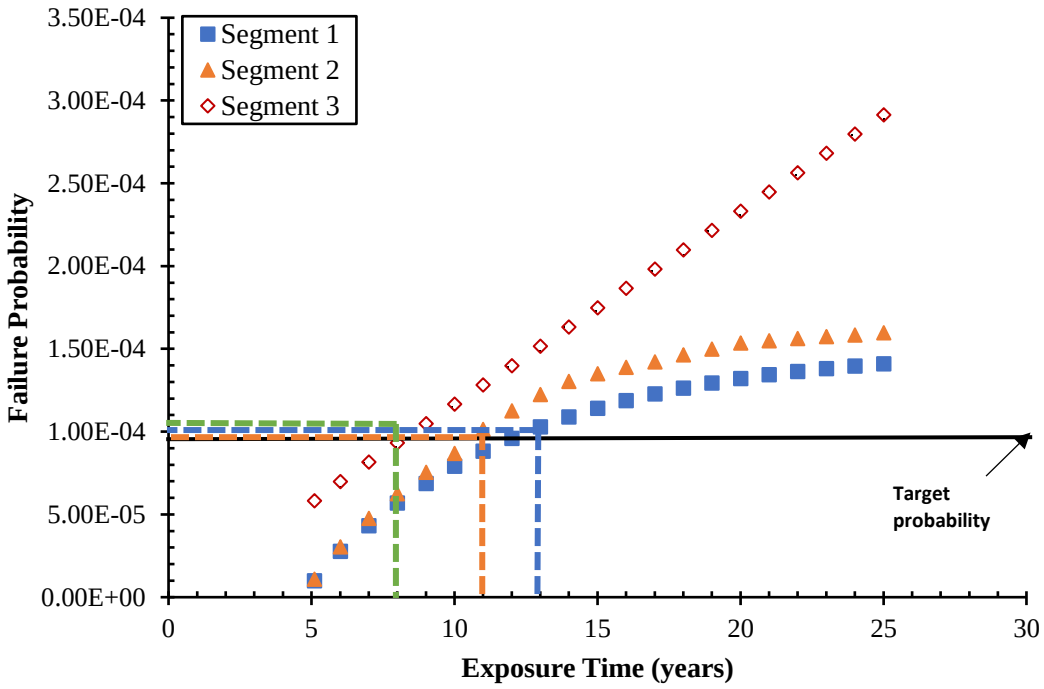

Figure 3.8. Time evolution failure probability of corroded subsea pipeline segment when the MIC rate is tripled

Table 3.7. Predicted failure probability for the subsea pipeline when the upper bound MIC rate is tripled.

Subsea Pipeline Segment	Critical Failure Probability	Critical Failure Year
Segment 1	1.08E-04	13
Segment 2	1.05E-04	11
Segment 3	1.15E-04	8

Figs. 3.9-3.11 present the time evolution MIC pit depth distribution for the three pipeline segments. The extreme upper bound MIC rate is tripled to reflect the dynamics of the MIC rate increase on pit depth distribution over time. It is found that the future pit depth distribution is significantly increased with an increase in depth and growth rate; this is in agreement with the previous research works [31–33]. However, for the first pipeline segment, the low corrosion category shows less significant growth over the pipeline's life cycle. This might be due to a low MIC rate and less influence from the contributory factors. A gradual or limited growth may be experienced at a specific corrosion rate lower than the low corrosion category threshold. The predicted time evolution pit depth distribution provides a guide on the likelihood of how microorganisms enhance the pit corrosion wastage in offshore pipelines. It is important to note that due to the complexity of microbial behaviors and colony formation, the MIC rate may exponentially increase and result in a sudden failure of the system.

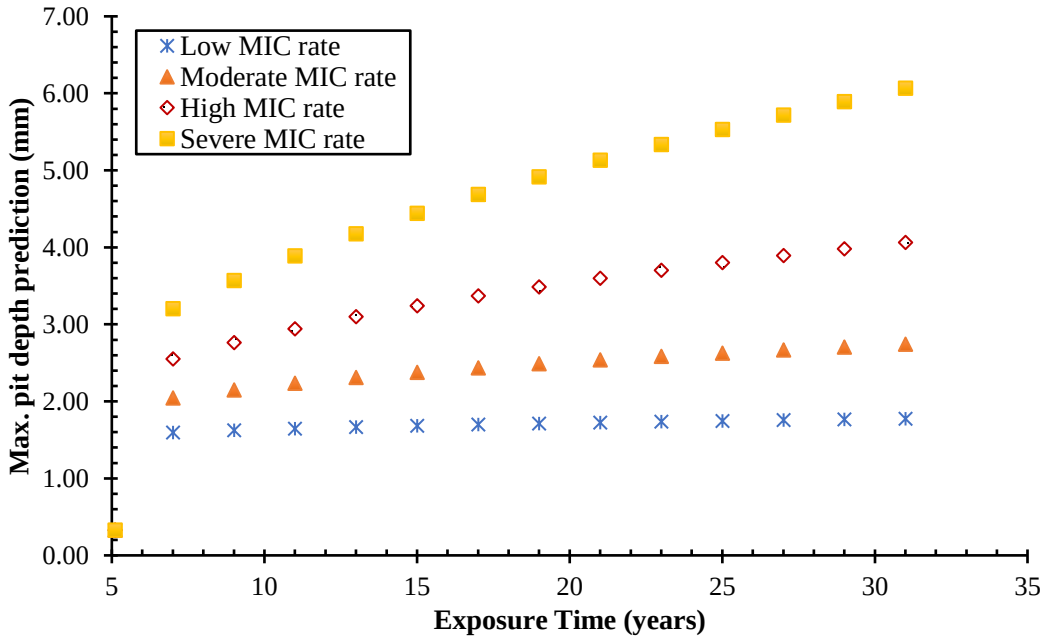

Figure 3.9. Future MIC pit depth distribution of corroded subsea pipeline segment 1 at tripled MIC rate

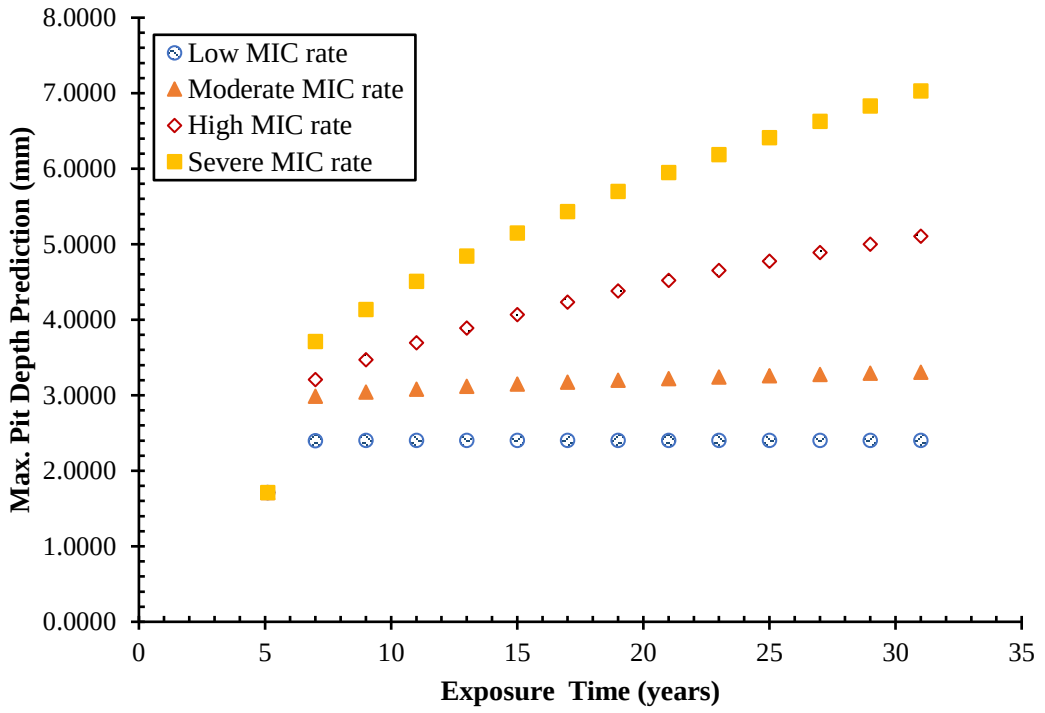

Figure 3.10. Future MIC pit depth distribution of corroded subsea pipeline segment 2 at tripled MIC rate

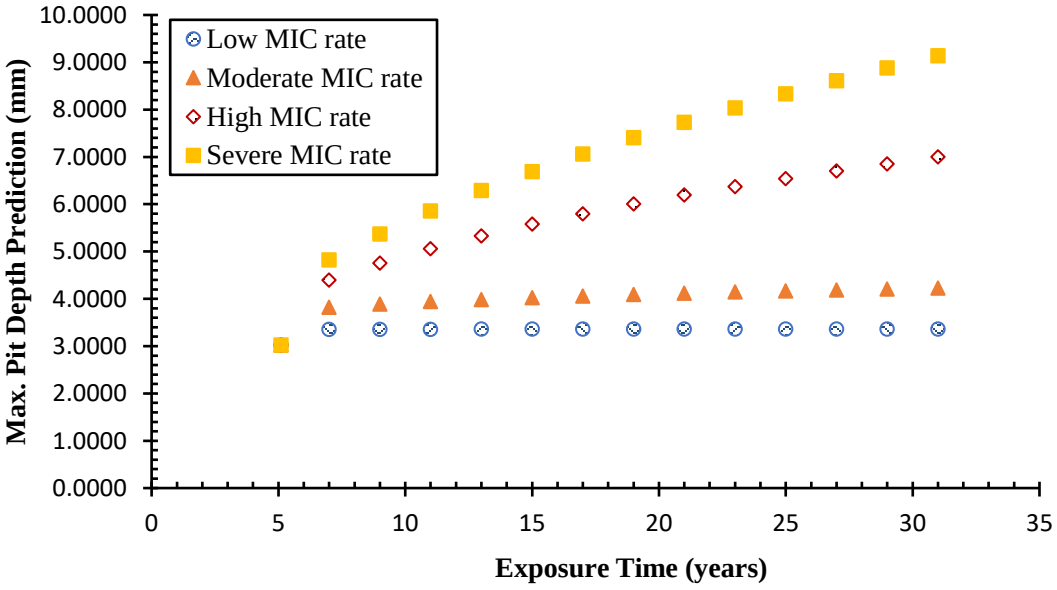

Figure 3.11. Future MIC pit depth distribution of corroded subsea pipeline segment 3 at tripled MIC rate

Fig. 3.12 displays the time evolution probabilities for the first and second corroded pipeline segments pit depth states 1 and 2, respectively. This is important to show the point of lower bound intersection between the two states' probabilities; this indicates the likely threshold for inspection or intervention (decision-making) to avoid a total failure. As mentioned earlier, in the 9th year of exposure, the pits depth states' probabilities for the first and intermediate states are at the midpoint. Based on Fig. 3.7, the predicted critical pit depth failure probability increases and exceeds the threshold as the year of exposure increases (e.g., at the 11th year, 14th year, and 18th year for the three pipe segments, respectively). The introduced method provides guidelines/tips for timely decision making to prevent the total failure of the corroding subsea pipeline. Hence, an optimal, cost-effective, and timely intervention plan could be implemented.

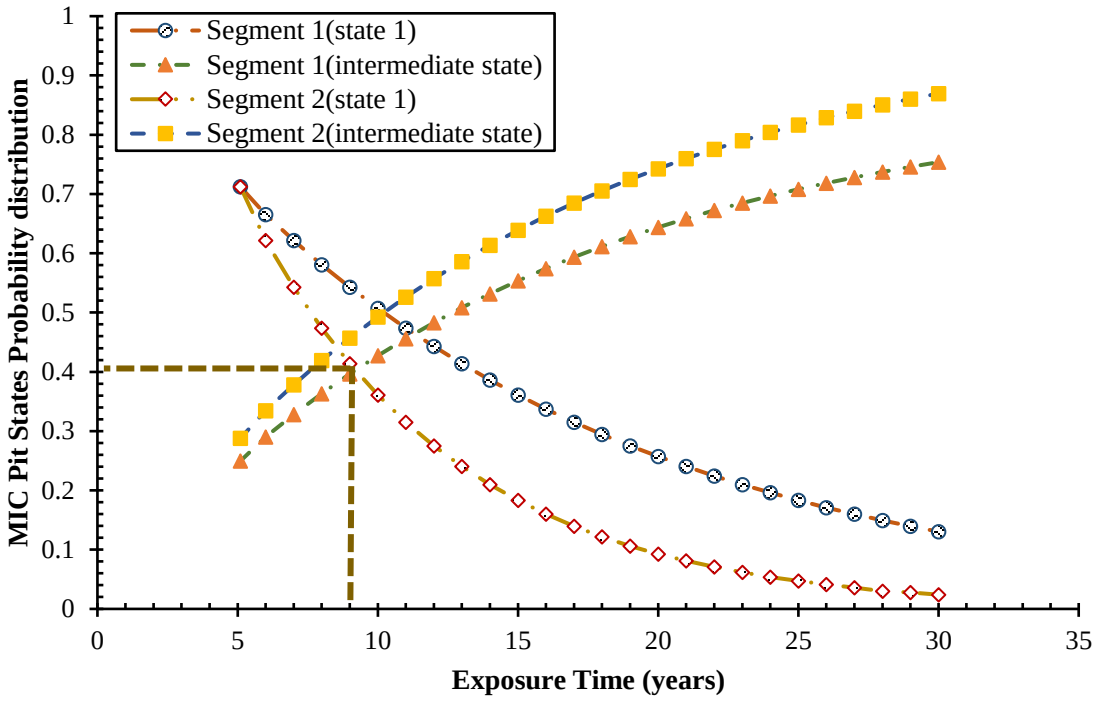

Figure 3.12. Time evolution of the first and intermediate states' probabilities for corroded subsea pipeline segments.

3.6. Conclusions

The present study demonstrates the application of an integrated BN-Markov methodology for the prediction of a time-dependent MIC rate, failure probability, and critical failure year of the corroding subsea pipeline. More emphasis is placed on the effects of the operating parameters and SRB on the MIC rate; this also covers the effect of MIC rate on the likelihood of failure of the pipeline after long-term exposure.

The developed model is tested using three corroded subsea pipeline segments; the BN demonstrates the potential for complex dependency modeling among the MIC rate influencing parameters, and quantitatively predicts their values. The degree of influence of the corrosion controlling parameters on the MIC rate is explored. The capacity of the BN is also assessed to update the MIC rate given a new set of information about the operating conditions of the pipeline. According to the parametric sensitivity analysis, temperature, fluid velocity, and SRB, among other factors, cause a severe effect on the MIC rate and the failure of the pipeline; this is also confirmed by the previous studies. The predicted MIC rate is used in the Markovian approach to predict the failure probability and critical failure year for the three segments under the same operating conditions, but with different MIC pit depth states. It is concluded that as the corrosion pit depth increases, the failure likelihood and risk of failure increase with time, while the critical failure time decreases. This is anticipated in aging corroded offshore pipelines. This further highlights the reliability and accuracy of the proposed approach. Nevertheless, only the linear defect growth corrosion model is considered for the future pit depth distribution.

Based on the results of the critical pit depth failure probability profile for the three pipeline segments, the following decision-making can be inferred: if the corroded pipe segments are assumed to be in series, failure of one segment constitutes pipeline failures; an optimal and cost-

effective 3.5-year inspection or intervention plan can be made. Otherwise, if the failure of all segments is required for the system to fail, an individual inspection plan may be required. For this case study, a 4-year (e.g., 9^{th} year, 13^{th} year, and 17^{th} year respectively) inspection or intervention plan can be implemented for the three corroded pipe segments to protect them from sudden failure and its consequences. In addition, improving material composition and pipeline design, practical parametric monitoring, and proper application of pigging and high-quality site-specific biocides can mitigate sudden failures due to MIC.

The proposed model presents an effective early warning and monitoring tool upon MIC formation on offshore components and for decision making. Nevertheless, the model can be improved in future research by considering the time-nonhomogeneous Markovian approach, nonlinear corrosion model integration, and multi-failure mechanisms under the multispecies biofilm structure.

Acknowledgments

The authors acknowledge the financial support provided by Genome Canada and their supporting partners, the Canada Research Chair (CRC) Tier I Program in Offshore Safety and Risk Engineering, and the Natural Sciences and Engineering Research Council of Canada (NSERC).

References

[1] Paik JK, Kim DK. Advanced method for the development of an empirical model to predict time-dependent corrosion wastage. Corros Sci 2012;63:51–8. https://doi.org/10.1016/j.corsci.2012.05.015.

[2] Little BJ, Lee JS. Microbiologivally Influenced Corrosion. John Wiley & Sons, Houston, New Jersey; 2007.

[3] Chandrasekaran S, Jain A. Ocean Structures: Construction, Materials and Operations. CRC press Taylor & Francis Group, LLC; 2016. https://doi.org/10.1201/9781315366692-2.

[4] Chandrasekaran S. Offshore Structural Engineering: Reliability and Risk Assessment. CRC press Taylor & Francis Group, LLC; 2016. https://doi.org/10.1017/CBO9781107415324.004.

[5] Papavinasam S, Doiron A, Panneerselvam T, Revie RW. Effect of Hydrocarbons on the Internal Corrosion of Oil and Gas Pipelines. Corrosion 2007:704–12.

[6] Papavinasam S, Doiron A, Revie RW. Model to Predict Internal Pitting Corrosion of Oil and Gas Pipelines. Corrosion 2010;66:1–11.

[7] Nesic S, Cai J, Lee KJ. A Multiphase Flow and Internal Corrosion Prediction Model for Mild Steel Pipelines. NACE Int. Corros. Conf., 2005, p. 1–35.

[8] Renpu W. Oil and gas well corrosion and corrosion prevention,. Adv. Well Complet. Eng. 3rd Editio, Gulf professional publishing, Boston; 2011, p. 619–39.

[9] Ibrahim A, Hawboldt K, Bottaro C, Khan F. Review and analysis of microbiologically influenced corrosion: the chemical environment in oil and gas facilities. Corros Eng Sci Technol 2018:1–15. https://doi.org/10.1080/1478422X.2018.1511326.

[10] Palmer A, King R. Subsea pipeline engineering. 2nd editio. Oklahoma USA: PennWell Corporation; 2008.

[11] Jepson WP. Study Looks at Corrosion in Hilly Terrain Pipe Lines. Pipeline Gas Ind 1996;8:27–32.

[12] Marciales A, Peralta Y, Haile T, Crosby T, Wolodko J. Mechanistic microbiologically influenced corrosion modeling — A review. Corros Sci 2019;146:99–111. https://doi.org/10.1016/j.corsci.2018.10.004.

[13] Beech IB, Gaylarde CC. Recent Advances in the Study of Biocorrosion - An Overview. Rev Microbiol 1999;30:177–90.

[14] Eckert R. Field Guide for Investigating Internal Corrosion of Pipelines. NACE International, Houston USA; 2003.

[15] Al-jaroudi S, Ul-hamid A, Al-Gahtani MM. Failure of crude oil pipeline due to microbiologically induced corrosion. Corros Eng Sci Technol 2011;46:568–79. https://doi.org/10.1179/147842210X12695149033819.

[16] Witt D, Ma K, Lee T. Field Studies of Microbiologically Influenced Corrosion of Mooring Chains. Offshore Technol. Conf., Houston, Texas USA: 2016.

[17] Machuca LL. Microbiologically influenced corrosion: A review focused on hydrotest fluids in subsea pipelines. Corros. Prev. Pap. 117, 2016.

[18] Gu T, Zhao K, Nesic S. A new mechanistic model for MIC based on a biocatalytic cathodic sulfate reduction theory. Corrosion 2009:1–12.

[19] Sørensen KB, Thomsen US, Juhler S, Larsen J. Cost Efficient MIC Management System based on Molecular Microbiological Methods. NACE Int. Conf. expo, 2012, p. 1–15.

[20] Al-Darbi MM, Agha K, Islam MR. Comprehensive Modelling of the Pitting Biocorrosion of Steel. Can J Chem Eng 2005;83:872–81. https://doi.org/10.1002/cjce.5450830509.

[21] Heyer A. Microbiologically influenced corrosion in ship ballast tanks. Universiteit Duisburg-Essen, Duitsland, 2013.

[22] Huang RT, McFarland BL, Hodgman RZ. Microbial Influenced Corrosion in Cargo Oil Tanks of Crude Oil Tankers. NACE Int. Corros. Conf., 1997.

[23] Liu H, Cheng YF. Mechanistic aspects of microbiologically influenced corrosion of X52 pipeline steel in a thin layer of soil solution containing sulphate-reducing bacteria under various gassing conditions. Corros Sci 2018;133:178–89.

https://doi.org/10.1016/j.corsci.2018.01.029.

[24] Taleb-berrouane M, Khan F, Hawboldt K, Eckert R, Skovhus TL. Model for microbiologically influenced corrosion potential assessment for the oil and gas industry. Corros Eng Sci Technol 2018:1–15. https://doi.org/10.1080/1478422X.2018.1483221.

[25] Wolodko J, Ecket R, Haile T, Hashemi S., Khan F, Taylor C, et al. Modeling of Microbiologically Influenced Corrosion (MIC) in the Oil and Gas Industry - Past, Present and Future. NACE Int. Conf. expo, 2018, p. 1–15.

[26] Pots BFM, John RC, Rippon IJ, Thomas MJJS, Kapusta SD, Girgis M., et al. Improvements of De Waard-Milliams Corrosion Prediction and Applications to Corrosion Managment. NACE Int. Corros. Conf. No. 02235, 2002, p. 1–19.

[27] Mahmoodian M, Li CQ. Reliability-Based Service Life Prediction of Corrosion-Affected Cast Iron Pipes Considering Multifailure Modes. J Infrastruct Syst 2018;24:1–8. https://doi.org/10.1061/(ASCE)IS.1943-555X.0000417.

[28] Caleyo F, Velázquez JC, Valor A, Hallen JM. Markov chain modelling of pitting corrosion in underground pipelines. Corros Sci 2009;51:2197–207. https://doi.org/10.1016/j.corsci.2009.06.014.

[29] Ossai CI, Boswell B, Davies IJ. Predictive Modelling of Internal Pitting Corrosion of Aged Non-Piggable Pipelines. J Electrochem Soc 2015;162:C251–9. https://doi.org/10.1149/2.0701506jes.

[30] Hong HP. Application of the Stochastic Process to Pitting Corrosion. Corros Sci 1999:10–6.

[31] Valor A, Caleyo F. Stochastic modeling of pitting corrosion : A new model for initiation and growth of multiple corrosion pits. Corros Sci 2007;49:559–79. https://doi.org/10.1016/j.corsci.2006.05.049.

[32] Valor A, Caleyo F, Alfonso L, Velázquez JC, Hallen JM. Markov Chain Models for the Stochastic Modeling of Pitting Corrosion. Math Probl Eng 2013;2013. https://doi.org/http://dx.doi.org/10.1155/2013/108386.

[33] Ossai CI, Boswell B, Davies I. Markov chain modelling for time evolution of internal pitting corrosion distribution of oil and gas pipelines. Eng Fail Anal 2016;60:209–28. https://doi.org/10.1016/j.engfailanal.2015.11.052.

[34] DNV. Risk based inspection of offshore topsides static mechanical equipment. RP-G101. 2010.

[35] Shabarchin O, Tesfamariam S. Internal corrosion hazard assessment of oil & gas pipelines using Bayesian belief network model. J Loss Prev Process Ind 2016;40:479–95. https://doi.org/10.1016/j.jlp.2016.02.001.

[36] Suarez LM, Polomka A. Microbiologically influenced corrosion in floating production systems. Microbiol Aust under Microsc 2018.

[37] Kaduková J, Škvareková E, Mikloš V, Marcinčáková R. Assessment of microbiologically influenced corrosion risk in slovak pipeline transmission network. J Fail Anal Prev 2014;14:191–6. https://doi.org/10.1007/s11668-014-9782-x.

[38] Bazán FAV, Beck AT. Stochastic process corrosion growth models for pipeline reliability. Corros Sci 2013;74:50–8. https://doi.org/10.1016/j.corsci.2013.04.011.

[39] Hasan S, Khan F, Kenny S. Probability assessment of burst limit state due to internal corrosion. Int J Press Vessel Pip 2012;89:48–58. https://doi.org/10.1016/j.ijpvp.2011.09.005.

[40] Nizamani Z, Mustaffa Z, Wen LL. Determination of extension of life of corroded offshore pipelines using form and monte carlo structural reliability. Int. Conf. Performance-based Life-cycle Struct. Eng., Brisbane, QLD, Australia: 2016, p. 1131–41. https://doi.org/10.14264/uql.2016.553.

[41] Mishra M, Keshavarzzadeh V, Noshadravan A. Reliability-based lifecycle management for corroding pipelines. Struct Saf 2019;76:1–14. https://doi.org/10.1016/j.strusafe.2018.06.007.

[42] Carellan IG De, Moustakidis S, Legg M, Dave R, Selcuk C, Jost P, et al. Characterization of Ultrasonic Wave Propagation in the Application of Prevention of Fouling on a Ship's Hull. Icmt2014 2014.

[43] Ahmed M, Eich M, Bernhard F. Design and Control of MIRA: A Lightweight Climbing Robot for Ship Inspection. Int Lett Chem Phys Astron 2015;55:130–7. https://doi.org/10.18052/www.scipress.com/ilcpa.55.130.

[44] Giurgiutiu V, Roman C, Lin B, Frankforter E. Omnidirectional piezo-optical ring sensor for enhanced guided wave structural health monitoring. Smart Mater Struct 2015;24. https://doi.org/10.1088/0964-1726/24/1/015008.

[45] Abbas M, Shafiee M. An overview of maintenance management strategies for corroded steel structures in extreme marine environments. Mar Struct 2020;71:102718. https://doi.org/10.1016/j.marstruc.2020.102718.

[46] Ghiasi MM, Bahadori A, Zendehboudi S, Chatzis I. Rigorous models to optimise stripping gas rate in natural gas dehydration units. Fuel 2015;140:421–8. https://doi.org/10.1016/j.fuel.2014.09.084.

[47] Kamari A, Bahadori A, Mohammadi AH, Zendehboudi S. New tools predict monoethylene glycol injection rate for natural gas hydrate inhibition. J Loss Prev Process Ind 2015;33:222–31. https://doi.org/10.1016/j.jlp.2014.12.013.

[48] Kamari A, Bahadori A, Mohammadi AH, Zendehboudi S. Evaluating the unloading gradient pressure in continuous gas-lift systems during petroleum production operations. Pet Sci Technol 2014;32:2961–8. https://doi.org/10.1080/10916466.2014.936455.

[49] Zendehboudi S, Rezaei N, Lohi A. Applications of hybrid models in chemical, petroleum, and energy systems: A systematic review. Appl Energy 2018;228:2539–66. https://doi.org/10.1016/j.apenergy.2018.06.051.

[50] Arabloo M, Bahadori A, Ghiasi MM, Lee M, Abbas A, Zendehboudi S. A novel modeling approach to optimize oxygen-steam ratios in coal gasification process. Fuel 2015;153:1–5. https://doi.org/10.1016/j.fuel.2015.02.083.

[51] Kamari A, Mohammadi AH, Bahadori A, Zendehboudi S. Prediction of air specific heat ratios at elevated pressures using a novel modeling approach. Chem Eng Technol 2014;37:2047–55. https://doi.org/10.1002/ceat.201400261.

[52] Adedigba SA, Khan F, Yang M. Process accident model considering dependency among

contributory factors. Process Saf Environ Prot 2016;102:633–47. https://doi.org/10.1016/j.psep.2016.05.004.

[53] Khakzad N, Khan F, Amyotte P. Quantitative risk analysis of offshore drilling operations: A Bayesian approach. Saf Sci 2013;57:108–17. https://doi.org/10.1016/j.ssci.2013.01.022.

[54] Islam R, Khan F, Abbassi R, Garaniya V. Human Error Probability Assessment During Maintenance Activities of Marine Systems. Saf Health Work 2018;9:42–52. https://doi.org/10.1016/j.shaw.2017.06.008.

[55] Chandrasekaran S. Advanced Marine Structures. CRC press Taylor & Francis Group, LLC; 2015. https://doi.org/10.1201/b18792.

[56] Bhandari J, Khan F, Abbassi R, Garaniya V. Pitting Degradation Modeling of Ocean Steel Structures Using Bayesian Network. J Offshore Mech Arct Eng 2017;139:1–11. https://doi.org/10.1115/1.4036832.

[57] Dawuda A-W. A mechanistic and a probabilistic model for prediciting and anlyzing microbiologically influenced corrosion. Master Thesis, Memorial Univeristy of Newfoundland, Canada, 2019.

[58] Adumene S, Khan F, Adedigba S. Operational safety assessment of offshore pipeline with multiple MIC defects. Comput Chem Eng 2020;138. https://doi.org/10.1016/j.compchemeng.2020.106819.

[59] Adedigba SA, Khan F, Yang M. Dynamic safety analysis of process systems using nonlinear and non-sequential accident model. Chem Eng Res Des 2016;111:169–83. https://doi.org/10.1016/j.cherd.2016.04.013.

[60] Jensen F V, Nielsen TD. Bayesian Networks and Decision Graphs. 2nd ed. Springer, New York; 2007.

[61] Palencia OG, Teixeira AP, Soares CG. Safety of Pipelines Subjected to Deterioration Processes Modeled Through Dynamic Bayesian Networks. J Offshore Mech Arct Eng 2019;141:1–11. https://doi.org/10.1115/1.4040573.

[62] Sheskin TJ. Markov Chains and Decision Processes for Engineers and Managers. CRC

press Taylor & Francis Group, LLC; 2011.

[63] Grabski F. Semi-Markov Processes : Applications in System Reliability and Maintenance. Elsevier B.V; 2015.

[64] Lisnianski A, Frenkel I, Ding Y. Multi-state system reliability analysis and optimization for engineers and industrial managers. 2010. https://doi.org/10.1007/978-1-84996-320-6.

[65] Arzaghi E, Mahdi M, Abbassi R, Reilly MO, Garaniya V, Penesis I. A Markovian approach to power generation capacity assessment of floating wave energy converters. Renew Energy 2020;146:2736–43. https://doi.org/10.1016/j.renene.2019.08.099.

[66] Ossai CI, Boswell B, Davies IJ. Application of Markov modelling and Monte Carlo simulation technique in failure probability estimation — A consideration of corrosion defects of internally corroded pipelines. Eng Fail Anal 2016;68:159–71. https://doi.org/10.1016/j.engfailanal.2016.06.004.

[67] Rinn P, Lind PG, Wächter M, Peinke J. The Langevin Approach : An R Package for Modeling Markov Processes. J Open Res Softw 2016:1–11.

[68] Guedes-Soares C, Garbatov Y, Zayed A, Wang G. Non-linear Corrosion Model for Immersed Steel Plates Accounting for Environmental Factors. SNAME Mar. Technol. Conf. Expo, 2005, p. 193–212.

[69] de Waard C, Lotz U, Milliams DE. Predictive Model for CO2 Corrosion Engineering in Wet Natural Gas Pipelines. Corrosion 1991;47:976–85. https://doi.org/10.5006/1.3585212.

[70] DNV. Corroded Pipelines - Dnv-Rp-F101. 2010. https://doi.org/DOI: 10.1016/B978-008044566-3.50040-3.

[71] Mahmoodian M, Li CQ. Failure assessment and safe life prediction of corroded oil and gas pipelines. J Pet Sci Eng 2017;151:434–8. https://doi.org/10.1016/j.petrol.2016.12.029.

[72] Witek M. Gas transmission pipeline failure probability estimation and defect repairs activities based on in-line inspection data. Eng Fail Anal 2018;70:255–72. https://doi.org/10.1016/j.engfailanal.2016.09.001.

[73] Liu X, Zhang H, Li M, Duan Q, Chen Y. Failure analysis of oil tubes containing corrosion

defects based on finite element method. Int J Electrochem Sci 2016;11:5180–96. https://doi.org/10.20964/2016.06.27.

[74] Mohd MH, Kee J. Investigation of the corrosion progress characteristics of offshore subsea oil well tubes. Corros Sci 2013;67:130–41. https://doi.org/10.1016/j.corsci.2012.10.008.

[75] NACE-RP0775. Recommended Practice Preparation, Installation, Analysis, and Interpretation of Corrosion Coupons in Oilfield Operations. NACE Int Houston, TX USA, 2005.

[76] Melchers RE. Effect of temperature on the marine immersion corrosion of carbon steels. Corrosion 2002;58:768–82. https://doi.org/10.5006/1.3277660.

[77] Melchers RE, Jeffrey R. The critical involvement of anaerobic bacterial activity in modelling the corrosion behaviour of mild steel in marine environments. Electrochim Acta 2008;54:80–5. https://doi.org/10.1016/j.electacta.2008.02.107.

[78] Aljaroudi A, Khan F, Akinturk A, Haddara M. Risk assessment of offshore crude oil pipeline failure. J Loss Prev Process Ind 2015;37:101–9. https://doi.org/10.1016/j.jlp.2015.07.004.

Chapter 4

Operational safety assessment of offshore pipeline with multiple MIC defects

Preface

A version of this chapter has been published in the ***Computers and Chemical Engineering 2020; 138: 106819.*** *I am the primary author along with the Co-authors, Faisal Khan, and Sunday Adedigba. I developed the conceptual framework for the model and carried out the literature review. I prepared the first draft of the manuscript and subsequently revised the manuscript based on the co-authors' and peer review feedbacks. Co-author Faisal Khan helped in the concept development, design of methodology, reviewing, and revising the manuscript. Co-author Sunday Adedigba provided support in implementing the concept and testing the model. The co-authors provided fundamental assistance in validating, reviewing, and correcting the model and results of the manuscript.*

Abstract

Microbiologically influenced corrosion (MIC) creates multiple defects. The interaction of MIC defects and their time dependence need to be considered for robust safety assessment of the asset.

This chapter presents a methodology for the dynamic safety assessment of the assets under the influence of MIC. The methodology is built by integrating the Bayesian Network (BN)-Markov Mixture (MM) technique with Monte Carlo simulation. The integration of BN and MM provides an empirical model to probabilistically predict the effective defect growth rate based on the multiple defects' interaction. A rate-dependent stochastic formulation is also developed for the remaining strength and safe operating pressure prediction using the Monte Carlo simulation. The proposed methodology dynamically predicts and captures the evolving effect of corrosion defects'

interaction and effective defect growth rate on the remaining strength and survival likelihood of an in-service corroding asset. The methodology is tested on an offshore pipeline, and the dynamic effects of corrosion influencing parameters and defects' interaction on the pipeline survivability were predicted. Critical safety influencing factors of the pipeline under complex microbial biofilm architecture were identified. The proposed methodology provides a parametric-based condition monitoring tool for effective management of MIC and ensuring safety in offshore systems.

Keywords: Residual strength, Bayesian network; Markov mixture, Pipeline, Dynamic safety, Defects' interaction, Microbiologically influenced corrosion, Monte Carlo Simulation

4.1. Introduction

Critical infrastructures in the marine and offshore industry are faced with high rates of degradation and failure due to corrosion defects, especially in harsh environments. The external factors enhance complex corrosion mechanisms that are unpredictable and often difficult to manage. These external factors include temperature, bacteria, biofouling, pH, nutrients, water velocity, carbonate solubility, salinity, suspended solids, material composition, and surface roughness [1]. Oil and gas production provides a regime that is corrosion stimulating (most commonly to pipelines). This stimulating environmental factor facilitates electrochemical reactions that enhance corrosion [2]. The corrosion defect growth is enhanced by bacteria's metabolic processes and the availability of nutrients. The corrosion defect rate depends on the steel composition and microstructural configuration, as well as the micro-organisms in the area of corrosion. Therefore, bacteria-infected environments promote severe material degradation, especially in the presence of sustainable nutrient sources [3,4]. Most importantly, the microorganism metabolism is enhanced

in crude oil pipelines where the oil and water phases serve as nutrient support sources to produce localized interacting and overlapping defects at the 6 o'clock position of the pipe.

For safety of the offshore systems in bacteria-infested environments, the system failure mechanisms should be properly understood. Failure of offshore systems due to microbiologically influenced defects occurs as a result of a dynamic degradation process accelerated by the metabolic activities of microorganisms [5]. Micro-organisms exist in the formation of biofilms due to fused microbial cells and extracellular polymeric substances (EPS) that provide a favorable mode of survival for microorganisms, even in an aggressive environment. The formation of polymers within the biofilm produces a heterogeneous complex array of dynamic corrosive microenvironments that enhance material deterioration. The colony of different micro-organisms further increases this complexity with various corrosion influencing potentials. There exists a synergistic community among the bacteria types that aggressively alter the electrochemical process of the steel structure, resulting in severe microbiologically influenced corrosion. For details on the complexity of multispecies biofilms architecture and its effects on multiple defects' interaction, readers can refer to [6–8].

The microbiologically influenced localized pit is formed when the structure becomes susceptible due to the breakdown of the thin passive oxide film that resists corrosion, and the defect grows across the length of the offshore system. This results in loss of structural integrity and subsequent collapse of the system. A better understanding of the propagation of these defects as it affects the residual strength and operating pressure is crucial for structural service life analysis and safety management of corroding offshore systems. The multiple interacting defects exist in multiple colonies on the offshore system internal surface and often overlap to produce a scalloped area of MIC damage to the system [9]. As the defects interact, knowledge of their effect on the failure

pressure and the strength characteristic of the offshore system is critical in remaining service life prediction and management. Hence, the interaction dynamics of the microbiologically influenced overlapping and interacting defects need to be investigated for effective time-dependent residual strength prediction and remaining useful life management of the corroding offshore system to prevent total failure.

Different approaches have been proposed to evaluate multiple defects' overlapping and interaction effects on the failure characteristic of corroding offshore systems [10–14]. However, the complexity associated with interaction among multiple defects, especially for microbiologically influenced multiple defects, demands continuous research. For accurate pits' interaction prediction and analysis, a clusterization method is proposed by [13]. The multiple defects are amalgamated into single or group defects' using the clusterization-based criteria. The proposed clusterization methodology is able to capture the randomness in the corrosion defects' parameters.

Chiodo & Ruggieri [15] used a plastic instability-based technique for failure prediction of a corroding offshore system subjected to multiple axial defects' interaction. They concluded that, along with the interaction among defects, defect size, and geometry greatly influenced the failure characteristic of a corroding pipeline. In another development, Cerit et al. [16] identified from a finite element analysis that the pit-depth-width ratio plays a critical role in the stress concentration factor, as well as the failure characteristic of the offshore system with pits' interaction. Undergoing multiple pits' interaction, the develop stress concentration factor at the corrosion defects follows the profile of two overlapped pits [17]. The recent improvement in failure characteristics prediction due to defects' interaction and overlap based on linear and non-linear finite element analysis can be found in [10–12]. However, none of the existing approaches have investigated the dynamics of microbiologically influenced multiple defects' interaction and their effect on predicting the

survival likelihood of corroding offshore systems. In addition, the dynamics of multispecies biofilms' architecture and microbiologically influenced contributory corrosion factors require dynamic-based models to predict the time-dependent defect rate for the merged defect and the strength loss over time.

Recent application of dynamic network-based probabilistic models such as the BN has demonstrated a capacity for MIC rate prediction and susceptibility analysis [18–21]. However, the existing applications have not considered multiple defects' interaction rate prediction for multispecies biofilms. Also, the dynamic effect of various defects' interaction on the structural strength loss over time and the survival likelihood of the microbiologically influenced corroding offshore system have not been investigated.

Moreover, there have been so far few studies on the complex behavior of microbiologically influenced defects' interaction and overlap effects on the defects' growth rate, time-variant structural strength loss, and safe operating pressure predictions for corroding offshore systems. The existing rules that predefined conditions for defects' interaction modeling have not considered the effect of defects' interaction on the microbial influenced defect growth rate in complex multispecies biofilms. Especially in scenarios where the interacting and overlapping defects are growing at different rates. To the best of the authors' knowledge, there exists no dynamic model for multiple defects' interaction rate prediction given a set of inspection data for an offshore system with multispecies biofilms architecture. These knowledge gaps, especially for microbiologically influenced corrosion, make the development of an integrated dynamic methodology for the safety assessment of in-service corroding offshore systems essential.

This chapter presents a methodology that integrates the Bayesian Network (BN)-Markov Mixture technique (MM) with Monte Carlo simulation and demonstrates its application for the dynamic

safety assessment of offshore assets under microbiologically influenced corrosion. The BN is used to dynamically predict the MIC rate, based on the monitored operating parameters, and the bacteria counts using a non-linear and interdependence network-based structure. The multiple interacting defects are clusterized into a single defect, and the history-based effective defect rate is predicted using a Markov Mixture technique (MM). A time-dependent stochastic formulation for structural strength loss and maximum safe operating pressure is developed using Monte Carlo Simulation (MCS). The hybrid methodology captures the complex interaction among the corrosion influencing parameters and the bacteria simultaneously and predicts its effects on the safety of the corroding assets under complex microbial biofilm architecture. This methodology provides a safer remaining life assessment tool for the management of the corroding asset under MIC. The proposed methodology and models are applied to an offshore pipeline.

The remaining part of the chapter is structured as follows: Section 4.2 presents an overview of safety assessment related to MIC defects and their interactions. Section 4.3 presents the proposed methodology. Section 4.4 describes the application of the methodology with a case study. Section 4.5 presents results and discussion, while section 4.6 gives the conclusions.

4.2. Overview of safety assessment related to MIC defects and their interactions

Safety assessment of offshore systems containing microbiologically influenced multiple defects in service is crucial for sustainable operations. Such corroding systems can continue to operate if the strength loss over time and if the maximum safe operating pressure is known to meet the reliability assessment criteria [22]. These criteria provide a better understanding of how to sustain operation based on the defect's characteristics and configuration, remaining strength, maximum safe

operating pressure, and survival likelihood of the offshore system in a corrosive environment. The following subsections briefly examine models' parameters for the safety assessment of in-service corroding offshore systems.

4.2.1 Remaining strength

As microbiologically influenced corrosion depth and density increases, the offshore system becomes more susceptible to total collapse due to strength loss and pressure loading. In a comprehensive research work of [23], the authors identified that changes in pipe design wall thickness due to corrosion and operational pressure dynamics play a critical role in the rate of failure and inspection of process systems. Such a reduction in the design wall thickness affects the structural performance of the system and poses a critical risk to humans, the economy, and the environment if failure occurs. Hence, it becomes imperative to evaluate the strength loss, based on the corrosion growth rate and its interactions, on the remaining service life of the defective system.

The variables that define the strength loss characteristics of a corroding system have associated uncertainties [24]. Hence, the strength loss of the corroding system over time can be stochastically modeled to capture these uncertainties. Several generic strength loss models, in terms of the burst capacity for a single (isolated) defect in corroding systems, such as Modified ASME B31G, RSTRENG, SHELL92, PCORRC, DNV model and CSA model are demonstrated by [14,25–30]. However, for complex-shaped defects and multiple defects' interaction and overlap, the DNV model is used and can be further enhanced mathematically to stochastically integrate the microbiologically influenced multiple defects' interaction effect based on the interaction rules. Further detail is presented in Section 4.3.

4.2.2 Corrosion defects' interaction and maximum operating pressure

The formation of a colony of corrosion defects under multispecies biofilms shows complex failure behavior, compared to isolated defects with the same characteristics. This complexity is most enhanced due to the interactions between adjacent defects, and the rate of defects growth due to multispecies biofilms. As each defect in the colony introduces its disturbances, it creates areas of influence within the pipeline structure that affect the stress and strain fields of the system beyond the border of the individual defects [31]. These interactions influence the stress field of the pipeline under loading by increasing the stress influencing factors at the bottom of the defects as the depth increases. As such, the failure pressure of the pipeline due to the colony of defects may be affected by the increase in the area of defects' influence in overlapping defects [31,32]. Fig. 4.1 is used to illustrate the interaction among pairs of defects generically. The various interaction rules, as shown in Table 4.1, are generically adopted based on the relation: $L_{ij} \leq \left(L_{ij}\right)_{Lim}$ and $W_{ij} \leq \left(W_{ij}\right)_{Lim}$. The offshore system with a colony of interacting and overlapping defects is susceptible to sudden and progressive failure under unstable or increased internal pressure. Therefore, to actually define the critical failure state or safe state of the corroding offshore system, the incorporation of the effects of the microbiologically influenced multiple defects' interactions on the maximum operating pressure is crucial.

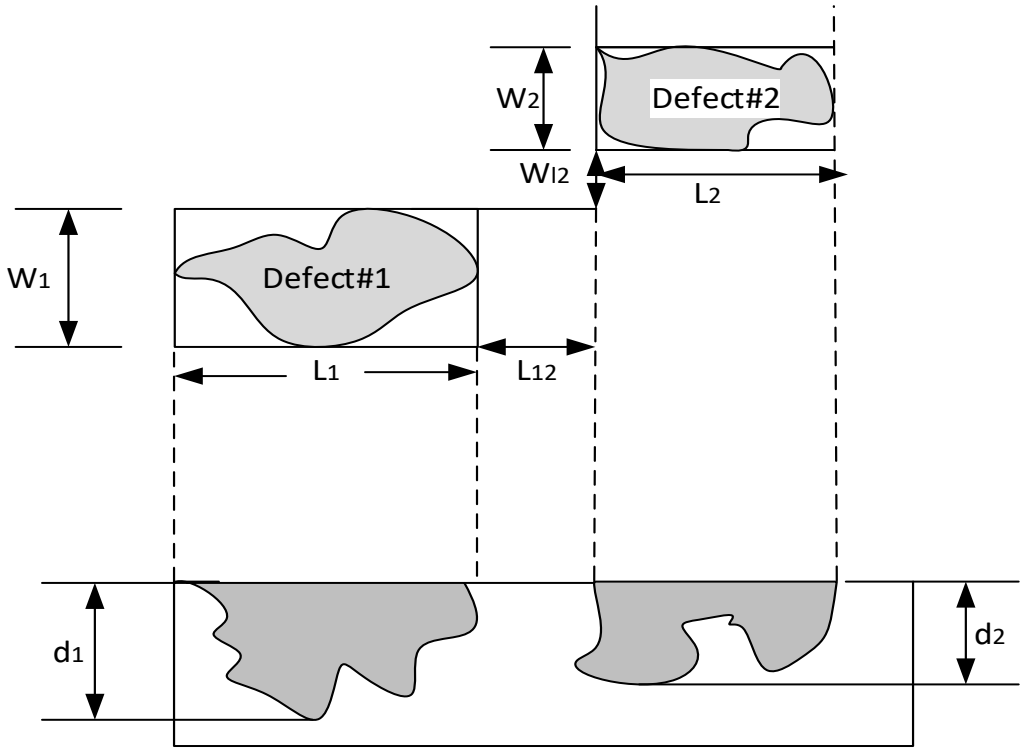

Figure 4.1. Schematic illustration of spacing between interacting defects

Table 4.1. Multiple defects interaction governing rules

Interaction rules	Longitudinal limit$(L_{ij})_{Lim}$	Circumferential limit$(W_{ij})_{Lim}$
DNV-RP-F101 code	$L_{ij} \leq 2.0\sqrt{Dwt}$	$W_{ij} \leq \pi\sqrt{Dwt}$
3WT rule	$L_{ij} \leq 3wt$	$W_{ij} \leq 3wt$
CW rule	$L_{ij} \leq min(L_1, L_2)$	$W_{ij} \leq min(w_1, w_2)$
6WT rule	$L_{ij} \leq 6wt$	$W_{ij} \leq 6wt$

where L_{ij} is the maximum longitudinal spacing, W_{ij} is the maximum circumferential spacing, D is the pipe diameter, wt is the pipe wall thickness,L_1 and L_2 are lengths of corrosion defects, and $w_1$and w_2 are widths of corrosion defects.

4.2.3 Safety assessment due to microbiologically influenced defects' interaction

Several model approaches have been demonstrated for safety and reliability-based remaining service life prediction for corroding systems [14,25–30,33–39]. However, there is little consideration of the effects of time-variant defects' interaction rate and multispecies biofilms' complexity on the strength loss over time. Due to the associated complexity with microbiologically influenced multiple defects' interaction, the integrated BN-Markov mixture model and Monte Carlo Simulation provide a better multivariate dependency modeling capability for MIC rate prediction under multispecies biofilms, defects' interaction rate prediction, time-variant strength loss prediction and survival likelihood prediction for corroding offshore systems.

4.3. The Proposed Methodology

The proposed hybrid BN-Markov Mixture (MM) and Monte Carlo Simulation methodology is shown in Fig. 4.2. It consists of three main steps to capture the dynamic relationship among key parameters for safety assessment. The following subsection gives the details of each of the steps in the methodology:

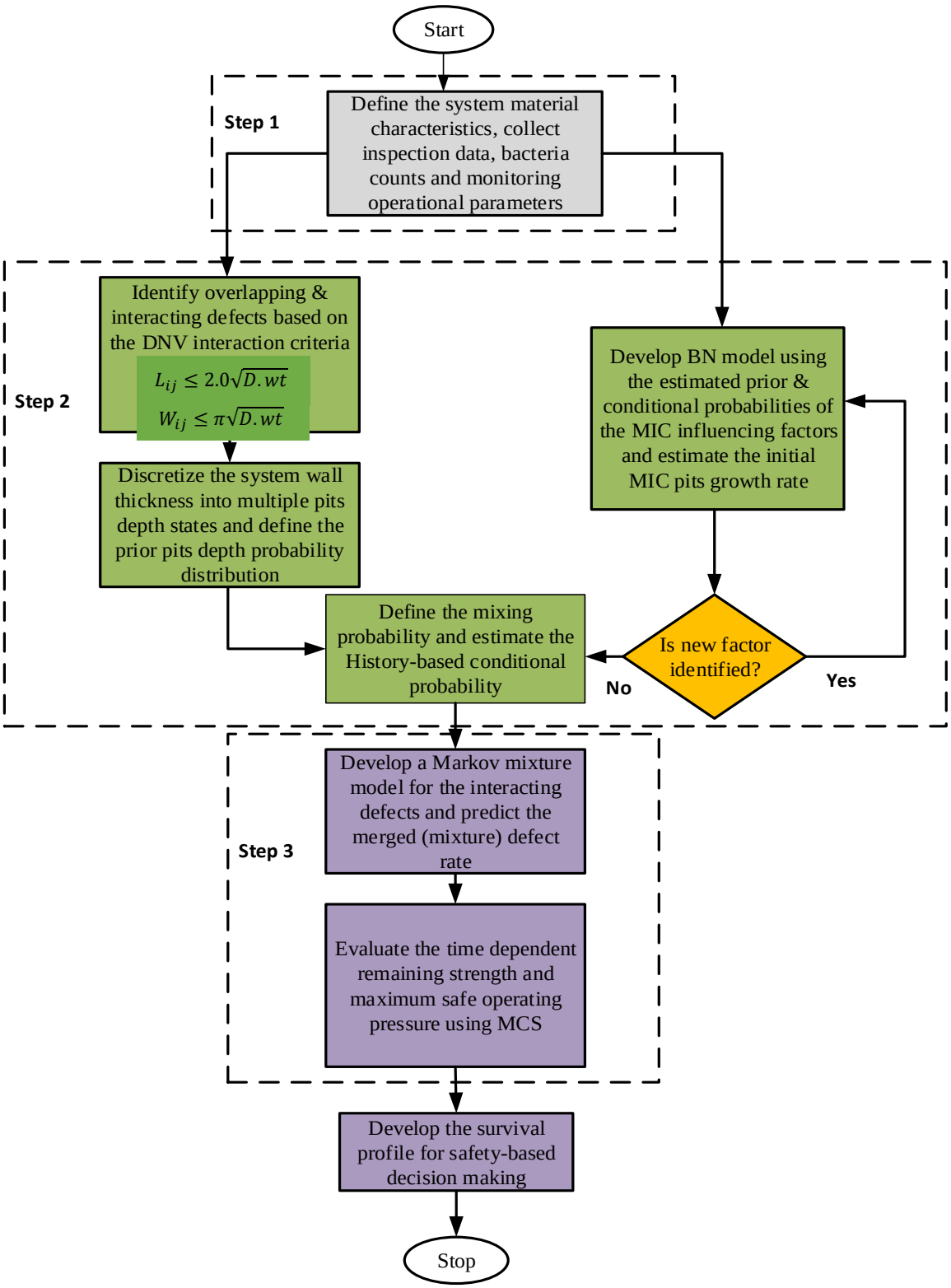

Figure 4.2. Flowchart of the proposed hybrid methodology

4.3.1 Data Collection

The first step of the methodology involves the following:

i). Define the corrosion, chemical, and mechanical characteristics of the offshore system having microbiologically influenced corrosion (MIC). These include but not limited to the corrosion defects length, width, depth, orientation, material type, alloy composition, and strength properties.

ii). Collect historical data/information on the monitoring operating parameters and environmental condition (such as salinity, temperature, velocity, pH, exposure time, alloy composition, sulfate ions, chloride ions, CO_2 partial pressure, water cut), and the bacteria characteristic (bacteria types, counts and the biofilm architecture). The collected operational data are processed into intervals to estimate their probabilities for the defined ranges, and the predicted probabilities are used as input data for the BN analysis.

4.3.2 Defects' interaction examination and corrosion rate prediction

4.3.2.1 Defects' interaction criteria

In this step, the available data on the defects' characteristics are further examined for defect interaction categorization. From Fig. 4.1, subsection 4.2.2, the longitudinal and circumferential characteristics of the multiple defects are assessed using the following criteria [14]:

$$L_{ij} \leq 2.0\sqrt{D.wt} \tag{4.1}$$

$$W_{ij} \leq \pi\sqrt{D.wt} \tag{4.2}$$

where D is the outside diameter of the system, and wt is the system web thickness.

If the longitudinal and transverse distances between the defects meet these criteria, there exists interaction among the defects. The identified defects that meet the interaction criteria are further

clusterized into single or groups of defects based on their depth, length, width, and orientation. The clusterized defect can then be characterized using the effective depth, length, and width D, L, W of the mixture (amalgamated) defect, which consists of interacting defects from number n to m, based on the criteria as shown in Eqs. (4.3) – (4.5) [13,14].

$$l_{nm} = l_m + \sum_{i=n}^{m-1} (l_i + l_{ii+1}), n, m = 1, \ldots\ldots, N \tag{4.3}$$

$$w_{nm} = w_m + \sum_{i=n}^{m-1} (w_i + w_{ii+1}), n, m = 1, \ldots\ldots, N \tag{4.4}$$

$$d_{nm} = \frac{\sum_{i=n}^{i=m} d_i l_i}{l_{nm}} \tag{4.5}$$

Furthermore, the offshore system wall thickness is discretized into defect depth states to represent the various degrees of corrosion penetration through the pipe wall, and a prior probability distribution is defined based on the state of the defects when the offshore system was inspected.

4.3.2.2 Estimation of microbiologically influenced corrosion rate using Bayesian network

The Bayesian network (BN) is a dynamic network-based probabilistic technique for modeling random variables under uncertainty and is able to capture multivariate interactions (dependence) among contributory factors of an underlying phenomenon. The complexity in the interaction within the bacteria colony, operating parameters, and the offshore system material surface as it affects the MIC rate can be represented using BN. For a detailed demonstration of BN and its capability to dynamically and quantitatively model complex system interdependency, readers are referred to [18,20,21,40–42]. Recent applications of the BN in microbiologically influenced corrosion susceptibility prediction have been demonstrated by [19–21]. The BN structure conditional probability table for each state of the nodes (variables) is developed based on the parent

states. This is derived from the study of the parent-child nodes' relationship using field data, theoretical models, and subject matter expert knowledge.

The BN configuration can be represented qualitatively and quantitatively. For a given set of random operating variables, $U = \{X_1, \ldots\ldots, X_n\}$, the chain rule and the joint probability distribution $P(U)$ of the variables based on conditional independence can be mathematically modeled using Eq. (4.6) [43].

$$P(U) = \prod_{i=1}^{n} P(X_i | P_x(X_i)) \tag{4.6}$$

where $P(U)$ is the joint probability distribution of the variables and $P_x(X_i)$ is the parent of variable X_i. Eq. (4.7) is used to estimate the probability X_i.

$$P(X_i) = \sum_{U \setminus X_i} P(U) \tag{4.7}$$

where the summation is taken for all the variables except X_i.

Given a new set of information or availability of data on the offshore system operating conditions (called evidence), the BN structure updates the prior probability of events using Bayes' theorem to produce the consequence probability (i.e., the posterior). This is illustrated mathematically by Eq. (4.8).

$$P(U|E) = \frac{P(U,E)}{P(E)} = \frac{P(U,E)}{\sum_U P(U,E)} \tag{4.8}$$

From the inspection data, bacteria types, their counts, and the operating parameters, a network-based structure is constructed using BN for the estimation of the MIC rate. From the collected monitoring operating parameters, inspection data, bacteria, and their counts, various set bounds

are established to estimate the prior probability for the operating parameters and categorize the MIC rate into low, moderate, high or severe, where applicable, depending on the degree of influence.

Fig. 4.3 shows a schematic representation of the BN structure as applied in this research to predict the individual corrosion defect rate considering the influence of the bacteria colony (sulfur-reducing bacteria (SRB), acid-producing bacteria (APB), and iron-reducing bacteria (IRB)) and the operating parameters. The bacteria influencing factors, such as the operating parameters and nutrients, are represented in a cause-consequence relationship (structural learning), as shown in the BN structure. Given the prior probabilities, which are estimated from the collected sample data, they serve as input probabilities for the MIC influencing factors. These are used for the parametric learning of the BN to predict the MIC rate.

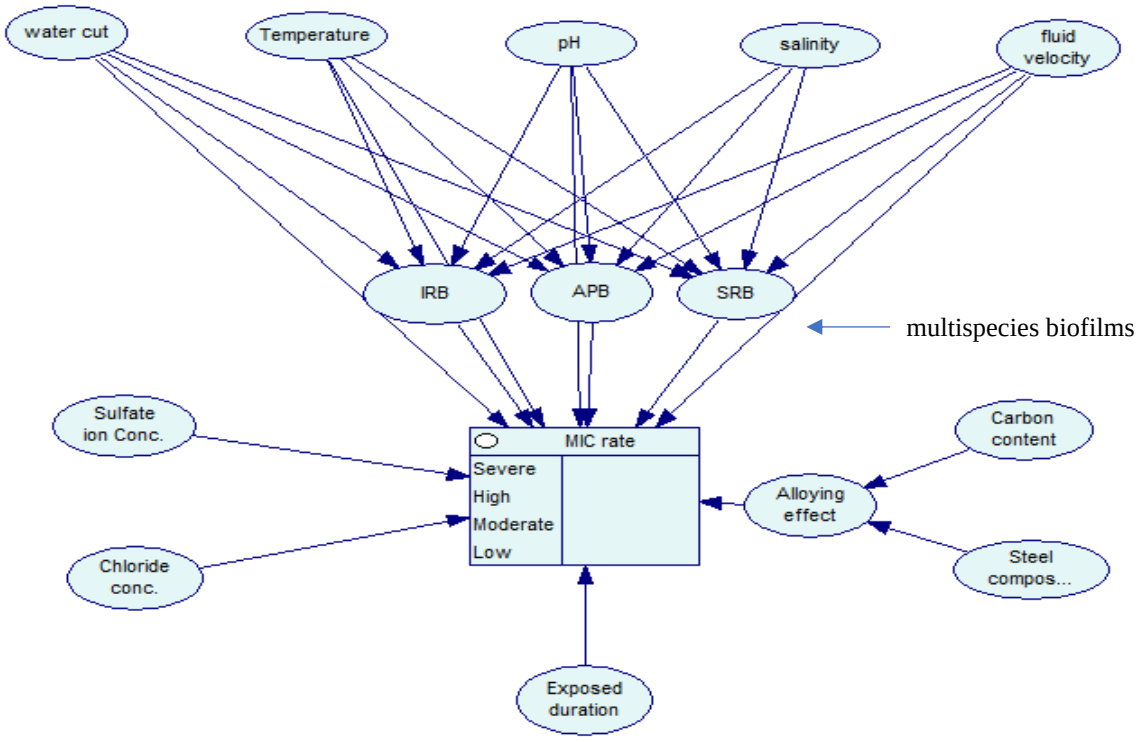

Figure 4.3. Schematic of BN structural learning for MIC rate prediction

Recent research has shown that within the multispecies biofilms, the complex interaction and dynamic behavior of APB and IRB can improve their survival under a wide range of conditions, as well as switching from an aerobic to an anaerobic metabolic process in the absence of oxygen [8,44,45]. As such, these bacteria can contribute to the degradation of the system, together with the SRB, in an anaerobic environment. Their contributory effects are factored into the BN structure for the MIC rate prediction, as shown in Fig. 4.3.

4.3.3 Clusterized defect rate and residual strength prediction

4.3.3.1 Defects' interaction rate prediction using Markov mixture model

The Markov mixture model is a machine learning and probabilistic approach, built from the convolution of different Markov chains, that describes an underlying phenomenon. It is built on the finite-state continuous time homogeneous Markovian principle, which states that for an observed indexed sequence of the given random variables, $\{Y_0, Y_1, Y_2, \cdots\cdots Y_N\}$ at different time steps over the system life cycle, the set of an observed sequence satisfies the Markov property, such that:

$$\mathbb{P}(Y_{t+1} = s|Y_t = s_t,\ Y_{t-1} = s_{t-1}, \cdots\cdots, Y_0 = s_0) = \mathbb{P}(Y_{t+1} = s|Y_t = s_t) \tag{4.9}$$

for all $t\ = 1, 2, 3, \ldots\ldots\ldots$ and for all states $s_0, s_1, \cdots\cdots\ s_t, s$.

For a defined state space of the continuous-time Markov chains that consist of sets of transient states $E = \{1,2, \ldots\ldots, n\}$, the states represent the corrosion wastage or penetration through the wall thickness of the offshore system. The absorbing state describes the unsafe critical state of the system with corrosion, which is characterized based on the safety criteria adopted in the analysis. For example, as shown in Fig. 4.4, μ^{ij} represents the transition intensity from one state to another

within the defined state space. Several demonstrations of the applicability of the Markov process for corrosion defect rate and depth prediction can be found in [35,46,47].

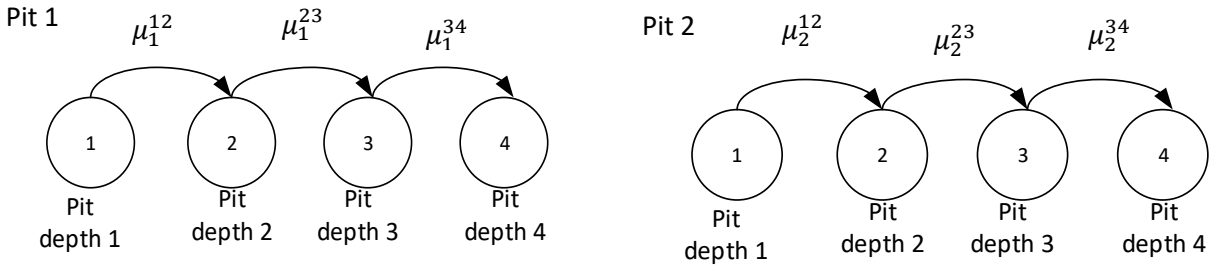

Figure 4.4. Discretize depth states for two interacting corrosion defects

The mixture of the individual Markov chains, as shown in Fig. 4.4 for the interacting defects, forms what is called a Markov mixture model. There are different approaches to the construction of a Markov mixture model [48–51].

A recent demonstration of the application of the Markov mixture model is presented in the work of [51], where a tractable model of heterogeneous behavior was constructed for individual health states. In the three-state Markov mixture process constructed, the transition intensities were conditioned on one's sickness history. The author applied the Markov mixture model and estimated the transition intensities based on the stochastic formulation proposed by [49], as represented by Eqs. (4.10) and (4.11).

$$\lambda^{ij} = \frac{1}{E_Z[P(\mathcal{H}_t|Z)]} E_Z\left[\lim_{h\to 0} \frac{P(X(t+h)=j|X(t)=i,Z)}{h} P(\mathcal{H}_t|Z)\right] \tag{4.10}$$

$$\lambda^{ij} = \frac{E_Z\left[\mu^{ij} Z^{ij} P(\mathcal{H}_t|Z)\right]}{E_Z[P(\mathcal{H}_t|Z)]} \tag{4.11}$$

where vector $Z = \{Z^{ij}, i, j \in \{1, 2, \ldots\ldots\ldots, q\}, i \neq j\}$ contains the mixing variables for the corresponding transition possibilities and $P(\mathcal{H}_t|Z)$ is the history-based conditional probability density up to time t, given the mixing variable. However, in the current research, a four-state Markovian mixture process is adopted to reduce the mathematical complexity associated with the complex multi-state configuration.

From the inspection data, the multiple defects that meet the interaction criteria are discretized into multi-state corrosion depths based on the pipe wall thickness. These defects form individual multi-state systems, and their growth process is modeled using the Markov Chain. The multi-state process is a stochastic process that is time and space-dependent based on a finite set of random variables. The process is characterized by the transition intensity (MIC rate), which describes the instantaneous rate of transition from one state to another within the space. The transition intensity is a time function and history-based process based on the Markovian assumptions.

To predict the merged defect rate, a simple discrete mixture of Markov chains with the same state space, $\mathcal{S}$, but distinct transition intensities (MIC rate) is constructed for the interacting defects. This is assumed for a scenario where the defects under complex multispecies biofilms have multiple growth rates.

Given a random variable M that represents the Markov chain, then for $m = 1,2, \ldots\ldots n,\ P(M = m)$ is a mixing probability associated with the Markov chains with predicted transition intensities (MIC rates) of $\{\mu_m^{ij}(t); i, j \in \mathcal{S}, i \neq j\}$ from the BN. Therefore, for three interacting defects with a four-state Markov process, the transition intensities (MIC rates) yield $\{\mu_1^{ij}(t); i, j \in \{1,2,3,4\}, i \neq j\}$, $\{\mu_2^{ij}(t); i, j \in \{1,2,3,4\}, i \neq j\}$ and $\{\mu_3^{ij}(t); i, j \in \{1,2,3,4\}, i \neq j\}$ respectively.

Using Aalen's [48] notation for the Markov mixture model transition intensity from the observable defect state, i, to the future observable defect state, j, the prediction for the clusterized defect growth rate is denoted by $\lambda^{ij}(t|\mathcal{H}_t)\ where\ i,j \in \{1,2,3,4\}\ and\ i \neq j$. This yields:

$$\lambda^{ij}(t|\mathcal{H}_t) = \mu_1^{ij} P(m=1|\mathcal{H}_t) + \mu_2^{ij} P(m=2|\mathcal{H}_t) + \mu_3^{ij} P(m=3|\mathcal{H}_t) \tag{4.12}$$

Eq. (4.12) shows that the transition intensity of the mixture model is dependent on the history of the corrosion process, which is based on the contributory factors (operating parameters) and the defects' depth states at the year of inspection through the conditional probabilities on the right-hand side.

Generically, for a mixture of n 4-state Markov chains, we have

$$\lambda^{ij}\left(t\middle|\mathcal{H}_t^k\right) = \frac{\sum_{m=1}^{n} \mu_m^{ij} P\left(\mathcal{H}_t^k\middle|M=m\right)P(M=m)}{\sum_{m=1}^{n} P\left(\mathcal{H}_t^k\middle|M=m\right)P(M=m)} \tag{4.13}$$

$$= \frac{1}{P(\mathcal{H}_t)} \sum_{m}^{n} \mu_t^{ij}\, P\left(\mathcal{H}_t^k\middle|M=m\right)P(M=m) \tag{4.14}$$

$$= \sum_{m=1}^{n} \mu_m^{ij}\, P\left(M=m\middle|\mathcal{H}_t^k\right) \tag{4.15}$$

where $P(M=m)$ is the mixing probabilities and $P\left(\mathcal{H}_t^k\middle|M=m\right)$ denotes the transition probabilities for the defects' states and is estimated by sets of Kolmogorov stochastic differential equations that are solved by Laplace Stieltjes transformation, while $P\left(M=m\middle|\mathcal{H}_t^k\right)$ is a history-based conditional probability and is estimated using Bayes' Rule:

$$P\left(M=m\middle|\mathcal{H}_t^k\right) = \frac{P\left(\mathcal{H}_t^k\middle|M=m\right)P(M=m)}{\sum_{m=1}^{n} P\left(\mathcal{H}_t^k\middle|M=m\right)P(M=m)} \tag{4.16}$$

Therefore, the resulting mixture model intensity function $\lambda^{ij}\left(t\middle|\mathcal{H}_t^k\right)$, which serves as the merged (mixture) defect rate, gives a phase-type distribution with a convolution of an exponential distribution. The results from the BN in subsection 4.3.2.2 are used as input parameters for the mixture model to predict the microbiologically influenced merged defect rate over the life cycle of the offshore system.

4.3.3.2 Remaining strength and operating pressure prediction using Monte Carlo Simulation

The Monte Carlo Simulation (MCS) is of diverse application for failure and safety analysis of engineering systems considering randomness. It is a probabilistic numerical method that relies on sampling the inherently random variables for engineering application [22,46,52]. Its usefulness in safety and reliability predictions is built on its simplicity and accuracy. Several applicable details for both stand-alone and hybrid methodologies that showcase the potency of MCS in safety and reliability analysis can be found in [53–56].

In this step, the output of the mixture model intensity (merged defects' rate) function serves as an input parameter to a time-dependent strength loss formulation. This is simulated using Monte Carlo Simulation. In this research, the independent variables that define the strength loss of the corroding offshore system are treated as random variables and are assumed to be normally uncorrelated.

To model the remaining strength of the microbiologically influenced corroding offshore system with multiple defects' interaction and overlap in terms of burst capacity, the following mathematical formulation based on the work of [14] is adopted.

$$P_{nm} = \frac{2\sigma_u wt}{(D - wt)}\left[\frac{1 - (d_{nm}/wt)}{1 - (d_{nm}/(Q_{nm}wt))}\right] \tag{4.17}$$

where d_{nm} denotes the effective depth of the combined defect from the interacting defects; σ_u is the tensile strength; wt is the system wall thickness; D is the outer diameter. For the time-variant prediction of P_{nm}, that is $P_{nm}(t)$, the integration of the mixture defect growth rate based on the pits' interaction criteria into the linear corrosion growth model by [57], yields:

$$d_{max}(T) = d_{nm}(0) + \lambda^{ij}\left(t\middle|\mathcal{H}_t^k\right) \cdot t \tag{4.18}$$

$$L_{eff}(T) = l_{nm}(0) + \lambda^{ij}\left(t\middle|\mathcal{H}_t^k\right) \cdot t \tag{4.19}$$

where $\lambda^{ij}\left(t\middle|\mathcal{H}_t^k\right)$ is the time-dependent transition intensity (Mixture defect growth rate) and l_{nm} is the combined length of all adjacent interacting defects. It is assumed that both the axial and radial corrosion growth rate, which is substituted for by the merged defect rate, is the same for the system's life period. It is important to note that the corrosion defects' depth and length changes over time, based on the associated randomness, which defines the degree of variability (dynamics) in the corrosion influencing parameters and the operating condition of the offshore system.

hence;

$$P_{nm}(t) = \frac{2\sigma_u wt}{(D - wt)}\left[\frac{1 - \left(\frac{d_{max}(T)}{wt}\right)}{1 - \left(\frac{d_{max}(T)}{Q_{nm}wt}\right)}\right] \tag{4.20}$$

$$P_{nm}(t) = \frac{2\sigma_u wt}{(D - wt)}\left[\frac{1 - \left(\frac{d_{nm}(0) + \lambda^{ij}(t|\mathcal{H}_t^k \cdot t)}{wt}\right)}{1 - \left(\frac{d_{nm}(0) + \lambda^{ij}(t|\mathcal{H}_t^k) \cdot t}{Q_{nm}wt}\right)}\right] \tag{4.21}$$

Thus, the remaining strength can be stochastically modeled in terms of the basic random variables as the primary contributing factors if their distribution is known. That is $P_{nm}(t) = f\left(l_{nm}(0), \sigma_y, d_{nm}(0), D, wt, \lambda^{ij}\left(t\middle|\mathcal{H}_t^k\right), t\right)$. With a predefined probability distribution for the

independent variables, the strength loss with its randomness over time is modeled using the Monte Carlo Simulation in the MATLAB environment.

The maximum safe operating pressure for the corroding offshore system is influenced by the acceptable defect depth and the corroded length. For the amalgamated defect (mixture), the maximum allowable operating pressure is predicted by the modified expression [14]:

$$P_{MSOP}(t) = \frac{2wt\sigma_u F}{(D - wt)}\left(\frac{1 - \frac{d_{max}(T)}{wt}}{1 - \frac{d_{max}(T)}{wtQ_{nm}}}\right) \tag{4.22}$$

where $Q_{nm} = \text{length correction factor} = \sqrt{1 + 0.31\left(\frac{l_{eff(T)}}{\sqrt{Dwt}}\right)^2}$ and F is the design factor, which is normally 0.72. This gives the time-variant maximum safe operating pressures, considering the time-dependent strength loss for the remaining useful life of the system.

The survival likelihood for the system is then estimated from the combination of the continuous-time phase-type distribution series model (acyclic Markov) and the strength loss profile over the remaining life of the offshore system. The result from the application of the methodology would provide safety criteria for determining the remaining useful life, the least critical operating pressure, the likely failure year, and the point of safety critical decision making for the in-service corroding offshore system.

The proposed methodology is demonstrated with a simplified example in the supplementary material (see page 261).

4.4. Application of the proposed methodology

The proposed methodology is applied to an API 5L Grade X42 offshore hydrocarbon transmission pipeline with microbiologically influenced corrosion [58]. The pipeline carried co-mingled fluids from a large number of offshore sources. Upon inspection, the pipeline contains localized internal pits and pits clustered at a different position along the internal surface of the pipeline. The pipeline operating data/information based on the inspection and investigation of the operating environment is shown in Tables 4.2, 4.3 and 4.4. The offshore pipeline contains multiple defects within the multispecies biofilm architecture that are longitudinally and circumferentially oriented and meet the defects' interaction criteria. The interactions between the multispecies biofilms and the material composition cause higher levels of variation and thus create a high degree of replication, which complicates the defects' interaction process [8,59].

Table 4.2 shows the data ranges for the monitoring operating parameters and the bacteria count used in the analysis. These parameters describe the prevailing operating condition of the pipeline for the period under consideration. Table 4.3 shows the probabilistic characteristics of the pipeline parameters and mechanical properties, while Table 4 shows the characteristic and composition of the multispecies biofilm architecture considered in the research analysis. Also, some of the missing data/additional parameters used in the analysis were adopted from these referenced works [18,60–63]. Assume at the time of inspection (i.e., 4.5years) during operation, and among the colony of defects, three defects at different pit depth states ($\text{defect 1 depth} = 5.4\text{mm};\ \text{defect 2 depth} = 2.8\text{mm};\ \text{defect 3 depth} = 1.9\text{mm}$) that meet the interaction criteria are used for the application. The proposed methodology is applied to the case study, while the computational procedure of the proposed methodology has been demonstrated in the supplementary material (see page 261).

Table 4.2. Monitoring operating parameters' data range and bacteria counts

Variables (Node)	Range	Variables (Node)	Range
pH	3.2 ~ 7.86	Water cut	1~ 10%
Temp(degree C)	0 ~ 50	Iron (ppm)	0.01 ~ 120
Flow rate(m/s)	0.01 ~ 1.116	Sulfate ion (ppm)	0.01 ~ 32000
Chlorine (ppm)	0.01~40000	Exposure period	Max. > 3.5yrs Mean 2.5-3.5yrs Min < 2.5yrs
APB	Low < 1000cfu/ml 1000 < Moderate <10000 High> 10000 cfu/ml	Organic liquid	90~95%
		Salinity	Present/Absent
SRB	Low < 10000cfu/ml 10000 < Moderate <100000 High> 100000 cfu/ml	IRB	Low < 1000cfu/ml 1000 < Moderate <10000 High> 10000 cfu/ml

Table 4.3. API 5L Grade X42 pipe defects and mechanical properties

Symbol	Variable	Unit	Distribution	Mean	Std. Dev
D_o	Internal diameter	mm	Normal	311.15	0
wt	Pipe wall thickness	mm	Normal	12.7	0.097
σ_y	Yield strength	MPa	Normal	290	10.23
l_{nm}	Mixture pit length	mm	Normal	98	26
w_{nm}	Mixture pit width	mm	Normal	103.4	27.5
d_{nm}	Mixture pit depth	mm	Normal	5.4	0.37
σ_u	Tensile strength	MPa	Normal	415	19.23

Table 4.4. Characteristics of the multispecies microbial biofilm architecture

Group	Survival mode	End Product	State
SRB	Anaerobic	H_2S, HS^-, FeS	Active
APB	Aerobic/Anaerobic (Facultative)	Organic acids	Active
IRB	Aerobic/Anaerobic (Facultative)	Soluble ferrous ion	Active

4.5. Results and discussion

The main objective of this research chapter is to develop a hybrid dynamic methodology that captures and predicts the dependencies' effect among corrosion influencing parameters on the MIC rate, multiple defects' interaction rate, and the safety of the corroding offshore pipeline. The hybrid

model provides a robust tool for the safety assessment of the offshore system under complex multispecies microbial biofilm architecture.

4.5.1 Modeling the MIC rate under complex biofilm architecture

The collected data/information on the case study, as shown in section 4.4, is used in the analysis. First, the impact of the corrosion influencing parameters, bacteria, and their interaction on the MIC rate is investigated. For this purpose, the BN structure is used to build the cause-effect relationship among the corrosion influencing parameter based on the available data to predict the MIC rate. The prior probabilities for the corrosion influencing parameters, as estimated, serve as the input probabilities for the parametric learning of the BN structure. The result of the parametric learning of the structure, as shown in Fig. 4.5, gives the MIC rate for the individual defects. The result shows the degree of influence of various microbiologically corrosion contributory factors based on their structural relationship built from the available data. Under the prevailing operating conditions of the pipeline, the predicted MIC rate gives 0.1604mm/year, 0.1936mm/year, 0.3123mm/year, 0.3337mm/year, for the low, moderate, high, and severe corrosion rate category, respectively.

Furthermore, the effect of the multispecies biofilm is investigated through a sensitivity analysis of the BN structure, as shown in Fig. 4.6. To do this, evidence is placed on the bacteria nodes, and their degrees of influence are predicted. The result indicates a 22.4% and 35.8% increase in the high and severe MIC rate, respectively. The result agreed with the findings of [5,7,8], which show that for multispecies biofilms, the high rate of survival of the SRB in their intertidal zones increase. As such, the SRB interaction with the facultative nature of the APB and IRB, promote their degradation ability and cause an increase in the rate of degradation of the offshore systems.

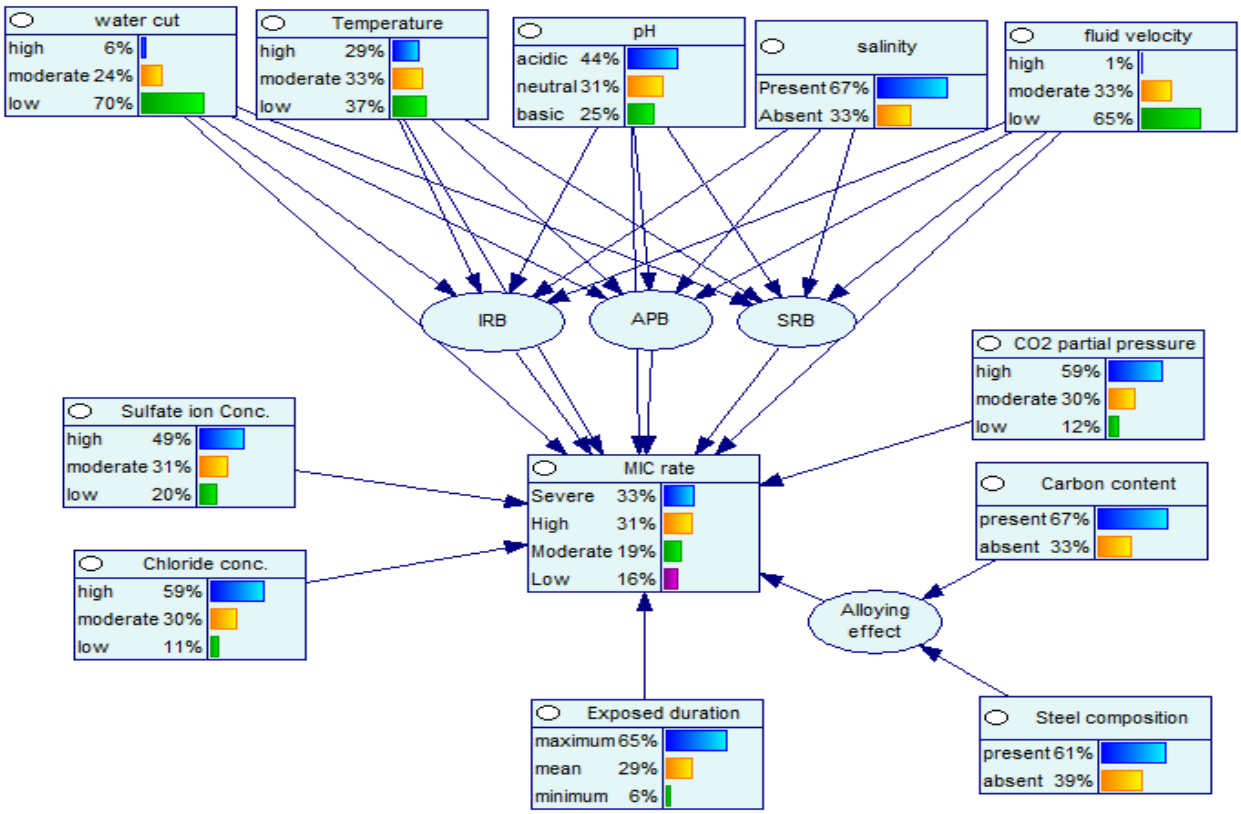

Figure 4.5. Predicted MIC rate based on the BN parametric learning using prior probabilities

These bacteria build a complex structure that protects them from temporary stress or harsh environments, therefore sustaining their degradation effect on the offshore system. Also, the mixed microbial communities under this multispecies biofilm are unstable with time, which causes a decrease in their diversity as the MIC depth increases, and the pH decreases. The decrease in pH is a result of the acidic state, which is a by-product of the APB metabolic activities. The produced acids' interaction with the SRB increases the corrosiveness under the biofilm. This also increases the corrosion rate under the predefined favorable conditions, as shown.

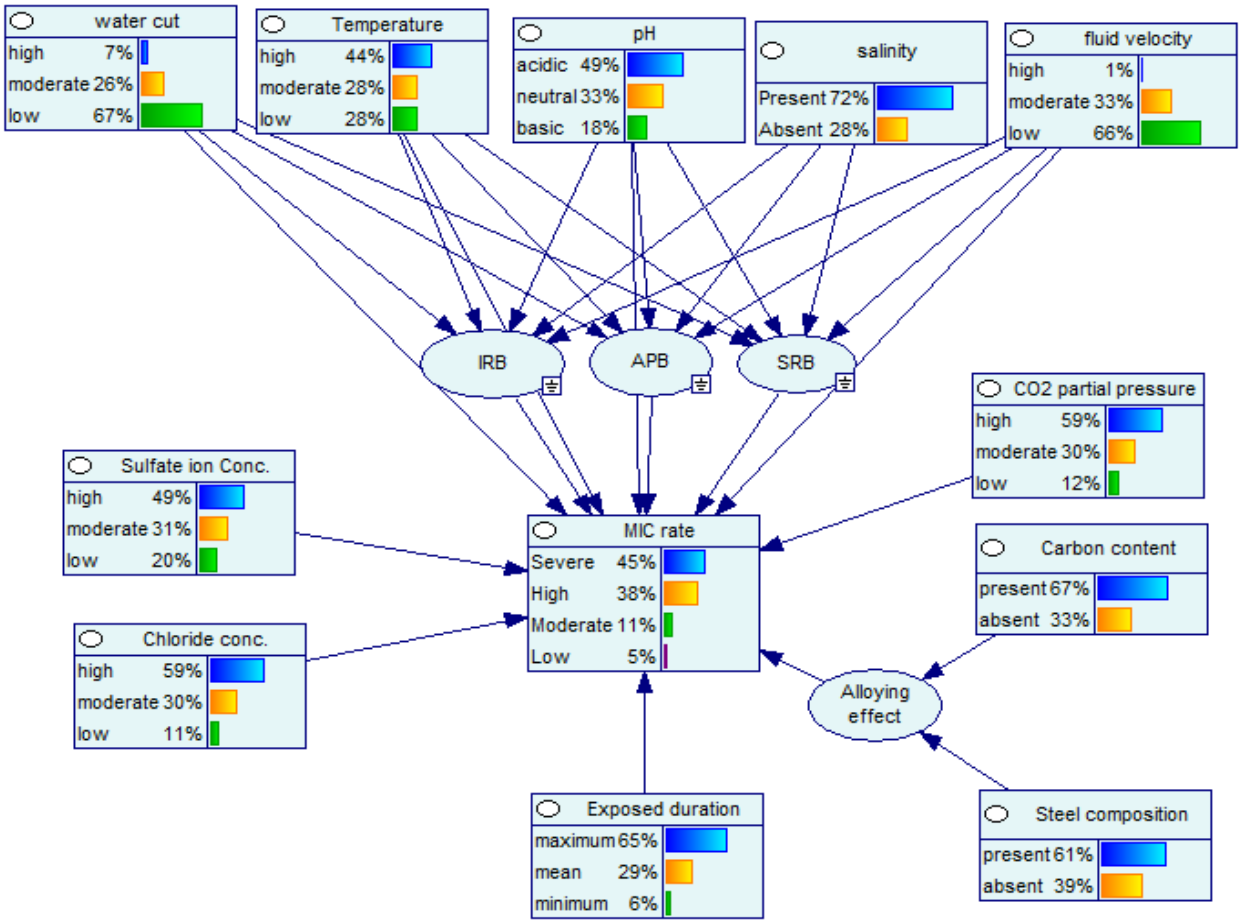

Figure 4.6. BN model for MIC rate with evidence on the bacteria nodes

Further analysis of the effect of the dynamic interactions among the operating parameters, the multispecies biofilm, heterogeneous material surfaces, and other nutrients on the MIC rate is shown in Fig. 4.7. In this case, the evidence is placed on all the nodes of the BN structure to learn their effects on the MIC rate under predefined conditions. The result shows that with favorable conditions or with hard evidence, the optimum contributory effects from the influencing parameters increase the severe corrosion rate over a hundred percent. This supports the findings that under the most favorable operating conditions which promote multispecies biofilms'

formation, the offshore system suffers severe degradation that results in sudden and catastrophic failures [64–66].

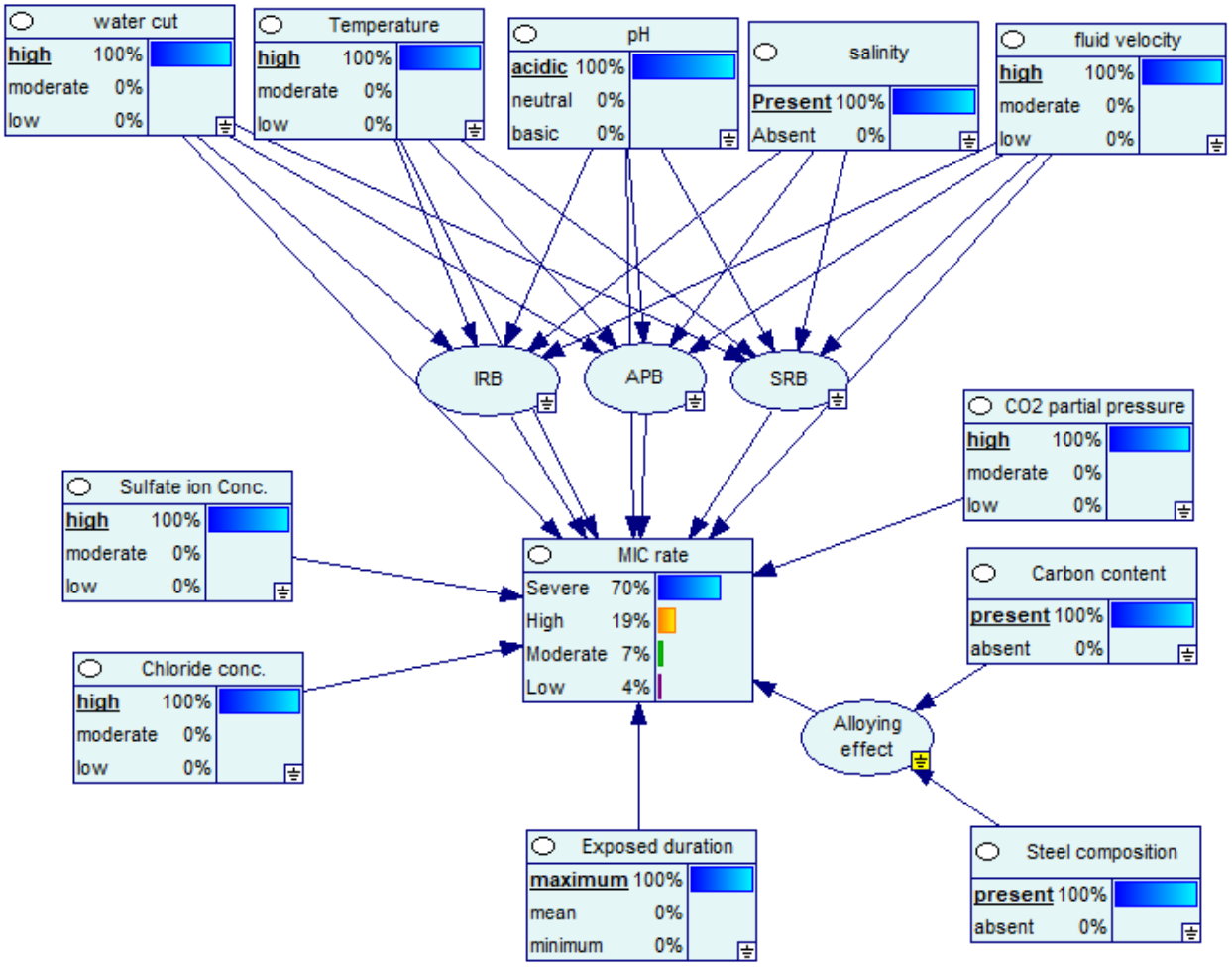

Figure 4.7. BN model for MIC rate with evidence on all contributory parameters' nodes

4.5.2 Modeling the effective defect rate due to multiple defects' interaction

The defects' characteristics from the inspection data are assessed based on the interaction criteria. Three defects that meet the criteria, as indicated in section 4, are discretized into pit depth states and clusterized into a single pit. The three defects are assumed to be growing at different rates, and the result from the BN is used based on the [67] corrosion rate categorization. The empirical

mixture model is built based on a 4-states Markovian mixture process, using the defects' historical data and the initial predicted MIC rate to predict the rate of the merged defect probabilistically. The Markov mixture technique is applied to the three interacting defects to predict their effective interaction rate, and the results are shown in Fig. 4.8. Fig. 4.8 shows the increasing trend of the time-variant effective defect rate under a sustainable microbial infested offshore environment.

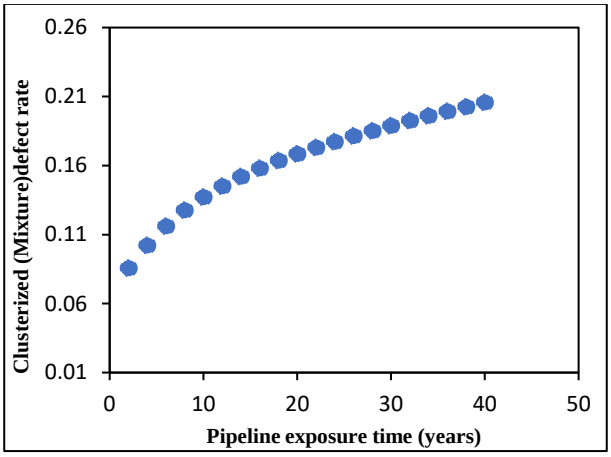

$(a)\ \lambda^{12}(t|\mathcal{H}_t^1)$

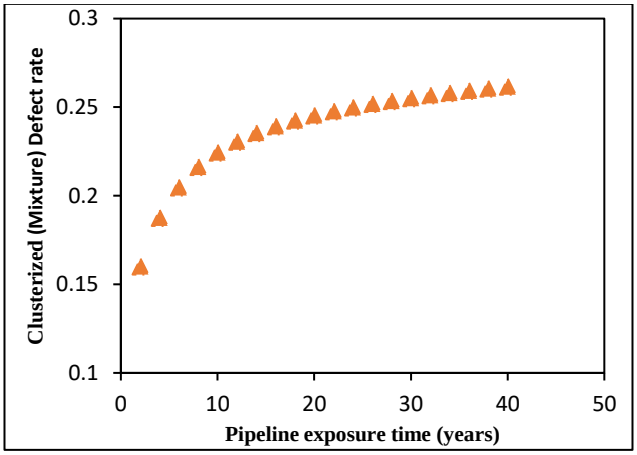

(b) $\lambda^{23}(t|\mathcal{H}_t^2)$

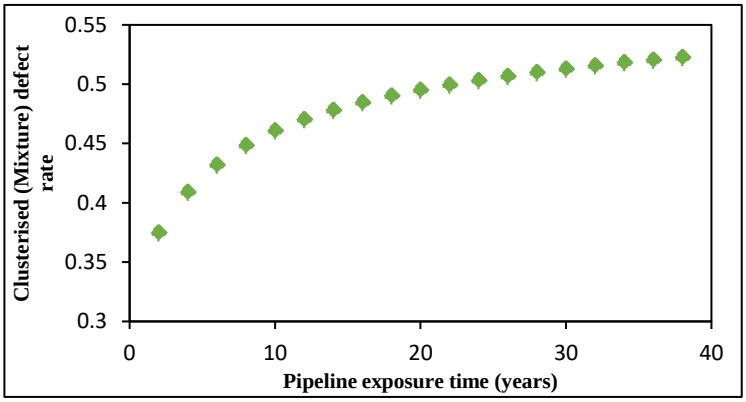

(c) $\lambda^{34}(t|\mathcal{H}_t^3)$

Figure 4.8. Time-evolution merged defect rate due to interaction at low, high and severe MIC rates

As shown in Fig. 4.8, $\lambda^{12}(t|\mathcal{H}_t^1)$; $\lambda^{23}(t|\mathcal{H}_t^2)$ and $\lambda^{34}(t|\mathcal{H}_t^3)$ provide the time-evolution profiles for the history-based merged defect rate for the low, high, and severe corrosion rates, and this is used for the defect depth and strength loss prediction over the exposure period. The profile reveals that under the favorable condition for multispecies biofilms' formation without intervention, the interaction effects among defects increase the merged defect growth rate sharply until a saturation point is reached. At the saturation point, a steady-state defect growth rate is observed, which follows an asymptotic limiting function as the exposure time increases. As such, the increase in the defects interaction rates causes a corresponding percentage effect in the pipe wall wastage and the remaining strength of the pipeline. The predicted result of the defect interacting rate as shown follows a similar trend of corrosion loss as a function of long time exposure to microbial corrosion, proposed by [60,68]. The resulting profile also agrees with the numerical findings of [69] based on the defect depth profiling, which describes the corrosion defect depth as a function of the defect growth rate with complex biofilms. This provides validation for the empirical defects' mixture model.

4.5.3 Modeling the strength loss (remaining strength) and safe operating pressure

With the purpose of demonstrating the robustness of the proposed hybrid methodology, the effects of the MIC rate, effective defect interaction rate, and the corrosion parameters on the time-variant strength loss and safe operating pressure of the pipeline are predicted. The MIC rate, effective defect rate, and corrosion parameters serve as input data to the time-dependent remaining strength formulation. The remaining strength was stochastically modeled by the Monte Carlo numerical simulation in the MATLAB environment using Eq. (4.21). The simulation captures the inherent randomness and statistical distribution associated with the structural strength influencing variables, and the results are shown in Fig. 4.9. The results reveal that as the defects grow in depth

and volume, the structure under the complex corrosion attack continues to experience structural strength loss. This is as a result of the corrosion damages cumulative effect as the time of exposure increases. It further causes a decrease in the burst capacity of the corroding pipeline, thereby limiting the resistance of the pipeline to total failure under unstable internal pressure loads. The structural degradation, in terms of strength loss under the combined effect of complex multispecies biofilm and multiple defects interaction, creates critical safety challenges for in-service corroding offshore pipeline management. It is important to note that the results in Fig. 4.9 is the time-variant strength loss prediction based on burst capacity formulation for multiple defects' interaction.

Considering the basic independent variables, it is noticed that the longitudinally oriented defects' interaction depth plays a critical role in the strength loss as the exposure time increases. This is as a result of the high-stress concentration that increases its distributive effect at the bottom of the deepest and overlapping pits. As the stress concentration builds up around the bottom of the deepest defect, the material strength may be exceeded as a result of the combined effect of the complex interactions among bacteria in the multispecies biofilms and the defects' interactions. This may result in sudden system failure.

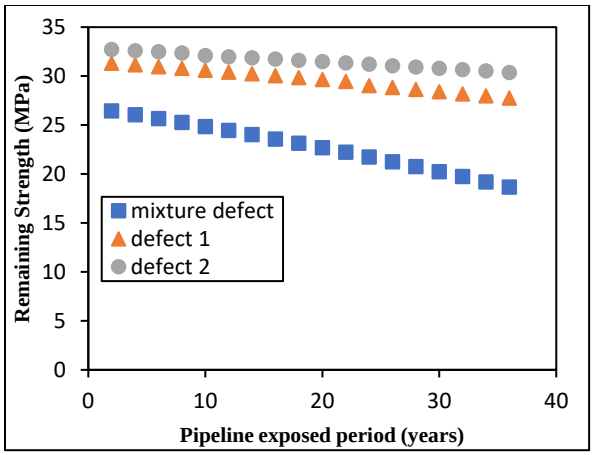

(a) low MIC rate

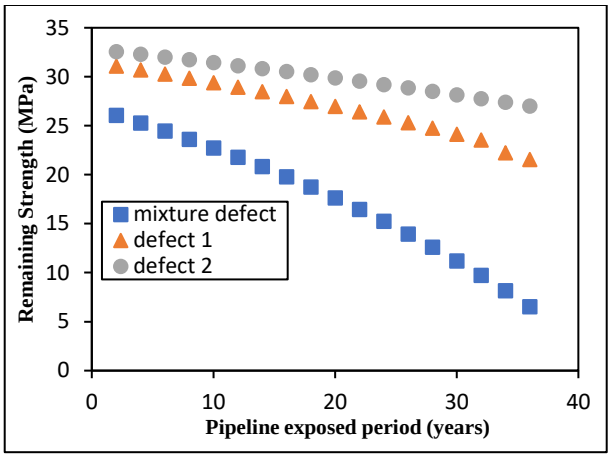

(b) high MIC rate

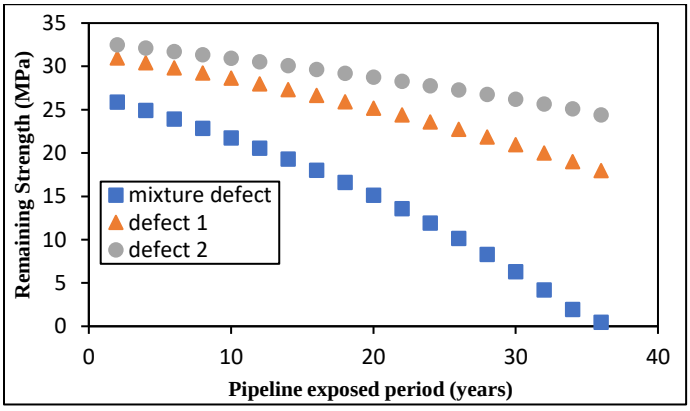

(c) Severe MIC rate

Figure 4.9. Time-evolution strength loss under microbiologically influenced corrosion

Further analysis of the degree of complex defects' interaction effect on the remaining strength for the exposed period at different rate is investigated. With the merged defect rate of $0.085mm/yr$, isolated defect 1 rate of 0.0541mm/yr and isolated defect 2 rate of 0.0407mm/yr, the remaining strengths decreased by 16.4% and 20.1% respectively for the low defects' interaction rate in comparison with that of the isolated (single) defects. Moreover, as the defect depth progressively increases with an increase in rate, the rate of strength loss increases by 21.8% and 22.4% for the high and severe MIC rates, respectively, as shown in Fig. 4.9(b & c). Consequently, the burst

capacity (failure pressure) of the corroding pipeline continues to decrease as the time-variant corrosion rate and the exposed period increases due to the complex multispecies biofilms. The result of the time-variant strength loss analysis is consistent with the findings of [10,11,70] in which they conclude, based on a non-linear finite element analysis of three mid-strength pipe grade failure pressure ratios $\left(P_{overlapped\ defects}/P_{isolated\ defect}\right)$, that the burst capacity of corroding pipeline decreases significantly with longitudinally oriented defects interactions. Moreover, the interaction of the bacteria within the multispecies biofilms as presented in this work further promotes a complex defects' interaction rate with deteriorating effects on the structural stability of the corroding offshore pipeline. This provides further validation for the proposed model.

From the strength loss results, the most critical safety-based decision may be inferred, which is primarily based on the time-variant MIC rate, defects' interaction rate, material characterization, and the dynamics of the operating environments. This provides a dynamic predictive methodology that could inform the operator of the safe operating conditions for the corroding offshore pipeline based on the estimated remaining strength over time and the safe operating pressure. Eq. (4.22) is used to stochastically predict the safe operating pressure, based on the merged defect rate profile. At each time-variant defect growth rate, the maximum safe operating pressure can be predicted. From the predicted time-evolution safe operating pressure over the remaining useful life of the corroding pipeline, its mean values, as shown in Fig. 4.10, provide key operational information to estimate the likely failure time if the pipeline is assumed to be operated at steady-state pressure from the year of inspection. Also, the result provides a time-evolution pressure-based operational envelope for safe life operation of the corroding offshore pipeline with defects interaction.

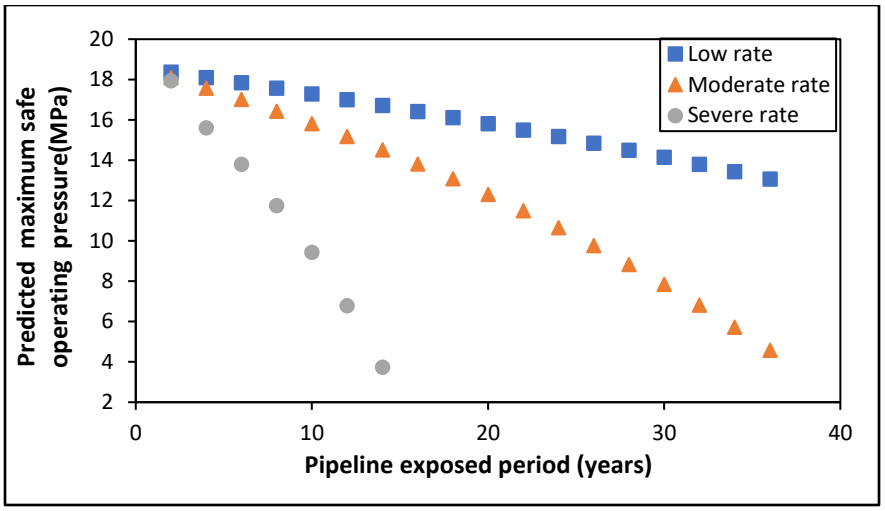

Figure 4.10. Time variant safe operating pressure profile for corroding pipeline with multiple defects' interaction

4.5.4 Develop the survivability profile for safety-based decision making

The predicted results from subsections 4.5.1, 4.5.2, and 4.5.3 are integrated to develop a survival curve for a robust safety-based decision making. Fig. 4.11 shows the developed survival curve for the offshore pipeline with a proposed minimum survivability likelihood of 0.4, which represents over 60% corrosion penetration of the system wall thickness. The survivability likelihood is proposed based on the dynamic and unstable mechanism of multispecies microbial biofilms, which in most cases result in multiple system failure mechanisms.

Further analysis shows that if there is no intervention during the exposure period, any slight increase in the defect growth rate and interaction rate decreases the remaining life (survival life) of the offshore pipeline as well as its safe operation, as shown in Fig. 4.11 (b & c). Assuming T_s is the likely maximum survival time based on the proposed survivability criteria, it can be predicted that the surviving time $T_s = 18\,\text{years}, 12\,\text{years}, \text{and } 9\,\text{years}$ respectively, for the offshore

pipeline, based on the merged defect growth rate for the three scenarios. This proves that as the defects' growth rate increases, the safe operating life of the corroding offshore pipeline decreases.

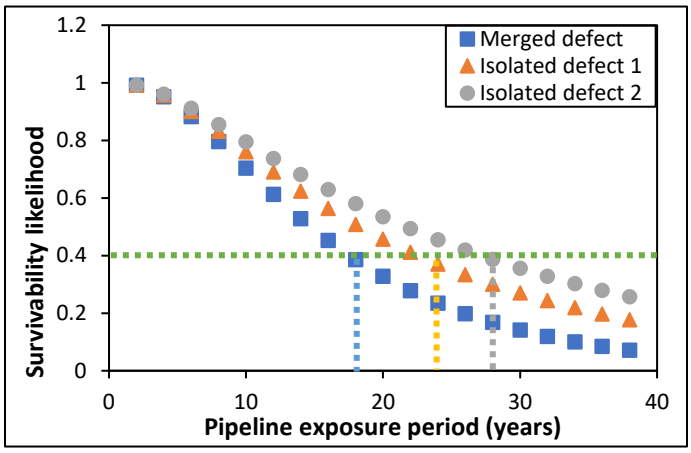

(a) initial defects' growth rate

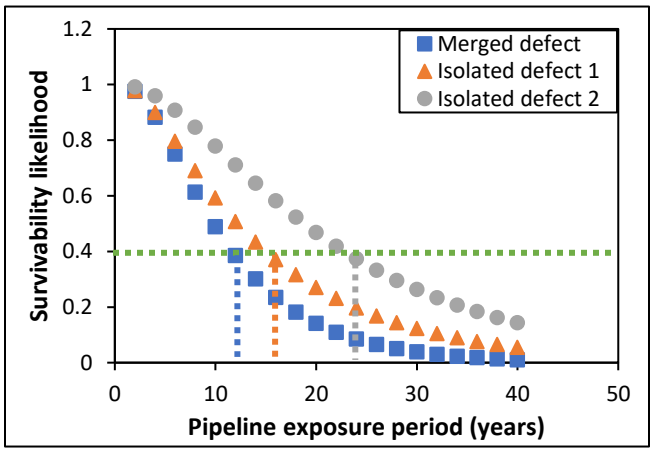

(b) 50% increase in defects' growth rate

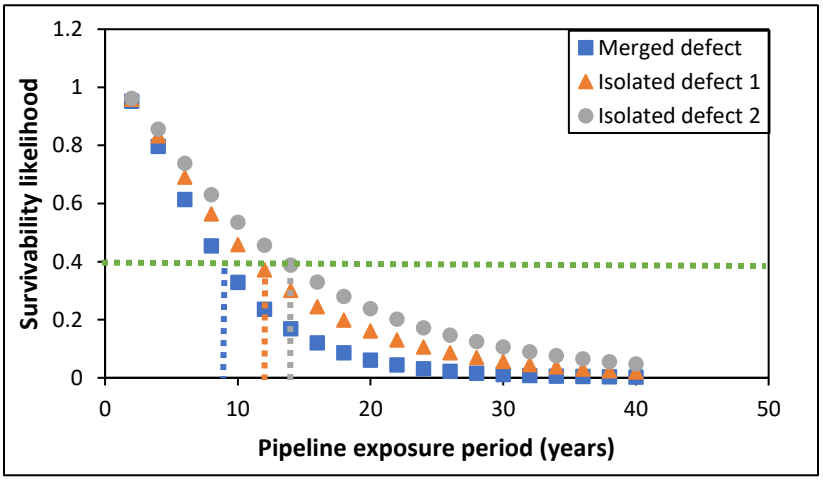

(c) 100% increase in defects' growth rate

Figure 4.11. Survival curve of the pipeline with time considering multiple defects interaction and isolated defects rates.

For practical application, T_s can also represent the time of first intervention or the end of the safe operating life for the pipeline with microbiologically influenced corrosion defects' interaction. The available information on T_s inferred from Fig. 4.11 is of significant practical application for pipeline operators and system integrity managers facing microbiologically influenced corrosion in the oil and gas industry.

The model provides a first-hand parametric-based tool that will guide decision making in prioritizing the point of intervention, such as repair or replacement of the damaged pipeline. It also provides guides to cost-effective, safe operations with an optimum maintenance strategy by determining with confidence the time when the pipeline will become unserviceable during operation.

As previously accentuated, it is important to note that beyond T_s, even if the corroding offshore pipeline has not totally failed, it will be unsafe to sustain operations based on the recommended survivability criteria.

The result of the current methodology in comparison with the probabilistic and mathematical approaches proposed by [19,20,60,68,69] provides a robust application. This is demonstrated by its capacity to predict the MIC rate from a set of inspection data, as well as the time-variant strength loss and likely survival time of the corroding pipeline. These performance capabilities of the current methodology are critical for the integrity management of microbiologically influenced corrosion in marine and offshore industries. Furthermore, there is the need to provide a reliable pipeline rating based on the predicted survivability criteria as a measure of the pipe-wall penetration. Details of the proposed rating are shown in Table 4.5, which gives a reliable calibrated survivability criterion for the in-service corroding pipeline with microbiologically influenced multiple defects' interaction. Also, the following critical safety influencing factors are identified,

and attention should be given to understand better their dynamics and mechanism for safe life condition monitoring of in-service corroding offshore pipelines under microbiologically influenced multiple defects. These are: (i) the multispecies biofilms characteristics; (ii) the longitudinal and circumferential spacing and interacting rate among defects; (iii) the depth, length, and rate of defects under sustainable growth support nutrient sources; (iv) operating parameters' characteristics; and (v) the mechanism of the overlapping defects.

Table 4.5. Corroding pipeline survivability likelihood as a function of % of pipe-wall Penetration

Survivability likelihood (*SL*)	Pipe-wall penetration	State	Action/critical parameters
≤ 0.4	over 60%	Critically unsafe	Repair or replacement
$0.4 - 0.6$	over 40%	Moderately unsafe	Critical condition monitoring of operating parameters, corrosion rate & pressure stability
$0.6 - 0.8$	over 20%	Marginally unsafe	Operating pressure monitoring against instability & corrosion rate
$0.8 - 0.9$	over 5%	Negligibly unsafe	Routine parametric monitoring

4.6. Conclusions

The present study has demonstrated the application of a hybrid BN-Markov Mixture and Monte Carlo simulation methodology for the safety assessment of an offshore pipeline with microbiologically influenced corrosion. The methodology reliably and dynamically predicts the

MIC rate of an offshore system considering complex interaction among the various corrosion influencing parameters. This is shown in the result of the parametric learning of the BN structure with and without evidence. The interaction among corrosion defects was captured to dynamically predict the effective defects interaction rate under the multispecies biofilm for the exposed period. It could be inferred that as the complexity of the interaction increases, the loss in the pipe wall thickness increases until a saturation point is reached where the growth rate becomes steady and gradually exhibits an asymptotic limiting function characteristic.

For the strength loss prediction, the model captures the dynamic effects of the MIC rate and the variability in the remaining strength influencing parameters. Among these effects, the mutual orientation of the defects, depth, spacing, and bacteria interaction play critical roles in the remaining strength prediction. It was observed that as the defects' rate increases, the safe life of the corroding pipeline decreases due to the increase in the rate of strength loss with exposure time under multiple defects' interaction.

The application of the methodology would offer the pipeline integrity managers a dynamic tool for effective survivability criteria inference for the offshore pipeline under low, high, and severe microbiologically influenced corrosion defect rates. With the information provided from the result of the model application on the pipeline and the predicted safe operating time under the predefined operating conditions, a safety-based cost-effective decision making can be inferred to aid integrity management of the corroding offshore pipeline.

Though the application of the proposed methodology confirms its usefulness in the safety assessment of microbiologically influenced corroding offshore systems, the model is scenario-based. It is limited to capture the non-linearity in the corrosion growth process, the spatial dependencies among corrosion parameters, and the time-nonhomogeneity in the Markovian

process. The proposed methodology could be further improved in future research by i) modeling dependencies among corrosion parameters and their characteristic effects on the remaining strength of the corroding assets. ii) considering the time-nonhomogeneous Markovian process to capture the effect of time-variant defects growth, iii) considering non-linear corrosion models and complex multi-failure modes' interaction on the survivability of corroding assets under a multispecies microbial biofilm.

Acknowledgments

The authors acknowledge the financial support provided by Genome Canada and their supporting partners, and the Canada Research Chair (CRC) Tier I Program in Offshore Safety and Risk Engineering.

References

[1] Little BJ, Lee JS. Microbiologically Influenced Corrosion. John Wiley & Sons, Houston, New Jersey; 2007.

[2] Renpu W. Oil and gas well corrosion and corrosion prevention,. Adv. Well Complet. Eng. 3rd Editio, Gulf professional publishing, Boston; 2011, p. 619–39.

[3] Marciales A, Peralta Y, Haile T, Crosby T, Wolodko J. Mechanistic microbiologically influenced corrosion modeling — A review. Corros Sci 2019;146:99–111. https://doi.org/10.1016/j.corsci.2018.10.004.

[4] Gu T, Jia R, Unsal T, Xu D. Toward a better understanding of microbiologically influenced corrosion caused by sulfate reducing bacteria. J Mater Sci Technol 2019;35:631–6. https://doi.org/10.1016/j.jmst.2018.10.026.

[5] Beech IB, Gaylarde CC. Recent Advances in the Study of Biocorrosion - An Overview. Rev

Microbiol 1999;30:177–90.

[6] Kadwa U. A study on biofilm formation in pipelines. Master's Thesis, University of KwaZulu-Natal, 2015.

[7] de Carvalho CCCR. Marine Biofilms : A Successful Microbial Strategy With Economic Implications. Front Mar Sci 2018;5:1–11. https://doi.org/10.3389/fmars.2018.00126.

[8] Marsili E, Kjelleberg S, Rice SA. Mixed community biofilms and microbiologically influenced corrosion. Focus Microbiol Aust 2018:152–7. https://doi.org/10.1071/MA18046.

[9] Palmer A, King R. Subsea pipeline engineering. 2nd editio. Oklahoma USA: PennWell Corporation; 2008.

[10] Chauhan V. Experimental validation of methods for assessing closely spaced corrosion metal loss defects in pipelines, PRCI Report Catalog No. L52007; 2004.

[11] Sun J, Cheng YF. Assessment by finite element modeling of the interaction of multiple corrosion defects and the effect on failure pressure of corroded pipelines. Eng Struct 2018;165:278–86. https://doi.org/10.1016/j.engstruct.2018.03.040.

[12] Xu LY, Cheng YF. Reliability and failure pressure prediction of various grades of pipeline steel in the presence of corrosion defects and pre-strain. Int J Press Vessel Pip 2012;89:75–84. https://doi.org/10.1016/j.ijpvp.2011.09.008.

[13] Timashev S, Bushinskaya A. Diagnostics and Reliability of Pipeline Systems. Springer Berlin Heidelberg; 2016.

[14] DNV. Corroded Pipelines - Dnv-Rp-F101. 2010. https://doi.org/DOI: 10.1016/B978-008044566-3.50040-3.

[15] Chiodo MSG, Ruggieri C. Failure assessments of corroded pipelines with axial defects using stress-based criteria : Numerical studies and verification analyses. Int J Press Vessel Pip 2009;86:164–76. https://doi.org/10.1016/j.ijpvp.2008.11.011.

[16] Cerit M, Genel K, Eksi S. Numerical investigation on stress concentration of corrosion pit. Eng Fail Anal 2009;16:2467–72. https://doi.org/10.1016/j.engfailanal.2009.04.004.

[17] Cerit M. Numerical investigation on torsional stress concentration factor at the semi elliptical corrosion pit. Corros Sci 2013;67:225–32. https://doi.org/10.1016/j.corsci.2012.10.028.

[18] Bhandari J, Khan F, Abbassi R, Garaniya V. Pitting Degradation Modeling of Ocean Steel Structures Using Bayesian Network. J Offshore Mech Arct Eng 2017;139:1–11. https://doi.org/10.1115/1.4036832.

[19] Dawuda A-W. A mechanistic and a probabilistic model for prediciting and anlyzing microbiologically influenced corrosion. Master Thesis, Memorial Univeristy of Newfoundland, Canada, 2019.

[20] Taleb-berrouane M, Khan F, Hawboldt K, Eckert R, Skovhus TL. Model for microbiologically influenced corrosion potential assessment for the oil and gas industry. Corros Eng Sci Technol 2018:1–15. https://doi.org/10.1080/1478422X.2018.1483221.

[21] Palencia OG, Teixeira AP, Soares CG. Safety of Pipelines Subjected to Deterioration Processes Modeled Through Dynamic Bayesian Networks. J Offshore Mech Arct Eng 2019;141:1–11. https://doi.org/10.1115/1.4040573.

[22] Teixeira AP, Soares CG, Netto TA, Estefen SF. Reliability of pipelines with corrosion defects. Int J Press Vessel Pip 2008;85:228–37. https://doi.org/10.1016/j.ijpvp.2007.09.002.

[23] Tak K, Kim J. Corrosion effect on inspection and replacement planning for a refinery plant. Comput Chem Eng 2018;117:97–104. https://doi.org/10.1016/j.compchemeng.2018.05.027.

[24] Wu W, Li Y, Cheng G, Zhang H, Kang J. Dynamic safety assessment of oil and gas pipeline containing internal corrosion defect using probability theory and possibility theory. Eng Fail Anal 2019;98:156–66. https://doi.org/10.1016/j.engfailanal.2019.01.080.

[25] Kiefner JF, Vieth PH. Evaluating pipe:new method corrects criterion for evaluating corroded pipe. Oil Gas J 1990.

[26] Leis BN, Stephens DR. An Alternative Approach to Assess the Integrity of Corroded Line Pipe - Part I : Current Status. Proc. Seventh Int. Offshore Polar Eng. Conf., vol. IV, 1997,

p. 624–34.

[27] Stephens DR, Leis BN. Development of an alternative criterion for residual strength of corrosion defects in moderate-to-high-toughness pipe. ASME Int. Pipeline Conf. Proceeding, vol. 2, 2000.

[28] Zhou W, Huang GX. Model error assessments of burst capacity models for corroded pipelines. Int J Press Vessel Pip 2012;99–100:1–8. https://doi.org/10.1016/j.ijpvp.2012.06.001.

[29] Amaya-gómez R, Sánchez-silva M, Bastidas-arteaga E, Schoefs F, Muñoz F. Reliability assessments of corroded pipelines based on internal pressure – A review. Eng Fail Anal 2019;98:190–214. https://doi.org/10.1016/j.engfailanal.2019.01.064.

[30] Mokhtari M, Melchers RE. A new approach to assess the remaining strength of corroded steel pipes. Eng Fail Anal 2018;93:144–56. https://doi.org/10.1016/j.engfailanal.2018.07.011.

[31] Benjamin AC, Freire LF, Vieira RD, Cunha DJS. Interaction of corrosion defects in pipelines Part 1 : Fundamentals. Int J Press Vessel Pip 2016;144:56–62. https://doi.org/10.1016/j.ijpvp.2016.05.007.

[32] Benjamin AC, Freire LF, Vieira RD, Cunha DJS. Interaction of corrosion defects in pipelines Part 2 : MTI JIP database of corroded pipe tests. Int J Press Vessel Pip 2016;145:41–59. https://doi.org/10.1016/j.ijpvp.2016.06.006.

[33] Mahmoodian M, Li CQ. Stochastic failure analysis of defected oil and gas pipelines. Handb. Mater. Fail. Anal. with Case Stud. from Oil Gas Ind., Elsevier Ltd.; 2016, p. 235–55. https://doi.org/10.1016/B978-0-08-100117-2.00014-5.

[34] Ossai CI, Boswell B, Davies I. Markov chain modelling for time evolution of internal pitting corrosion distribution of oil and gas pipelines. Eng Fail Anal 2016;60:209–28. https://doi.org/10.1016/j.engfailanal.2015.11.052.

[35] Xie Y, Zhang J, Aldemir T, Denning R. Multi-state Markov modeling of pitting corrosion in stainless steel exposed to chloride-containing environment. Reliab Eng Syst Saf 2018;172:239–48. https://doi.org/10.1016/j.ress.2017.12.015.

[36] Mohd MH, Kee J. Investigation of the corrosion progress characteristics of offshore subsea oil well tubes. Corros Sci 2013;67:130–41. https://doi.org/10.1016/j.corsci.2012.10.008.

[37] Smith MQ, Antonio S, Grigory SC. New procedures for the residual assessment of corroded pipe subjected to combined loads. ASME Int. Pipeline Conf. Proceeding, vol. 1, 1996.

[38] Pawar U. Residual Strength of Steel Coupons and Plates Subjected to Corrosion Damage. University of Akron, 2018.

[39] Chen Y, Zhang H, Zhang J, Li X, Zhou J. Failure analysis of high strength pipeline with single and multiple corrosions. Mater Des 2015;67:552–7. https://doi.org/10.1016/j.matdes.2014.10.088.

[40] Adedigba SA, Khan F, Yang M. Dynamic safety analysis of process systems using nonlinear and non-sequential accident model. Chem Eng Res Des 2016;111:169–83. https://doi.org/10.1016/j.cherd.2016.04.013.

[41] Khakzad N, Khan F, Amyotte P. Quantitative risk analysis of offshore drilling operations: A Bayesian approach. Saf Sci 2013;57:108–17. https://doi.org/10.1016/j.ssci.2013.01.022.

[42] Adedigba SA, Khan F, Yang M. Process accident model considering dependency among contributory factors. Process Saf Environ Prot 2016;102:633–47. https://doi.org/10.1016/j.psep.2016.05.004.

[43] Jensen F V, Nielsen TD. Bayesian Networks and Decision Graphs. 2nd ed. Springer, New York; 2007.

[44] Bond DR, Holmes DE, Tender LM, Lovley DR. Electrode-Reducing Microorganisms That Harvest Energy from Marine Sediments. Science (80-) 2002;295:483–6.

[45] Ibrahim A, Hawboldt K, Bottaro C, Khan F. Review and analysis of microbiologically influenced corrosion: the chemical environment in oil and gas facilities. Corros Eng Sci Technol 2018:1–15. https://doi.org/10.1080/1478422X.2018.1511326.

[46] Ossai CI, Boswell B, Davies IJ. Application of Markov modelling and Monte Carlo simulation technique in failure probability estimation — A consideration of corrosion defects of internally corroded pipelines. Eng Fail Anal 2016;68:159–71.

https://doi.org/10.1016/j.engfailanal.2016.06.004.

[47] Valor A, Caleyo F, Alfonso L, Velázquez JC, Hallen JM. Markov Chain Models for the Stochastic Modeling of Pitting Corrosion. Math Probl Eng 2013;2013. https://doi.org/http://dx.doi.org/10.1155/2013/108386.

[48] Aalen O. Dynamic description of a Markov chain with random time scale. Mathamatical Sci 1988;13:90–103.

[49] Aalen O. Mixing Distributions on a Markov Chain. Scand J Stat 1987;14:281–9.

[50] Liu X, Lin XS. A subordinated Markov model for stochastic mortality. Eur Actuar J 2012;2:105–27. https://doi.org/10.1007/s13385-012-0047-3.

[51] Zhang Y. Actuarial Modelling with Mixtures of Markov Chains. PhD Thesis, Unversity of Western Ontario, Canada, 2016.

[52] Jones MN, Frutiger J, Ince NG, Sin G. The Monte Carlo driven and machine learning enhanced process simulator. Comput Chem Eng 2019;125:324–38. https://doi.org/10.1016/j.compchemeng.2019.03.016.

[53] El M, Ben A, Keshtegar B, Correia JAFO, Lesiuk G, De Jesus AMP. Reliability analysis based on hybrid algorithm of M5 model tree and Monte Carlo simulation for corroded pipelines : Case of study X60 Steel grade pipes. Eng Fail Anal 2019;97:793–803. https://doi.org/10.1016/j.engfailanal.2019.01.061.

[54] Li S, Yu S, Zeng H, Li J, Liang R. Predicting corrosion remaining life of underground pipelines with a mechanically-based probabilistic model. J Pet Sci Eng 2009;65:162–6. https://doi.org/10.1016/j.petrol.2008.12.023.

[55] Liu A, Chen K, Huang X, Chen J, Zhou J, Xu W. Corrosion failure probability analysis of buried gas pipelines based on subset simulation. J Loss Prev Process Ind 2019;57:25–33. https://doi.org/10.1016/j.jlp.2018.11.008.

[56] Wen K, Hea L, Liub J, Gong J. An optimization of artificial neural network modeling methodology for the reliability assessment of corroding natural gas pipelines. J Loss Prev Process Ind 2019:1–8.

[57] Witek M. Gas transmission pipeline failure probability estimation and defect repairs activities based on in-line inspection data. Eng Fail Anal 2018;70:255–72. https://doi.org/10.1016/j.engfailanal.2016.09.001.

[58] Eckert R. Field Guide for Investigating Internal Corrosion of Pipelines. NACE International, Houston USA; 2003.

[59] Alabbas FM, Mishra B. Microbiologically Influenced Corrosion of Pipelines in the Oil & Gas Industry. 8th Pacific Rim Int. Congr. Adv. Mater. Process. Miner. Met. Mater. Soc., 2013, p. 3441–8.

[60] Melchers RE, Jeffrey R. The critical involvement of anaerobic bacterial activity in modelling the corrosion behaviour of mild steel in marine environments. Electrochim Acta 2008;54:80–5. https://doi.org/10.1016/j.electacta.2008.02.107.

[61] Melchers RE. Development of new applied models for steel corrosion in marine applications including shipping. Ships Offshore Struct 2008;3:135–44. https://doi.org/10.1080/17445300701799851.

[62] Wang X, Melchers RE. Corrosion of carbon steel in presence of mixed deposits under stagnant seawater conditions. J Loss Prev Process Ind 2017;45:29–42. https://doi.org/10.1016/j.jlp.2016.11.013.

[63] Bhandari J, Khan F, Abbassi R, Garaniya V, Ojeda R. Modelling of Pitting Corrosion in Marine and Offshore Steel Structures - A Technical Review. J Loss Prev Process Ind 2015;37:39–62. https://doi.org/10.1016/j.jlp.2015.06.008.

[64] Al-jaroudi S, Ul-hamid A, Al-Gahtani MM. Failure of crude oil pipeline due to microbiologically induced corrosion. Corros Eng Sci Technol 2011;46:568–79. https://doi.org/10.1179/147842210X12695149033819.

[65] Pots BFM, John RC, Rippon IJ, Thomas MJJS, Kapusta SD, Girgis M., et al. Improvements of De Waard-Milliams Corrosion Prediction and Applications to Corrosion Managment. NACE Int. Corros. Conf. No. 02235, 2002, p. 1–19.

[66] Vigneron A, Head IM, Tsesmetzis N. Damage to offshore production facilities by corrosive microbial biofilms. Appl Microbiol Biotechnol 2018.

https://doi.org/https://doi.org/10.1007/s00253-018-8808-9.

[67] NACE-RP0775. Recommended Practice Preparation, Installation, Analysis, and Interpretation of Corrosion Coupons in Oilfield Operations. NACE Int Houston, TX USA, 2005.

[68] Melchers RE. Extreme value statistics and long-term marine pitting corrosion of steel. Probabilistic Eng Mech 2008;23:482–8. https://doi.org/10.1016/j.probengmech.2007.09.003.

[69] Al-Darbi MM, Agha K, Islam MR. Comprehensive Modelling of the Pitting Biocorrosion of Steel. Can J Chem Eng 2005;83:872–81. https://doi.org/10.1002/cjce.5450830509.

[70] Su C, Li X, Zhou J. Failure Pressure Analysis of Corroded Moderate-to-High Strength Pipelines *. China Ocean Eng 2016;30:69–82. https://doi.org/10.1007/s13344-016-0004-z.

Chapter 5

Offshore system safety and reliability considering microbial influenced multiple failure modes and their interdependencies

Preface

A version of this chapter has been published in the ***Reliability Engineering and System Safety 2021; 215: 107862.*** *I am the primary author along with the Co-authors, Faisal Khan, Sundady Adedigba, and Sohrab Zendehboudi. I developed the conceptual framework for the reliability assessment model and carried out the literature review. I prepared the first draft of the manuscript and subsequently revised the manuscript based on the co-authors' feedbacks. Co-author Faisal Khan helped in the concept development, design of methodology, reviewing, and revising the manuscript. Co-author Sunday Adedigba provided support in implementing the concept and testing the model. Co-author Sohrab Zendehboudi provided fundamental assistance in validating, reviewing, and correcting the model and results. The co-authors also contributed to the review and revision of the manuscript.*

Abstract

The stochastic nature of microbial corrosion creates spatial interdependencies among random corrosion parameters and their failure modes. These interdependencies need to be captured for robust offshore system reliability prediction considering complex multispecies biofilms.

This research chapter presents a hybrid methodology for the prediction of system reliability, considering multiple failure modes' interdependencies. The methodology integrates the Bayesian Network with Copula-based Monte Carlo (BN-CMC) simulation. The BN captures the dynamic interactions among physio-chemical parameters and microbes to predict the corrosion rate of an offshore system. The random corrosion parameters dependencies and the failure modes that define

the performance functions under microbial corrosion are modeled using CMC. The methodology is assessed with an example, and the impact of dynamic interactions of the parameters and their failure modes on the system reliability is investigated. The results reveal that the system's probability of failure differs diversely as the degree of dependencies among the random corrosion parameters and their failure modes increases. The proposed methodology can predict the failure indexes that could aid system integrity management for a sustainable offshore operation experiencing microbial corrosion.

Keywords: Microbial corrosion; Bayesian network; Offshore system reliability; Monte Carlo simulation; Failure probability; Parameters interactions

5.1. Introduction

Offshore systems in the marine environment face a high degree of corrosion-related damage due to dynamic environmental and operational factors. This poses critical safety and integrity issues, especially in remote and harsh offshore environments. These systems, which include offshore pipelines and equipment, are essential infrastructures for oil and gas transportation. The offshore systems suffer severe degradation due to microbial corrosion induced failure mechanisms in the harsh dynamic environment. The diverse and complex microbial corrosion mechanisms create unpredictable and correlated failure modes with associated high risks in marine and offshore systems. There are several studies in the literature with focus on material composition, coating technology, and their response to aggressive microenvironment in marine and offshore systems (e.g., pipeline) [1]. However, the long exposure of these systems to a dynamic corrosive microbial environment makes them vulnerable to a high deterioration rate, especially in sour oil field operations. Therefore, it is important to understand the dynamics of the system environment (in

terms of operating conditions) and the material response in terms of the failure mechanisms and their interdependencies on the corresponding infrastructure life cycle. Moreover, the influential corrosion parameters interact among themselves, and their dependencies affect the morphology of the corrosion products [2–4]. These parameters' interactions complicate the corrosion induced failure mechanisms, especially in bacteria-infested environments.

Micro-organisms at the point of corrosion initiation play a crucial role in the dynamics of system failure modes. They introduce a complex underlying phenomenon that alters the electrochemical configuration and the corrosion induced failure mechanisms in offshore systems. These bacteria survive within the complex multispecies biofilm, and the extracellular polymeric substances act as primary organic carbon/nutrient sources for the biofilm configuration. The bacteria, such as Sulphate Reducing Bacteria (SRB), act as an electron acceptor, which aids the metabolic activities to produce H_2S and HS^- as byproducts [5,6]. These byproducts are aggressive corrosion enhancing substances for steel and iron materials. The bacteria colony, especially multispecies biofilms, interacts with various key variables/factors involved in corrosion to create complex multiple failure mechanisms that are often difficult to manage. It has been shown that the mixed consortium of micro-organisms may lead to more severe and unstable microbiological degradation with unpredictable characteristics [7].

An adaptive reliability approach is required to better understand the sustainability and response of corroding marine and offshore systems in dynamic bacteria-infested environments. This will help in the safety classification with a predefined index for sustainable operation of offshore systems/processes. Also, the associated failure mechanisms and their dynamics need to be

investigated considering the complex interactions among the physio-chemical parameters and the spatial interrelationships of corrosion parameters. This understanding will help define the limit state functions that best describe safe operating envelope of the system when experiencing microbial corrosion. The literature indicates that steel pipelines exhibit different failure modes, such as fracture, strength failure, leakage, buckling, and plastic collapse, which might be due to various levels and types of corrosion defects and applied stress [8–10]. However, there is no comprehensive study in the open sources which investigates the offshore pipeline multi-failure modes and their random response parameters' correlation when the multispecies microbial biofilm condition is maintained.

Various approaches for reliability prediction of both onshore and offshore systems with corrosion defects have been recently introduced [8,11–16]. For instance, Qian et al. [17] applied Monte Carlo simulation for failure prediction of a ductile metal pipeline for a single limit state function based on operating pressure and burst pressure. The approach captures the influence of the variability in the coefficient of variation on the failure probability prediction. However, it is unable to capture the physio-chemical parameters and the multiple failure modes' effects on the system reliability. Some research studies employed reliability methods for single failure mode by stochastically modeling the random corrosion variables with their characterized randomness [14,18,19]. Teixeira et al. [20] applied Monte Carlo simulation and the First-Order Reliability Method (FORM) for reliability prediction of the corroded pipeline under internal pressure load. The literature review reveals that the dynamic effect of multiple failure modes and the correlation among their random response parameters on the overall reliability of microbially influenced corroding systems has not been investigated yet.

Qin [21] analyzed the reliability of a corroding energy pipeline under three potential failure mechanisms, namely small leak, large leak, and rupture. This study introduced a Monte Carlo simulation-based methodology to predict the overall system reliability. A recent improvement in prediction of system reliability considering multiple failure modes and linear correlation can be found in the open sources [9,10]. Recently, Adumene et al. [22] proposed a hybrid model for dynamic safety analysis of offshore pipelines when microbially influenced corrosion occurs. The dynamic model captures the interaction effects of defects on the survival likelihood of the offshore system in the presence of multispecies biofilms. However, the reviewed models are inadequate to capture the complex interactions among the physio-chemical parameters and the nonlinear interdependencies among random corrosion variables and multiple failure modes simultaneously.

Several researchers have demonstrated the application of the copula function for spatial variability and dependencies modeling in complex nonlinear engineering systems and economic risk analysis [23–25]. Nevertheless, there is a limited number of research investigations to adequately explore the complex failure modes' and their random response parameters dependencies with focus on Microbially Influenced Corrosion (MIC) of offshore systems. This knowledge gap has hindered the development of robust and effective reliability prediction and failure prevention strategies for offshore operations suffering MIC. To the best of our knowledge, there is no dynamic model to consider MIC induced multi-failure modes and parametric dependencies' effect on the system reliability with multispecies biofilm architecture. The interactions among the key parameters of microbial corrosion and random corrosion parameters' dependencies in a multispecies biofilm condition have not yet been studied for reliability prediction.

The dynamic mixed bacteria communities and their interactions with steel material create complex multi-failure mechanisms that are unstable and unpredictable. The complex instability of the failure modes due to mixed microbial communities and the physio-chemical parameters' interactions, which affect the system safety and reliability, should be systematically investigated. These knowledge gaps necessitate the development of a dynamic model to capture the impact of the physio-chemical parameters' interactions, random response parameters' interdependencies, and their failure modes on offshore system reliability prediction.

This current chapter presents a hybrid connectionist methodology that integrates a Bayesian Network with Copula-based Monte Carlo (BN-CMC) simulation; the developed approach is used for system reliability prediction, considering multiple failure modes and their response variables interdependencies under multispecies microbial biofilms architecture. The BN is built to predict the dynamic corrosion rate, where the complex interactions among the physio-chemical parameters, bacteria, and environmental factors are considered. The dependencies among random corrosion parameters as well as the limit state functions for reliability prediction are evaluated using Copula-based Monte Carlo simulation (CMC). The hybrid model provides a practical and robust tool for the reliability assessment of corroding assets, considering interrelationships between parameters and complex microbial corrosion induced failure mechanisms. The application of the proposed hybrid methodology is demonstrated for a pipeline case in the marine environment.

The remaining part of the chapter is structured as follows: Section 5.2 gives an overview of performance functions for MIC induced multi-failure modes. Section 5.3 presents the proposed research methodology. Section 5.4 describes the implementation of the methodology through an example. Section 5.5 includes results and discussion, and Section 5.6 provides the conclusions.

5.2. Overview of microbial corrosion induced multi-failure modes

Microbial corrosion presents complex characteristics of mixed bacteria communities with different degradation potentials. This complexity can be described by the dynamic failure modes and their unpredictable nature during operations. To assess the failure state of the offshore assets, limit state functions are defined. The limit state functions describe the safe operating region of the offshore system with MIC defects. The limit state functions are formulated based on structural reliability theory [26].

The limit state functions take into account the geometry and morphology of the defects and the propagation rate. The morphology of MIC defects in the offshore pipeline is unstable and complex; the morphology is best described as localized corrosion (pitting corrosion). The pit cross-section may take several appearances in the form of cavernous, parabolic, elliptical, sub-surface, deep, and narrow attacks on the material structures [27]. Also, the offshore system is exposed to stress-related cracks due to the corrosive environment supported by the bacteria and H_2S. Comprehensive studies on hydrogen-induced and sulfide stress cracks' related failures and the predisposed crack-in-corrosion induced failure scenarios can be found in the literature [28–30]. The defects/crack growth is a function of the corrosion rate/crack propagation rate, which is dependent on the biofilm characteristics, material composition, operating parameters, and applied stresses. These vital

corrosion factors affect the failure rate, failure probability, system reliability, and critical failure year of the corroding assets.

To predict the material susceptibility and the microbial corrosion rate, several methods have been proposed, given the prevailing operating environmental conditions of the offshore assets [31–35]. However, due to sparse data availability, uncertainties, dependencies, randomness, and the complex nature of MIC influential parameters, a dynamic probabilistic approach (e.g., BN) has shown a higher capability for MIC potential modeling [22,36,37]. The BN is a network-based probabilistic tool (see Fig. 5.1) that systematically captures the interactions among the key factors and the bacteria growth to predict the corrosion defect rates [38,39]. The CMC simulation finds the dependencies among the corrosion parameters, the failure modes, and their randomness with the associated probability distributions. For the system reliability analysis, multiple limit state functions are formulated, as described in Section 5.3.

5.3. Research methodology

The dynamic nature of MIC under complex multispecies biofilm architecture presents complicated failure mechanisms with complex dependencies. For this reason, the failure functions are formulated to integrate possible failure modes considering various scenarios. Fig. 5.2 depicts the proposed methodology for system reliability analysis under MIC induced multi-failure modes. The following subsections describe the main steps of the proposed hybrid approach.

5.3.1 Data collection and probability estimation

Information about the corroding offshore assets is collected in step 1; this includes but is not limited to the physio-chemical parameters characteristics, defects characteristics, mechanical

characteristics, microbial characteristics, and their counts. The physio-chemical parameters (or MIC influential factors) are formatted by data partitioning into ranges (high, moderate, and low), to assess their probabilities, as illustrated in step 2. The obtained probabilistic data based on the physio-chemical parameters are used as the input data for the BN analysis.

5.3.2 Prediction of corrosion rate

The MIC influential factors are represented in a network-based structure using BN to illustrate the interrelationships among physio-chemical parameters and their effects on the MIC rate prediction (see step 3 in Fig. 5.2). The BN structural learning is built on the previous research works [40–46]. It shows that there are dependencies and dynamic nonlinear interactions among the physio-chemical parameters. For parameter learning of the BN structure, the estimated prior probability data from step 2 are used as the input data; the conditional probability table is constructed based on available corrosion models and the knowledge/experience of subject matter experts. The presence of the bacteria in the complex biofilm community introduces an interdependency among the bacteria types. This mutualistic relationship occurs such that the metabolites of some micro-organisms serve as substrates or energy sources for other bacteria [7]. The mutual complexity of multispecies biofilm structures complicates the biocorrosion and its rate prediction.

In this research, one of the objectives is to further understand the dynamic effect of the nonlinear interactions among temperature, CO_2 partial pressure, pH, H_2S partial pressure, salinity, and bacteria on the corrosion rate of the offshore pipeline. This is depicted by the directed arc drawn among these parameters, as demonstrated in Fig. 5.1. The predictive (or forward) analysis in the BN structure describes the probability of occurrence of any node of the network based on the prior probabilities of the root nodes and the conditional probability which captures the conditional

dependence (nonlinear interactions) of each node. The demonstration of the parameters interaction's effect on the corrosion rate is given in Section 5.5. For more details on the development of the MIC based BN structure for parametric and structural learning, readers are encouraged to visit these research studies [38,47–50].

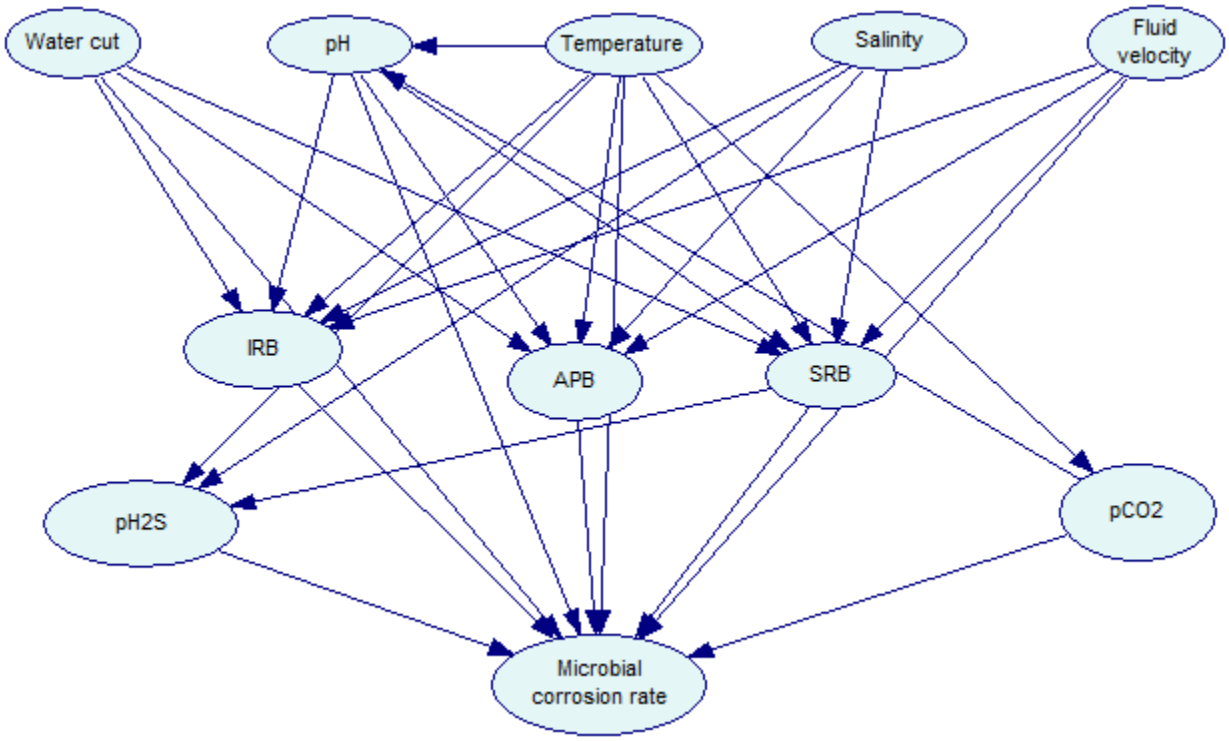

Figure 5.1. Schematic of BN structure considering nonlinear interactions among MIC vital factors

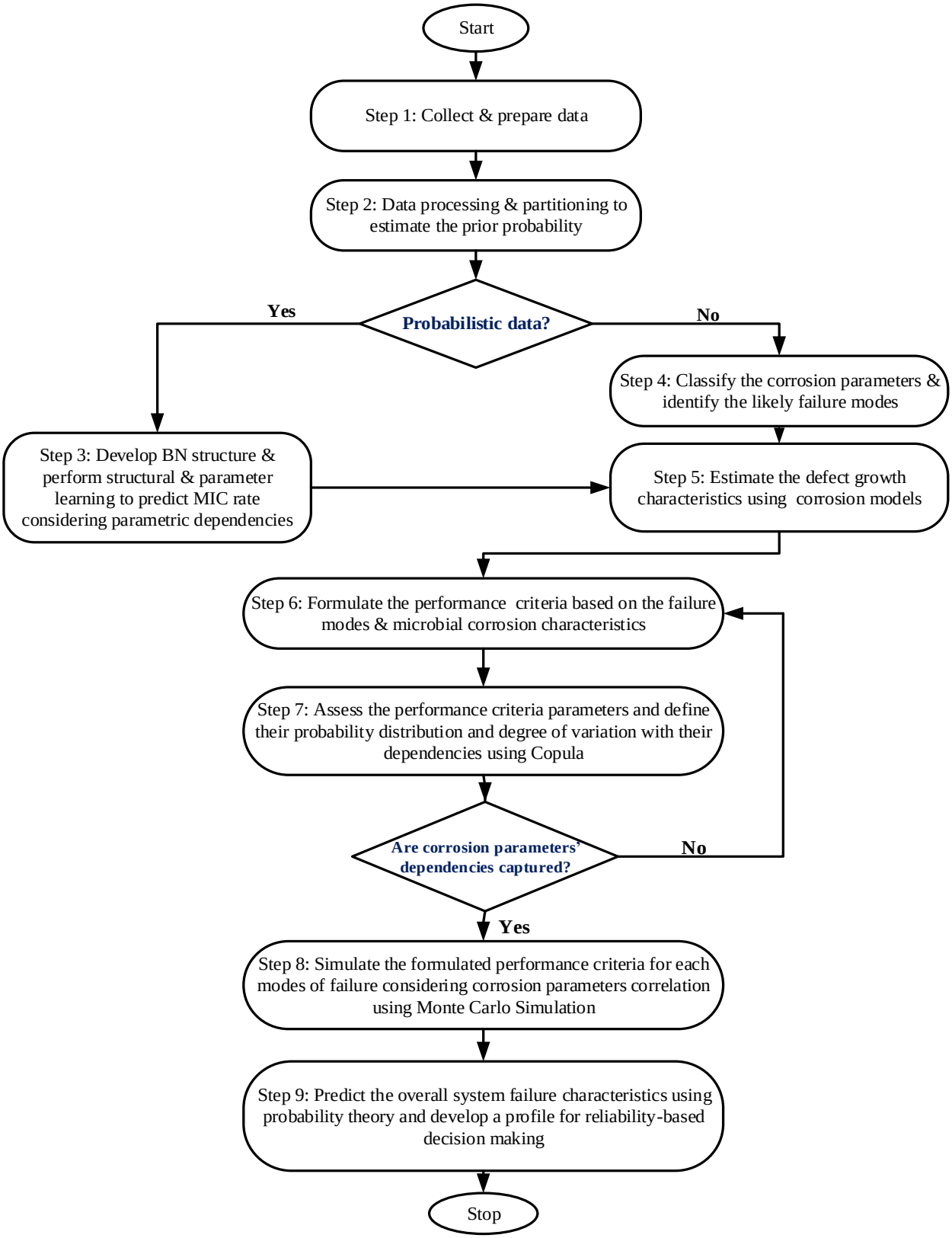

Figure 5.2. Flowchart of the proposed hybrid methodology

5.3.3 Limit state functions and random corrosion parameters' dependencies

In step 4, the inspection data are further assessed to identify defect characteristics and random response dependencies. This is necessary to ensure that the performance function represents the actual state of the corrosion characteristics based on the available data. Further analysis of the defects' growth is made using the linear corrosion models in step 5. The linear growth model is assumed for the corrosion defect growth as expressed by Eqs. (5.1) and (5.2) [18,51,52].

$$d(t) = d_0 + a_d \cdot t \tag{5.1}$$

$$L(t) = L_0 + a_l \cdot t \tag{5.2}$$

where d_0 and L_0 symbolize the initial defect depth and length, respectively, and a_d and a_l refer to the radial and axial corrosion rates. Due to the sparse data availability, the MIC rate is predicted based on the available single inspection data using BN as discussed in step 3. The predicted MIC rate is taken as the radial corrosion rate. Also, a percentage of the radial corrosion rate is used for the axial corrosion rate, based on the correlation between the corrosion depth and length. Fig. 5.3 provides a flowchart for the prediction of multi-failure modes.

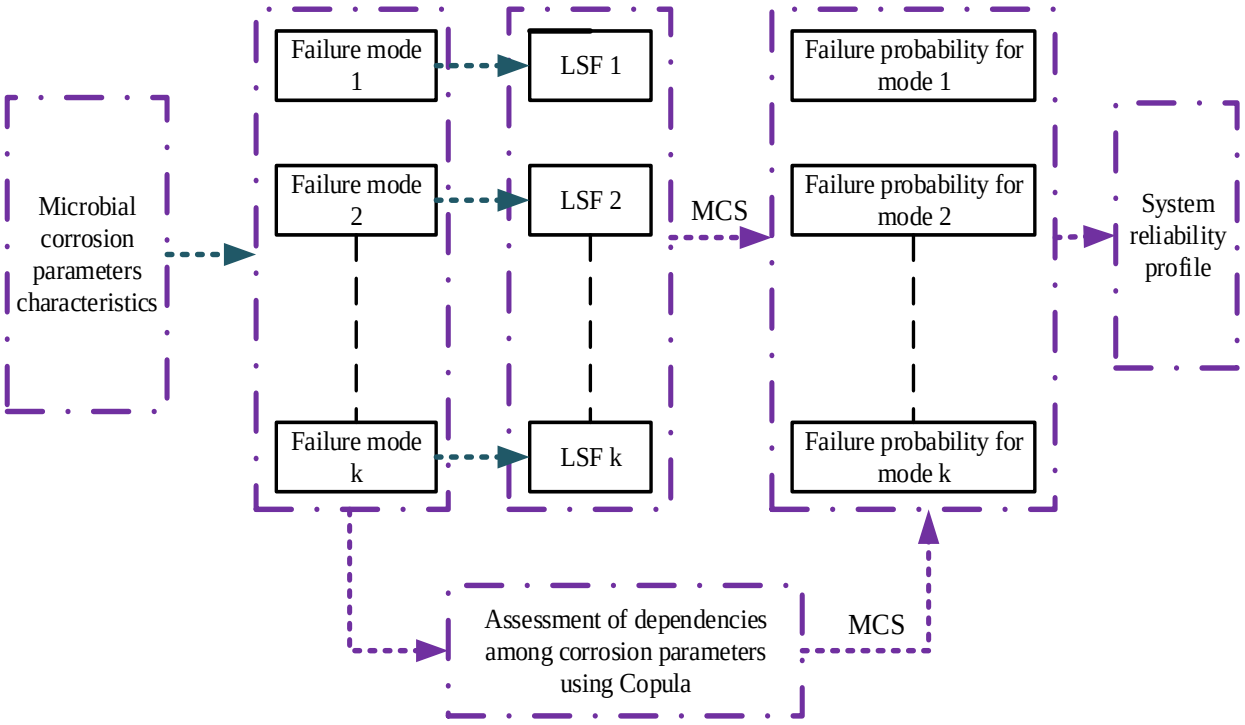

Figure 5.3. Flowchart to obtain reliability profile using failure function models

5.3.3.1 MIC induced leak failure

The corroded offshore system can be assessed to determine if operations should continue based on predefined reliability criteria [20]. The common condition for unsafe pipe operation due to leakage is benchmarked at the condition when the pipeline defect depth is more than 80% of the wall thickness [53]. In this case, the operation of the pipeline becomes critically unsafe, and replacement is recommended. Therefore, for safe operation, a failure function for the corrosion induced leak failure is defined by Eq. (5.3):

$$g_1(wt, d, t) = 0.8wt - d(t) \tag{5.3}$$

where wt introduces the pipe-wall thickness, and $d(t)$ stands for the corrosion defect depth at the time, t

5.3.3.2 Burst failure

Burst failure is mostly experienced due to clusters of multiple and interacting defects. The performance criterion based on the burst capacity is given by Eq. (5.4):

$$g_2\,(r_b, P_o, t) = r_b(t) - P_o \tag{5.4}$$

where $r_b(t)$ is the burst capacity, and P_o stands for the operating pressure. In this research study, the pipeline burst capacity is predicted using the FITNET FFS model, as given below [17][54]:

$$r_b(t) = \frac{2\sigma_u wt\left(1/2\right)^{\left(65/\sigma_y\right)}}{D - wt}\left[\frac{1 - \frac{d(t)}{wt}}{1 - \frac{d(t)}{wtQ}}\right] \tag{5.5}$$

where Q is the length correction factor which equals $\sqrt{1 + 0.8\frac{L(t)}{\sqrt{Dwt}}}$; and $D, \sigma_u, \sigma_y, wt,\ d(t),$ and $L(t)$ represent the external diameter, ultimate tensile strength, yield stress, wall thickness, defect depth, and corrosion defect length of the pipeline, respectively.

5.3.3.3 Fracture failure (MIC induced crack failure)

Fracture failures occur due to crack formation, which propagates under favorable environmental conditions. In sour oilfield production, the bacteria metabolites and their interactions with the environment enhance corrosive substances (e.g., H_2S), which cause rapid crack-in-corrosion of the steel pipe [29,41,55]. This cracking may be sulfide stress and hydrogen-induced cracking, a form of Stress Corrosion Cracking (SCC). These are possible scenarios of the bacteria interactions and the effect of oilfield production with high hydrogen sulfide concentration [41,56].

A formulated limit state function for the estimation of crack-in corrosion failure probability considering the R6 procedure is given in Eq. (5.6). This method provides an elasto-plastic based analysis by an equivalent comparison of the J_{app} (in the J-terminology) with the material toughness, $J_{mat}(\Delta a)$ [57,58].

$$g_3\left(J_{mat,}, J_{app}, t\right) = J_{mat}(\Delta a) - J_{app} \tag{5.6}$$

where J_{app} denotes the applied J and is expressed as a function of the stress intensity factor as follows [58]:

$$J_{app} = \frac{K^2}{E} \cdot [f(L_r)]^{-2} \tag{5.7}$$

An empirical model, presented in the literature [59,60], is adopted for the crack-in corrosion (stress corrosion cracking) propagation rate and the stress intensity factor for the J_{app}. The model is expressed as $\beta\sigma\sqrt{\pi(a_f + \int_{t_f}^{t} C(\Delta K)^m dt}$. For the empirical model derivation, readers are referred to the research studies [59,61]; where a_f accounts for the defect size at the transition to crack; σ is the stress load; β refers to the shape parameter for the crack; ΔK can be expressed as $K_{max} - K_{ISCC}$, where K_{max} is the maximum stress intensity factor and K_{ISCC} denotes the stress intensity factor threshold of the SCC; m and C are the parameters of crack-in corrosion propagation rate model; t_f is the time of transition for crack propagation; Δa introduces the ductile crack extension; E symbolizes the Young's modulus of the material[62]; and $f(L_r)$ represents the yielding correction function and is expressed as $(1 - 0.14L_r^2)\left(0.3 + 0.7exp(-0.65L_r^6)\right)$[57] for the plastic collapse cut-off on the Failure Assessment Diagram (FAD), where $L_r < L_r^{max} \equiv \frac{1}{2}\left(1 + \frac{\sigma_{uts}}{\sigma_{ys}}\right)$.

The J_{mat} is expressed as a function of the material fracture toughness (K_{mat}) as follows [57]:

$$J_{mat}(\Delta a) = \frac{K_{mat}^2(\Delta a)}{E'} \tag{5.8}$$

where $E' = E$ and $E/(1 - v^2)$ stand for the plane stress and plane strain states, respectively; and v is the Poisson ratio.

5.3.3.4 Rupture failure

The failure criterion for rupture failure is defined by Eq. (5.9):

$$g_4(r_{rp}, P_o, t) = r_{rp}(t) - P_o \tag{5.9}$$

The flow stress-dependent failure criterion proposed by Kiefner et al. [63] is given below:

$$r_{rp}(t) = \frac{2wt\sigma_f}{MD} \tag{5.10}$$

where

$$M = \begin{cases} \sqrt{1 + \dfrac{0.6275L^2}{Dwt} - \dfrac{0.003375L^4}{D^2wt^2}}, & \text{for } \dfrac{L^2}{(Dwt)} \leq 50 \\ \dfrac{0.032L^2}{Dwt} + 3.3, & \text{for } \dfrac{L^2}{(Dwt)} > 50 \end{cases} \tag{5.11}$$

in which, M symbolizes the folias factor; and σ_f is the flow stress and is defined as $0.9\sigma_u$. The corrosion defect in the axial direction can be expressed as a function of time (see Eq. 5.2). The random corrosion parameters are used to model the performance criteria for rupture failure stochastically. This is applicable only for the corrosion defects.

For the microbially influenced corroding offshore pipeline, the failure state (f_s) can be summarized using the limit state function and intersection $(\cap)$ of $g_1, g_2, g_3,$ and g_4, according to the following expression [64]:

$$f_s = \begin{cases} g_1 \leq 0 \cap g_2 > 0 & \text{leak} \\ g_1 > 0 \cap g_2 \leq 0 & \text{burst} \\ g_1 > 0 \cap g_2 \leq 0 \cap g_3 \leq 0 & \text{fracture} \\ g_1 > 0 \cap g_2 \leq 0 \cap g_3 \leq 0 \cap g_4 \leq 0 & \text{rupture} \end{cases} \tag{5.12}$$

5.3.4 Corrosion parameters and failure modes' interdependencies

In step 7, the Copula is adopted to model the dependencies among random corrosion parameters and failure modes, considering the dynamic operating conditions of the offshore assets.

The Copula can capture different characteristic variability among random variables (rvs) [65]. The copula function can model the joint probability distribution of rvs with different individual marginal probability distribution functions. Sklar [66] used the "copula" concept and provided the mathematical background that describes the copula function, linking marginal distributions to a joint probability distribution. Sklar's theorem states that a function $\mathrm{F}: \mathbb{R}^d \rightarrow [0,1]$ is the joint distribution function of a random vector $(X_1, \ldots\ldots, X_d)$ if there is a copula $\mathrm{C}: [0,1]^{\mathrm{d}} \rightarrow [0,1]$ and univariate distribution function $\mathrm{F}_1, \ldots\ldots, \mathrm{F}_{\mathrm{d}}: \mathbb{R} \rightarrow [0,1]$ such that

$$F(x_1, \ldots\ldots, x_d) = C\big(F_1(x_1), \ldots\ldots, F_d(x_d)\big), x_1, \ldots\ldots, x_d \in \mathbb{R} \tag{5.13}$$

This is defined for all functions $F_1, \ldots\ldots, F_d$ being continuous.

Copula type selection is based on the goodness-of-fit tests of the data set. However, in the case of sparse data availability, Gong and Frangopol [23] demonstrated the application of the Archimedean copula family to model the dependence structure among random corrosion parameters. In this research, the Archimedean copula family is adopted. It includes the Clayton, Gumbel, and Frank with different formulations for copula parameter estimation. The general Archimedean copula function is given below [65]:

$$C\varphi(u_1, \ldots\ldots, u_d) = \varphi(\varphi^{-1}(u_1) + \varphi^{-1}(u_2) + \cdots + \varphi^{-1}(u_d)) \tag{5.14}$$

where for a suitable, non-increasing function $\varphi: [0, \infty]$ with $\varphi(0) = 1$ and $\lim_{x \to \infty} \varphi(x) = 0$ is the Archimedean generator; $\varphi(\cdot)$ is the generator function; and $\varphi^{-1}(\cdot)$ is its inverse. The single argument θ is used to characterize the Archimedean generator and its inverse function.

The concordance measure among random variables that defines the copula parameter is called Kendall's tau. It is a non-parametric measure that does not vary with the marginal probability distribution of the random variables. For any two random variables Y_1 and Y_2, the Kendall's tau between them is the difference in the concordance and discordance probability of (Y_1, Y_1') and (Y_2, Y_2'), where Y_1' and Y_2' are the independent copies of Y_1 and Y_2 respectively. The link between the copula function and Kendall's tau can be expressed by Eq. (5.15). For more details on the copula formulation and its applications, interested readers are referred to the referenced literature [67,68].

$$\tau = 4 \int_0^1 \int_0^1 C(y_1 y_2)\, dC(y_1 y_2) - 1 \tag{5.15}$$

where $y_1$and y_2 are the values of Y_1 and Y_2, respectively.

Tables 5.1 and 5.2 describe the copula generator and its inverse functions, and the one-to-one relation between Kendall's tau and the argument, respectively [65,67].

Table 5.1. Description of the copula generator and its inverse function

Copula	Generator $\varphi(\cdot)$	Inverse function $\varphi^{-1}(\cdot)$	Argument θ
Gumbel	$[-\ln(\cdot)]^{\theta}$	$e^{-(\cdot)^{\theta^{-1}}}$	$[1, \infty]$
Clayton	$\frac{(\cdot)^{-\theta}-1}{\theta}$	$[1+(\cdot)]^{-\theta^{-1}}$	$[-1, \infty], \{0\}$
Frank	$\frac{-\ln e^{-\theta(\cdot)}-1}{e^{-\theta}-1}$	$-\theta^{-1}\ln\left[1-\left(1-e^{-\theta}\right)e^{-(\cdot)}\right]$	$[-\infty, \infty], \{0\}$

Table 5.2. Description of the relationship between Kendall's tau and the Argument Θ

Copula	Kendall's tau
Gaussian	$\tau = \frac{2}{\rho}\arcsin(\rho)$
Gumbel	$\tau = 1-\theta^{-1}$
Clayton	$\tau = \frac{\theta}{\theta+2}$
Frank	$\tau = 1+\frac{4}{\theta}\left(\frac{1}{\theta}\int_0^{\theta}\frac{t}{e^t-1}dt-1\right)$

where ρ represents the Pearson's correlation coefficients.

The limit state function response's parameters are assessed to define their probabilistic characteristics and identify dependencies among them. Further analysis is performed through considering the random disturbance of the load effect on the performance characteristics of the offshore system. The impact of this disturbance on the structural failure shows that the basic response parameters may be positively interrelated within the segment of a given offshore pipeline. These correlated response parameters may include the corrosion depth, length, axial and radial corrosion rate, crack size, stress intensity, wall thickness, pipe diameter, yield strength, and tensile strength; they are modeled using copula.

5.3.5 Probability of failure estimation and system reliability prediction

Monte Carlo simulation is a powerful probabilistic tool widely used in engineering and non-engineering systems analysis. It provides a straightforward failure probability estimation approach based on the probabilistic characteristics of the response parameters of the failure functions [20,22]. In step 8 shown in Fig. 5.2, the characteristic random variables and their dependencies are modeled by the Copula. The results serve as the input parameters to the limit state functions as described in subsection 5.3.3, and the various failure probabilities for each mode are predicted. Fig. 5.4 shows the MCS flow chart for failure probability prediction for each failure mode.

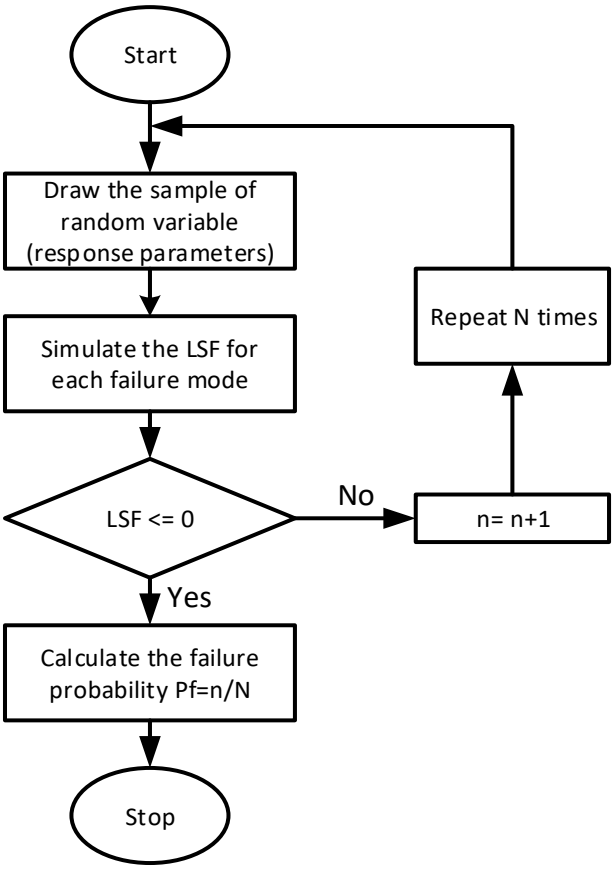

Figure 5.4. Model segment flowchart for failure probability prediction

Further consideration of random corrosion response parameters dependencies and their failure modes helps to predict the dynamic effect of correlation and operating parameters on the offshore system reliability. For an offshore asset that is considered as a series system, the system reliability based on the formulated four modes of failure can be expressed using the probability theory, as given below:

$$R_{sys}(t) = 1 - P\left(\bigcup_{i=1}^{m}(g_i(X) \leq 0)\right) \tag{5.16}$$

$$R_{sys}(t)$$

$$= 1$$

$$- \ P\left[g_1(wt, d, t) \leq 0 \cup g_2(r_b, P_o, t) \leq 0 \cup g_3\left(J_{mat}, J_{app}, t\right) \leq 0 \cup g_4\left(r_{rp}, P_o, t\right)\right.$$

$$\left. \leq 0\right] \quad (5.17)$$

Therefore, the upper bound system failure probability (considering correlation (dependencies) structures among the random corrosion parameters) and the failure modes can be captured under the complex multispecies biofilm by the Copula function at any given time t, as follows [68]:

$$P_{fsys}(t) = P(g_1(X_1) \leq 0, g_2(X_2) \leq 0, \dots \dots \dots, g_n(X_n) \leq 0) \quad (5.18)$$

$$P_{fsys}(t)$$

$$= \sum_{i=1}^{n} P(g_i(X) \leq 0) + \sum_{1 \leq i_1 < i_2 \leq n}^{n} P\left(g_{i_1}(X) \leq 0, g_{i_2}(X) \leq 0\right) + \cdots \dots$$

$$+ (-1)^k \sum_{1 \leq i_1 < i_2 < \cdots \dots < i_k < n}^{n} P\left(g_{i_1}(X) \leq 0, g_{i_2}(X) \leq 0, \dots \dots g_{i_k}(X) \leq 0\right)$$

$$+ (-1)^n P(g_1(X) \leq 0, g_2(X) \leq 0, \dots \dots \dots, g_n(X)$$

$$\leq 0) \quad (5.19)$$

$$P_{fsys}(t) = \sum_{i=1}^{n} F_i(t) + \sum_{1 \leq i_1 < i_2 \leq n}^{n} C_{g_{i_1} g_{i_2}}\left(F_{i_1}(t), F_{i_2}(t)\right) + \cdots \dots \dots \dots \dots \dots \dots +$$

$$+ (-1)^k \sum_{1 \leq i_1 < i_2 < \cdots < i_k \leq n}^{n} C_{g_{i_1} g_{i_2} \dots \dots g_{i_k}}\left(F_{i_1}(t), F_{i_2}(t), \dots \dots \dots, F_{i_k}(t)\right)$$

$$+ \ (-1)^n C_{g_1 g_2 \dots \dots g_n}(F_1(t), F_2(t), \dots \dots \dots, F_n(t)) \quad (5.20)$$

where $F_i(t)$ $(i = 1,2 \dots . n)$ is the probability of failure for the i^{th} failure mode at time t; $F_i(\cdot)$ represents the probability distribution function of the i^{th} failure mode; and $C_{g_1 g_2 \dots \dots g_n}$ is the

Copula function for the joint probability distribution of the limit state functions of $\left(g_1(x_1), g_2(x_2), \ldots\ldots\ldots, g_n(x_n)\right)$.

The co-occurrences of the failure modes, as presented by Eq. (5.12), are investigated to establish diverse scenarios of the system reliability profile for holistic decision-making in offshore operations.

5.4. Methodology implementation

The application of the proposed hybrid connectionist methodology is demonstrated on a 2 km crude oil transmission pipeline made of grade X60 steel. The 762 mm outer diameter (DN 750) pipeline operates in a sour oil field production with characteristic bacteria in the marine environment [69]. To simplify the analysis, it is assumed that the pipeline segment contains localized defects on the internal surface based on inline inspection, as shown in Table 5.3.

Table 5.3. Geometry of the corrosion parameters

	Defect I		Defect 2		Defect 3	
	Mean	Std dev	Mean	Std dev	Mean	Std dev
Depth (mm)	4.24	0.43	2.95	0.38	1.46	0.26
Length (mm)	95	32	110	42	155	53

The operating and environmental conditions of the pipeline are shown in Tables 5.4 and 5.5. The working condition is assumed to be the same for the period under study. The defects exist under complex multispecies microbial biofilm architectures. Additional data/information on the

corrosion influencing factors and the crack-in-corrosion characteristics can be found in the references [38,70–72]. It is assumed that the inspection of the pipeline is carried out in the 4th year of the operation.

Table 5.4. Description of the physio-chemical field data and their node states

	θ_t℃	pCO_2(MPa)	$V(m/s)$	pH_2S(MPa)	SO_4(mg/l)	CL (mg/l)	WC(%)	pH
				Low state				
Min	15	0.02	0.06	0.03	2	88	1	4.6
Max	35	0.25	1.01	0.26	2600	2200	89	9.8
Mean	30.1	0.19	0.87	0.17	1201	1944	32	5.2
				Moderate state				
Min	18	0.12	0.59	0.14	6	117	10	3.2
Max	55	0.32	2.03	0.37	3050	2500	95	8.1
Mean	42	0.22	1.27	0.28	1620	1988	45	4.2
				High state				
Min	35	0.19	0.86	0.17	108	205	35	2.2
Max	65	0.44	3.04	0.52	4300	4600	95	7.6
Mean	42	0.33	2.04	0.32	1908	2010	58	3.4

θ_t: Temperature (℃); pCO_2: CO_2 partial pressure (MPa); V: Fluid flow rate (m/s)
pH_2S: H_sS partial pressure (MPa); pH: pH of the fluid; SO_4: Sulfate ion (mg/l)
CL: Chloride ion (mg/l); WC: Water cut (%)

Table 5.5. Description of the biofilm characteristics and categorization of the bacteria node states

State	SRB (cfu/ml)	IRB (cfu/ml)	APB (cfu/ml)
Low	≤ 10000	≤ 1000	≤ 1000
Moderate	$10000 - 50000$	$1000 - 10000$	$1000 - 10000$
High	≥ 50000	≥ 10000	≥ 10000

The pipeline mechanical properties, crack properties, and their probabilistic characteristics are shown in Table 5.6 and Table 5.7. Furthermore, the following assumptions are made for the proposed methodology application: i) the data bounds, as shown in Tables 5.3-5.7, depict the prevailing operating/environmental conditions for the pipeline, ii) the corrosion influencing parameters exhibit complex interactions, and the random corrosion parameters show parametric dependencies, iii) the defects and crack-in-corrosion are assumed to be stable and growing; they are exposed to the same operating conditions, iv) Kendall $\tau's$ values of 0.28, 0.53, 0.91 are assumed to capture the dependencies among the random response parameters for the research analysis, and iv) the crack-in corrosion propagation rate is assumed to follow the empirical model proposed by the research study [59].

Table 5.6. Description of the pipe variables and mechanical properties

Symbol	Variable	Unit	Distribution[c]	Mean	COV
D	Outer diameter	mm	Normal	762	–
wt	Pipe wall thickness	mm	Normal	7.92	0.009
σ_y	Yield strength	MPa	Normal	461	0.035
σ_u	Tensile strength	MPa	Lognormal	517	0.037
P_0	Operating pressure	MPa	Lognormal	5.7	0.058
a_d	Radial corrosion rate	mm/yr	Normal	0.3020[a]	0.6
a_l	Axial corrosion rate	mm/yr	Normal	6.04[b]	0.4

a: a_d value is a mean value estimated from the predicted MIC rate

b: $a_l$value is based on the percentage proportionality of a_d

c: The probability distribution for the random response variables are adopted from the work [17]

Table 5.7. Description of the crack-in-corrosion characteristics

Symbol	Variable	Unit	Distribution	Mean	COV
a_0	Initial crack size	mm	Normal	0.1984	0.202
σ	Hoop stress	MPa	Normal	400	0.051
K_{mat}	Fracture toughness for mode I fracture	$\mathrm{MPa}/\sqrt{\mathrm{m}}$	Normal	200	–
E	Young modulus	$\mathrm{GP_a}$	–	206	–
d_c	Defect depth	mm	Normal	1.46	0.18
C	Crack propagation model constant	–	Normal	$2.8e^{-11}$	–
β	crack shape parameter	–	–	2.6	–
m	model parameter for crack propagation	–	Normal	1.16	0.052
σ_a	stress amplitude	MPa	Normal	90	0.026

5.5. Results and discussion

The research objective was to develop a hybrid connectionist methodology that simultaneously captures the impacts of physio-chemical parameters' nonlinear interactions, random corrosion parameters interdependencies, and their failure modes on the offshore system reliability in the presence of multispecies microbial biofilms.

5.5.1 Impact of physio-chemical parameters' interactions on the corrosion rate

The dynamic structure that represents the complex interactions among the parameters is built using BN. Thus, the dependencies and dynamic interactions among the physio-chemical parameters (e.g., temperature, CO_2, pH, H_2S, and salinity) and their data range effects are captured for the prediction of the microbial corrosion rate. The collected data on the physio-chemical parameters are processed into probabilistic data for the BN modeling. Fig. 5.5 shows the results of the parameter learning of the BN structure that reveal the dynamic interactions among the physio-chemical parameters and bacteria and their effects on the corrosion rate. The estimated corrosion rate is in agreement with the recommended corrosion rate categorization [73].

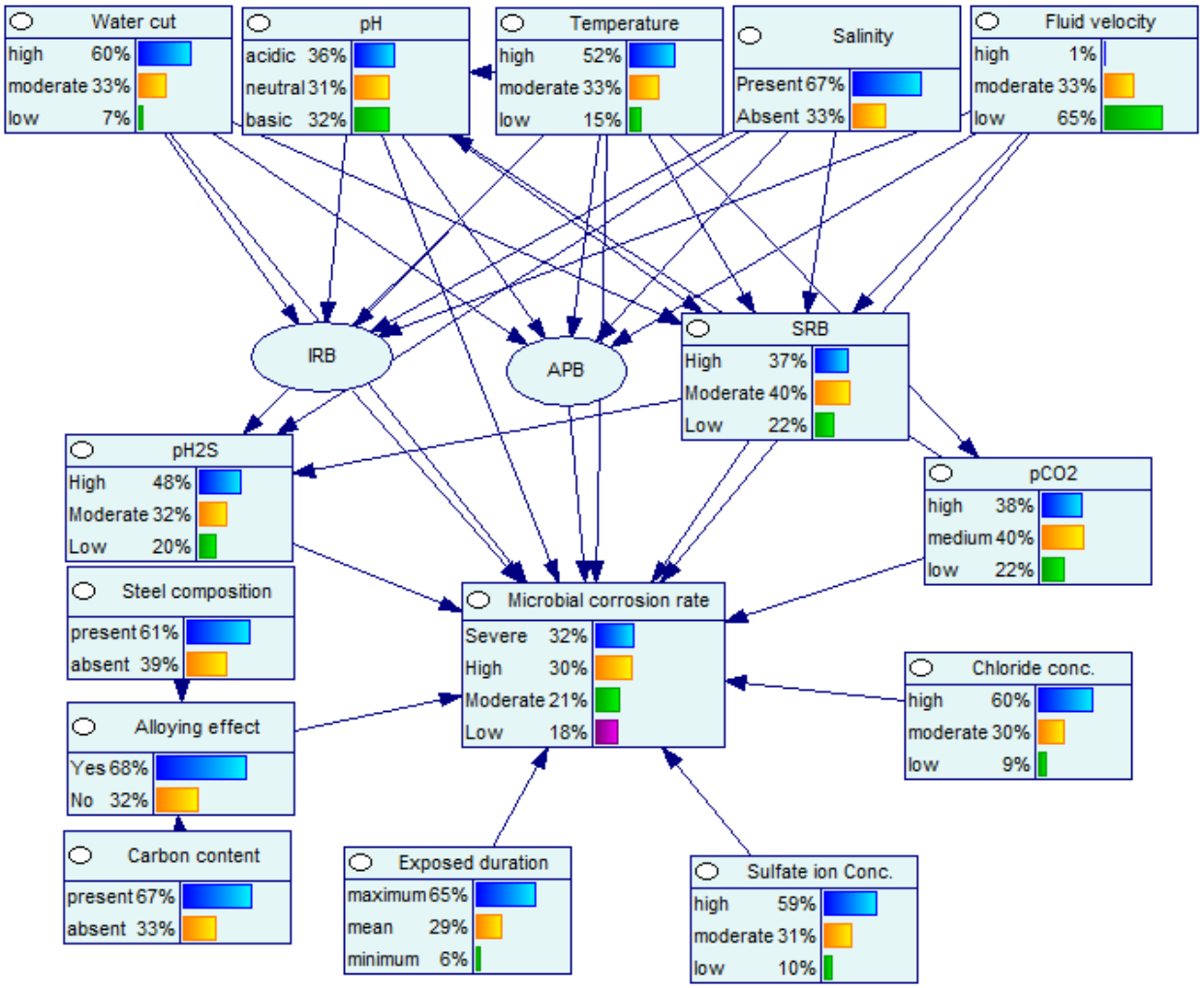

Figure 5.5. BN structure for microbial corrosion rate prediction, considering the interrelationship between physio-chemical parameters

Fig. 5.6 demonstrates the cumulative impact of the physio-chemical parameters' interactions on the corrosion defect rate while dealing with multispecies biofilm structure. The impact of the interactions among temperature, CO_2, H_2S, salinity, and SRB on the corrosion rate is assessed by placing evidence on their respective nodes (see Fig. 5.6). The results show a 13.4% and 24% increase in the corrosion rate for the high and severe corrosion rate categories, respectively. The model provides a robust and dynamic tool for corrosion rate prediction by showing the importance

level of the operational and environmental parameters. This model can be updated upon the availability of a new set of data/information on the operating condition of the pipeline. It is important to note that for a sour oil field operation, the H_2S and bacteria interactions enhance severe degradation rate of the infrastructures. They also participate in the structural crack failure as a result of Fe_2S formation and hydrogen embrittlement.

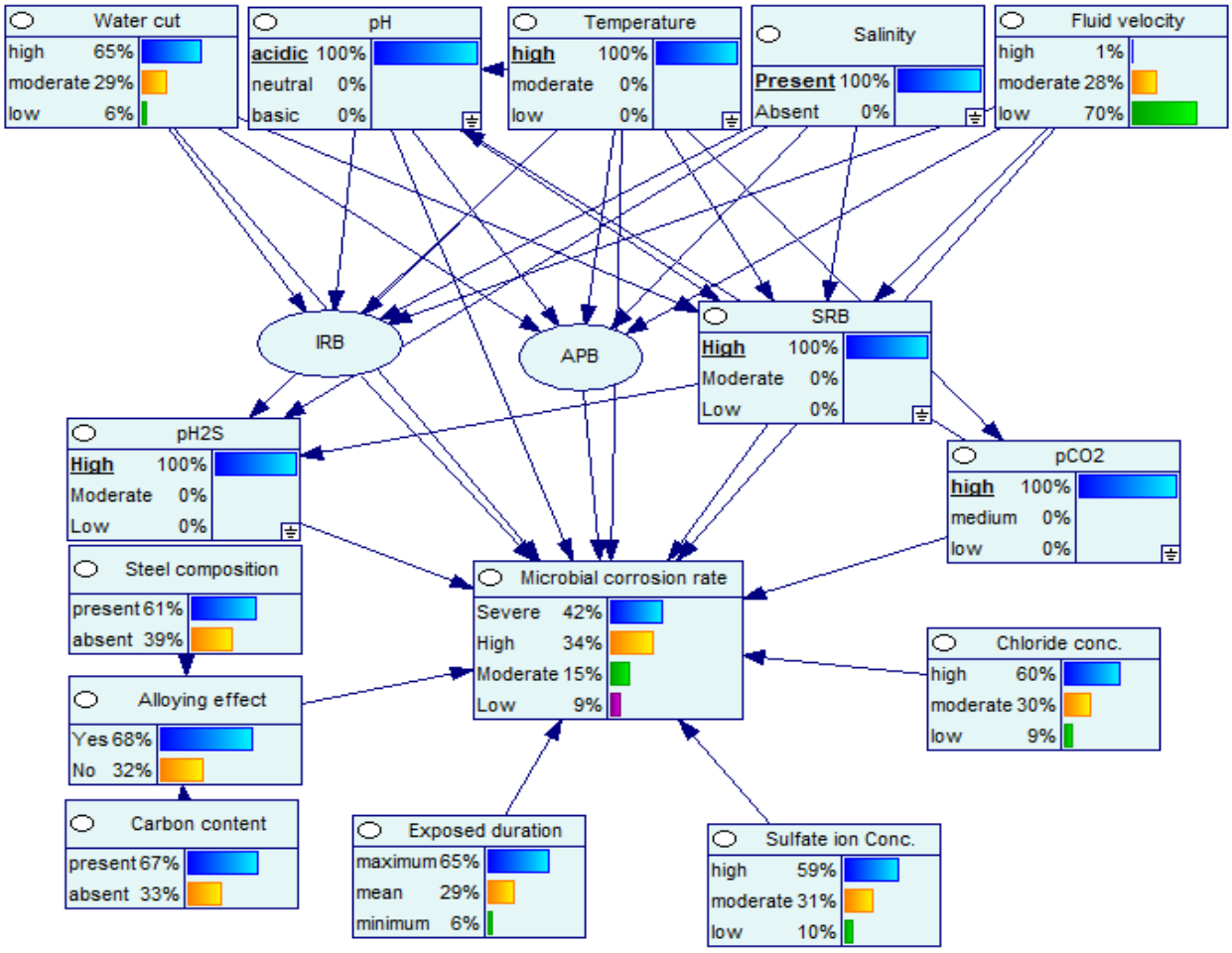

Figure 5.6. Combined effects of temperature, CO_2, H_2S, pH, salinity, and SRB interactions on microbial corrosion rate

5.5.2 Performance functions analysis based on microbial corrosion defects characteristics

To analyze the effect of the failure modes on the system reliability, the non-probabilistic data are assessed to determine their probability characteristics and distributions. The probabilistic properties of the random corrosion variables are used to predict the time-dependent defect growth rate for the three defects depth. A total number of 10^5 Monte Carlo simulation trials in the MATLAB environment are used to evaluate the failure characteristics for the offshore pipeline and each failure mode for both cases. Fig. 5.7 presents the predicted failure characteristics and critical failure year under a prevailing multispecies biofilm condition.

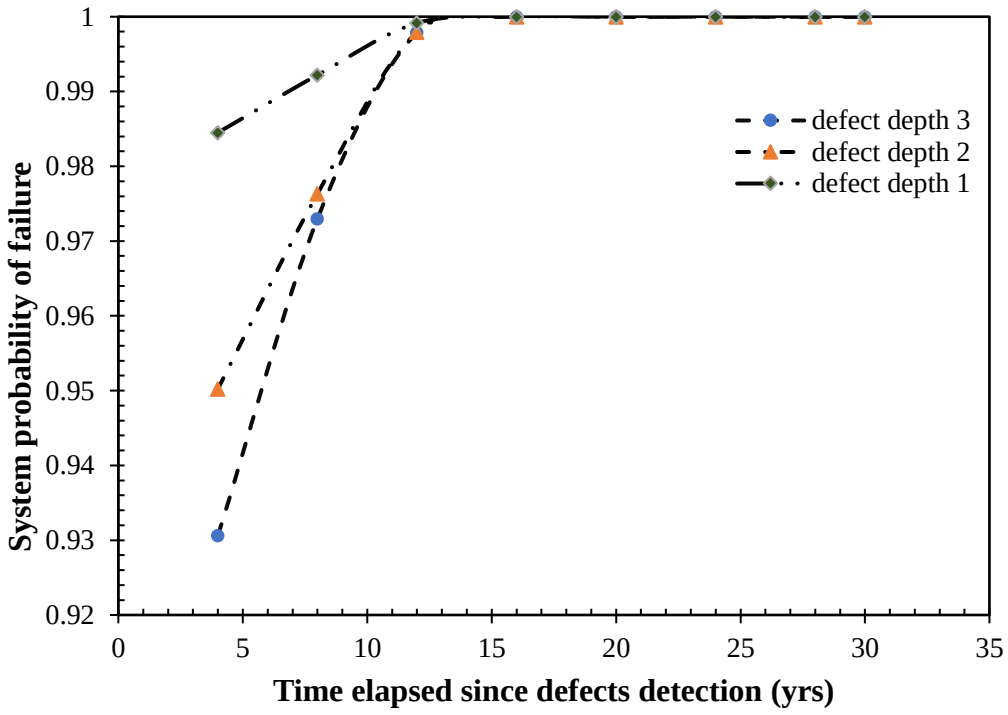

Figure 5.7. System failure probability for multi-failure modes and different corrosion defect depths without correlation effect

Based on Fig. 5.7, the point of coincidence of the failure profiles for the defect depth provides an absolute critical failure year of the offshore system. Consequently, the likely probability of failure due to leak, burst, crack, and rupture can be estimated from Figs. 5.8-5.11, respectively. Fig. 5.8 illustrates the impact of microbial corrosion defect size on the leak failure probability prediction. It reveals that at the 12th year of exposure, the likely failure probability due to leakage increases by 40.9% and 77.1%, as the defect depth increases from 1.46mm to 2.95mm and 4.24mm, respectively. The defect with the maximum defect depth under a severe degradation rate shows the highest likelihood of failure due to leakage, resulting in the system failure.

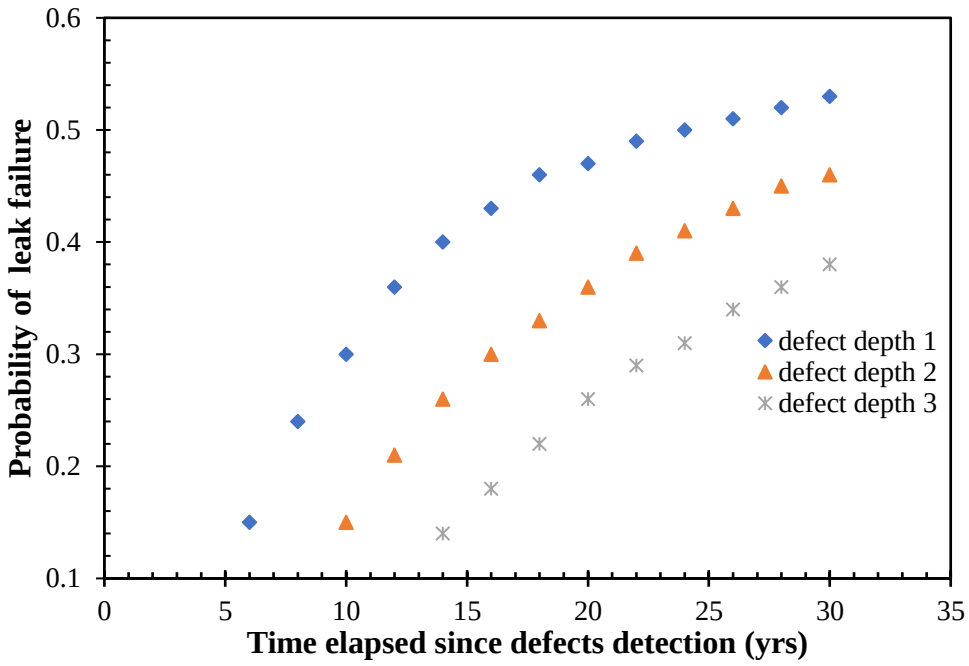

Figure 5.8. Effects of defects depth and rate on the failure probability due to perforation

The performance function due to burst capacity versus time is shown in Fig. 5.9. The burst capacity of the offshore pipeline is characterized by its failure pressure under unstable pressure loads during operation. The influence of this pressure disturbance on the structural failure shows that as the

defect size increases, the system failure pressure reduces due to strength loss over time. In this case, the system may experience stochastic failure characteristics at any point along the internal surface of the pipeline with multispecies biofilms. According to Fig. 5.9, the analysis of the effect of the defect sizes and severe corrosion rate shows a 19.3% and 37.8% increase in the burst failure probability for long term exposure. According to the results, the burst failure contributes about 36.5% to the overall offshore system reliability under microbial corrosion.

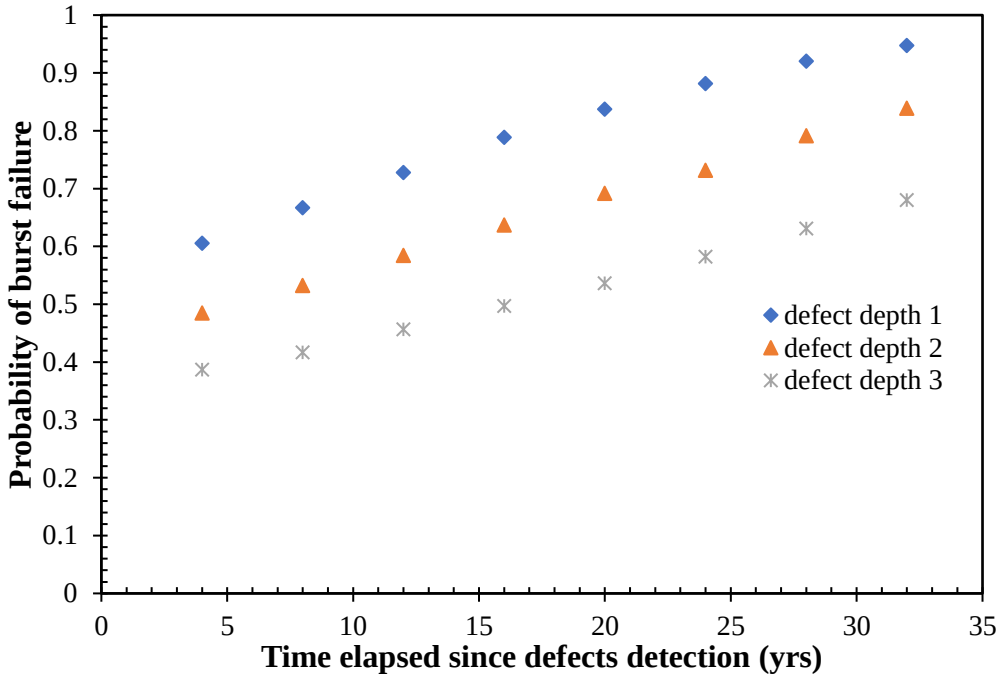

Figure 5.9. Effect of defects depth on the probability of burst failure due to microbial corrosion

As the corrosion defects increase in depth, the stress intensity factors increase at the bottom of the deepest defect, based on its morphology. In this case, the stress field of the pipeline increases under unstable pressure loads. This dynamic pressure disturbance complicates the failure mechanisms, mainly due to the stochastic nature of the microbial corrosion. The limit state function results for

the rupture and stress corrosion cracking (fracture) induced failures are shown in Figs. 5.10-5.11. The output shows that in the 12th year of exposure, the likelihood of rupture failures under an unstable stress field increases with an increase in corrosion defect size. A parametric sensitivity analysis reveals that the longitudinal defect characteristics and flow stress produce an increasing impact on the likelihood of rupture failure caused by a complex multispecies biofilm. Note that the dynamic interactions among the bacteria types in the multispecies biofilm constitute a complex phenomenon that can dynamically alter the stress effects at any time during operation. This is further demonstrated by the crack induced failure prediction in Fig. 5.11.

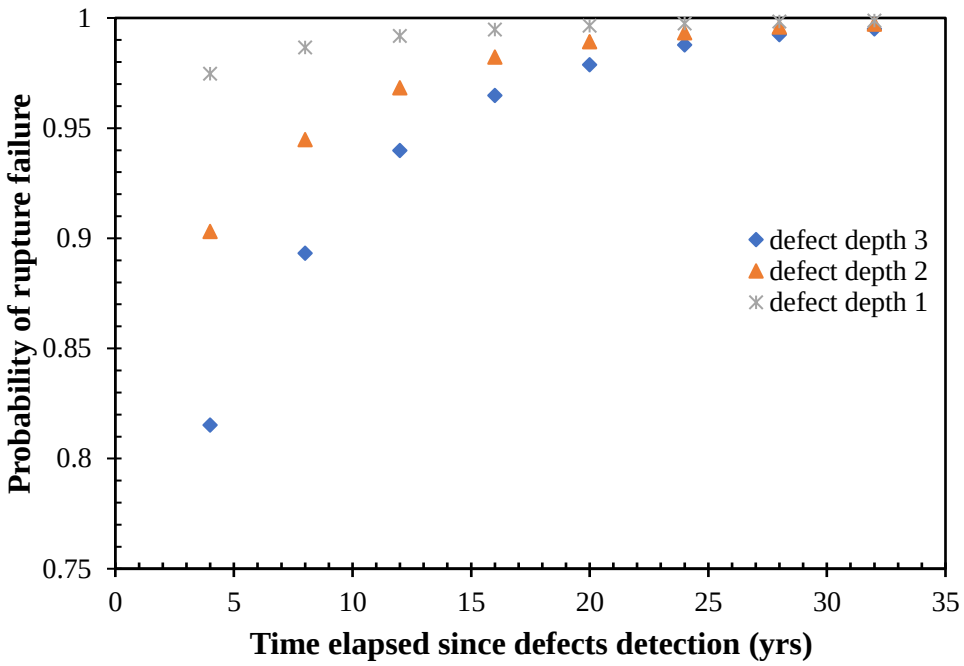

Figure 5.10. Effect of defects depth on the probability of rupture failure due to microbial corrosion

The results in Fig. 5.11 show the effect of stress intensity factors (which is defined by the crack size, far-field stress level, geometry, and microstructural stability) on the failure characteristic of a cracked offshore pipeline segment. Under microbial corrosion, the interactions among the

physio-chemical parameters and the SRB promote an environment that supports the cracking of the steel material. This is likely a result of hydrogen embrittlement and sulfide stress cracking. The characteristic function for the crack induced failure is probabilistically formulated by Eq. (5.6), and the predicted result at the 12^{th} year of exposure gives an upper bound probability of 0.7762. To capture the variability and possible lower bound probability of failure, a 10% lower bounds error interval profile for crack propagation due to the prevailing complex multispecies biofilm is presented.

It is important to note that the rupture and crack modes show a higher degree of influence on the overall system's failure likelihood and the critical failure year. This behavior is due to the cumulative effects of the stress intensity parameters, random fluctuation of the internal pressure, and the dynamic bacteria interactions when there is a considerable reduction in the pipe wall thickness. The percentage contribution of the individual failure modes on the pipeline's overall failure profile at the 12^{th} year of exposure is shown in Table 5.8.

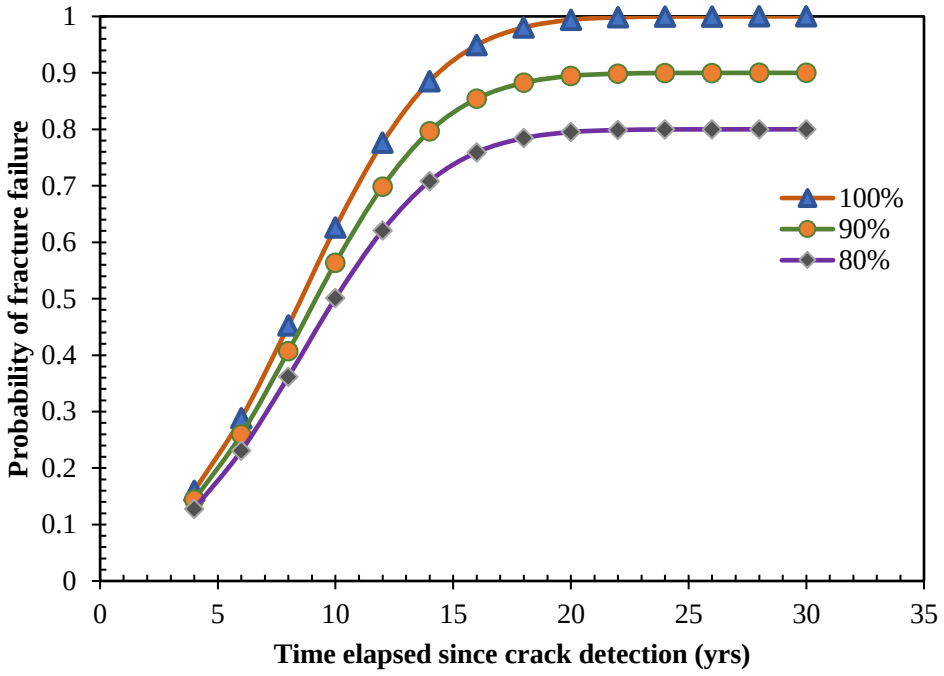

Figure 5.11. Time evolution probability of failure due to MIC induced cracking

Furthermore, the effects of the physio-chemical parameters on the leak failure probability are illustrated in Fig. 5.12. An increase in the corrosion rate is observed due to the interactions among the vital parameters and by placing evidence on their upper bound probability state. The corrosion rate serves as the input parameter to the leak failure limit state function to forecast the effects of the physio-chemical parameters on the leak failure probability (see Fig. 5.12). It is observed that at the 12th year of exposure to the microenvironments, the leak failure probability increases by 23.4%, 13.3%, and 2.6%, respectively. This increase is due to the combined effect of physio-chemical parameters (CO_2, pH, and temperature) interactions and bacteria. This confirms the finding presented in the literature [41,42], implying that in a dynamic microbial-chemical environment, the dynamic dependencies among physio-chemical parameters increase the

corrosion rate and its propagation. Although the degree of influence may be unstable, a parametric impact assessment on the system reliability can be inferred by considering multiple scenarios.

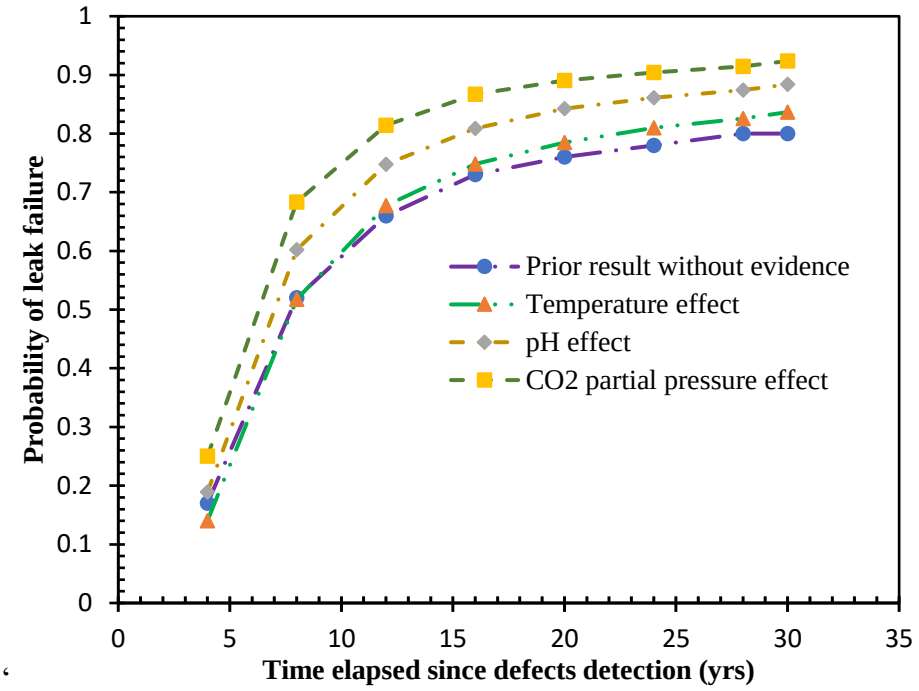

Figure 5.12. Results of the physio-chemical parameters' effect on leak failure mode caused by microbial corrosion

Table 5.8. Critical failure characteristics of an offshore pipeline with microbial corrosion induced multi-failure modes

Critical failure year	Failure modes probabilities											
	Leak			Burst			Crack			Rupture		
	defect 1	defect 2	defect 3	defect 1	defect 2	defect 3	80%	90%	100%	defect 1	defect 2	defect 3
12th year	0.372	0.234	0.093	0.731	0.585	0.459	0.6209	0.6986	0.7762	0.991	0.969	0.945

5.5.3 Corrosion parameters correlation and failure modes effects on the system reliability

The Copula function is adopted to model the impact of the interdependencies among the random corrosion parameters and their failure modes. Its unique advantage helps model the joint probability distribution for the response parameters. The system probability of failure for the likely failure modes is evaluated by Eq. (5.20) using a Copula-based Monte Carlo simulation in the MATLAB environment. For the correlation's effect modeling, an Archimedean Copula family is implemented to predict the copula parameter and Kendall's tau, which defines the dependence measure among the random response parameters. Fig. 5.13 shows the generated sample uniform distribution of the parameters for the Archimedean Copula family. The plot is created based on 1000 samples using the method presented in the reference [67]. The Clayton Copula approach shows relatively stable dependencies in the lower tail of the structure, while the Gumbel Copula reveals a significant dependence at the upper tail. The Frank Copula shows a symmetric profile along the positive correlation axis. In this research, the characterized Kendall's tau values are used as the concordance measure of the parameters, and the Copula is adopted for their joint probability distribution function.

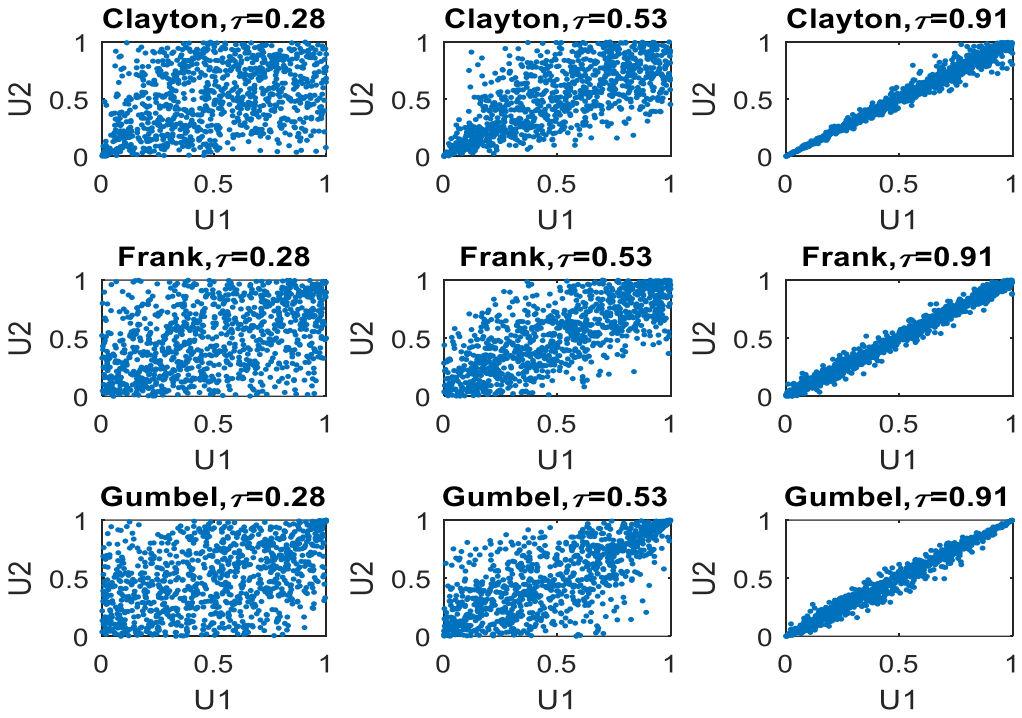

Figure 5.13. Generated standard uniform samples for Kendall's τ values of 0.28, 0.53, and 0.91, respectively

The copula function based on the Kendall's tau values captures the dependencies among the random response parameters for the leak failure probability prediction under the influence of the multispecies biofilm. The overall analysis captures the influence of the physio-chemical parameters and their nonlinear interdependencies on the leak failure probability for long term exposure, as seen in Fig. 5.14. It is found that the leak failure probability decreases by 5.3%, 7.2%, and 9.0% for Kendall's $\tau = 0.28$, Kendall's $\tau = 0.53$, and Kendall's $\tau = 0.91$, respectively, as the exposure time increases. This again confirms that as the value of the dependences measure (Kendall's τ) increases among the response random corrosion variables and the physio-chemical parameters, there is a corresponding decrease in the leak failure probability with time. Although

the decreasing rate is low, the results depict the real case scenario for the corroding offshore pipeline that is exposed to a long term microbial infested environment. This is in agreement with the findings of previous studies [9,33,74]. This provides initial validation for the model application.

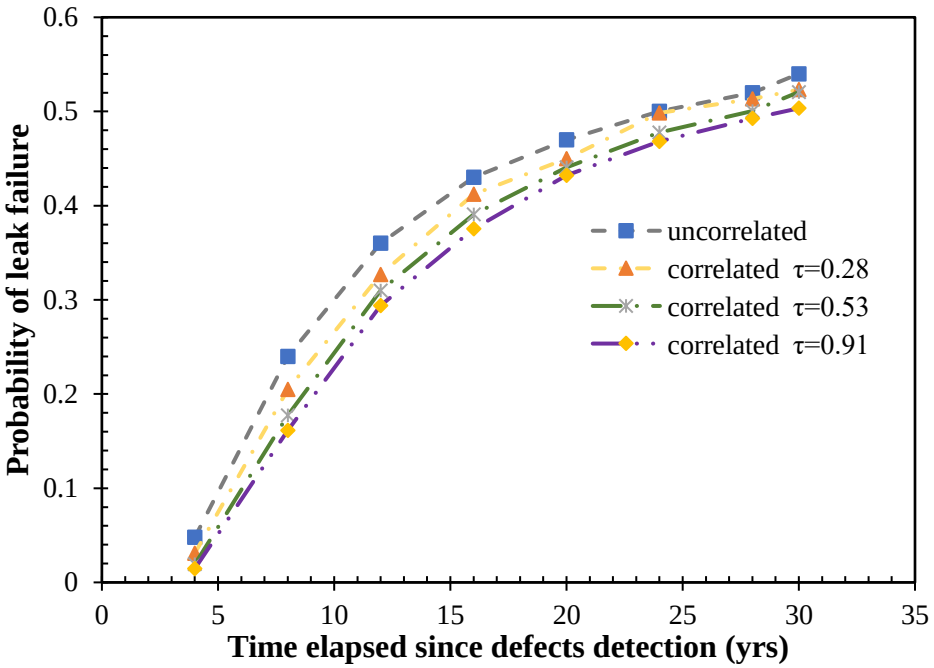

Figure 5.14. Effects of corrosion parameters' dependences on the leak failure probability for the maximum defect size

The proposed model captures the complex interactions among MIC influential factors and the random response parameters' dependencies for the system reliability prediction. According to the results, for long term exposure, the system failure probability decreases by 9.82%, 13.70%, and 19.30% at $\tau = 0.28, \tau = 0.53,$ and $\tau = 0.91$ respectively (see Fig. 5.15). The resulting trend shows a monotonic effect on the system failure probability as the coefficient of rank correlation increases. This finding agrees with the results presented in the literature [9,25]. This further validates the applicability of the proposed approach. Based on the dependencies' cumulative

impact, the likely critical failure year inferred from the system failure profile (in Fig. 5.15) occurs at the 16th year of exposure. Two different indexing scenarios are then employed to predict the leak mode's upper bound failure year and the most critical worst-case scenario for the system reliability, considering dependencies. The results of the analysis are given in Table 5.9. Since the offshore system is treated as a series system, the overall results provide critical information on the system reliability necessary for a precise, effective, and proactive integrity management plan to minimize unnecessary inspection costs and sudden failure for sustainable operations. It could be observed that the results are highly conservative (i.e., overestimated) upon ignoring dependencies, compared to the results when interdependencies of the failure modes' random response parameters are captured. The results provide practical and reliable information on the actual state of the offshore pipeline and its associated failure characteristics for the period under consideration.

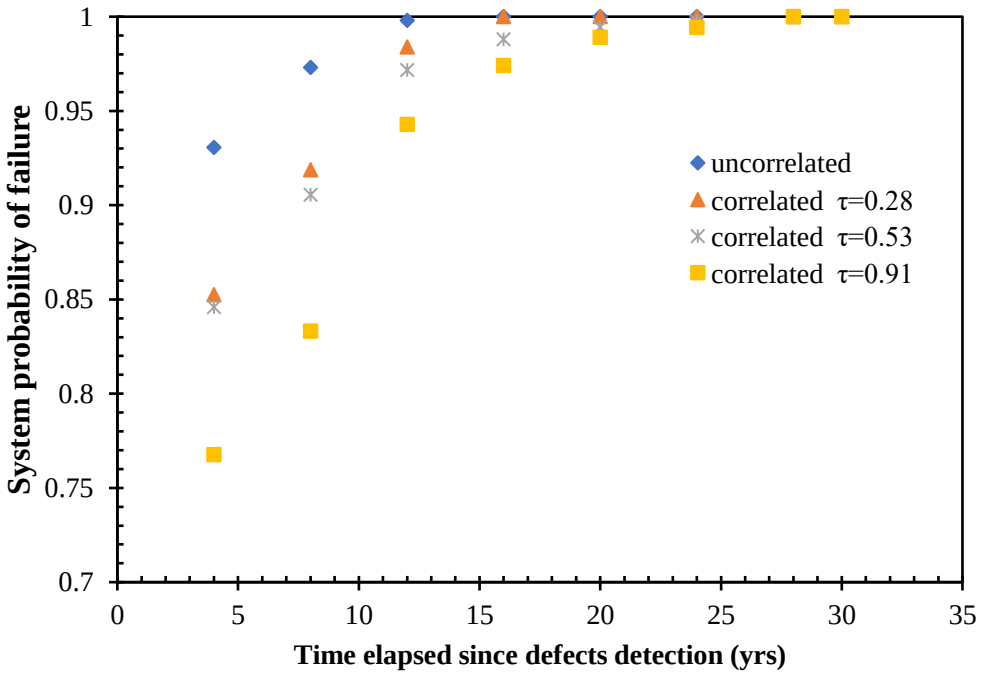

Figure 5.15. Effects of corrosion parameters interdependencies on the system failure probability

Table 5.9. Critical failure year for leak mode and system failure at different indexes

Leak mode (failure time, years)					System mode (failure time, years)				
Failure index	uncorrelated	correlated			Worst-case scenario index	uncorrelated	correlated		
		τ=0.28	τ=0.53	τ=0.91			τ=0.28	τ=0.53	τ=0.91
0.3	9.8	11	11.8	12.5	0.9	4.5	5.9	8	9.9

The results obtained at the prevailing operating conditions are used for reliability-based decision making, as shown in Fig. 5.16. A decision-making strategy is provided in Fig. 5.16 by showing the likely failure year based on the failure probability and the degree of correlation among the random corrosion parameters. Consequently, a reliable inspection and maintenance interval can be inferred based on the main operating conditions of the offshore pipeline.

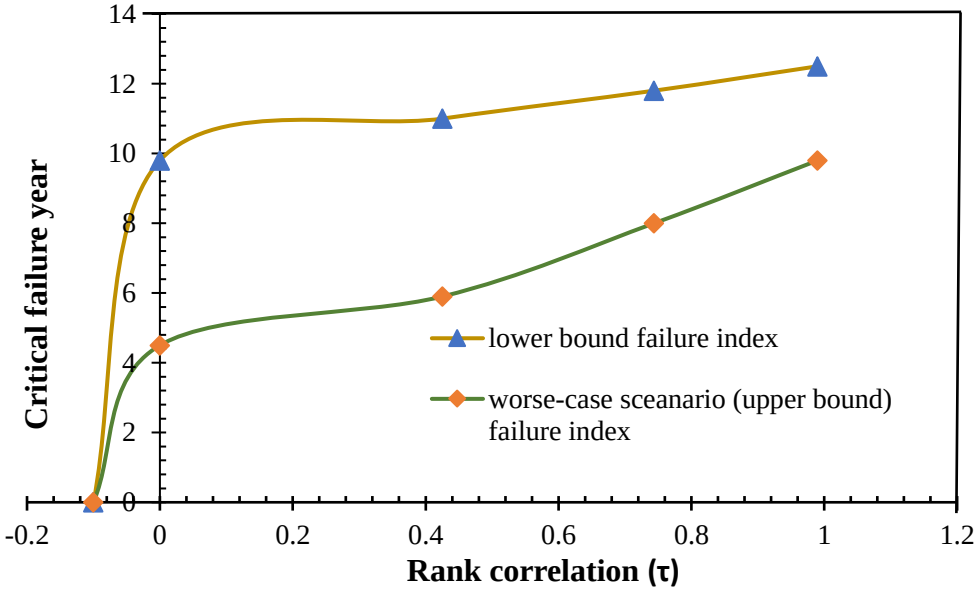

Figure 5.16. Effect of corrosion parameters dependencies on the critical failure year for the offshore pipeline at different failure indexes

The current study offers robust dynamic condition assessment criteria based on the associated dependencies among random corrosion parameters and failure modes for pipeline reliability under MIC. However, the hybrid methodology may have some limitations. The major setback in the BN is the associated subjectivity with the prior and posterior probability estimation. The substantial influence of the probability distribution of the monitoring operating parameters and the random corrosion response variables may introduce further subjectivity in the CMC model analysis. Also, the proposed approach does not consider the multiple defects interactions.

5.6. Conclusions

The current research demonstrates the application of a hybrid connectionist methodology, and the integration of BN and Copula-based Monte Carlo simulation (BN-CMC), for reliability prediction of a corroding offshore pipeline. The methodology captures the effects of dynamic nonlinear interactions among the physio-chemical parameters, and the failure modes on the system reliability. It is found that the complex interplay among the physio-chemical parameters increases the corrosion rate and the likelihood of leak failure when dealing with multispecies biofilms. However, due to the instability in the dependencies among the corrosion's influential parameters, the critical failure year due to leak failure increases for long term exposure cases. The reason for this behavior might be that for long term exposure, the effect of the physio-chemical parameters interactions and the bacteria diversity decreases, and the growth rate of corrosion defects becomes steady, exhibiting a limiting factor.

Furthermore, the instability in the physio-chemical parameters' interactions with the bacteria and the failure modes diversely affects the system reliability at different levels of factors'

dependencies. It is concluded that an increase in the offshore pipeline's critical failure year is experienced as the value of the Kendall tau increases. This is due to the likely decrease in the upper bound failure probability as the exposure time increases under the combined effects of the physio-chemical parameters' interactions and random corrosion variables' dependencies. It is important to note that the complex instability in mixed microbial communities and the variability in the response parameters of failure modes are the vital factors of critical safety in corroding offshore systems. The effects of the complex interactions and instability among the microbial corrosion parameters are captured through the failure index analysis for the leak mode and system mode, respectively.

The introduced methodology offers a robust and dynamic tool for risk-based inspection and maintenance planning to sustain offshore operations experiencing microbial corrosion. Certainly, the model could be improved in future research by i) considering multiple defects interactions under multi-failure modes' dependencies and multispecies biofilm architecture, and ii) considering the effects of probability distribution types and the changes in the coefficient of variation of the random response variables and the operating pressure on the pipeline failure behavior under parametric interdependencies.

Acknowledgments

The authors acknowledge the financial support provided by Genome Canada and their supporting partners, and the Canada Research Chair (CRC) Tier I Program in Offshore Safety and Risk Engineering.

References

[1] Shifler DA. Understanding material interactions in marine environments to promote extended structural life. Corros Sci 2005;47:2335–52. https://doi.org/10.1016/j.corsci.2004.09.027.

[2] Alaba PA, Adedigba SA, Olupinla SF, Agboola O, Sanni SE. Unveiling Corrosion Behavior of Pipeline Steels in CO2-Containing Oilfield Produced Water: Towards Combating the Corrosion Curse. Crit Rev Solid State Mater Sci 2019:1–22. https://doi.org/10.1080/10408436.2019.1588706.

[3] Silva SC da, de Souza EA, Pessu F, Hua Y, Barker R, Neville A, et al. Cracking mechanism in API 5L X65 steel in a CO2-saturated environment. Eng Fail Anal 2019;99:273–91. https://doi.org/10.1016/j.engfailanal.2019.02.031.

[4] Sui P, Sun J, Hua Y, Liu H, Zhou M, Zhang Y, et al. Effect of temperature and pressure on corrosion behavior of X65 carbon steel in water-saturated CO2 transport environments mixed with H2S. Int J Greenh Gas Control 2018;73:60–9. https://doi.org/10.1016/j.ijggc.2018.04.003.

[5] Ibrahim A, Hawboldt K, Bottaro C, Khan F. Review and analysis of microbiologically influenced corrosion: the chemical environment in oil and gas facilities. Corros Eng Sci Technol 2018:1–15. https://doi.org/10.1080/1478422X.2018.1511326.

[6] Abbas M, Shafiee M. An overview of maintenance management strategies for corroded steel structures in extreme marine environments. Mar Struct 2020;71:102718. https://doi.org/10.1016/j.marstruc.2020.102718.

[7] Xiaoxia S. Biofilm Formation and Its Induced Biocorrosion of Metals in Seawater. PhD Thesis, National University of Singapore, 2007.

[8] El M, Ben A, Keshtegar B, Correia JAFO, Lesiuk G, De Jesus AMP. Reliability analysis based on hybrid algorithm of M5 model tree and Monte Carlo simulation for corroded pipelines : Case of study X60 Steel grade pipes. Eng Fail Anal 2019;97:793–803. https://doi.org/10.1016/j.engfailanal.2019.01.061.

[9] Fu G, Yang W, Li C, Shi W. Reliability analysis of corrosion affected underground steel pipes considering multiple failure modes and their stochastic correlations. Tunn Undergr Sp Technol 2019;87:56–63. https://doi.org/10.1016/j.tust.2019.02.005.

[10] Zhang P, Su L, Qin G, Kong X, Peng Y. Failure probability of corroded pipeline considering the correlation of random variables. Eng Fail Anal 2019;99:34–45. https://doi.org/10.1016/j.engfailanal.2019.02.002.

[11] Yang X, Saevik S, Sun L. Numerical analysis of buckling failure in flexible pipe tensile armor wires. Ocean Eng 2015;108:594–605. https://doi.org/10.1016/j.oceaneng.2015.08.011.

[12] Gong C, Zhou W. Importance sampling-based system reliability analysis of corroding pipelines considering multiple failure modes. Reliab Eng Syst Saf 2018;169:199–208. https://doi.org/10.1016/j.ress.2017.08.023.

[13] Gong C, Zhou W. First-order reliability method-based system reliability analyses of corroding pipelines considering multiple defects and failure modes. Struct Infrastruct Eng 2017;2479:1–11. https://doi.org/10.1080/15732479.2017.1285330.

[14] Mahmoodian M, Aryai V. Structural failure assessment of buried steel water pipes subject to corrosive environment. Urban Water J 2017;14:1023–30. https://doi.org/10.1080/1573062X.2017.1325500.

[15] Song J, Lu Z. Moment method based on fuzzy reliability sensitivity analysis for a degradable structural system. Chinese J Aeronaut 2008;21:518–25. https://doi.org/10.1016/S1000-9361(08)60169-7.

[16] Lu Z, Song J, Song S, Yue Z, Wang J. Reliability sensitivity by method of moments. Appl Math Model 2010;34:2860–71. https://doi.org/10.1016/j.apm.2009.12.020.

[17] Qian G, Niffenegger M, Li S. Probabilistic analysis of pipelines with corrosion defects by using FITNET FFS procedure. Corros Sci 2011;53:855–61. https://doi.org/10.1016/j.corsci.2010.10.014.

[18] Mahmoodian M, Li CQ. Failure assessment and safe life prediction of corroded oil and gas pipelines. J Pet Sci Eng 2017;151:434–8. https://doi.org/10.1016/j.petrol.2016.12.029.

[19] Mahmoodian M, Li CQ. Stochastic failure analysis of defected oil and gas pipelines. Handb. Mater. Fail. Anal. with Case Stud. from Oil Gas Ind., Elsevier Ltd.; 2016, p. 235–55. https://doi.org/10.1016/B978-0-08-100117-2.00014-5.

[20] Teixeira AP, Soares CG, Netto TA, Estefen SF. Reliability of pipelines with corrosion defects. Int J Press Vessel Pip 2008;85:228–37. https://doi.org/10.1016/j.ijpvp.2007.09.002.

[21] Qin H. Probabilistic Modeling and Bayesian Inference of Metal-Loss Corrosion with Application in Reliability Analysis for Energy Pipelines. Master Thesis; University of Western Ontario, 2014.

[22] Adumene S, Khan F, Adedigba S. Operational safety assessment of offshore pipeline with multiple MIC defects. Comput Chem Eng 2020;138. https://doi.org/10.1016/j.compchemeng.2020.106819.

[23] Gong C, Frangopol DM. Time-variant hull girder reliability considering spatial dependence of corrosion growth, geometric and material properties. Reliab Eng Syst Saf 2020;193. https://doi.org/10.1016/j.ress.2019.106612.

[24] Hashemi SJ, Ahmed S, Khan FI. Loss scenario analysis and loss aggregation for process facilities. Chem Eng Sci 2015;128:119–29. https://doi.org/10.1016/j.ces.2015.01.061.

[25] Zhou W, Hong HP, Zhang S. Impact of dependent stochastic defect growth on system reliability of corroding pipelines. Int J Press Vessel Pip 2012;96–97:68–77. https://doi.org/10.1016/j.ijpvp.2012.06.005.

[26] Melchers RE, Beck AT. Structural Reliability Analysis and Prediction. 3rd ed. John Wiley & Sons, Chichester; 2018.

[27] Eckert R. Field Guide for Investigating Internal Corrosion of Pipelines. NACE International, Houston USA; 2003.

[28] Dwivedi SK, Vishwakarma M. Effect of hydrogen in advanced high strength steel materials. Int J Hydrogen Energy 2019;44:28007–30. https://doi.org/10.1016/j.ijhydene.2019.08.149.

[29] Mohtadi-Bonab MA, Eskandari M. A focus on different factors affecting hydrogen induced

cracking in oil and natural gas pipeline steel. Eng Fail Anal 2017;79:351–60. https://doi.org/10.1016/j.engfailanal.2017.05.022.

[30] Wang S, Nagao A, Sofronis P, Robertson IM. Assessment of the impact of hydrogen on the stress developed ahead of a fatigue crack. Acta Mater 2019;174:181–8. https://doi.org/10.1016/j.actamat.2019.05.028.

[31] Gu T, Zhao K, Nesic S. A new mechanistic model for MIC based on a biocatalytic cathodic sulfate reduction theory. Corrosion 2009:1–12.

[32] Marciales A, Peralta Y, Haile T, Crosby T, Wolodko J. Mechanistic microbiologically influenced corrosion modeling — A review. Corros Sci 2019;146:99–111. https://doi.org/10.1016/j.corsci.2018.10.004.

[33] Melchers RE, Jeffrey R. The critical involvement of anaerobic bacterial activity in modelling the corrosion behaviour of mild steel in marine environments. Electrochim Acta 2008;54:80–5. https://doi.org/10.1016/j.electacta.2008.02.107.

[34] Mokhtari M, Melchers RE. A new approach to assess the remaining strength of corroded steel pipes. Eng Fail Anal 2018;93:144–56. https://doi.org/10.1016/j.engfailanal.2018.07.011.

[35] Melchers RE. Corrosion uncertainty modelling for steel structures. J Constr Steel Res 1999;52:3–19. https://doi.org/10.1016/S0143-974X(99)00010-3.

[36] Kammouh O, Gardoni P, Cimellaro GP. Probabilistic framework to evaluate the resilience of engineering systems using Bayesian and dynamic Bayesian networks. Reliab Eng Syst Saf 2020;198:106813. https://doi.org/10.1016/j.ress.2020.106813.

[37] Kannan P, Kotu SP, Pasman H, Vaddiraju S, Jayaraman A, Mannan MS. A systems-based approach for modeling of microbiologically influenced corrosion implemented using static and dynamic Bayesian networks. J Loss Prev Process Ind 2020;65:104108. https://doi.org/10.1016/j.jlp.2020.104108.

[38] Adumene S, Khan F, Adedigba S, Zendehboudi S, Shiri H. Dynamic risk analysis of marine and offshore systems suffering microbial induced stochastic degradation. Reliab Eng Syst Saf 2020;207:107388. https://doi.org/10.1016/j.ress.2020.107388.

[39] Mamudu A, Khan F, Zendehboudi S, Adedigba S. Dynamic risk assessment of reservoir production using data-driven probabilistic approach. J Pet Sci Eng 2020;184. https://doi.org/10.1016/j.petrol.2019.106486.

[40] Pak KR, Lee HJ, Lee HK, Kim YK, Oh YS, Choi SC. Involvement of organic acid during corrosion of iron coupon by Desulfovibrio desulfuricans. J Microbiol Biotechnol 2003;13:937–41.

[41] Palmer A, King R. Subsea pipeline engineering. 2nd editio. Oklahoma USA: PennWell Corporation; 2008.

[42] Bai H, Wang Y, Ma Y, Zhang Q, Zhang N. Effect of CO2 partial pressure on the corrosion behavior of J55 carbon steel in 30% crude oil/brine mixture. Materials (Basel) 2018;11. https://doi.org/10.3390/ma11091765.

[43] Renpu W. Oil and gas well corrosion and corrosion prevention,. Adv. Well Complet. Eng. 3rd Editio, Gulf professional publishing, Boston; 2011, p. 619–39.

[44] Garbatov Y, Guedes Soares C. Spatial corrosion wastage modeling of steel plates exposed to marine environments. J Offshore Mech Arct Eng 2019;141:1–6. https://doi.org/10.1115/1.4041991.

[45] Guedes-Soares C, Garbatov Y, Zayed A, Wang G. Non-linear Corrosion Model for Immersed Steel Plates Accounting for Environmental Factors. SNAME Mar. Technol. Conf. Expo, 2005, p. 193–212.

[46] Melchers RE. Effect of temperature on the marine immersion corrosion of carbon steels. Corrosion 2002;58:768–82. https://doi.org/10.5006/1.3277660.

[47] Bhandari J, Khan F, Abbassi R, Garaniya V. Pitting Degradation Modeling of Ocean Steel Structures Using Bayesian Network. J Offshore Mech Arct Eng 2017;139:1–11. https://doi.org/10.1115/1.4036832.

[48] Taleb-berrouane M, Khan F, Hawboldt K, Eckert R, Skovhus TL. Model for microbiologically influenced corrosion potential assessment for the oil and gas industry. Corros Eng Sci Technol 2018:1–15. https://doi.org/10.1080/1478422X.2018.1483221.

[49] Palencia OG, Teixeira AP, Soares CG. Safety of Pipelines Subjected to Deterioration Processes Modeled Through Dynamic Bayesian Networks. J Offshore Mech Arct Eng 2019;141:1–11. https://doi.org/10.1115/1.4040573.

[50] Adumene S, Adedigba S, Khan F, Zendehboudi S. An integrated dynamic failure assessment model for offshore components under microbiologically influenced corrosion. Ocean Eng 2020;218. https://doi.org/10.1016/j.oceaneng.2020.108082.

[51] Witek M. Gas transmission pipeline failure probability estimation and defect repairs activities based on in-line inspection data. Eng Fail Anal 2018;70:255–72. https://doi.org/10.1016/j.engfailanal.2016.09.001.

[52] Bhardwaj U, Teixeira AP, Guedes Soares C. Uncertainty in reliability of thick high strength pipelines with corrosion defects subjected to internal pressure. Int J Press Vessel Pip 2020;188:104170. https://doi.org/10.1016/j.ijpvp.2020.104170.

[53] DNV. Corroded Pipelines - Dnv-Rp-F101. 2010. https://doi.org/DOI: 10.1016/B978-008044566-3.50040-3.

[54] Cicero S, Lacalle R, Cicero R, Ferren D. Assessment of local thin areas in a marine pipeline by using the FITNET FFS corrosion module. Int J Press Vessel Pip 2009;86:329–34. https://doi.org/10.1016/j.ijpvp.2008.11.021.

[55] Fang BY, Atrens A, Wang JQ, Han EH, Zhu ZY, Ke W. Review of stress corrosion cracking of pipeline steels in “low” and “high” pH solutions. J Mater Sci 2003;38:127–32. https://doi.org/10.1023/A:1021126202539.

[56] Depover T, Laureys A, Escobar DP, Van den Eeckhout E, Wallaert E, Verbeken K. Understanding the interaction between a steel microstructure and hydrogen. Materials (Basel) 2018;11. https://doi.org/10.3390/ma11050698.

[57] Budden PJ, Sharples JK, Dowling AR. The R6 procedure: Recent developments and comparison with alternative approaches. Int J Press Vessel Pip 2001;77:895–903. https://doi.org/10.1016/S0308-0161(01)00012-6.

[58] Zerbst U, Kiyak Y, Madia M, Burgold A, Riedel G. Reference loads for plates with semi-elliptical surface cracks subjected to tension and bending for application within R6 type

flaw assessment. Eng Fract Mech 2013;99:132–40. https://doi.org/10.1016/j.engfracmech.2012.11.017.

[59] Xie C, Huang HZ. A Probabilistic Physics of Failure Approach for Structure Corrosion Reliability Analysis. Int J Corros 2016;2016. https://doi.org/10.1155/2016/1343587.

[60] Hasan SM, Khan F, Kenny S. Probabilistic transgranular stress corrosion cracking analysis for oil and gas pipelines. J Press Vessel Technol Trans ASME 2012;134:1–9. https://doi.org/10.1115/1.4006125.

[61] Wu G. A Probabilistic-Mechanistic Approach to Modelling Stress Corrosion Cracking Propagation in Alloy 600 Components with Applications. University of Maryland, College Park, USA, 2011.

[62] Dong Y, Teixeira AP, Guedes Soares C. Application of adaptive surrogate models in time-variant fatigue reliability assessment of welded joints with surface cracks. Reliab Eng Syst Saf 2020;195:106730. https://doi.org/10.1016/j.ress.2019.106730.

[63] Kiefner JF, A MW, Eiber RJ, Duffy AR. Failure stress levels of flaws in pressurized cylinders, Progress in flaw growth and fracture toughness testing. ASTM STP 536, Am Soc Test Mater 1973.

[64] Ossai CI, Boswell B, Davies IJ. Application of Markov modelling and Monte Carlo simulation technique in failure probability estimation — A consideration of corrosion defects of internally corroded pipelines. Eng Fail Anal 2016;68:159–71. https://doi.org/10.1016/j.engfailanal.2016.06.004.

[65] Mai J-F, Scherer M. Financial Engineering with Copulas Explained. 1st Editio. UK: Palgrave Macmillan; 2014. https://doi.org/10.1017/CBO9781107415324.004.

[66] Sklar A. Fonctions de R{é}partition {à} n Dimensions et Leurs Marges. Publ L'Institut Stat L'Universit{é} Paris 1959.

[67] Cherubini U, Luciano E, Vecchiato W. Copula methods in finance. 1st Editio. John Wiley & Sons, Ltd, UK; 2004. https://doi.org/10.1017/CBO9781107415324.004.

[68] Gu YK, Fan CJ, Liang LQ, Zhang J. Reliability calculation method based on the Copula

function for mechanical systems with dependent failure. Ann Oper Res 2019. https://doi.org/10.1007/s10479-019-03202-5.

[69] Okoro C, Ekun OA, Nwume MI, Lin J. Molecular analysis of microbial community structures in Nigerian oil production and processing facilities in order to access souring corrosion and methanogenesis. Corros Sci 2016;103:242–54.

[70] Al-jaroudi S, Ul-hamid A, Al-Gahtani MM. Failure of crude oil pipeline due to microbiologically induced corrosion. Corros Eng Sci Technol 2011;46:568–79. https://doi.org/10.1179/147842210X12695149033819.

[71] Yang S, Li CQ, Yang W. Analytical model of elastic fracture toughness for steel pipes with internal cracks. Eng Fract Mech 2016;153:50–60. https://doi.org/10.1016/j.engfracmech.2015.11.014.

[72] Yang W, Fu G, Li C-Q. Elastic Fracture Toughness of Ductile Materials. J Eng Mech 2017;143:04017111. https://doi.org/10.1061/(asce)em.1943-7889.0001321.

[73] NACE-RP0775. Recommended Practice Preparation, Installation, Analysis, and Interpretation of Corrosion Coupons in Oilfield Operations. NACE Int Houston, TX USA, 2005.

[74] Al-Darbi MM, Agha K, Islam MR. Comprehensive Modelling of the Pitting Biocorrosion of Steel. Can J Chem Eng 2005;83:872–81. https://doi.org/10.1002/cjce.5450830509.

Chapter 6

Offshore pipeline integrity assessment considering material and parametric uncertainty

Preface

A version of this chapter has been submitted to the ***Journal of Pipeline Science and Engineering.*** *I am the primary author along with the Co-authors, Faisal Khan, Sundady Adedigba, Sohrab Zendehboudi, and Hodjat Shiri. I developed the conceptual framework for the integrity assessment model and carried out the literature review. I prepared the first draft of the manuscript and subsequently revised the manuscript based on the co-authors' feedbacks. Co-author Faisal Khan helped in the concept development, design of methodology, reviewing, and revising the manuscript. Co-author Sunday Adedigba provided support in implementing the concept and testing the model. Co-author Sohrab Zendehboudi provided fundamental assistance in validating, reviewing, and correcting the model and results. Co-author Hodjat Shiri provided support in reviewing and correcting the manuscript. The co-authors also contributed to the review and revision of the manuscript.*

Abstract

This chapter presents a methodology that integrates the semi-empirical corrosion models with probabilistic analysis to study steel structural failure behavior considering material and parametric uncertainties. The semi-empirical models are used to assess the asset's susceptibility, system degradation rate, and defect growth over time under harsh corrosive environments. The developed model is translated into a limit state function in a probabilistic framework to define the asset's safe operating envelope. The probabilistic framework is simulated considering the variation in the material properties of steel grades, corrosion response parameters, and different susceptibility

models. The variabilities in the ultimate tensile strength, operating pressure, and wall thickness exhibit the highest contributions to pipeline failure behavior in a harsh offshore environment. It is also observed that the failure probability of the pipeline increases with an increase in the coefficient of variation at the lower bound of failure, while it decreases at the upper bound of failure. The coefficient of variation for the tensile strength shows a 32.2% (the highest) impact on the limit state function performance as the year of exposure progresses. The proposed approach offers a systematic framework for an appropriate material selection and risk-based integrity management strategy for offshore structures, including pipelines.

Keywords: Mixed corrosion environment; Offshore steel pipelines; Monte Carlo simulation; Failure probability; Uncertainty; Parametric variability

6.1. Introduction

Offshore pipeline failure in the ocean environment is influenced by the environment, material chemical composition, and the material microstructural formation. These factors pose different potential effects on the susceptibility of the steel structure over time. They are also crucial factors in the pipeline selection process and life cycle prediction/management during operation, especially in harsh ocean environments. Several studies have indicated that material microstructural variability of steel structures plays a vital role in their corrosion susceptibility potentials [1–3]. Offshore steel structures present complex failure characteristics due to high variability in microstructural parameters and their interactions with the harsh environment. A comprehensive understanding of the system's failure behavior is needed for a proactive integrity management strategy. The interplay of these influencing factors' variability on the offshore steel pipelines'

structural behavior under different susceptibility models is critical for system integrity management, especially in bacteria-infested offshore environments.

The material elements and corrosion influential factors present complex interdependent characteristics. This dependency could influence the failure behavior of the steel structure. The failure complexity is characterized by the difference in the potential of the heterogeneities in the material structure. These heterogeneities could result from the atomic to microns scales, including defects in the metal crystal structure, non-metallic inclusion, chemical phase structure, elements, and/or phase segregation [3,4]. Therefore, it is essential to adequately understand the correlation of corrosion with the microstructural/material formation of the system.

Various studies have focused on the effect of microstructure/material properties on corrosion susceptibility of engineering systems [4–12]. For example, Hwang et al. [4] experimentally investigated the correlation of microstructure and fracture properties of steel pipelines based on the pressed notch drop-weight tear test (DWTT) and Charpy V-notch (CVN) impact test, and the authors concluded that change in the alloying elements (such as Mo, C, Cu) and the high-toughness steel pipe (API X70) show different crack susceptibility potentials. There is an increase in the fracture properties as indicated by the highest upper self-energy (USE). Bastos et al. [10] experimentally examined the corrosion susceptibility of UNS32750 steels under three different microstructures in harsh environmental conditions. They found that the steel's corrosion characteristic strongly correlates with the microstructure, especially under the combined effect of very high hydrogen sulphide and chloride concentration. As the steel is exposed to harsh environmental conditions under increasing temperature, the pitting resistance is decreased due to precipitation.

Furthermore, the impact of carbon steel microstructure on the corrosion rate and sulphide stress cracking (SSC) susceptibility has been discussed in the literature [3,9,13]. Xue and Cheng [13] showed that the material microstructure influences the rate of corrosion of the carbon steel. This is evidenced in the localized corrosion susceptibility potentials and the presence of pearlite bands in the steel microstructure. The polarization curves and permeation measurement show that the high-strength steel pipe with a martensitic microstructure is most susceptible to SSC at all temperatures. Sun et al. [6] investigated the impacts of material microstructure and its carbon content on steel pipelines' corrosion properties. It was observed that an increase in the carbon content decreases the ferrite and increases the cathode/anode area ratio. This results in an increase in the corrosion rate from 0.30 to 0.90 mm/year when the carbon content increases from 0.05 to 0.13 wt%. Katiyar et al. [8] studied the corrosion behavior of coarse, medium, and fine ferrite-pearlite, martensite, and tempered martensite microstructure reinforced bars. It was concluded that the corrosion susceptibility increases based on their material microstructural formation in a high pH environment.

To further understand the variability in the material elements and corrosion response parameters, Lee et al. [14] proposed the application of a probabilistic strategy. The authors introduced the integration of the homogenization method with Monte Carlo simulation (MCS) to estimate the equivalent microstructure and behavior of the fiber and matrix constituents of glass/epoxy compositions. The main objective is to capture the variability in the basic microstructural elements/properties and to minimize uncertainty. The stochastic analysis shows the effect of variability and probability distribution type on the steel's macroscopic mechanical properties. Further information/discussion on probabilistic/stochastic models for microstructural analysis can be found in the literature [15–19].

The reviewed literature has shown the potential influence of the microstructural/material properties on steel pipelines' integrity. However, there is a limited understanding of how the degree of impact propagates to the system's failure in a harsh bacteria-infested environment. It is clear from the reviewed literature that there are a low number of studies that investigated the effect of microstructural element variability on the offshore systems failure characteristic. The offshore system microstructural response in a mixed chloride-CO_2-H_2S-bacteria-infested/corrosive environment has not been studied. The effects of microstructural elements' variability on the offshore systems' failure need to be further explored. The associated failure dependency on the material formation and its corresponding parametric uncertainty in the steel pipe still requires further research. Thus, we need to study and understand the offshore pipeline failure behavior under different corrosion susceptibility models in a mixed corrosive environment, for risk-based integrity management.

Moreover, the diversity in alloying elements (nickel, chromium, niobium, carbon, and sulfur) inclusion in steels of the same grade among different manufacturers presents complexity in prediction of their corrosion susceptibility behaviors. The interaction of the material elements and the chemical composition in a mixed chloride-CO_2-H_2S-bacteria-infested (corrosive) environment could further complicate the material degradation potential. This will increase the chance of the steel pipeline failure. These knowledge gaps necessitate the development of an integrated probabilistic approach for a comparative study of the steel grades microstructural and parametric uncertainties' effects on the pipeline's integrity by considering different corrosion susceptibility models.

The current research presents the integration of semi-empirical models with MCS for a comparative analysis of internally corroding offshore systems failure behavior considering

different material microstructure (steel grade) and susceptibility models. The semi-empirical models capture various corrosion susceptibility response parameters for defect propagation prediction for different material structures. The semiempirical models' outputs are mapped into the likely failure modes formulation under a complex and mixed corrosion environment. The developed failure state equations are modeled using the Monte Carlo algorithm considering the randomness in the essential random variables and the stochastic nature of the microbial corrosion phenomenon. The proposed approach is demonstrated on three different steel grade pipelines with corrosion defects under different susceptibility models. The model explores: i) the effects of heterogeneities' characteristics and mixed corrosive environment on the failure behavior of the steel pipelines, ii) the impact of the susceptibility model on the strength loss over time under a mixed corrosive environment, and iii) the variability in the material microstructure and corrosion response parameters for failure behavior prediction and integrity management. The proposed approach provides a risk-based tool for a well-informed material selection, condition monitoring, and treatments/environmental control strategy in corroding systems integrity management.

6.2. Offshore pipeline corrosion susceptibility analysis

The environmental influential factors' interaction with the steel pipes' microstructural/material formation could enhance their corrosion susceptibility potentials. The literature has shown that the corrosion rates of the steel pipes increase in different material microstructures, such as pearlitic steel, bainitic steel, spheroidized steel, martensitic steel, and tempered martensitic steel [1]. Robust models are required to model the susceptibility potentials and the propagation rate of the corrosion defect under a complex microenvironment. Some empirical, phenomenological, probabilistic and semi-empirical corrosion susceptibility models have been recently reported in the literature

[20,21,30,31,22–29]. An overview of the common susceptibility models for both external and internal corrosion is shown in Table 1.

Table 6.1. Empirical/semi-empirical corrosion susceptibility models for offshore systems

Model	Application	Source
Southwell's linear model; $$d(t) = 0.076d + 0.038t$$	Steel structure	[32]
Southwell's bi-linear model; $$d(t) = \begin{cases} 0.09t & 0 \le t < 1.46y \\ 0.76 + 0.038t & 1.46 \le t < 16y \end{cases}$$	Steel structure	[32]
Melchers-Southwell's nonlinear model: $$d(t) = 0.84t^{0.823}$$	Marine structure	[33]
Melcher's power law model: $$d(t) = 0.1207t^{0.6257}$$	Marine structure	[33]
Melcher's tri-linear model: $$d(t) = \begin{cases} 0.170t & 0 \le t < y \\ 0.152 + 0.0186t & 1 \le t < 8y \\ -0.364 + 0.083t & 8 \le t < 16y \end{cases}$$	Marine steel structure	[29,33]
Yamamoto-Ikegami's nonlinear model: $$d(t) = C_1(t - T_0 - T_t)^{C_2}$$	Ship structure	[34]
Paik's nonlinear model: $$d(t) = C_1(t - t_{cl})^{C_2}$$	Ship structure	[35]
Paik & Kim model: $$d_C = \frac{\alpha}{\beta}\left(\frac{Y_e}{\beta}\right)^{\alpha-1} exp\left[-\left(\frac{Y_e}{\beta}\right)^{\alpha}\right]$$ $$\alpha = 0.0020Y_e^3 - 0.0994Y_e^2 + 1.5604Y_e - 6.0025$$ $$\beta = 0.0004Y_e^3 - 0.0248Y_e^2 + 0.4793Y_e - 2.3812$$	Ship structure	[21]
Soares and Garbatov model: $$d(t) = d_\infty\left[1 - e^{\left(\frac{t-T_c}{T_t}\right)}\right]$$	Ship structure	[36]

Mohd & Kee model: $$f_c = \frac{\alpha}{\beta}\left(\frac{Y_e}{\beta}\right)^{\alpha-1} exp\left[-\left(\frac{Y_e}{\beta}\right)^{\alpha}\right]$$ $$\alpha = -0.02287Y_e^2 + 0.61835Y_e - 0.94398$$ $$\beta = 0.001347Y_e^2 + 0.004688Y_e + 0.292059$$	Subsea/offshore structure	[25]
Generic linear model: $$d(t) = d_0 + c_d \cdot T$$ $$L(t) = L_0 + c_l \cdot T$$	Pipeline structures	[37]
Ossai model: $$D_{max}(t) = \begin{cases} 0.12t^{0.771}\ for\ low \\ 0.2687t^{0.7408}\ for\ moderate \\ 0.3887t^{0.7879}\ for\ high \\ 0.6508t^{0.8657}\ for\ severe \\ 0.695t^{0.7689}\ for\ all\ data \end{cases}$$	Pipeline structures	[38]

6.3. Methodology

The complex nature of the offshore systems' operating environment promotes stochastic failure characteristics during operation. The failure behavior also depends on the microstructural formation and the variability of the steel structure parameters. The interaction of the microstructural/material elements and the environmental factors with their variability can be modeled using a robust probabilistic framework. The following sections describe the procedure of the proposed methodology:

6.3.1 Collection of relevant information on the offshore structures

Information on the systems under study is collected. The required information includes but is not limited to the microstructure composition, mechanical properties, operating/environmental

condition/properties, microbial availability/counts, corrosion types, morphology, and corrosion flaws characteristics.

6.3.2 Corrosion susceptibility model assessment

The susceptibility of a steel structure in corrosive environments is complex and difficult to predict. This is due to the mixed corrosive elements and their interaction with the steel's material parameters. Several studies for the development of empirical, phenomenological, probabilistic, and semi-empirical susceptibility models from different corrosion influential factors' perspectives have been conducted. However, there are a limited number of comprehensive models in the literature that can capture all the influential parameters in a mixed corrosion environment. In this research, four of these models (i.e., the power law model, Ossai's model, Mohd and Kee's model, and linear growth model) are adopted to demonstrate their effects on the failure behavior of three different steel grade pipeline structures in a mixed corrosive environment.

It is important to note that for the offshore assets' degradation rate under a mixed corrosive environment, the predicted results presented by the references [27,39] are adopted for the research analysis. The approach demonstrates the application of a probabilistic network-based structure to capture the dynamic and nonlinear interactions among the corrosive elements in a mixed corrosion environment. The corrosion rates are used as the input data for the susceptibility model prediction in this research. For more detail on the corrosion rate prediction, interested readers are referred to our previous works [27,39].

6.3.3 Failure assessment model

Corrosion induced failures are complex and stochastic in nature. The failures' influencing variables such as the microstructural elements, corrosion response parameters, and monitoring

operating parameters have associated uncertainties. Therefore, the failure prediction over time is stochastically structured. Several generic failure (strength loss) models have been introduced for system plastic collapse modeling [40–47]. However, the PCORRC model (see Eq. 6.1) is a validated model which is mostly suitable and applicable for moderate-to-high toughness pipe failure prediction [48].

$$\text{PCORRC} = \begin{cases} P_b(t) = \dfrac{2wt\sigma_u}{D}\left[1 - \dfrac{d_{max}}{wt}\left(1 - exp\left(\dfrac{-0.157L}{\sqrt{\dfrac{D(wt - d_{max})}{2}}}\right)\right)\right] \\ L \leq 2D \; and \; \dfrac{d_{max}}{wt} \leq 0.8 \end{cases} \tag{6.1}$$

where $P_b(t), D, \sigma_u, wt, \; d_{max}$ and L represent the burst capacity, external diameter, ultimate tensile strength, wall thickness, defect depth, and corrosion defect length of the pipeline, respectively.

The PCORRC model is adopted in this research study. The model captures the material mechanical and fracture properties.

6.3.4 Limit state formulation for failure probability prediction

The failure behavior of the moderate-to-high toughness pipe can be forecasted based on the small leak modes, large leak modes, and/or crack failure. However, in the current study, we consider the leak and burst failure modes while employing multiple corrosion susceptibility models. The limit state formulation (LSF) for corroding systems is based on the fitness for service criteria as a function of the considerable wall thickness reduction [49].

Corrosion induced leak failure. Offshore oil and gas pipelines leaks are a function of the considerable wall thickness reduction and pit hole formation. Different criteria to define the safe

operating envelope for leak failure mode are available in the open sources [43,45,50]. In this study, the limit state formulation for small leak failure mode is based on the DNV criteria [43], as presented by Eq. (6.2).

$$g_1(wt, d, t) = 0.8wt - d(t) \tag{6.2}$$

where wt refers to the pipe-wall thickness, and $d(t)$ defines the corrosion defect depth at the time, t.

Burst failure criteria. For a given limit state function, as shown by Eq (6.3), the failure envelope which is described by the probability of failure, can be predicted using Eq. (6.4) .

$$G(R, L, t) = R(t) - L(t) \tag{6.3}$$

where $L(t)$ introduces the time-dependent load or load effect and $R(t)$ describes the structural resistance.

$$P_f(t) = P[G(R, L, t) \leq 0] = P[L(t) \geq R(t)] \tag{6.4}$$

where P is the probability of occurrence of an event.

Different models of burst failure prediction for moderate-to-high toughness steel pipes have been introduced as a function of considerable reduction in wall thickness and unstable pressure loads [42]. The dynamic pressure loads or stresses could result in system failure at any time. The complexity in the microstructural elements' response in a mixed chloride-CO_2-H_2S-microbial corrosive environment plays an important role in the burst or plastic collapse failure characteristic. Eq. (6.5) introduces the limit state function for failure mode based on the burst capacity.

$$g_2\left(P_b, P_{op}, t\right) = P_b(t) - P_{op} \tag{6.5}$$

where $P_b(t)$ denotes the burst capacity (see Eq. 6.1), and P_{op} symbolizes the operating pressure.

Uncertainty propagation in the failure prediction. The failure behavior of corroding offshore pipelines is a very random phenomenon based on its basic response parameters. Therefore, the formulation for failure prediction can be stochastically defined in terms of the basic material and corrosion response parameters. These parameters play a key role in the variability and dynamics of the material strength loss in a mixed chloride-CO_2-H_2S-microbial corrosive environment. The random response parameters' uncertainty can be propagated using the MCS that generates a vector form of the random parameters, as given below [51,52]:

$$P_b(t) = f\left(wt, \sigma_y, \sigma_u C_d, C_L, D, L, d_{max}\right) \tag{6.6}$$

where $wt, \sigma_y, \sigma_u, c_d, c_l, D, L,$ and d_{max} represent the basic random independent variables that describe the pipe wall thickness, yield strength, ultimate strength, radial and axial corrosion rate, outer pipe diameter, mean initial corrosion length, and depth, respectively. For definite probabilistic characteristics of the random variables, $P_b(t)$ can be predicted using MCS.

The MCS is a probabilistic numerical tool that relies on the sampling inherent variability in random variables [27]. It has been broadly used in engineering and economic risk analysis [49,53,54]. The associated material structure and corrosion response parameters and their characterized probability distribution are captured by the MCS algorithm. Fig. 6.1 shows the MCS algorithm for failure probability prediction for the studied steel structures.

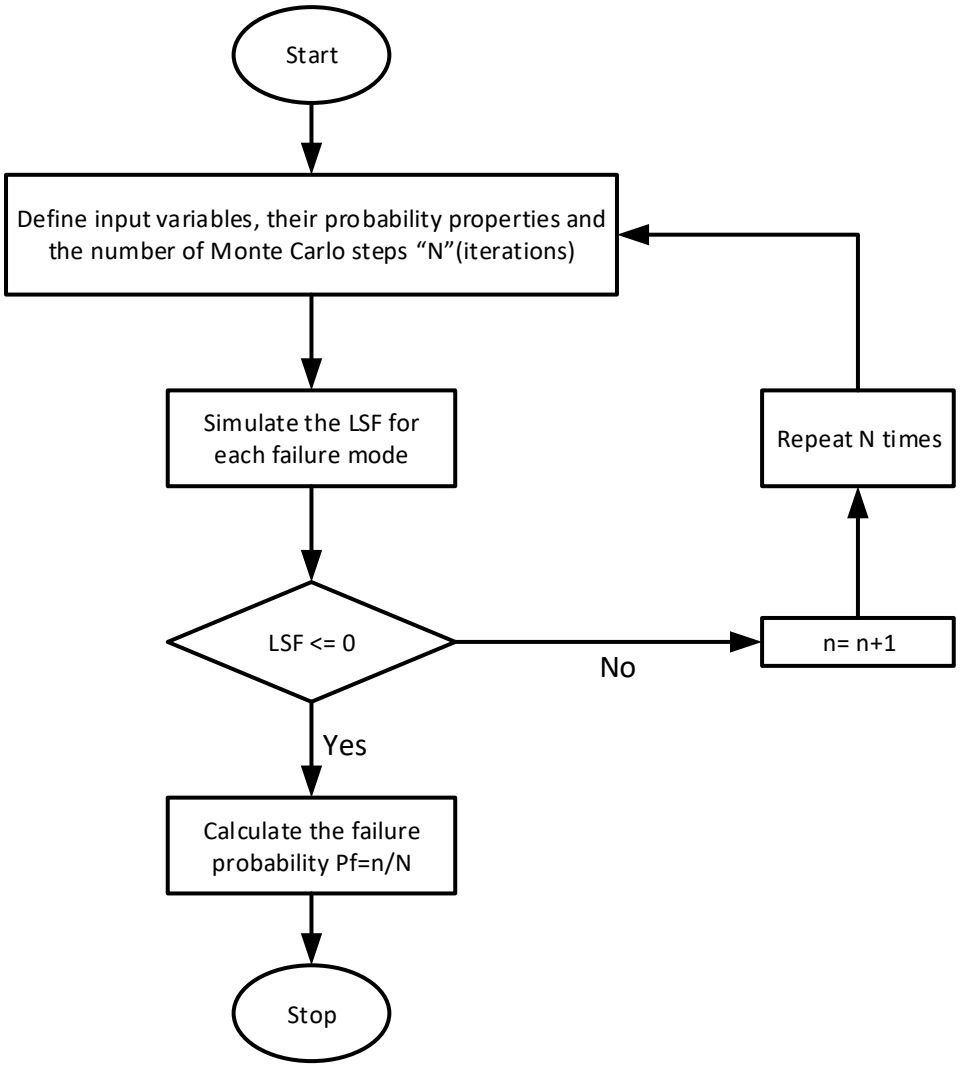

Figure 6.1. An algorithm for failure probability prediction using MCS

The microstructural/material formation and the environmental impact due to chloride, CO_2, H_2S, and microbial interaction could lead to fracture or corrosion induced failure. Crack failure could result from hydrogen-induced and sulfide stress cracking (a form of stress corrosion cracking) [55]. This is predominant in a sour oil field operation, where hydrogen embrittlement is enhanced [56]. The reported interaction presents a problematic corrosion induced failure mechanism, especially in a mixed corrosive environment. A sensitivity analysis is carried out to capture the effects of the random response parameters on the limit state function performance for the exposed

period. It is important to note that the current study does not consider the fracture failure mode and the effect of correlation among material/corrosion response parameters.

The algorithm is demonstrated on three steel grade structures under different corrosion susceptibility models. The steel pipelines' failure characteristic is predicted for comparative risk-based analysis and optimal decision-making to aid terrain specific material selection and corrosion management strategy.

6.4. Case study

The current hybrid methodology is demonstrated on three different steel grade pipelines (API 5L X52, API 5L X65, and API 5L X70) under different corrosion susceptibility models [39,42]. The steel structures are assumed to operate in a mixed chloride-CO_2-H_2S-microbial corrosive environment with internal corrosion defect depth. In a mixed corrosion environment, CO_2 synergistically interacts with the sulphate reducing bacteria (SRB) and increases the corrosion rate of the steel pipeline [57]. The pipeline's fluid temperature plays a critical role in the subsea pipelines' microstructural response to CO_2 corrosion, H_2S corrosion, and microbial corrosion [58–60]. The mechanical properties of the pipelines are listed in Table 2. The corrosion geometry, defect depth characteristics (mean of 2.2mm; standard deviation of 0.81), and defect length (mean of 95mm; standard deviation of 32) are used in the analysis [61].

Table 6.2. Mechanical and fracture properties for offshore steel pipelines

Grade	Yield Stress (MPa)	Ultimate Tensile Strength (MPa)	Charpy Upper-Shelf Energy (ft-Ib)	Strain Hardening Coefficient (n)
X52	411	508	32	0.0832
X65	483	625	122	0.0881
X70	525	601	70	0.0856

Table 6.3 shows the probabilistic properties of the random response variables of the steel structures used in this research. The probabilistic characteristics were extracted from the literature [50,61].

Table 6.3. Probabilistic properties for random response variables

X52					
Parameters	D(mm)	wt (mm)	P_{op} (MPa)	σ_y (MPa)	σ_u (MPa)
Mean value	508	12.7	7.8	411	508
Standard deviation	12.43	1.214	0.231	11.44	15.149
Distribution	Normal	Normal	Lognormal	Normal	Lognormal

X65					
Parameters	D(mm)	wt (mm)	P_{op} (MPa)	σ_y (MPa)	σ_u (MPa)
Mean value	762	9.92	9.8	483	625
Standard deviation	14.288	0.713	0.331	16.135	19.129
Distribution	Normal	Normal	Lognormal	Normal	Lognormal

X70					
Parameters	D(mm)	wt (mm)	P_{op} (MPa)	σ_y (MPa)	σ_u (MPa)
Mean value	682.4	15.9	10.2	525	601
Standard deviation	13.87	2.09	0.658	12.6	14
Distribution	Normal	Normal	Lognormal	Normal	Lognormal

Additional data/information on the radial and axial corrosion rate under the mixed corrosive environments are found in the literature [27,39]. The corrosion susceptibility models presented in the open sources [25,33,37,38] are adopted for the numerical demonstration of the proposed approach. Furthermore, the following assumptions are made: i) the pipelines are exposed to mixed corrosive environments, as presented in [39], and the predicted corrosion rate is adopted for the research analysis, ii) the microstructural and corrosion response variables are treated as mutually

independent, iii) the fracture failure mode and the correlation among key failure influencing factors are not considered in the current study, iv) the pipelines are subjected to four different susceptibility modeling for the defect propagation prediction over time, v) empirical values are assumed for the power law model coefficients (parameters) for the purpose of demonstration, and vi) different coefficient of variation (cov) values are assumed for the random structural parameters.

The proposed computational procedure is applied to the numerical example based on the data, as summarized in Tables 6.1-6.3, with additional information from the referenced literature.

6.5. Results and discussion

The current research presents a probabilistic methodology that integrates the empirical corrosion susceptibility models with the Monte Carlo algorithm for a comparative failure prediction of steel pipelines under mixed corrosive environments. The current study utilizes the results of our previous research work that uses a network-based probabilistic formalism to capture the nonlinear interactions among the mixed corrosive elements for corrosion rate prediction [39]. The predicted corrosion rate is adopted and used as input data for the pipeline susceptibility prediction. Three grades of offshore steel pipeline failure profile are predicted under a mixed corrosive environment. A 10^6 number of simulations based on the Monte Carlo algorithm are carried out in the MATLAB environment for the failure probability prediction.

6.5.1 Leak failure behavior of offshore steel pipelines in a mixed corrosive environment

Three steel pipelines (API 5L X52, API 5L X65, and API 5L X70) are subjected to a mixed corrosive environment and different susceptibility models to study their failure behavior. The goal is to capture the microstructural and parametric interactions' effects on the failure characteristics

of these steel pipelines. To do this, emphasis is placed on the material microstructural elements' configuration, based on their impact on the strength and resistivity of the steel structure to corrosion and leak failure. The results of the formulated leak limit state function are depicted in Fig. 6.2. It is found that for a severe corrosion rate of 0.3776, the steel structures show diverse failure profiles across the grades.

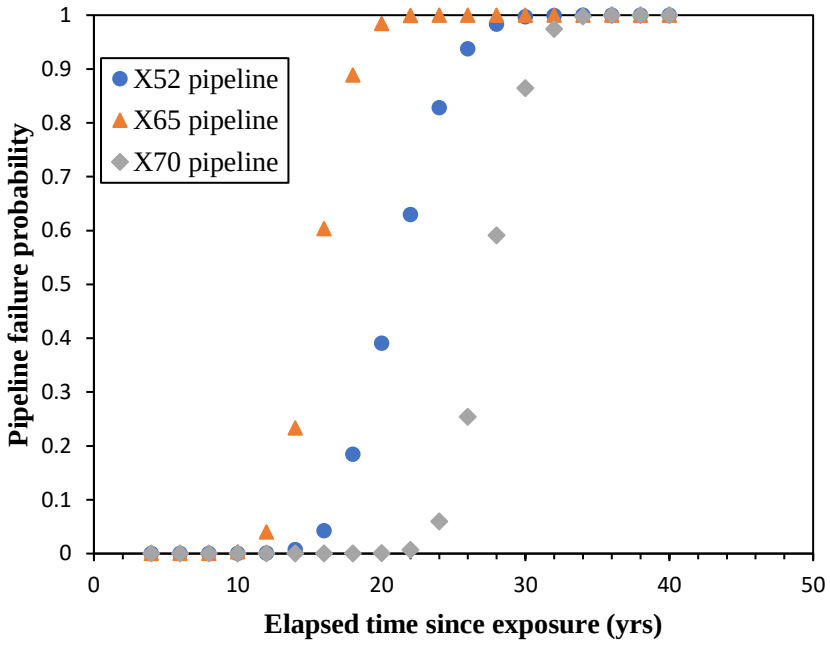

Figure 6.2. Impact of steel grades on leak failure probability in mixed corrosive environments

It can be concluded that, given the predefined mixed corrosive environments, the likely time of failure at an upper bound leak failure probability of 0.9741 occurs after 16 years, 26 years, and 32 years of exposure for the X65, X52, and X70 pipelines, respectively. Further analysis of the susceptibility model performance on the leak limit state function is shown in Fig. 6.3.

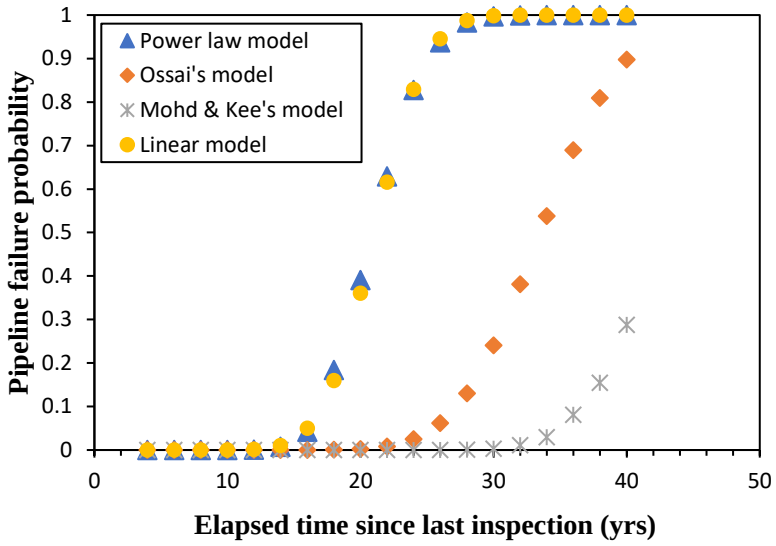

Figure 6.3. Impact of susceptibility models on the leak failure behavior of X52 steel pipeline

As indicated in Fig. 6.3, the failure profile of the X52 pipeline based on the power law model follows a similar trend as with the linear corrosion growth model. It further shows that there is a considerable divergence in the pipeline failure profile for Ossai's model and Mohd & Kee's model. This indicates the performance state of the semi-empirical models, which depends on the model's assumptions and the prevailing operating conditions of the pipeline. One can conclude that the choice of susceptibility model influences the failure profile of the steel structures. Thus, for the predefined mixed corrosive environments, the power law model and linear corrosion growth model adequately forecast the susceptibility characteristics of the X52 pipeline under leak failure mode.

6.5.2 Impact of corrosion susceptibility models on burst failure characteristics

The flow stress and corrosive elements significantly affect the steel structures' burst capacity in the offshore environment as a result of pressure disturbances and bacteria. These disturbances could result in the steel pipeline failure from a considerable reduction in the pipe wall thickness.

The susceptibility models are defined by the defects' characteristics and the corrosion rate. The susceptibility models' results are integrated into the formulated burst pressure model for the pipeline failure probability prediction, as demonstrated in Fig. 6.4. Fig. 6.4(a) reveals the corrosion susceptibility models' effect on the burst failure profile of the API 5L X52 steel pipeline. The burst failure probability, based on the power law and linear corrosion growth models, increases gradually with exposure time. An intersection is observed at the failure probability of 0.7433 with a corresponding failure year at the 26th year of exposure.

Further analysis reveals the inadequacy of Mohd & Kee's model to capture the susceptibility/failure trends of the X52 pipeline under the predefined mixed corrosive operating conditions. In Fig. 6.4(b), the intersection of the two models' result occurs at the 32 year of exposure with a corresponding burst failure probability of 0.4766. The Ossai's and Mohd & Kee's models show an inadequate capacity to capture the X70 steel structure's susceptibility trend under the predefined mixed corrosive environments. However, for the X65 steel structures, the four susceptibility models' applicability is shown in Fig. 6.4(c).

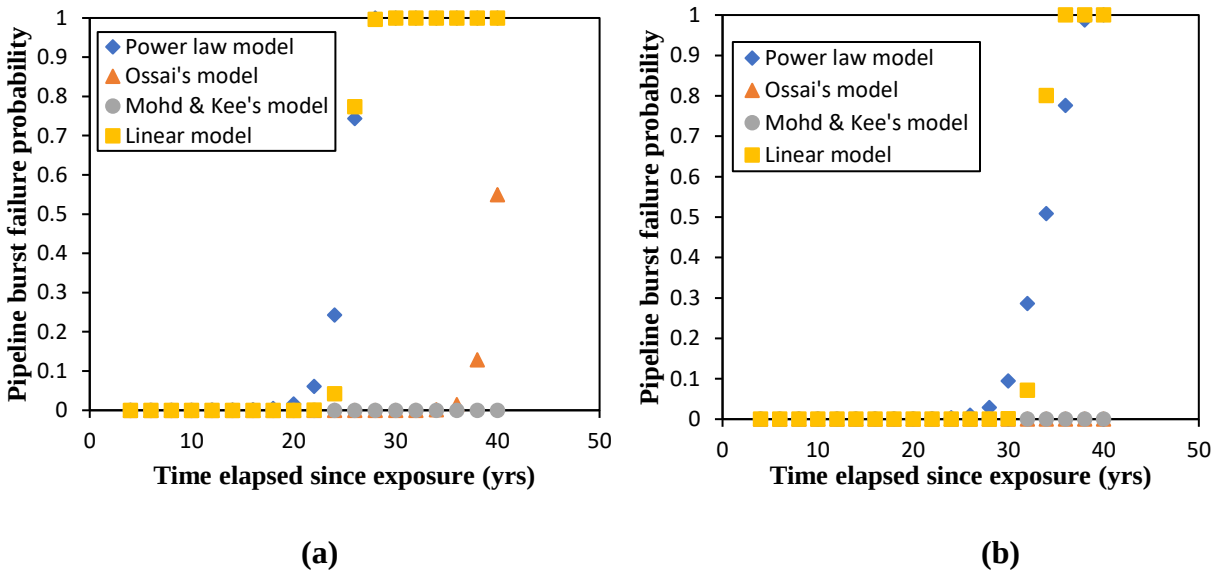

(a) (b)

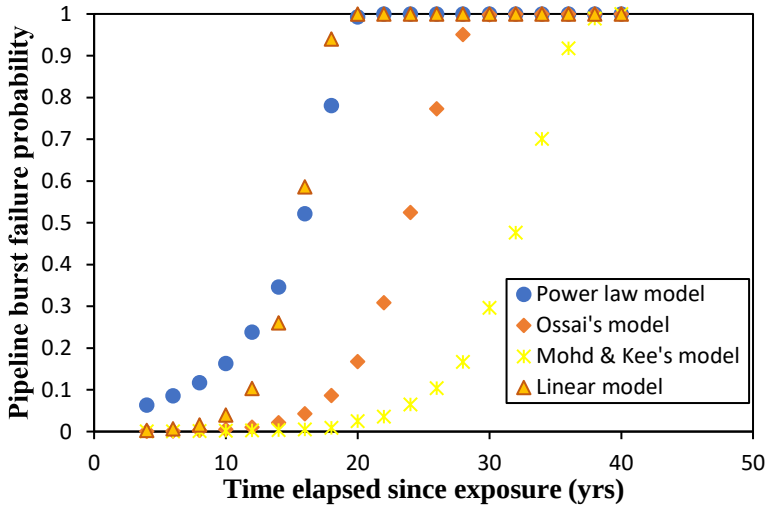

(c)

Figure 6.4. Impact of susceptibility models on burst failure probability:
(a) X52 pipeline, (b) X70 pipeline, and (c) X65 pipeline

The linear growth and power law models show some degree of concordance compared to the other models. It is observed that the failure profiles based on Ossai's model and Mohd & Kee's model differ greatly in comparison with that obtained from the power-law and linear corrosion growth model. This could be attributed to the model parameters' characterization, uncertainty, and the

environmental variability, which could represent the conservatism, as shown in the failure profile. Hence, these models may be highly conservative (i.e., overestimate or underestimate the susceptibility rate) for the given operating conditions. However, the results provide key operational and technical information that could aid decision-making in the failure assessment models' appropriateness and in risk-based integrity management strategy for the corroding steel structures. The characterized diversity in the steel grades' response to the mixed corrosive environments is dependent on the microstructural, mechanical, and strength properties, as demonstrated in the result analysis. The results agree with the previous research studies [50,61–64]. This provides initial validation for the presented approach.

6.5.3 Effect of uncertainty/variability in the response parameters on the pipeline failure

The burst failure probability of the corroding steel pipeline in a mixed corrosive environment under microstructural and parametric uncertainty is depicted in Fig. 6.5. This is evaluated by the coefficient of variation (cov) of the random response parameters, which measure the degree of relative uncertainty in the mean values and their standard deviation. The characterized burst failures are predicted by changing the standard deviation of the random response parameters while keeping their mean constant.

Fig. 6.5(a) shows the impact of the coefficient of variation of the operating pressure (written as cov (p_{op})) on the burst failure probability with time. The result indicates a slight increase in the failure probability as the cov (p_{op}) increases below the 50% failure probability. It can be seen that at the upper bound failure, the X52 likely failure decreases with an increase in the cov (p_{op}) This indicates the likely failure profile of the steel structure, which is domain-specific for any given bounds of the pressure disturbance in mixed corrosive environments. The stress distribution and the influence of corrosion depth may increase the pipeline stress influencing factors under unstable

loading conditions. Hence, the failure domain increases above the 50% failure probability of the pipeline.

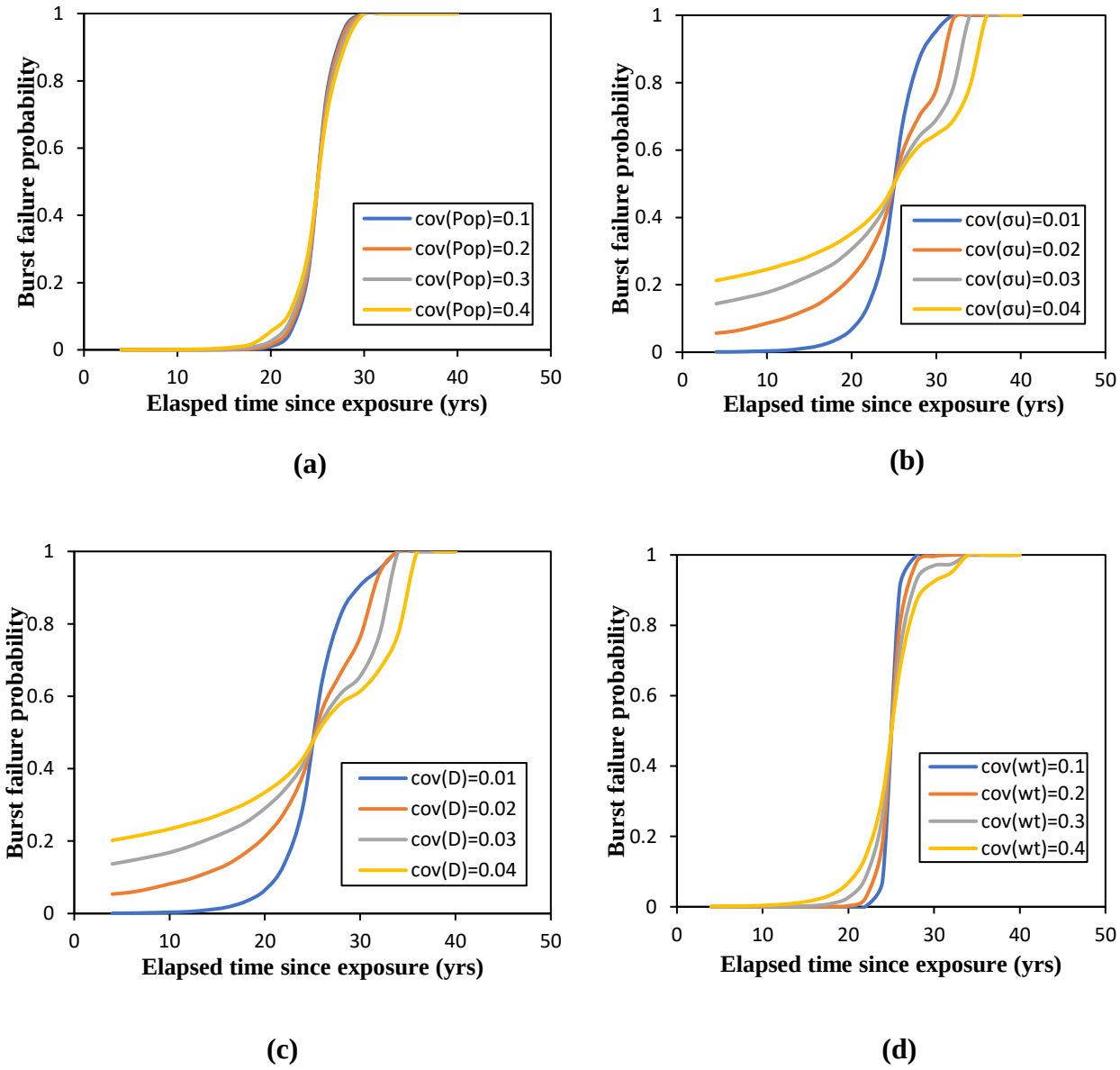

Figure 6.5. Effect of parametric variation on burst failure probability of X52 steel pipeline: (a) cov (p_{op}), (b) cov (σ_u), (c) cov (D), and (d) cov (wt)

Fig. 6.5(b) and Fig.6.5(c) illustrate the effect of cov (σ_u) and cov (D) on the burst failure probability of the X52 pipeline as the time of exposure increases. The failure probability increases with increasing cov for both cases, as shown, until 25 years of exposure. When the failure probability exceeds 50%, the burst likely failure year increases with increasing cov. It can be concluded that at 26 years of exposure to the mixed corrosive environment, the burst failure probability decreases by 12.20%, 16.96%, and 18.85% across the cov in the ultimate tensile strength for the X52 pipeline. The result of cov (wt), as shown in Fig. 6.5(d), follows a similar trend with that of cov (p_{op}). However, the failure probability based on the cov (wt) values becomes more significant at the upper bound of the failure profile.

Fig. 6.6 shows the influence of the coefficient of variation in the material's microstructural and corrosion parameters on the X65 steel pipeline's burst capacity. According to Fig. 6.6(a), the failure likelihood increases with increasing cov (p_{op}) at the lower bound of the failure profile but becomes insensitive toward the upper bound of the profile. This can be attributed to the unstable and complex characteristics of the corrosion influential factors, such as the H_2S, bacteria, and the stress factor over time.

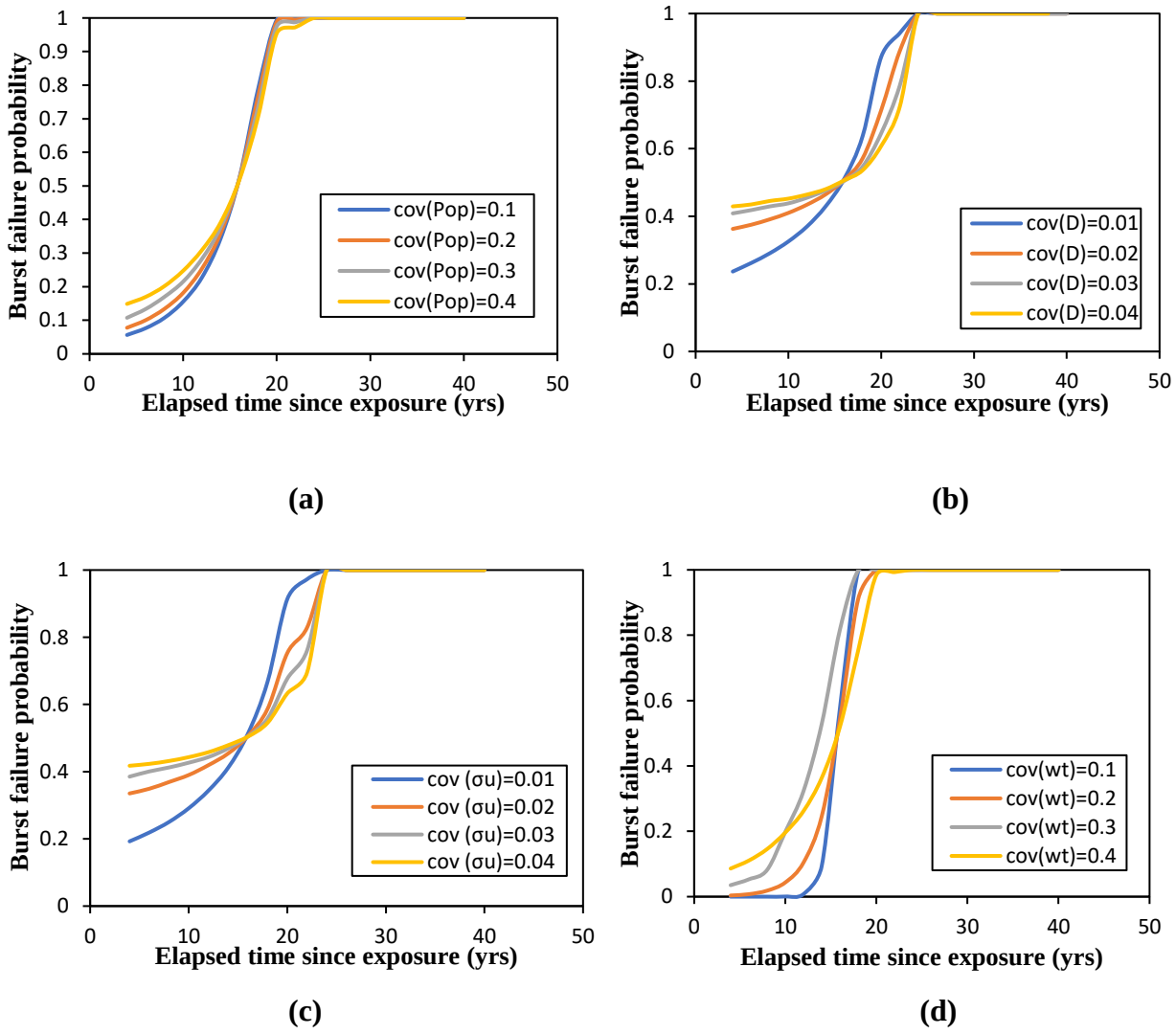

Figure 6.6. Effect of parametric variation on burst failure probability of X65 steel pipeline: (a) cov (p_{op}), (b) cov (σ_u), (c) cov (D), and (d) cov (wt)

In Fig. 6.6(b) and Fig. 6.6(c), the burst failure probability increases with increasing cov until about 15th year of exposure to the mixed corrosive environments. Based on the results, the likely total failure of the X65 pipeline will occur at 24 years of exposure under the predefined operating conditions. Fig. 6.6(d) displays an early failure of the pipeline as the cov (wt) increases with

exposure time. The pipe wall thickness and its variability could influence the leak failure likelihood in most cases by accounting for the corrosion allowance in pipeline design safety optimization.

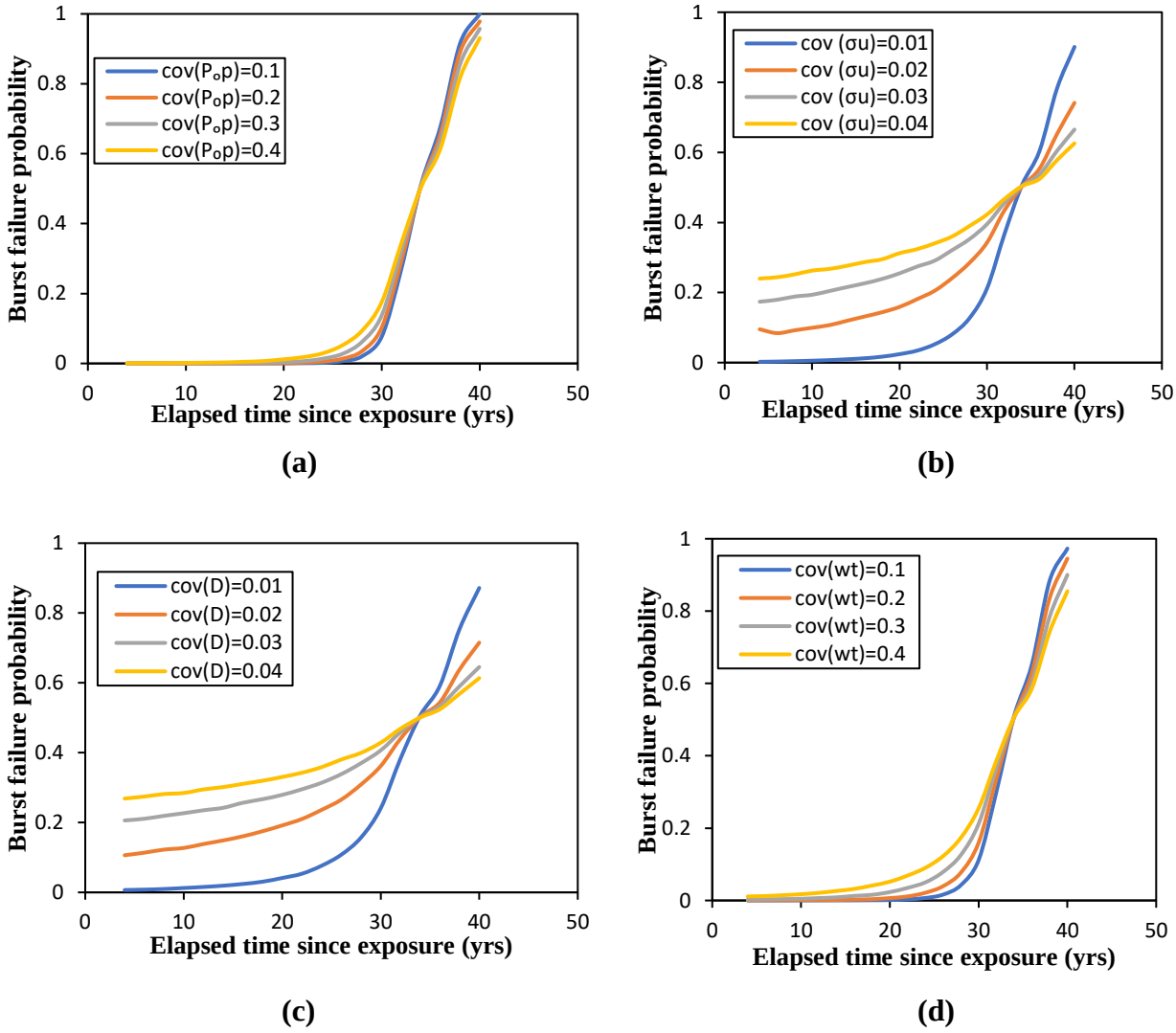

Figure 6.7. Effect of elapsed time on burst failure probability of X70 steel pipeline: (a) cov (p_{op}), (b) cov (σ_u), (c) cov (D), and (d) cov (wt)

The effect of uncertainty in the structural elements of the X70 steel pipeline is shown in Fig. 6.7. For the case of cov (p_{op}), as shown in Fig. 6.7(a), the burst failure probability increases with increasing cov at the lower bound of the failure profile until about 34years of exposure. However,

at the upper bound of the failure profile, the cov exhibits less impact on the failure likelihood. The same trend is reflected in the cov (wt), as demonstrated in Fig. 6.7(d). As seen in Fig. 6.7(b) and Fig. 6.7(c), the failure probability increases with increasing cov. For instance, at 25 years of exposure, the burst failure probability increases by 18.9%, 35.8%, and 82.9%, respectively, at the lower bound of the failure profile. However, toward the upper failure domain, as illustrated in Fig. 6.7(c), the failure probability decreases with increasing cov. This is reflected by the burst failure probability of 0.8717, 0.7152, 0.6453, and 0.6135, for the cov (σ_u) of 0.01, 0.02, 0.03, and 0.04, respectively. It is important to note that a similar trend is observed in the failure profile due to cov (D). Fig. 6.7(d) depicts the cov (wt) effect on the failure probability of the X70 pipeline. The effect of cov (wt) follows a similar trend as the failure profile due to cov (p_{op}). At the upper failure domain of the failure profile due to cov (wt), the burst failure likelihood decreases by 2.8%, 7.5%, and 9.4% as the cov increases over the exposure period.

Furthermore, a sensitivity analysis to explore the random response parameters' effect on the performance function is conducted (see Fig. 6.8). Fig. 6.8(a) shows the percentage impact of the mean value of the cov results on the limit state function for the X52 steel pipeline. The percentage mean value of the cov (σ_u) represents a 32.2% (the highest) impact on the limit state function result at 24 years of exposure. This impact is dominant at the upper bound of the failure domain for the given offshore pipeline. At 18 years of exposure, the mean values of the cov (wt) and cov (p_{op}) exhibit more significant influence on the limit state function value for the X65 steel pipeline. The degree of influence could vary across the steel structures' failure profile, based on the corrosivity of the operating environment. Fig. 6.8(c) shows the cov mean values' effect on the limit state function performance for the X70 pipeline at the 24th year of exposure. It is observed that at the upper bound of the failure probability profile, the cov (D) and cov (σ_u) show dominant effects.

This is reflected in their percentage impact on the overall limit state function performance at 24 years. The results are in agreement with previous studies [50,65]. This further validates the applicability and reliability of the proposed approach. It is important to note that the degree of influence of these random variables may stochastically change as the system operating condition changes.

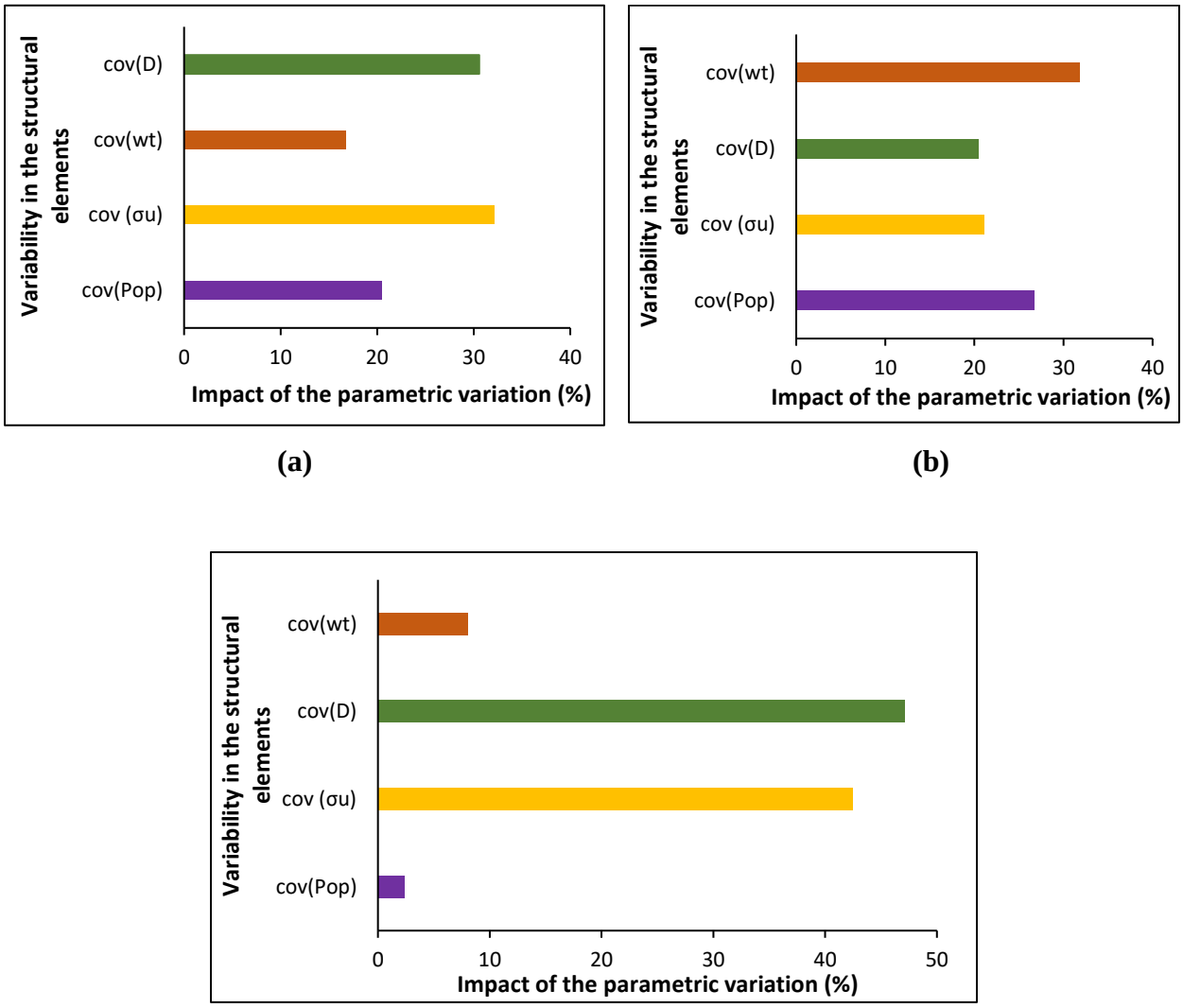

Figure 6.8. Effect of variation of variables (%) on the limit state function: (a) X52 @ T=24 years, (b) X65 @ T=18 years, and (c) X70 @ T=24years

The results' analysis shows the degree of influence of the structural parameters on the lower and upper bound failure probability of the steel pipelines. It is found that the limit state function increases with an increase in the mean value and the cov of the structural response parameters. This affects the susceptibility characteristics across the steel grades, with the X65 pipeline showing an earlier failure time due to considerable reduction in wall thickness and unstable pressure disturbances. The effects of the wall thickness and the pipeline diameter are clearly reflected in the X52 and X70 failure profiles, respectively. Therefore, priority should be given to precise determination of the structural response parameters, corrosion defect characteristics, and their associated variability for integrity management.

A risk-based integrity management strategy is recommended based on the results' analysis, considering the effects of the susceptibility models and the microstructural variability. A 4-year inspection plan and corrosion control measures (both batch and continuous biocide, and corrosion inhibitor application) could enhance the survivability of the X65 pipeline, while for the X52 and X70 pipelines, a 5-year and 7-year inspection plan is recommended under continuous subsea well fluid treatment and environmental control measures.

6.6. Conclusions

The current study demonstrates a probabilistic methodology that integrates the corrosion susceptibility models with the Monte Carlo algorithm for failure probability prediction of steel pipelines. The approach explores the key factors that affect the degradation of steel structures in a mixed corrosive environment (chloride-CO_2-H_2S-bacteria). The microstructural elements and their variability effects on the failure profile are predicted. The model demonstrates the capacity to capture the diversity in the susceptibility models and the parametric uncertainty for the failure

behavior prediction of API 5L X52, API 5L X65, and API 5L X70 in a mixed corrosive environment. The following conclusions are drawn from the current study:

- The presented approach serves as a useful tool to predict the offshore pipelines' failure behavior under different susceptibility characteristics.
- The power-law model and linear corrosion model show good potential in the susceptibility modeling of corroding pipelines under the predefined operating conditions.
- The failure probability increases with increasing cov of the structural and corrosion response parameters at the lower bound failure domain.
- The degree of influence of the structural elements stochastically changes along with the steel pipelines' failure profile over time in a mixed corrosive environment.
- This study offers key operational information that will aid condition monitoring and corroding systems' integrity management strategy under uncertainty.

The proposed approach is a useful tool for the integrity assessment of corroding offshore steel pipelines. However, the model could be improved by considering parametric dependencies/ correlation and comparative life cycle cost modeling.

Acknowledgments

The authors acknowledge the financial support provided by Genome Canada and their supporting partners and the Canada Research Chair (CRC) Tier I Program in Offshore Safety and Risk Engineering.

References

[1] Katiyar PK, Misra S, Mondal K. Comparative Corrosion Behavior of Five Microstructures (Pearlite, Bainite, Spheroidized, Martensite, and Tempered Martensite) Made from a High Carbon Steel. Metall Mater Trans A Phys Metall Mater Sci 2019;50:1489–501. https://doi.org/10.1007/s11661-018-5086-1.

[2] Dugstad A, Hemmer H, Seiersten M. Effect of steel microstructure upon corrosion rate and protective iron carbonate film formation. NACE - Int Corros Conf Ser 2000;2000-March:369–78.

[3] Clover D, Kinsella B, Pejcic B, De Marco R. The influence of microstructure on the corrosion rate of various carbon steels. J Appl Electrochem 2005;35:139–49. https://doi.org/10.1007/s10800-004-6207-7.

[4] Hwang B, Kim YM, Lee S, Kim NJ, Ahn SS. Correlation of microstructure and fracture properties of API X70 pipeline steels. Metall Mater Trans A 2005;36:725–39. https://doi.org/10.1007/s11661-005-0188-y.

[5] Handoko W, Pahlevani F, Sahajwalla V. Enhancing corrosion resistance and hardness properties of carbon steel through modification of microstructure. Materials (Basel) 2018;11. https://doi.org/10.3390/ma11122404.

[6] Sun F, Li X, Cheng X. Effects of carbon content and microstructure on corrosion property of new developed steels in acidic salt solutions. Acta Metall Sin (English Lett 2014;27:115–23. https://doi.org/10.1007/s40195-013-0007-1.

[7] Xiao XM, Peng Y, Ma CY, Tian ZL. Effects of Alloy Element and Microstructure on Corrosion Resistant Property of Deposited Metals of Weathering Steel. J Iron Steel Res Int 2016;23:171–7. https://doi.org/10.1016/S1006-706X(16)30030-9.

[8] Katiyar PK, Behera PK, Misra S, Mondal K. Effect of Microstructures on the Corrosion Behavior of Reinforcing Bars (Rebar) Embedded in Concrete. Met Mater Int 2019;25:1209–26. https://doi.org/10.1007/s12540-019-00288-1.

[9] Ramírez E, González-Rodriguez JG, Torres-Islas A, Serna S, Campillo B, Dominguez-

Patiño G, et al. Effect of microstructure on the sulphide stress cracking susceptibility of a high strength pipeline steel. Corros Sci 2008;50:3534–41. https://doi.org/10.1016/j.corsci.2008.09.014.

[10] Bastos IN, Tavares SSM, Dalard F, Nogueira RP. Effect of microstructure on corrosion behavior of superduplex stainless steel at critical environment conditions. Scr Mater 2007;57:913–6. https://doi.org/10.1016/j.scriptamat.2007.07.037.

[11] Arafin MA, Szpunar JA. Effect of bainitic microstructure on the susceptibility of pipeline steels to hydrogen induced cracking. Mater Sci Eng A 2011;528:4927–40. https://doi.org/10.1016/j.msea.2011.03.036.

[12] Singh MP, Arora KS, Kumar R, Shukla DK, Siva Prasad S. Influence of heat input on microstructure and fracture toughness property in different zones of X80 pipeline steel weldments. Fatigue Fract Eng Mater Struct 2020:1–16. https://doi.org/10.1111/ffe.13333.

[13] Xue HB, Cheng YF. Characterization of inclusions of X80 pipeline steel and its correlation with hydrogen-induced cracking. Corros Sci 2011;53:1201–8. https://doi.org/10.1016/j.corsci.2010.12.011.

[14] Lee SP, Jin JW, Kang KW. Probabilistic analysis for mechanical properties of glass/epoxy composites using homogenization method and Monte Carlo simulation. Renew Energy 2014;65:219–26. https://doi.org/10.1016/j.renene.2013.09.012.

[15] Khristenko U, Constantinescu A, Tallec P Le, Oden JT. A statistical framework for generating microstructures of two-phase random materials: application to fatigue analysis ∗. 2019.

[16] Li HX. Mechanics of Materials Limit analysis of composite materials with anisotropic microstructures : A homogenization approach 2011;43:574–85. https://doi.org/10.1016/j.mechmat.2011.06.007.

[17] Nastac L, Stefanescu DM, Simul M, Sci M, Musaddique M, Rafique A. Stochastic modelling of microstructure formation in solidification processes. Model Simul Mater Sci Eng 1997;5:391–420.

[18] Hadi I, Jabbareh MA, Nikbakht R, Assadi H. Modelling of microstructure evolution during

thermal processes - A hybrid deterministic-probabilistic approach. Mater Sci Forum 2012;704–705:63–70. https://doi.org/10.4028/www.scientific.net/MSF.704-705.63.

[19] Köhnen P, Létang M, Voshage M, Schleifenbaum JH, Haase C. Understanding the process-microstructure correlations for tailoring the mechanical properties of L-PBF produced austenitic advanced high strength steel. Addit Manuf 2019;30:100914. https://doi.org/10.1016/j.addma.2019.100914.

[20] Abbas M, Shafiee M. An overview of maintenance management strategies for corroded steel structures in extreme marine environments. Mar Struct 2020;71:102718. https://doi.org/10.1016/j.marstruc.2020.102718.

[21] Paik JK, Kim DK. Advanced method for the development of an empirical model to predict time-dependent corrosion wastage. Corros Sci 2012;63:51–8. https://doi.org/10.1016/j.corsci.2012.05.015.

[22] Shabarchin O, Tesfamariam S. Internal corrosion hazard assessment of oil & gas pipelines using Bayesian belief network model. J Loss Prev Process Ind 2016;40:479–95. https://doi.org/10.1016/j.jlp.2016.02.001.

[23] Xie Y, Zhang J, Aldemir T, Denning R. Multi-state Markov modeling of pitting corrosion in stainless steel exposed to chloride-containing environment. Reliab Eng Syst Saf 2018;172:239–48. https://doi.org/10.1016/j.ress.2017.12.015.

[24] Pots BFM, John RC, Rippon IJ, Thomas MJJS, Kapusta SD, Girgis M., et al. Improvements of De Waard-Milliams Corrosion Prediction and Applications to Corrosion Managment. NACE Int. Corros. Conf. No. 02235, 2002, p. 1–19.

[25] Mohd MH, Kee J. Investigation of the corrosion progress characteristics of offshore subsea oil well tubes. Corros Sci 2013;67:130–41. https://doi.org/10.1016/j.corsci.2012.10.008.

[26] Liu X, Zhang H, Li M, Duan Q, Chen Y. Failure analysis of oil tubes containing corrosion defects based on finite element method. Int J Electrochem Sci 2016;11:5180–96. https://doi.org/10.20964/2016.06.27.

[27] Adumene S, Khan F, Adedigba S. Operational safety assessment of offshore pipeline with multiple MIC defects. Comput Chem Eng 2020;138.

https://doi.org/10.1016/j.compchemeng.2020.106819.

[28] Melchers RE, Jeffrey R. The critical involvement of anaerobic bacterial activity in modelling the corrosion behaviour of mild steel in marine environments. Electrochim Acta 2008;54:80–5. https://doi.org/10.1016/j.electacta.2008.02.107.

[29] Melchers RE. Development of new applied models for steel corrosion in marine applications including shipping. Ships Offshore Struct 2008;3:135–44. https://doi.org/10.1080/17445300701799851.

[30] Melchers RE, Wells T. Models for the anaerobic phases of marine immersion corrosion. Corros Sci 2006;48:1791–811. https://doi.org/10.1016/j.corsci.2005.05.039.

[31] Garbatov Y, Guedes Soares C. Spatial corrosion wastage modeling of steel plates exposed to marine environments. J Offshore Mech Arct Eng 2019;141:1–6. https://doi.org/10.1115/1.4041991.

[32] Schumacher M. Seawater Corrosion handbook. Noyes Data Corp.; 1979.

[33] Melchers RE. Corrosion uncertainty modelling for steel structures. J Constr Steel Res 1999;52:3–19. https://doi.org/10.1016/S0143-974X(99)00010-3.

[34] Yamamoto N, Ikegami K. A study on the degradation of coating and corrosion of ship's hull based on the probabilistic approach. J Offshore Mech Arct Eng 1998;120:120–8. https://doi.org/10.1115/1.2829532.

[35] Paik JK, Thayamballi AK, Park Y Il, Hwang JS. A time-dependent corrosion wastage model for seawater ballast tank structures of ships. Corros Sci 2004;46:471–86. https://doi.org/10.1016/S0010-938X(03)00145-8.

[36] Soares G, Garbatov Y. Reliability of maintained, corrosion protected plates subjected to non-linear corrosion and compressive loads. Mar Struct 1999;12:425–45. https://doi.org/10.1016/S0951-8339(99)00028-3.

[37] Witek M. Gas transmission pipeline failure probability estimation and defect repairs activities based on in-line inspection data. Eng Fail Anal 2018;70:255–72. https://doi.org/10.1016/j.engfailanal.2016.09.001.

[38] Ossai CI, Boswell B, Davies IJ. Predictive Modelling of Internal Pitting Corrosion of Aged Non-Piggable Pipelines. J Electrochem Soc 2015;162:C251–9. https://doi.org/10.1149/2.0701506jes.

[39] Adumene S, Khan F, Adedigba S, Zendehboudi S, Shiri H. Dynamic risk analysis of marine and offshore systems suffering microbial induced stochastic degradation. Reliab Eng Syst Saf 2020;207:107388. https://doi.org/10.1016/j.ress.2020.107388.

[40] Kiefner JF, Vieth PH. Evaluating pipe:new method corrects criterion for evaluating corroded pipe. Oil Gas J 1990.

[41] Leis BN, Stephens DR. An Alternative Approach to Assess the Integrity of Corroded Line Pipe - Part I : Current Status. Proc. Seventh Int. Offshore Polar Eng. Conf., vol. IV, 1997, p. 624–34.

[42] Stephens DR, Leis BN. Development of an alternative criterion for residual strength of corrosion defects in moderate-to-high-toughness pipe. ASME Int. Pipeline Conf. Proceeding, vol. 2, 2000.

[43] DNV. Corroded Pipelines - Dnv-Rp-F101. 2010. https://doi.org/DOI: 10.1016/B978-008044566-3.50040-3.

[44] Zhou W, Huang GX. Model error assessments of burst capacity models for corroded pipelines. Int J Press Vessel Pip 2012;99–100:1–8. https://doi.org/10.1016/j.ijpvp.2012.06.001.

[45] Amaya-gómez R, Sánchez-silva M, Bastidas-arteaga E, Schoefs F, Muñoz F. Reliability assessments of corroded pipelines based on internal pressure – A review. Eng Fail Anal 2019;98:190–214. https://doi.org/10.1016/j.engfailanal.2019.01.064.

[46] Mokhtari M, Melchers RE. A new approach to assess the remaining strength of corroded steel pipes. Eng Fail Anal 2018;93:144–56. https://doi.org/10.1016/j.engfailanal.2018.07.011.

[47] Gao J, Yang P, Li X, Zhou J, Liu J. Analytical prediction of failure pressure for pipeline with long corrosion defect. Ocean Eng 2019;191:106497. https://doi.org/10.1016/j.oceaneng.2019.106497.

[48] Nasser-Muthanna BG, Bouledroua O, Meriem-Benziane M, Setvati MR, Djukic MB. Assessment of corroded API 5L X52 pipe elbow using a modified failure assessment diagram. Press Vessel Pip 2020:104743. https://doi.org/10.1016/j.ijpvp.2020.104291.

[49] Teixeira AP, Soares CG, Netto TA, Estefen SF. Reliability of pipelines with corrosion defects. Int J Press Vessel Pip 2008;85:228–37. https://doi.org/10.1016/j.ijpvp.2007.09.002.

[50] Qian G, Niffenegger M, Li S. Probabilistic analysis of pipelines with corrosion defects by using FITNET FFS procedure. Corros Sci 2011;53:855–61. https://doi.org/10.1016/j.corsci.2010.10.014.

[51] Bhardwaj U, Teixeira AP, Guedes Soares C. Uncertainty quantification of burst pressure models of corroded pipelines. Int J Press Vessel Pip 2020;188:104208. https://doi.org/10.1016/j.ijpvp.2020.104208.

[52] Bhardwaj U, Teixeira AP, Guedes Soares C. Uncertainty in reliability of thick high strength pipelines with corrosion defects subjected to internal pressure. Int J Press Vessel Pip 2020;188:104170. https://doi.org/10.1016/j.ijpvp.2020.104170.

[53] Jones MN, Frutiger J, Ince NG, Sin G. The Monte Carlo driven and machine learning enhanced process simulator. Comput Chem Eng 2019;125:324–38. https://doi.org/10.1016/j.compchemeng.2019.03.016.

[54] Ossai CI, Boswell B, Davies IJ. Application of Markov modelling and Monte Carlo simulation technique in failure probability estimation — A consideration of corrosion defects of internally corroded pipelines. Eng Fail Anal 2016;68:159–71. https://doi.org/10.1016/j.engfailanal.2016.06.004.

[55] Depover T, Laureys A, Escobar DP, Van den Eeckhout E, Wallaert E, Verbeken K. Understanding the interaction between a steel microstructure and hydrogen. Materials (Basel) 2018;11. https://doi.org/10.3390/ma11050698.

[56] Laureys A, Pinson M, Claeys L, Seranno T De, Depover T, Verbeken K. Initiation of hydrogen induced cracks at secondary phase particles 2020;52:113–27. https://doi.org/10.3221/IGF-ESIS.52.10.

[57] Liu H, Cheng YF. Mechanistic aspects of microbially influenced corrosion of X52 pipeline steel in a thin layer of soil solution containing sulphate-reducing bacteria under various gassing conditions. Corros Sci 2018;133:178–89. https://doi.org/10.1016/j.corsci.2018.01.029.

[58] Zhu Y, Xu Y, Wang M, Wang X, Liu G, Huang Y. Understanding the influences of temperature and microstructure on localized corrosion of subsea pipeline weldment using an integrated multi-electrode array. Ocean Eng 2019;189:106351. https://doi.org/10.1016/j.oceaneng.2019.106351.

[59] Adumene S, Adedigba S, Khan F, Zendehboudi S. An integrated dynamic failure assessment model for offshore components under microbiologically influenced corrosion. Ocean Eng 2020;218. https://doi.org/10.1016/j.oceaneng.2020.108082.

[60] Fang BY, Atrens A, Wang JQ, Han EH, Zhu ZY, Ke W. Review of stress corrosion cracking of pipeline steels in “low” and “high” pH solutions. J Mater Sci 2003;38:127–32. https://doi.org/10.1023/A:1021126202539.

[61] Mahmoodian M, Li CQ. Failure assessment and safe life prediction of corroded oil and gas pipelines. J Pet Sci Eng 2017;151:434–8. https://doi.org/10.1016/j.petrol.2016.12.029.

[62] Mahmoodian M, Aryai V. Structural failure assessment of buried steel water pipes subject to corrosive environment. Urban Water J 2017;14:1023–30. https://doi.org/10.1080/1573062X.2017.1325500.

[63] Mahmoodian M, Li CQ. Stochastic failure analysis of defected oil and gas pipelines. Handb. Mater. Fail. Anal. with Case Stud. from Oil Gas Ind., Elsevier Ltd.; 2016, p. 235–55. https://doi.org/10.1016/B978-0-08-100117-2.00014-5.

[64] Maes MA, Dann M, Salama MM. Influence of grade on the reliability of corroding pipelines 2008;93:447–55. https://doi.org/10.1016/j.ress.2006.12.009.

[65] Caleyo F, González JL, Hallen JM. A study on the reliability assessment methodology for pipelines with active corrosion defects. Int J Press Vessel Pip 2002;79:77–86. https://doi.org/10.1016/S0308-0161(01)00124-7.

Chapter 7

Dynamic risk analysis of marine and offshore systems suffering microbial induced stochastic degradation

Preface

A version of this chapter has been published in the ***Reliability Engineering and System Safety 2021; 207: 107388.*** *I am the primary author along with the Co-authors, Faisal Khan, Sundady Adedigba, Sohrab Zendehboudi, and Hodjat Shiri. I developed the conceptual framework for the dynamic risk assessment model and carried out the literature review. I prepared the first draft of the manuscript and subsequently revised the manuscript based on the co-authors' feedbacks. Co-author Faisal Khan provided supervision and helped in the concept development, design of methodology, reviewing, and revising the manuscript. Co-author Sunday Adedigba provided support in implementing the concept and testing the model. Co-author Sohrab Zendehboudi provided fundamental assistance in validating, reviewing, and correcting the model and results. Co-author Hodjat Shiri provided support in reviewing and correcting the manuscript. The co-authors also contributed to the review and revision of the manuscript.*

Abstract

This research chapter presents a methodology that integrates the dynamic Bayesian network (DBN) with a loss aggregation technique for microbial corrosion risk prediction. The DBN captures the dynamic interrelationships among microbial corrosion influencing variables to predict the rate of system degradation and failure probability. The model captures the dynamic and time-evolution effect of the degradation propagation on the consequences of failure. The loss aggregation technique is used to forecast the expected economic loss associated with the different loss scenarios. The proposed methodology is tested on a subsea pipeline to assess risks of failure

upon microbial corrosion. The outcomes reveal that the interplay among the vital variables results in severe deterioration of the offshore/marine system; thus, it increases the risk in terms of economic losses. Three critical loss scenarios are examined as the consequences of microbial corrosion induced failure to capture the effect of the soft and hard failures of the safety barriers/actions on the expected total economic loss. At the 95% confidence interval, the upper and lower bound economic losses (value at risk) increase by 40.3% and 57.5%, respectively. The proposed methodology provides a risk-based prognostic tool for offshore and marine systems suffering from microbial corrosion.

Keywords: Microbial corrosion; Dynamic Bayesian network; Offshore systems; Loss aggregation technique; Dynamic risk; Expected economic loss

7.1. Introduction

Important engineering infrastructures in the ocean environments are prone to a high rate of degradation. The degradation of the infrastructures is influenced by biotic and abiotic factors that are operational and environmentally dependent. The biotic factors (e.g., bacteria, fungi, and algae) play a significant role in the deterioration of the marine and offshore oil and gas systems such as ship hull fouling and cargo tank leakage [1,2], pipeline corrosion [3,4], and reservoir souring [5,6]. Catastrophic failure and high-risk events are still a challenge in marine and offshore oil and gas industries as a result of microbial induced degradation. This is attributed to the uncertain and stochastic nature of microbially influenced corrosion (MIC) and its influential operational parameters. The complexity in the formation and propagation of the MIC under multispecies biofilm architecture complicates its failure induced prediction and the direct and indirect

consequences. Limited understanding of the associated stochasticity of MIC induced failure could result in making risky and uncertain operational decisions.

A few models for MIC risk analysis are available in the literature [7–11]. For instance, Maxwell and Campbell [9] proposed a risk-based mitigation model for predicting biocide performance and MIC monitoring in field operations. They adopted the Monod kinetics framework to model the biofilm development under inhibitor application and integrate it into the Pots et al. [12] model. The authors scaled the MIC risk level based on the amount of sulfide production in the microbial biofilm. The model only offers a diagnostic risk-based monitoring capacity by using key performance indicators, without quantitatively predicting the risk of MIC-induced system failure under various operational scenarios. Sørensen et al. [8] developed a semi-quantitative MIC risk assessment model based on the sulfate-reducing prokaryotes (SRP), and the methanogens (MET) counts. The model includes the sulfate reduction rate and CO_2 reduction rate to formulate an integrated MIC risk factor (IMRF) to estimate the MIC initiation time and the potential pit generation rate (PPGR) under biofilm. The model can quantify the risks in terms of the microbial counts and the pit generation rate for long-term exposure by integrated molecular microbiological methods. The available approaches are mechanistically structured and are inadequate to capture the parametric variability and dynamic/non-linear interactions among the key corrosion influencing factors for MIC quantitative risk modeling.

The recent improvement in corrosion risk modeling has been demonstrated by the use of probabilistic-based models such as the Markov, fuzzy, Petri nets, Monte Carlo simulation, and Bayesian belief network (BBN) models [13–20]. For instance, Zhang et al. [17] proposed a fuzzy-based model to develop a risk matrix for the failure prediction of subsea connectors. The matrix captures the failure occurrence probability and the associated risk factors' impact level by the

defuzzification of expert elicitation. The results provide operational safety guidelines/tips under uncertainties. To capture the corrosion risk at the design stage of the subsea systems, Hasan et al. [14] proposed the integration of Monte Carlo simulation with a finite element model. The hybridized probabilistic model captures the corrosion response parameters' uncertainties to assess the system's mechanical integrity under burst capacity. However, the dependencies among corrosion influencing factors and their effect on risk modeling of corroding marine systems are not considered.

To explore the dependencies and interdependencies among vital factors of any given phenomenon, the Bayesian network (BN) technique has shown great potentials [15,21–24]. This is originated from its capability to capture multivariate interactions and dynamic dependence among risk influencing factors [25,26]. For instance, Shabarchin and Tesfamariam [15] employed a network-based probabilistic model (BN) for internal corrosion risk modeling of oil and gas pipelines. The authors integrated the multiple corrosion and failure models into a dynamic and flexible structure to forecast defects propagation and failure probability. The model could determine the degree of influence of the vital failure factors and the pipeline segments' vulnerability likelihood. Kannan et al. [27] proposed a systemic-based approach for MIC potential modeling using BN and dynamic Bayesian network. This approach combines the heuristic and quantitative states of the key parameters for MIC susceptibility prediction. The approach provides a systematic safety assessment tool for the oil and gas industry.

Furthermore, for a time evolution probability of failure prediction under stochastic degradation, Arzaghi et al. [13] and Yuanjiang et al. [19] applied the dynamic Bayesian network (DBN). The

authors demonstrated the DBN application for pitting and corrosion-fatigue damage, and corrosion risk of subsea pipelines and subsea wellheads. The results showed the model's capability to capture the temporal dependencies, stochastic growth rate, and failure likelihood of corroding subsea systems. The model further integrates the various degrees of influence of the failure-induced variables for the failure probability prediction in every time slice structurally. Further applications of the BN and DBN for risk, safety, reliability, and resilience modeling are detailed in the literature [21,28–31]

The DBN has the capability of capturing the temporal interrelationship among failure-induced factors, as demonstrated in the open sources. However, its application to investigate and predict the microbially influenced corrosion induced failures and corresponding consequences has not been adequately reported. The multispecies microbial biofilm characteristics and their effects on corroding offshore system risk propagation phenomenon have not yet been studied. The associated loss scenarios induced by the system failure have not been considered in the literature to predict the likely value at risk in terms of economic losses in the investment. There is no adequate understanding of the effect of safety barriers' degree of failure in terms of financial risks on a corroding offshore system overall risk profile. The reported knowledge gaps necessitate the development of a dynamic and robust model that can capture the varying influencing parameters and the biofilm characteristics effects to predict the propagation of microbial corrosion induced failure and the corresponding consequences in terms of financial losses at different time periods.

Moreover, the MIC induced failure presents a complex mechanism due to the dynamic and facultative nature of the acid-producing bacteria (APB) and iron-reducing bacteria (IRB) under a

multispecies biofilm architecture. This unstable tendency in the bacteria colony can present multidimensional degradation potentials [32]. The degradation diversity due to the multispecies biofilm architecture needs to be captured to predict its impact on the consequences of failure likelihood. This is depicted in the proposed DBN model by the SRB, APB, and IRB nodes, based on their relative abundance for the risk analysis.

The current research work presents a hybrid methodology that integrates the DBN with a loss aggregation technique and demonstrates its novel application for MIC risk prediction, considering complex multispecies biofilm architecture. The DBN is structured to incorporate the risk influencing factors and capture their dependencies for the offshore system degradation rate. This involves the prediction of the failure probability and the likelihood of failure consequences based on the health state of the safety barriers/actions. The loss aggregation technique is adopted to determine the expected economic losses for the likely loss scenarios induced by microbial corrosion. This provides the value at risk in terms of financial losses at the operational phase of the offshore infrastructures. The application of the proposed methodology is tested on a subsea pipeline suffering microbial corrosion. The integrated dynamic model can capture the MIC's time-dependent behavior and its influential parameters to forecast the complex degradation mechanisms, the likelihood of failure, and the associated loss scenarios in offshore operations.

The structure of the remaining sections of the chapter is as follows: Section 7.2 gives an overview of offshore systems corrosion risk assessment. Section 7.3 presents the proposed methodology. Section 7.4 describes the methodology implementation with a case study. Section 7.5 includes the results and discussion, and Section 7.6 provides the conclusions.

7.2. Overview of corrosion risk assessment of offshore systems

Microbial corrosion initiation and propagation pose safety and integrity threats to sustainable offshore operations, especially in harsh ocean environments. The deterioration of the systems causes them to fail with associated consequences, which describe MIC's risk. Dynamic risk assessment employs a method that is capable of updating the estimated risks with respect to the deteriorating state of the system changes in terms of performance, safety, and maintenance activities [33]. This approach will help operators and integrity managers track changes occurring in the system's health state to define decision-making criteria and set a tolerable risk level during operations. The following subsection briefly describes the dynamic probabilistic approach for risk assessment.

Dynamic Bayesian networks: The conventional Bayesian network (BN) is a technique that models the random variables under uncertainty using a directed acyclic graph structure. This approach has been used for both qualitative and quantitative risk-based analysis under uncertainty [33–39]. BN captures dependencies among random variables and integrates the concept of conditional independence and the chain rule to estimate the joint probability distribution of random variables, as given in Eq. (7.1). Bayes' theorem (see Eq. (7.2)) is a governing equation in the BN that enhances updating upon the availability of new information, called evidence (E).

$$P(U) = P(Y_1, Y_2, \ldots\ldots, Y_n) = \prod_{i=1}^{n} P\left(Y_i | P_y(Y_i)\right) \tag{7.1}$$

where $P_y(Y_i)$ is the parent of the random variable Y_i and P(U) refers to the joint probability distribution.

$$P(U|E) = \frac{P(U,E)}{P(E)} = \frac{P(U,E)}{\sum_U P(U,E)} \tag{7.2}$$

The DBN is an extension of the BN for modeling an evolving stochastic process by capturing the temporal relationship among random variables nodes [13,21,30,40–42]. The temporal relationship among nodes is time-indexed, and the multidimensional probabilistic dependencies among the random variables are captured. This proves the merits of DBN over the conventional BN.

For instance, if $\mathbb{R}$ denotes a set of random variables $Y_1, Y_2, \ldots\ldots, Y_n$ $(\text{i.e.}, \text{Y} \in \mathbb{R})$, the temporal interrelationship across the time elements for a DBN can be expressed by Eq. (7.3).

$$P(\mathbb{R}_t|\mathbb{R}_{t-1}) = \prod_{i=1}^{n} P\left(\mathbb{R}_{i,t}\middle|P_a\left(\mathbb{R}_{i,t}\right)\right) \tag{7.3}$$

where $\mathbb{R}_{i,t}$ stands for the i^{th} node at time t; $P_a\left(\mathbb{R}_{i,t}\right)$ is the parent nodes of $\mathbb{R}_{i,t}$ from the same time and previous time elements, and n refers to the number of nodes in the network.

The joint probability distribution for a DBN structure for time, $t = 1\ to\ N$, can be expressed by Eq. (7.4). For conditional probability table (CPT) estimation in DBN, it is assumed that Y_i is represented at time step j by a node $n_{(i,j)} \in N$ with a finite number of states $\mathcal{S}_{n_i}: \{S_1^{n_i}, \ldots\ldots S_M^{n_i}\}$; $y_j^{n_i}$ denotes the probability distribution over these states at time step *k*, which defines the transition-probabilities (CPT) between the variable node states at time step j and time step $j+1$. This evolutionary process leads to determining the CPT (transition probability distribution) relative to the inter-time steps [43]. This implies that the future $(j+1)$ is conditionally independent of the past, given the present (j). Hence, the CPT $P\left(n_{i,j+1}\middle|P_a\left(n_{i,j+1}\right)\right)$ follows the Markovian assumption.

$$P(\mathbb{R}_{1:N}) = \prod_{t=1}^{N} \prod_{i=1}^{n} P\left(\mathbb{R}_{i,t} \middle| P_a(\mathbb{R}_{i,t})\right) \quad (7.4)$$

The DBN application enables forecasting the future degradation state, the failure probability of the corroding offshore system, and the associated risks of failure based on an iterative inference algorithm. For more details on the DBN learning and inference algorithms, interested readers are referred to the work conducted by Murphy [44].

7.3. Proposed methodology

Microbially influenced corrosion complexity makes the prediction of its failure-induced risk challenging. This results from the unstable interplay among the key factors, such as bacteria and the operating parameters. An understanding of the metabolic complexity and adaptability of bacteria within the multispecies bacteria colony is crucial for the development of a robust risk prediction model under MIC. Fig. 7.1 shows the proposed dynamic and robust methodology for risk prediction of offshore systems suffering MIC. The following steps describe the procedure of model development and its application:

Step 1: Assess the system's operational data, inspection data, and microbial induced flaws' characteristics. This provides detailed information on the environmental condition and various monitoring operating parameters, such as CO_2 partial pressure, H_2S partial pressure, oxygen, water cut, chloride ions, temperature, salinity, velocity, alloy composition, exposure time, pH, sulfate ions, bacteria types, counts/relative abundance, and biofilm architecture. For operational data collection in the offshore oil and gas industry, sensors and intelligent pigging tools such as the magnetic flux leakage (MFL), ultrasound, and probes are mostly used for defects detection, data collection, and mapping; on-line condition monitoring for monitoring operating parameters; and

the use of API-RP-38 serial dilution techniques and molecular microbiological methods for microorganisms detection/analysis. These tools/methods have been satisfactorily validated for the oil and gas industry.

Step 2: The system's health is further examined based on the inspection data. The collected monitoring operational data are assigned to various intervals to assess their probabilities for high, moderate, and low ranges. The data partitioning enhances a better understanding of the bounds of the influence of system failure's vital factors. The data partitioning approach for probability estimation has been demonstrated in previous research studies [15,45].

Step 3: Assess the system state and identify the various consequences of MIC induced failures under different operation scenarios. This is built based on the likely failure modes caused by MIC. The consideration of the possible failure modes requires the analysis of the outcomes. The outcomes in this research are grouped into four (e.g., one safe outcome and three critical consequences). These are safe, C_1; small economic loss and environmental pollution, C_2; huge economic loss and environmental pollution, C_3; and catastrophic economic loss and environmental pollution, C_4. The safe, C_1 outcome, as assumed in this research, denotes the operational state where intervention upon detection of the defects is successful, such as perfect detection, maintenance, and replacement of the corroding segments before failure.

The consequences of failure-induced financial loss evaluated include production loss/shutdown costs, inspection costs, segment repair/replacement costs, environmental impacts, and loss of reputation costs. The losses are cost elements of the loss scenarios, which vary based on the severity of the scenarios. When a failure occurs, there will be system shutdown and business interruption, which may result in loss of market share investment and trust from the negative public perception of the organization's safety performance. This will directly and/or indirectly cause

additional losses to the organization's reputation. Similarly, other losses can be assessed based on the magnitude of the failure events. For the subsea pipeline, the lower baseline financial loss/cost used in this research analysis is extracted from the literature [46–49], with an annual inflation rate of 2%.

Step 4: The system and its failure-induced consequences are further assessed to identify and establish safety barriers/actions that could mitigate the corrosion defects propagation (failure events). This is expected to represent all critical safety actions that could affect risk aversion from design to operation and failure of the system. However, the trade-off between cost and safety also plays an essential role in the selection of safety barriers/actions. In this work, the safety actions are grouped into four core barriers, namely treatment and environmental control, SB1 (i.e., pH/buffering, corrosion inhibition, scale inhibition, biocide application, oxygen scavenging, H_2S scavenging, dehydration, and pigging); condition monitoring and assessment, SB2 (i.e., inspection, corrosion monitoring, defects detection, fluid sampling, and leak detection); maintenance action, SB3 (i.e., minor repair, and preventive maintenance); and management/emergency action, SB4 (i.e., competent action, emergency intervention systems/shutdown, and operational decision making). To capture the dependencies among the barriers, the Domino theory principle and the structural dependency, presented by Khakzad et al. [50], are adopted in this research analysis. The safety barriers' functionality depends on the accurate understanding of the fluid characteristics and the operational instability posed by the key influencing factors. Any changes in the production well/fluid characteristics may affect the treatment and environmental control procedure. Therefore, an adequate understanding of the subsea well sampling and the sample characteristics and analysis accuracy are crucial for an effective mitigation plan against MIC. Hence, if dependencies exist among key safety barriers, any

error or failure of one safety action affects the others. In such a complex operational scenario, a robust and dynamic predictive tool is essential. It is important to note that for this research, we assume sequential and functional dependency among the safety barriers/actions, as discussed by Khakzad et al. [50]. However, the causal arcs drawn from the MIC induced failure node to the safety barriers (see Fig. 7.2) reveal the dependence for those safety barriers/actions whose performance/failure depends on the failure and/or the state of failure of the asset.

Step 5: A consequence-based dynamic network structure is developed to capture the propagating event (MIC), the safety barriers/action, and the likely consequences using DBN. The safety barrier/actions are categorized into two states (success and failure).

Step 6: The system wall thickness is discretized into four states to represent different degradation profiles (e.g., corrosion depth). The pipe wall thickness is discretized into four pit depth states based on the corrosion penetration percentage. For instance, the four pit depth states are 0-25%, 25-50%, 50-75% and >75%. The pit depth state >75% represents the critical depth that can lead to leak failure. The failure state is formulated based on the critical pit depth (>75%) penetration of the system's wall thickness. This approach was employed by [45]. However, the system can fail by rupture under high flow stresses, hydrogen-induced cracking, sulfide stress loads, and pressure disturbances at considerable wall thickness deterioration due to MIC. The discretized states, defined by the prior probability distribution, are based on the system's health state at operating and inspection conditions. This serves as the input data to the dynamic node in step 7 for the failure probability prediction.

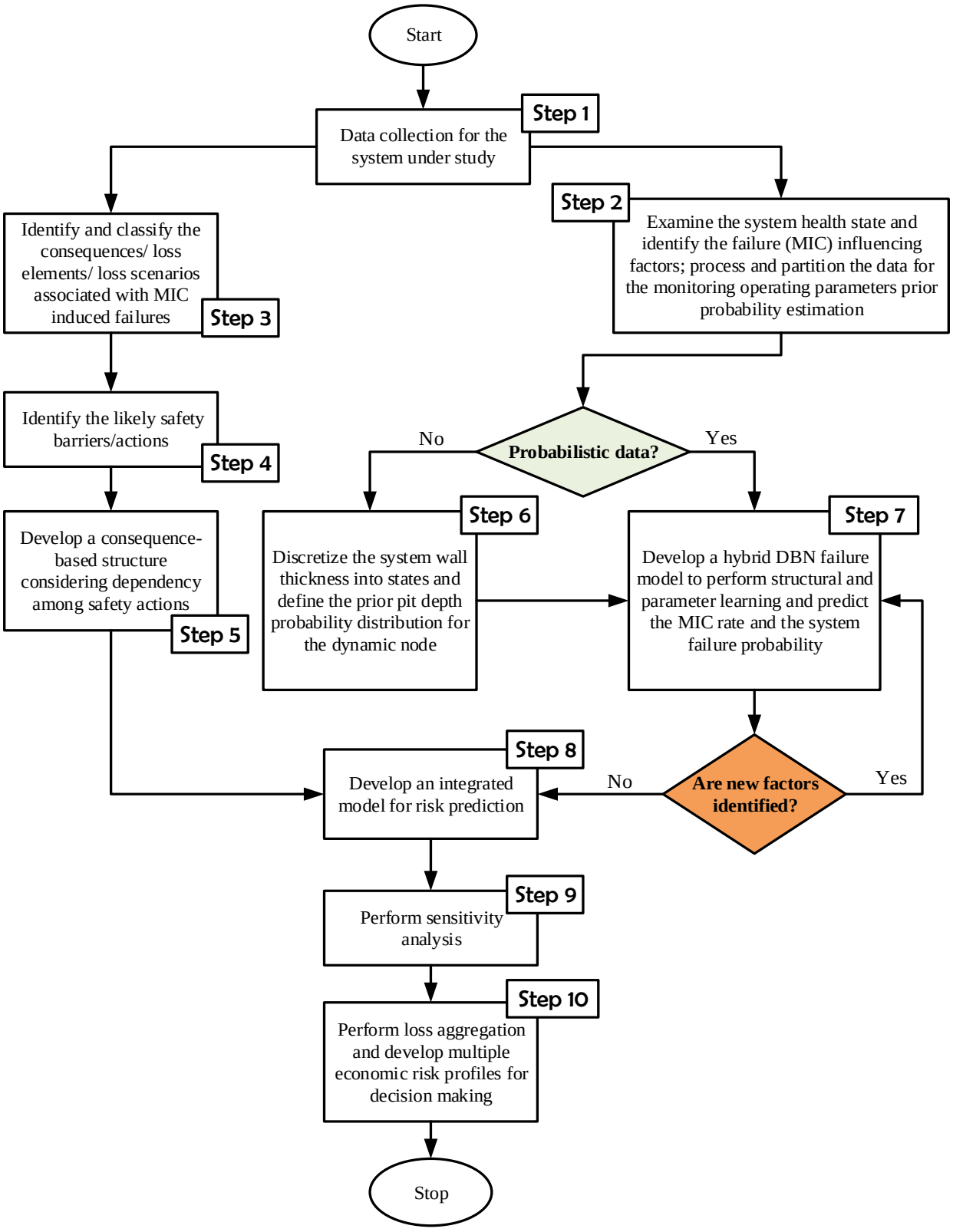

Figure 7.1. Schematic of an integrated dynamic model for microbial corrosion risk prediction

Step 7: The probabilistic data are used to develop the hybrid DBN for structurally and parametric learning, and to investigate the important factors' effects on the MIC rate and the system failure state. The interactions among temperature, CO_2 concentration, pH, salinity, and H_2S content are captured in the structure. Several researchers have shown that the operating conditions/parameters significantly affect the bacteria degradation activities and their metabolisms [51–54]. The available data range of these influencing parameters enhances the survival of the corrosive multispecies biofilm on the offshore system's surface. Under the mixed microbial biofilm architecture, the diversity in the degradation potentials and the mutual dependencies among the bacteria pose a severe threat to offshore systems' survivability. To capture the governing mechanisms, the influencing parameter nodes and bacteria nodes are categorized into high, moderate, and low states, while the MIC node is classified into severe, high, moderate, and low, respectively. This represents the system's likely degradation rates due to MIC based on the recommended rate categorization [55]. The probabilistic data estimated in step 2 and system state prior probability distribution from step 6 are used as the input data for the DBN structure to predict the MIC rate and the failure probability, as shown in Fig. 7.2. The conditional probability table (CPT) is built using corrosion models [12,53,56], expert knowledge, and the state of defects in the offshore system.

Furthermore, the dynamic interplay among the operating parameters (such as CO_2, pH, H_2S, and temperature) and their influence on the bacteria growth, corrosion rate, and failure probability are investigated. The hybrid DBN has demonstrated considerable merits for analysis of small and incomplete data sets, an explicit treatment of uncertainty, structural and parametric learning in evolving time steps, and a combination of multiple knowledge sources [34,54].

Step 8: A dynamic risk model is developed by integrating the DBN failure model with the consequences-based probabilistic model. In this model, the dynamic node (MIC induced failure state) in the DBN framework serves as the initiating event, and the predicted failure probability is used as the input data (see Fig. 7.2). To explore the dynamic and stochastic nature of MIC, the time evolution effect on the failure probability is propagated to the consequences. Hence, for different operational scenarios, the likelihood of the failure outcomes changes the risk prediction. All the DBNs in this work are simulated in the GeNIe™ software environment.

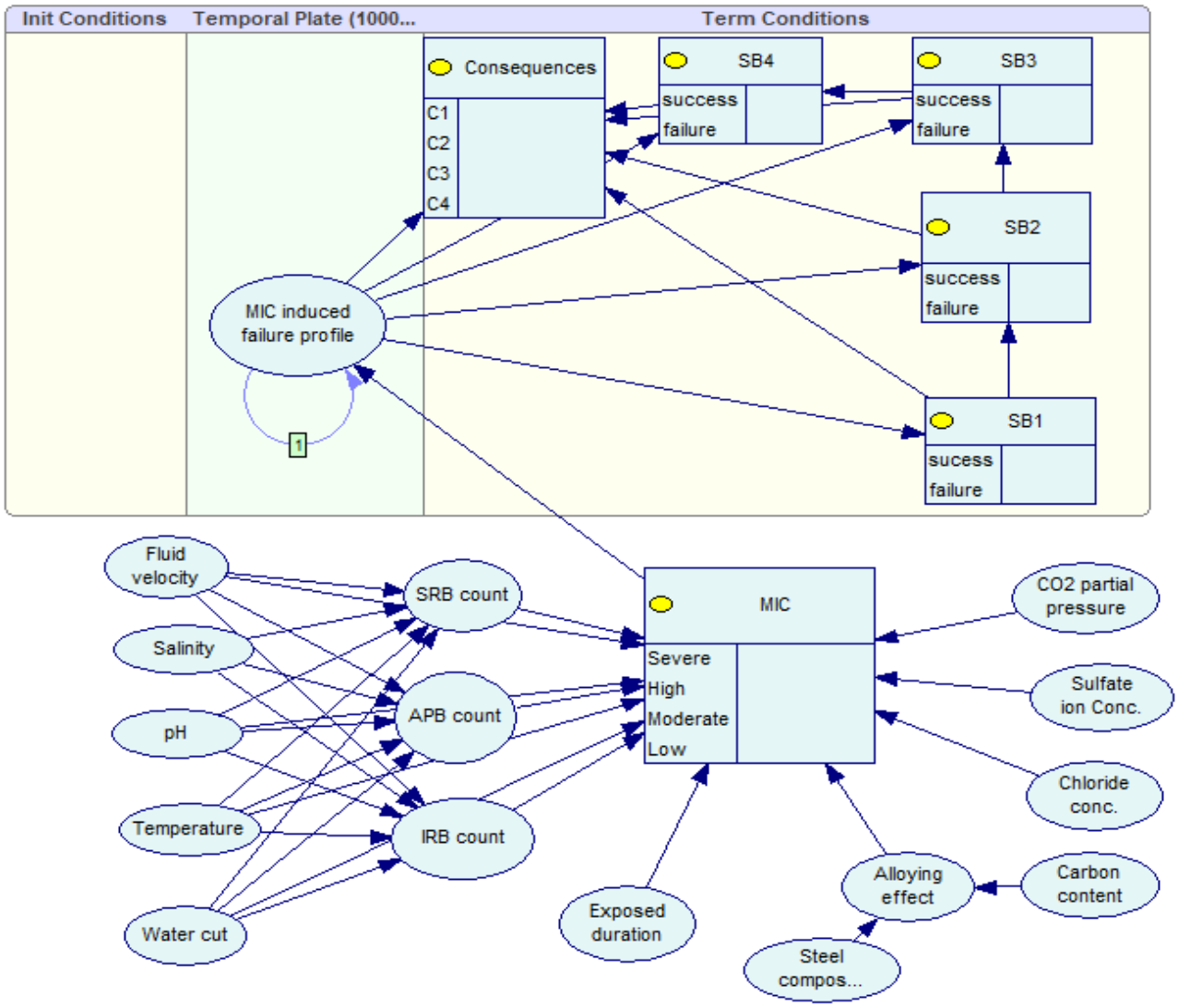

Figure 7.2. Schematic of the hybrid DBN structure for MIC risk prediction

Step 9: A parametric sensitivity analysis is carried out to identify the degree of influence of the various monitoring operating parameters and environmental factors' nodes on the failure modes and possible consequences. The sensitivity analysis of the hybrid DBN technically helps to identify critical input factors that significantly impact the risk propagation upon MIC formation. The DBN model is able to capture and propagate the parameters' associated uncertainty. Thus, it enhances the prioritization of the additional data needed for system modeling and optimization [15]. Different techniques have been proposed in the open sources for sensitivity analysis, which include entropy reduction, change ratio, variance of beliefs, and variance reduction [15,57–59]. For this research, the percentage change ratio technique is adopted for the sensitivity analysis to identify the influential factors under multiple operational scenarios.

Step 10: Further analysis is carried out to evaluate the value at risk in terms of economic loss on the investment incurred due to failure. The associated loss elements of microbial corrosion induced failures include but are not limited to operational loss, business interruption loss, reputational loss, asset loss, production loss, human health loss, and environmental clean-up loss. These loss elements are considered in the three critical consequences that represent the loss scenarios of the possible failure modes of microbial corrosion (i.e., small leak loss scenario, large leak loss scenario, and catastrophic loss scenario). To model these loss scenarios, a loss aggregation technique, proposed by [47], is given below:

$$E\{L_{scenario1}\} = \frac{1}{J}\sum_{j=1}^{J} L_{scenario1}^{j} \tag{7.5}$$

where J is the number of simulation runs. For any given failure (loss) scenario, the expected economic loss value, and the variance of the overall economic loss are the sum of the individual loss elements' mean value and variance, respectively.

A modified formulation is presented for the stochastic process to capture the probability of occurrence of the loss elements/scenarios. The formulation is used for the evaluation of the total economic loss value and variance based on the expectation probability theory, as shown by the following equations:

$$\mathbb{E}[L_E] = \sum_{d=1}^{D} E[L_d] \cdot \mathbb{P}(L_d) \tag{7.6}$$

$$Var[L_E] = \sum_{d=1}^{D} Var\,(L_d) \cdot \mathbb{P}(L_d) + 2 \sum_{d=1}^{D} \sum_{d'<d}^{D-1} Cov(L_d, L_{d'}) \tag{7.7}$$

where $\mathbb{E}[\cdot]$ is the expectation operator; $Var\{L_d\}$ symbolizes the variance of each loss element L_d; $Cov\{L_d, L_{d'}\}$ introduces the covariance between L_d and $L_{d'}$; $\mathbb{P}(L_d)$ refers to the probability of the loss element/scenario (failure) occurrence; $L_{1\ldots\ldots} L_d$ are the random variables that represent the elements of a given loss (failure) scenario; and $d = 1, \ldots\ldots\ldots, D$ designates the number of the loss scenarios. This formulation is also applied to estimate the expected economic loss incurred due to the safety barriers/actions. The cumulative expected loss for any of the loss scenarios can be expressed as follows:

$$L_{scenario} = \int_{0}^{t} E[L_i(\mu_t, \sigma_t)] \cdot \mathbb{P}(L_i, t)\, dt \tag{7.8}$$

where $E[L_i(\mu_t, \sigma_t)]$ represents the unit expected economic loss value for the loss element i and $\mathbb{P}(L_i, t)$ refers to the probability of its occurrence within [0, t]. This approach captures the likely cost (expected economic loss value) incurred for the various safety barriers/actions in the year of system failure. This technique aggregates the financial loss incurred on the safety barriers with the cost of the consequences using a loss aggregation function for decision making. However, for this

research, the $Cov\{L_d, L_{d'}\}$ is assumed to be zero, and multiple economic loss profiles are developed to define the various values at risk in terms of financial losses for the different loss scenarios. The result provides guidelines for system economic loss management plans and operational integrity decision making.

To capture the variability associated with the loss elements, a probability distribution is assumed for their prediction. The loss elements are considered to be normally distributed, and the predicted expected economic loss distribution is validated using the Kolmogorov-Smirnov and Shapiro-Wilk tests of normality, as depicted in Eqs. (7.9)-(7.11), respectively.

For an empirical distribution function F_n, the n number of independent and identical distribution events Y_i gives:

$$F_n(y) = \frac{1}{n}\sum_{i=1}^{n} \mathrm{I}_{[-\infty,\mathrm{y}]}(\mathrm{Y_i}) \tag{7.9}$$

where $\mathrm{I}_{[-\infty,\mathrm{y}]}(Y_i)$ is the indicator function, equal to 1 if $Y_i \leq y$, otherwise 0. Hence, the Kolmogorov -Smirnov test statistic for a given cumulative distribution function $F(y)$ is expressed below:

$$D_n = \sup_{\mathrm{y}} |F_n(y) - F(y)| \tag{7.10}$$

where $\sup_{\mathrm{y}}$ denotes the supremum of the set of distances.

The Shapiro-Wilk test statistic is defined as follows:

$$W = \frac{\left(\sum_{i=1}^{n} a_i y_{(i)}\right)^2}{\sum_{i=1}^{n}(y_i - \bar{y})^2} \tag{7.11}$$

where y_i is the random sample (loss elements cost); $\overline{y}$ introduces the sample mean; and a_i resembles the coefficient of the expected value of the order statistics. For this research, SPSS software is used for the test of normality analysis.

The integrated model provides a dynamic and robust prognostic tool for new applications in microbial corrosion risk prediction.

7.4. Case study

The proposed hybrid connectionist methodology is demonstrated on a 203 km oil transmission externally coated pipeline made of grade API 5L X-60 steel. The 762 mm outer diameter pipeline operates in a subsea oil field production with characterized bacteria-influenced failure in the marine environment [60]. An investigation of the subsea pipeline has revealed that the pipe has experienced severe localized defects at the 6 o'clock position of the pipe section. The pipeline is buried in a deep trench and influenced by the bacteria on the internal pipe surface, resulting in excessive wall thickness reduction and failure of the pipeline. The pipeline has a corrosion monitoring/fluid analysis procedure with an oil corrosion inhibitor dose of 4.70 ppm continuously applied and in batch quarterly application of biocide. The assessed information on the pipeline's operating/environmental conditions is shown in Table 7.1. The pipeline's mechanical properties include: wall thickness of 17.48mm, out diameter of 762mm, operating pressure of 9.3MPa, design pressure of 13.7MPa and pipeline length of 203km. The system operating state is assessed based on the historical data of the monitoring corrosion influencing variables and the inspection data (see Table 7.1). The monitoring operating variables data are processed through partitioning to estimate their prior probability and to train the designed network. More information on data partitioning for prior probability estimation can be found in our previous research studies [26,45]. These MIC

influencing parameters are integrated into a network structure using the DBN for the system failure prediction.

Table 7.1. Pipeline operating conditions and other important information

Parameters (Node)	Range	Parameters (Node)	Range
pH	3.4 ~ 9.89	pCO_2 (MPa)	0.01~ 0.19
Temp (°C)	15 ~ 65	Iron (ppm)	0.23 ~ 128
Flow rate: (a)	Oil(BOPD) 194,502	Sulfate ion (ppm)	1 ~ 3410
(b)	Water cut (%) 1~7	pH_2S (MPa)	0.137 ~ 0.514
Chlorine (ppm)	1 ~ 4430		Max. > 4.0 yrs
Flow velocity (m/s)	0.5 ~ 0.89	Exposure period	Mean 2.5 - 4.0 yrs
			Min < 2.5 yrs
APB counts	Low < 10^3 cfu/ml	Volatile fatty acids	Present/Absent
	10^3 < Moderate <10^4	Organic liquid	90 ~ 92%
	High> 10^4 cfu/ml		
		Salinity	Present/Absent
SRB counts	Low < 10^4 cfu/ml	IRB counts	Low < 10^3 cfu/ml
	10^4 < Moderate < 10^5		10^3 < Moderate < 10^4
	High > 10^5 cfu/ml		High > 10^4 cfu/ml

Additional data/information for the research analysis is adopted from the project database [61] and the relevant literature [15,45,52]. More probability data for the safety barriers/actions and essential events are adopted from the literature [14,16,62]. The baseline costs for the predefined loss

elements and loss scenarios modeling are taken from the literature [47,49,63]. The following assumptions are considered for the model application:

i) The data/information, as shown in Table 7.1, present the prevailing operating/environmental conditions of the pipeline.
ii) The corrosion influencing parameters exhibit complex interactions with the corrosion response parameters.
iii) The internal defects are stable and could result in the failure of the subsea pipeline.
iv) The system is subjected to two worst-case scenarios: scenario-1 is predicted based on the marginal probability of the safety barriers and the consequence likelihood, while scenario-2 is predicted by placing hard evidence on the safety barriers and the corresponding consequence likelihood.
v) The cost associated with the failure scenarios is expressed in terms of the economic loss (value at risk) for the research analysis.
vi) The loss elements are uncorrelated and normally distributed; this assumption is validated using the test of normality analysis.

7.5. Results and discussion

The current research objective is to develop a dynamic probabilistic methodology that simultaneously captures the key factors affecting microbial corrosion induced failure and their dependencies for: i) determining the MIC induced degradation of the asset under multispecies biofilm architecture using BN, ii) determining the failure probability and the corresponding consequences over time with DBN, and iii) determining the cumulative economic loss distribution with loss function technique using the Monte Carlo simulation algorithm under different loss

scenarios. The DBN captures the interrelationships among the failure factors and their time-dependent effects. The results of the parametric learning of the DBN structure are presented in Fig. 7.3. The DBN parameter learning uses the prior probabilities estimated from the influential corrosion variables as the input data, with the conditional probability assessed using corrosion models and subject expert knowledge. The outcomes of this phase show that the degradation rate ranges from 0.18mm/year to 0.317mm/year. This is premised on the available data and their ranges of probabilities.

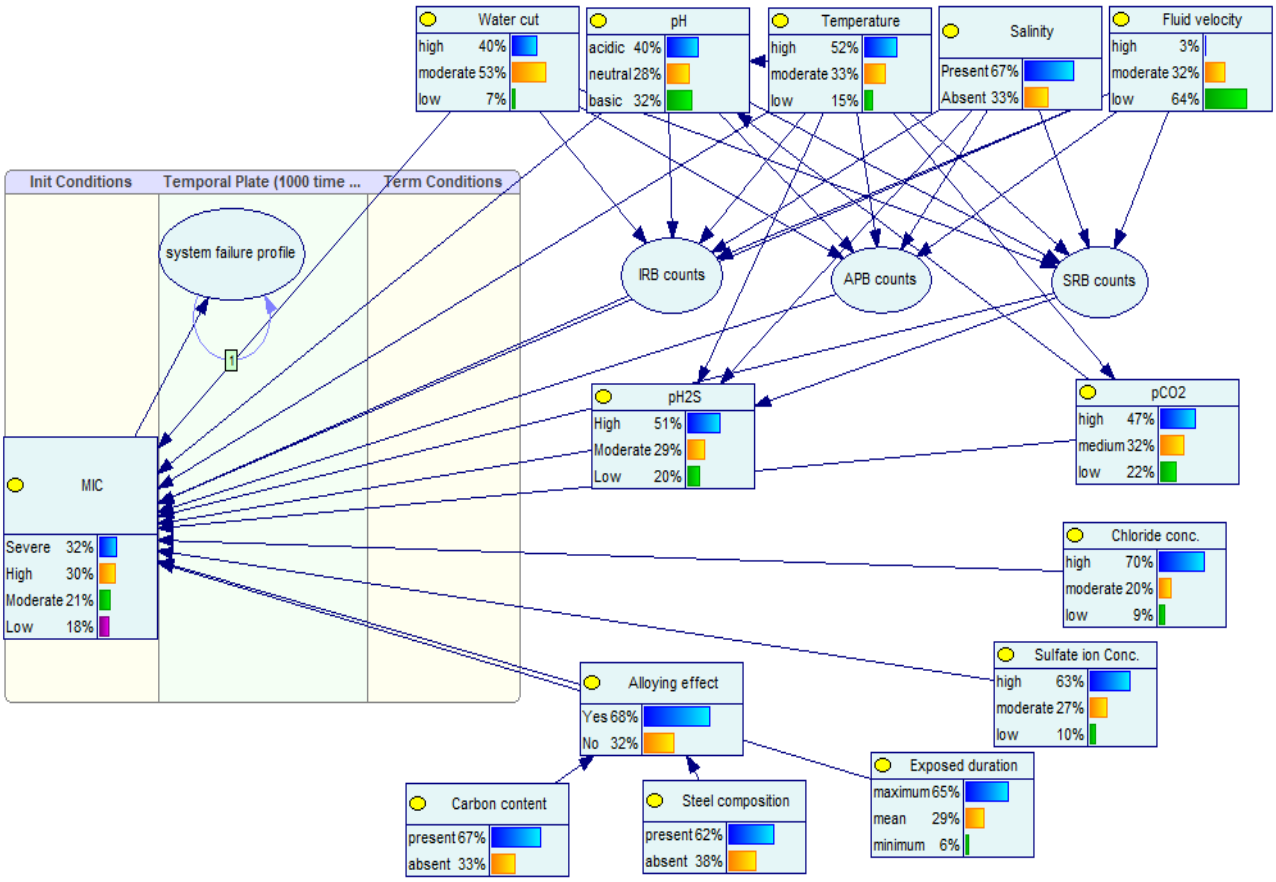

Figure 7.3. DBN parametric learning for microbial corrosion rate and failure probability prediction, considering dependencies among influencing parameters

Fig. 7.4 and Fig. 7.5 illustrate the impact of the dynamic interaction and dependencies among the vital corrosion influencing parameters and the bacteria on the system degradation rate under a multispecies biofilm. This is assessed by placing evidence on the multispecies bacteria nodes and the upper bound probabilities of the monitoring operating parameters' nodes, respectively. According to the results, the severe degradation rate increases for the two cases by 27.5% and 60.3%, respectively. This implies that as the sessile bacteria (Desulfovibrio, Desulfotomaculum, and Clostridium aceticum) counts increase, the system's deterioration severely increases. The byproducts of the bacteria metabolism, such as H_2S partial pressure and volatile fatty acid, enhance the corrosivity of the operating environment and promote severe degradation of the system. The results follow a similar trend with the findings of the previous works [45,64]. The dynamic node, as shown in Figs. 5.3-5.7, utilizes the prior state probability distribution based on the system's health state, defect depths, and the corrosion rate for the failure probability prediction. The prior probability distribution forms the dynamic node's CPT, which evolves over time-steps, based on the corrosion rate that serves as the transition intensity. The directed arc linking the variables (belonging to the different time-steps) reveals the random variables' temporal dependencies. For this analysis, up to 1000 time-steps are simulated for the failure probability prediction by the model.

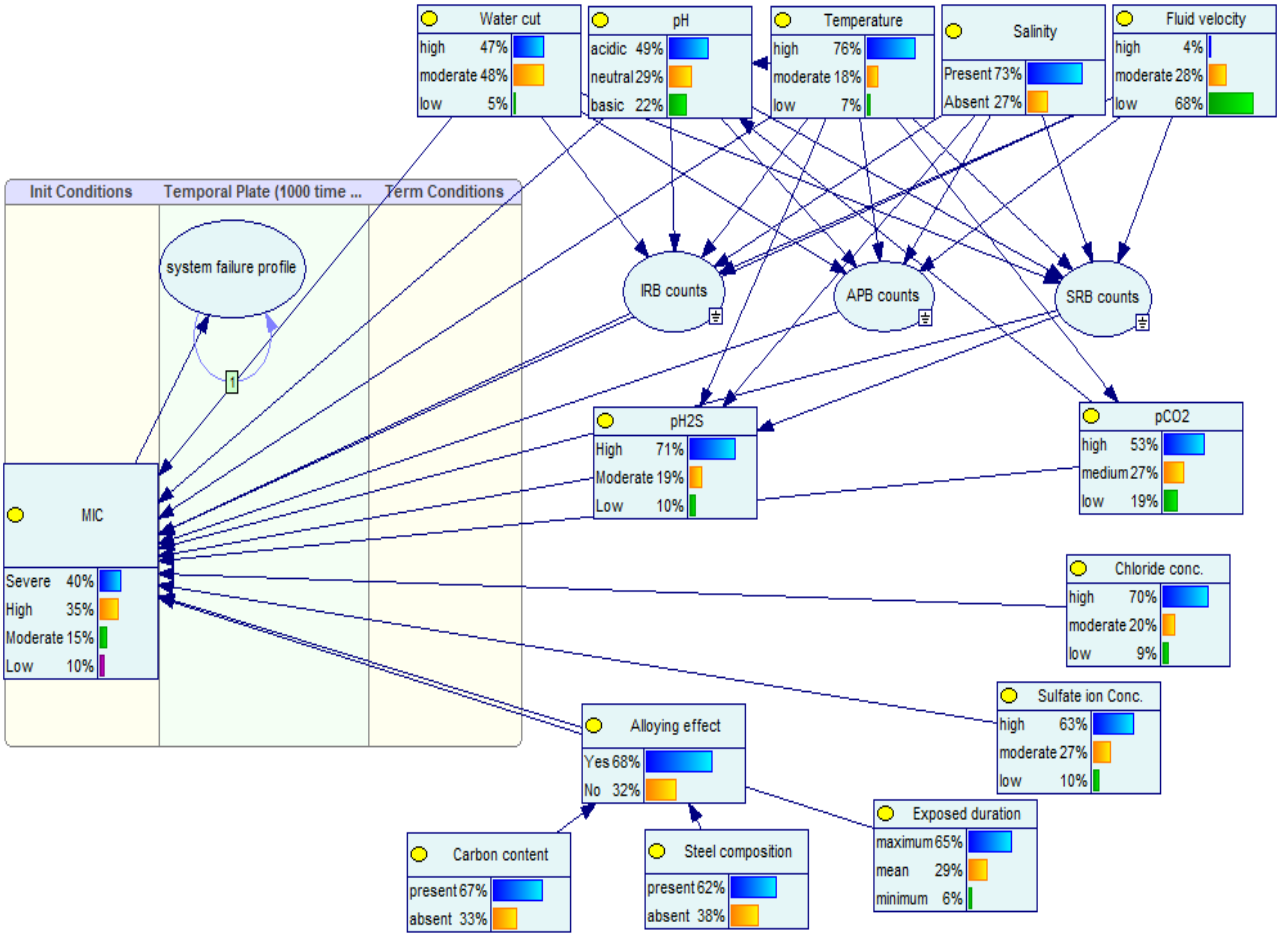

Figure 7.4. DBN structure for failure probability prediction with evidence on the bacteria nodes

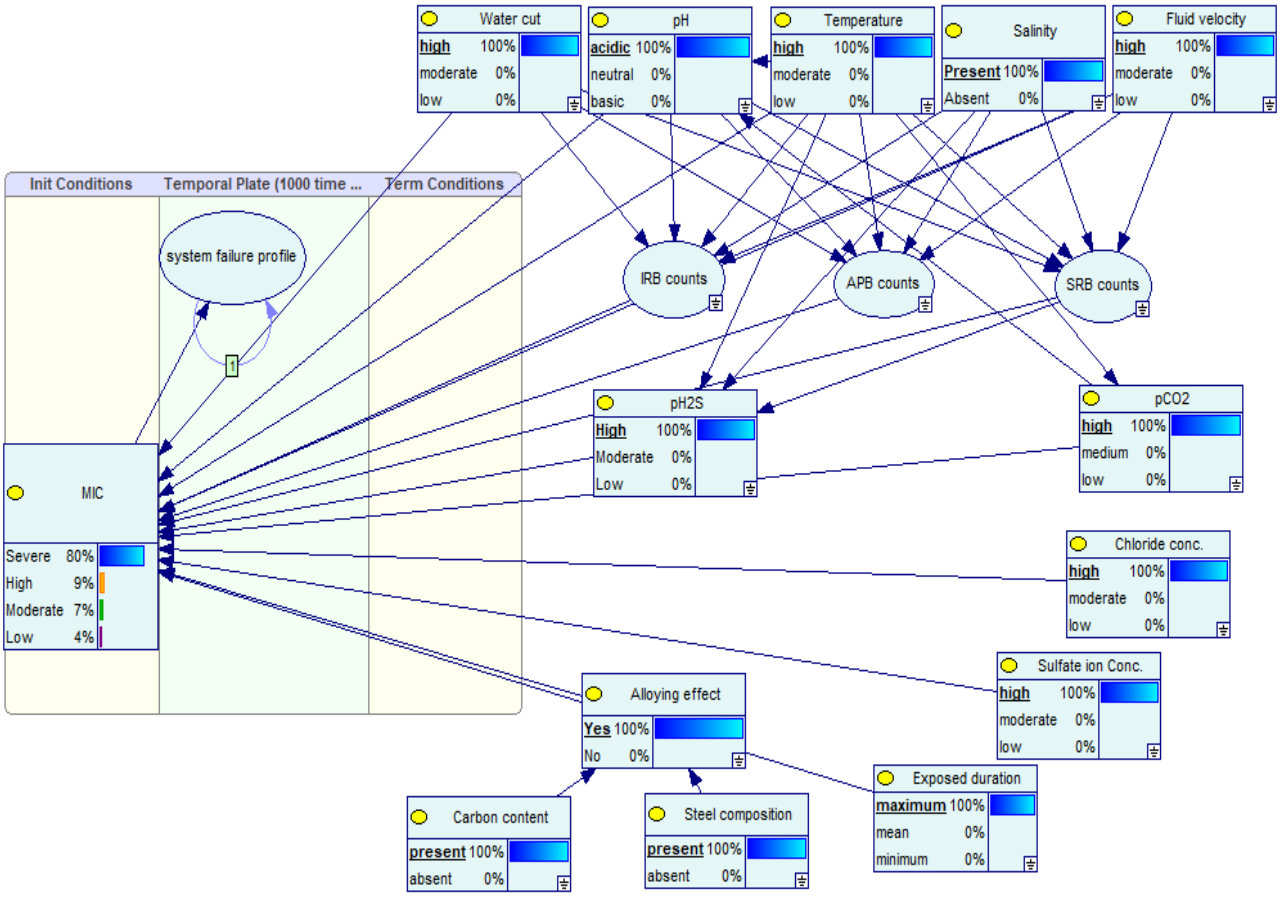

Figure 7.5. DBN structure for corrosion rate and failure probability prediction with evidence on the key factors nodes' upper bound probabilities

Furthermore, the predicted failure probability is mapped into a consequence-based structure for its likelihood prediction. A ten slices failure profile is used for the consequences analysis upon the formation and propagation of the MIC at the predicted corrosion rates. The likely safety barriers/actions are grouped into four and are represented to capture their impacts on the failure outcomes upon the formation of MIC. The simulation results based on the two worst-case scenarios are shown in Figs. 7.6-7.7. Scenario-1 presents the case that involves the formation of the MIC with its associated failure probability; the prior marginal likelihood of the safety barriers is used to determine the consequence likelihood (see Fig. 7.6). For the four consequence scenarios, as

depicted in Fig. 7.6, the magnitudes of the probability are equal to 0.526, 0.153, 0.12, and 0.201 for C_1, C_2, C_3, and C_4, respectively.

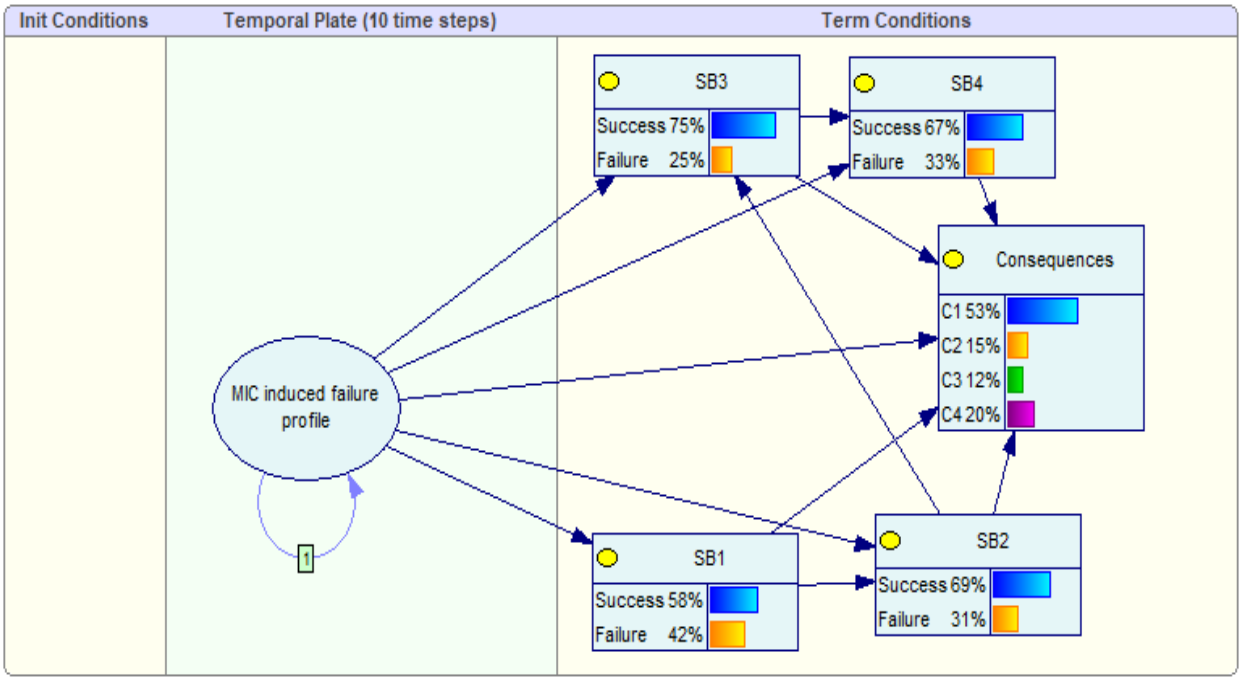

Figure 7.6. Results of consequence analysis under severe microbial corrosion rate

The analysis of the consequence likelihood for scenario-2 is presented in Fig. 7.7. In this case, the effects of the safety actions are taken into account to predict the consequences likelihood, as demonstrated in Fig. 7.7, when hard evidence is placed on the failure state of the safety barriers nodes. It shows a 44.6% increase in the probability of catastrophic economic loss and environmental pollution, signifying the likely occurrence of rupture failure upon MIC propagation. The rupture failure could occur at any time during operation, with considerable wall thickness deterioration under unstable pressure loads and stress-induced cracking as a result of H_2S presence. For the other failure outcomes, a progressive decrease in their occurrence likelihood can occur, given the safety barriers' failed state. The presented scenarios reveal the diversity of the state of

the failure outcomes as a function of the propagating corrosion degradation rate and its time evolution probability and safety barriers/actions. Therefore, it is essential to investigate the evolving effects of the safety barriers/actions and their likelihood on the overall failure outcomes for real-time risk prediction.

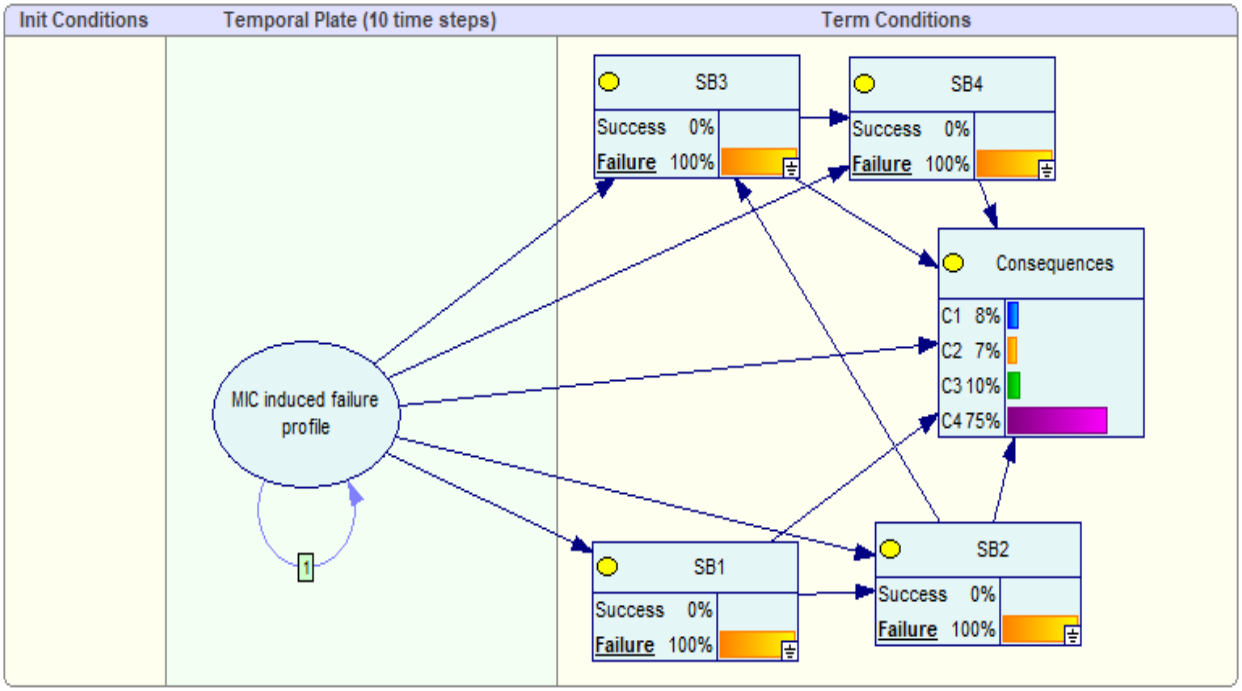

Figure 7.7. Results of consequence analysis under failed safety barriers/actions

A sensitivity analysis was carried out to establish the degree of influence of the monitoring operating parameters on the severe degradation rate and system failure (see Fig. 7.8). Using the modeling outcomes, the degree of influence of the vital factors is determined. It follows that the pCO_2 and pH_2S (partial pressures of CO_2 and H_2S) nodes have the highest contribution to the MIC node's, using the evidence of the severe degradation rate, accounting for 23% and 20%, respectively. This finding is in agreement with the previous studies [15,65]. This provides initial validation of the hybrid model. The high degree of the pCO_2 influence results from the formation

of carbonic acid due to the CO_2 dissolution in the oil-in-water phase medium. The carbonic acid plays a critical role in internal microbial corrosion and other forms of corrosion by cracking down the protective corrosion product [66]. The H_2S, which is the byproduct of the SRB's metabolism, is an aggressive substance that participates in and enhances the propagation of steel and iron materials' corrosion. Moreover, in sour oil field production, system degradation can be exponentially increased by H_2S presence. The pH and temperature are favorable stimulants for microbial growth and metabolism.

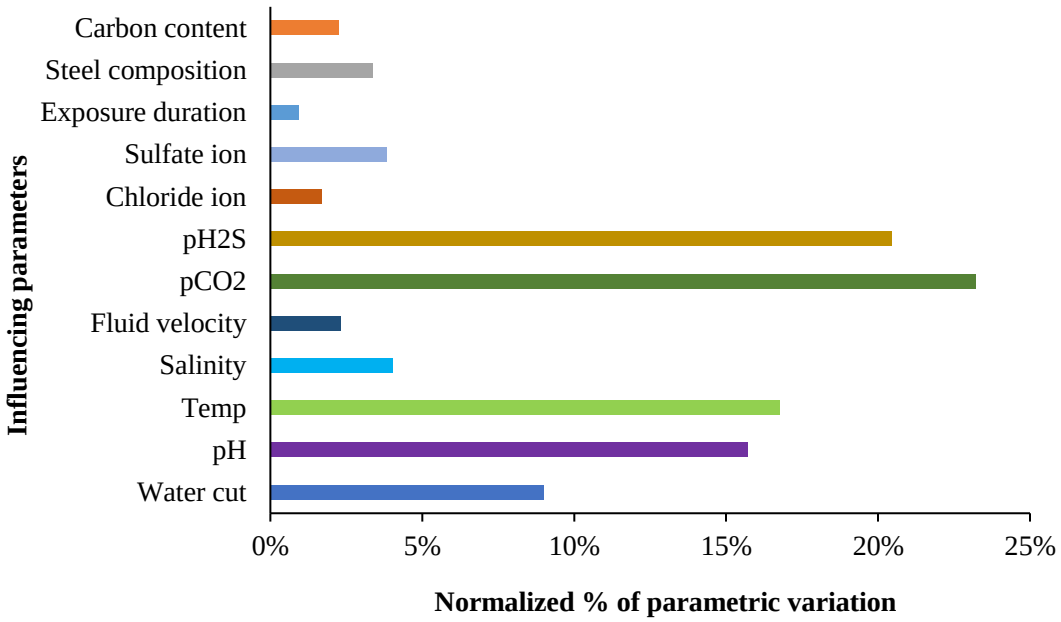

Figure 7.8. Sensitivity analysis of the MIC node due to the influence of various vital influencing parameters on the severe corrosion rate

The normalized percentages' influence of the pH and temperature on the severe degradation rate, as seen in Fig. 7.8, are 17% and 18%, respectively. It is found that the pipe surface is exposed to degradation due to the breakdown of protective films when the pH is low (acidic state), which supports the findings of [67]. The adaptive nature of microorganisms and their diversity under

multispecies biofilm enhances their survival at different temperature ranges. However, the normalized percentage influence reveals the significance of temperature on the subsea system's degradation rate. The flow velocity of about 0.8 m/s, which is considerably below the minimum recommended velocity, provides favorable conditions for possible segregation. This leads to the accumulation of water in the subsea pipeline's low laying areas and promotes the bacteria growth and metabolism; thus, it increases the pipeline wall degradation rate. Several other factors and their degree of influence can be deduced from Fig. 7.8. These key failure factors have combinatory impacts on bacteria growth and the system degradation process. The results exhibit a good match with the previous research investigations [15,62,68]. The combinatory effect of the influencing variables is captured in the DBN structure, and the identified variation due to their degree of influence reveals the critical parameters that should be monitored appropriately and controlled at every level of mitigation. Therefore, a parametric impact assessment on the system failure could be inferred by considering multiple scenarios.

Upon the formation of MIC, there is a progressive increase in the system failure probability with time. This failure or deviation in the system's performance capability is associated with consequences that are classified as loss or economic losses on the investment. Furthermore, the cost incurred on the safety systems for failure mitigation could be taken into account as economic losses when a failure event occurs. 10^4 simulation runs are conducted using Monte Carlo simulation to model the loss aggregation function (see Eq. (7.6)) in the MATLAB environment for the expected economic loss prediction. The results for the various loss (failure) scenarios ($L_{scenarios}$), with respect to their cumulative occurrence probability, are presented in Figs. 7.9-7.11. As shown in Figs. 7.9-7.11, for any known likelihood of occurrence of the loss scenarios

based on the predefined loss elements, the expected economic loss value (in USD) can be estimated.

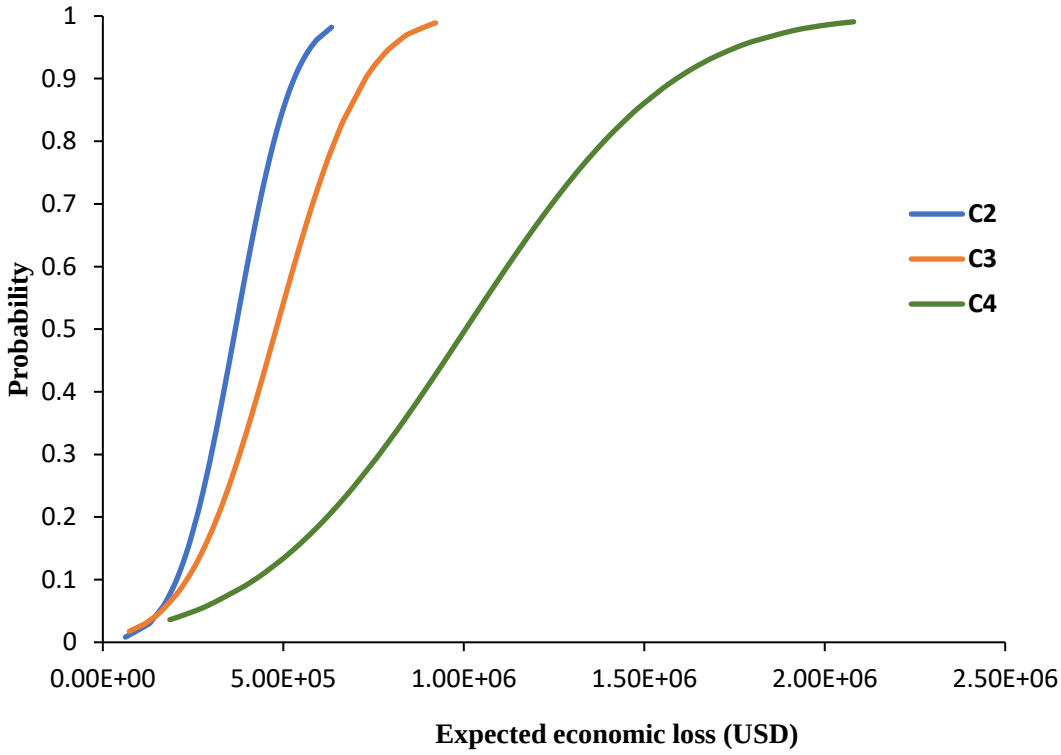

Figure 7.9. Expected economic loss (E_{Loss}) curve for scenario-1 based on the likelihood of the consequences

The induced costs associated with the loss scenarios are stochastically modeled; they are assumed to be normally distributed. The results provided in Fig. 7.9 are based on scenario-1 (see Fig.7.6), implying that the 95% upper bound confidence intervals for the expected value increase by 22.3%, 56.33%, and 64.3% for the loss scenarios of C_2, C_3, and C_4, respectively. Fig. 7.10 illustrates the effect of total failure of the safety barriers/actions (see Fig. 7.7) on the expected economic loss value, which accounts for a 70% increase in the 95% upper bound confidence interval of the expected loss value for loss scenario C_4. It is concluded that as the safety actions have failed to

mitigate against MIC propagation under unstable pressure disturbances/stress-induced cracking, the likelihood of loss scenario C_4 increases, as shown in Fig. 7.7. This increase in the probability of occurrence leads to an increase in its associated expected economic risk. The predicted results give an overview of the expected monetary loss (in USD) incurred based on the probability of occurrence of the various loss scenarios. The modeling results can be useful in operational cost planning and investment risk management. This provides practical tips for risk-based integrity and corrosion cost management. Furthermore, the total expected economic losses (in USD) based on the loss scenarios and the failure of the safety barriers are captured at the critical failure year (see Fig. 7.11). As shown in Fig. 7.11, there is an increase in the expected economic loss value across the loss scenarios with and without the cost incurred on safety barriers/actions.

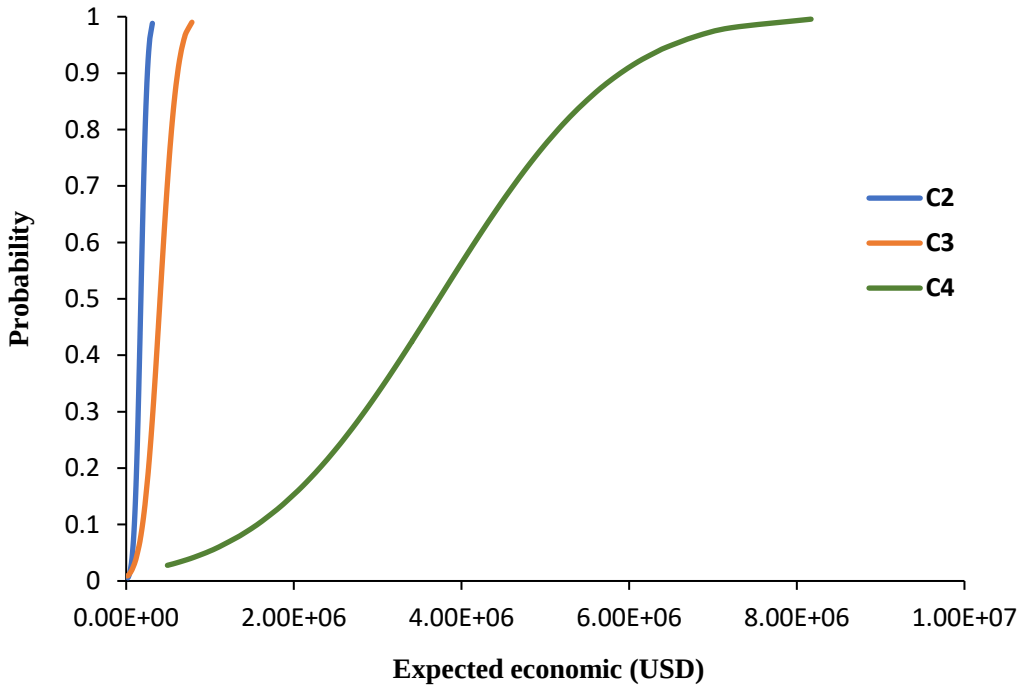

Figure 7.10. Expected economic loss (E_{Loss}) curve for scenario-2 based on the likelihood of the consequences

To validate the assumed probability distribution that captures the variability in the loss elements and the expected economic loss value, a normality test is carried out in the SPSS software environment; the results are reported in Table 7.2. EVAR1 and EVAR2 indicate the total expected loss value with and without the cost incurred because of the safety barriers, respectively. As shown in Table 7.2, the Kolmogorov-Smirnov and Shapiro-Wilk hypotheses are used for the normality test. It is found that the Shapiro-Wilk test gives better analysis, compared to the Kolmogorov-Smirnov test of statistics. Based on the alpha $(\alpha) = 5\%$ significance hypothesis, it is confirmed that the economic loss elements are normally distributed.

Table 7.2. Test for normality of the expected economic loss value

	Kolmogorov-Smirnov[a]			Shapiro-Wilk		
Expected Loss	Statistic	df	Sig.	Statistic	df	Sig.
EVAR1	0.060	100	0.200*	0.982	100	0.180
EVAR2	0.060	100	0.200*	0.987	100	0.446

*This is a lower bound of the true significance
a. Lilliefors significance correction

where df is the degree of freedom and Sig. represents the significance test value.

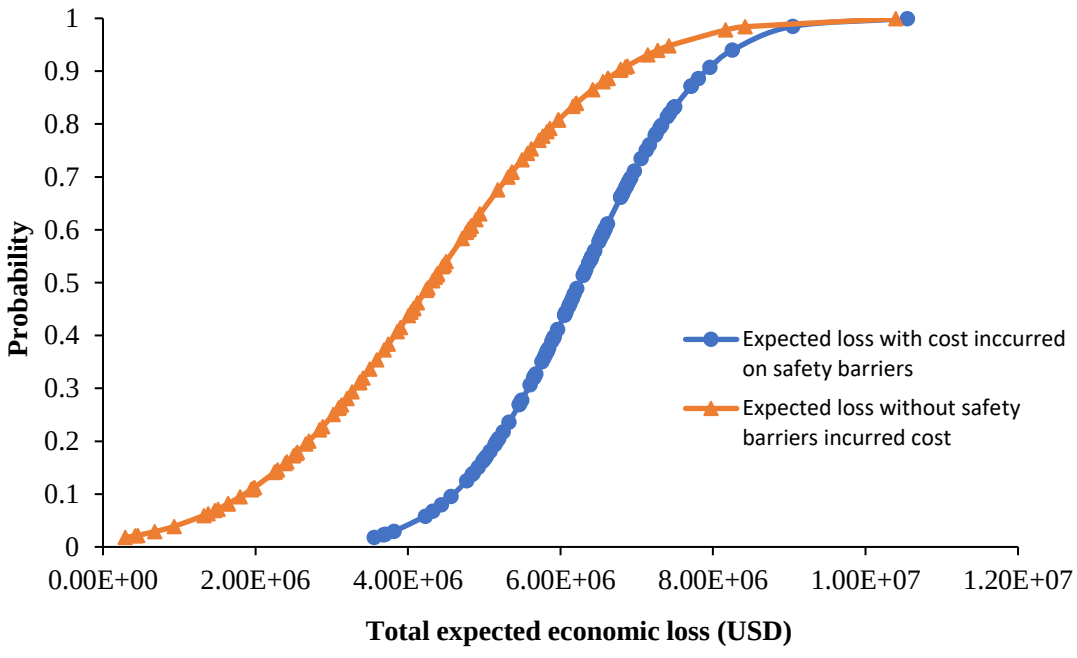

Figure 7.11. Total expected economic loss (E_{Loss}^{T}) curve for loss scenarios with and without the cost incurred on the safety barriers/actions at the critical year of failure

According to Fig. 7.11, the 95% upper bound of expected economic losses, which describe the total value at risk due to failure, is US$6.4 million with a variance (σ^2) of 1.261×10^{12}. The result analysis provides critical risk-based information that will help to forecast the economic losses based on the health state of the offshore system and the safety barriers. It is important to note that there is diversity in cost parameter characteristics, which is dependent on the system's operating terrain and the market influencing factors. This varies across the region of operations and case studies, which could be reflected in the overall predicted value at risk.

The current hybridized methodology, in comparison with the mechanistic and probabilistic approaches proposed by other researchers [7,8,11,15], offers a robust risk-based application. This is validated by its capacity to dynamically capture the vital influencing factors for failure and economic loss/risk prediction at different time-slices under multispecies biofilm architecture. Therefore, it is essential to integrate all likely losses and their variability as a result of failures and safety barriers/actions performance for the overall economic risk analysis. This is exhibited by the current model for well-informed risk-based decision making and loss/risk minimization strategies during the operation of offshore systems.

The proposed model provides an effective risk/economic loss monitoring (and predictive tool) for system operators and integrity managers. This shows the model's real-time monitoring capability for the system's health state and failure probability upon MIC formation; this approach can capture the value at risk based on the likelihood of the consequences over time. The dynamic model is of benefit to the marine and offshore oil and gas industries in assets integrity management and loss prevention strategy.

7.6. Conclusions

The present research demonstrates the integration and application of the DBN and loss aggregation technique for microbial corrosion risk prediction. The methodology explores the vital corrosion risk factors and their dependencies to predict the rate of degradation, failure, and consequences of failure in terms of economic losses in any time-period/step. It is observed that among the key factors, p_{CO2} and p_{H2S} show a significant impact on the severe degradation rate and failure of the system. The interplay between these influential factors plays a vital combinatory role that enhances the bacteria growth and the corrosion rate. Also, their associated instability and the bacteria diversity potentials complicate the failure characteristics of the corroding offshore systems. The proposed connectionist model demonstrates the capacity to simultaneously predict MIC induced failures and the associated risks during offshore operations. This section summarizes the key outcomes of the current research work:

- The developed model serves as a useful tool for dynamic corrosion risk assessment of marine and offshore systems.
- The model captures the dynamic non-linear interactions among corrosion influencing factors to predict the offshore system's degradation rate in operation.
- The hybridized model can propagate the offshore system's degradation rate for the prediction of the failure likelihood and consequences of failure in different time-slices.
- The model offers an integrated framework for the expected economic losses (value at risk) prediction based on the likely failure modes and their consequences under the multispecies biofilm structure.

- The hybridized model utilizes a probabilistic tool that integrates the soft and hard failure of the safety barriers/actions on the investment's overall financial losses. The results show a 40.3% and 57.5% increase in the total economic losses (value at risk) at the 95% upper and lower bound confidence intervals for the worst-case scenarios.
- The developed risk assessment methodology offers a dynamic and robust early warning and prognostic tool for economic risk-based decision making in offshore operations experiencing microbial corrosion.
- The marine and offshore oil and gas industries can benefit from the developed dynamic model in system degradation and failure propagation monitoring and forecasting. The associated risk/financial losses as a result of the system failure can be monitored through real-time risk modeling of offshore operations under MIC.

The dynamic model application confirms its benefits in risk assessment of microbial corrosion induced failure in offshore operations. However, the model can be further enhanced in future research by integrating copula modeling, market risk influencing factors, and stochastic dominance rules for loss elements/scenarios dependency analysis and risk minimization decision making criteria under uncertainty.

Acknowledgments

The authors acknowledge the financial support provided by Genome Canada and their supporting partners, and the Canada Research Chair (CRC) Tier I Program in Offshore Safety and Risk Engineering.

References

[1] Alasvand K, Ravishankar Z V. Identification of the traditional and non-traditional sulfate-reducing bacteria associated with corroded ship hull. 3 Biotech 2016;6:1–8. https://doi.org/10.1007/s13205-016-0507-6.

[2] Huang RT, McFarland BL, Hodgman RZ. Microbial Influenced Corrosion in Cargo Oil Tanks of Crude Oil Tankers. NACE Int. Corros. Conf., 1997.

[3] Eckert R. Field Guide for Investigating Internal Corrosion of Pipelines. NACE International, Houston USA; 2003.

[4] Paik JK, Kim DK. Advanced method for the development of an empirical model to predict time-dependent corrosion wastage. Corros Sci 2012;63:51–8. https://doi.org/10.1016/j.corsci.2012.05.015.

[5] Beech IB, Gaylarde CC. Recent Advances in the Study of Biocorrosion - An Overview. Rev Microbiol 1999;30:177–90.

[6] Gieg LM, Jack TR, Foght JM. Biological souring and mitigation in oil reservoirs. Appl Microbiol Biotechnol 2011;92:263–82. https://doi.org/10.1007/s00253-011-3542-6.

[7] Kaduková J, Škvareková E, Mikloš V, Marcinčáková R. Assessment of microbially influenced corrosion risk in slovak pipeline transmission network. J Fail Anal Prev 2014;14:191–6. https://doi.org/10.1007/s11668-014-9782-x.

[8] Sørensen KB, Thomsen US, Juhler S, Larsen J. Cost Efficient MIC Management System based on Molecular Microbiological Methods. NACE Int. Conf. expo, 2012, p. 1–15.

[9] Maxwell S, Campbell S. Monitoring the Mitigaation of MIC Risk in Pipelines. Corros. NACExpo; 61st Annu. Conf. &E Expo., 2006, p. 1–10.

[10] Vigneron A, Head IM, Tsesmetzis N. Damage to offshore production facilities by corrosive microbial biofilms. Appl Microbiol Biotechnol 2018. https://doi.org/https://doi.org/10.1007/s00253-018-8808-9.

[11] Skovhus TL, Andersen ES, Hillier E. Management of Microbiologically Influenced

Corrosion in Risk-Based Inspection Analysis. SPE Annu. Tech. Conf. Exhib., 2018, p. 122–30.

[12] Pots BFM, John RC, Rippon IJ, Thomas MJJS, Kapusta SD, Girgis M., et al. Improvements of De Waard-Milliams Corrosion Prediction and Applications to Corrosion Managment. NACE Int. Corros. Conf. No. 02235, 2002, p. 1–19.

[13] Arzaghi E, Abbassi R, Garaniya V, Binns J, Chin C, Khakzad N, et al. Developing a dynamic model for pitting and corrosion-fatigue damage of subsea pipelines. Ocean Eng 2018;150:391–6. https://doi.org/10.1016/j.oceaneng.2017.12.014.

[14] Hasan S, Sweet L, Hults J, Valbuena G, Singh B. Corrosion risk-based subsea pipeline design. Int J Press Vessel Pip 2018;159:1–14. https://doi.org/10.1016/j.ijpvp.2017.10.003.

[15] Shabarchin O, Tesfamariam S. Internal corrosion hazard assessment of oil & gas pipelines using Bayesian belief network model. J Loss Prev Process Ind 2016;40:479–95. https://doi.org/10.1016/j.jlp.2016.02.001.

[16] Yang Y, Khan F, Thodi P, Abbassi R. Corrosion induced failure analysis of subsea pipelines. Reliab Eng Syst Saf 2017;159:214–22. https://doi.org/10.1016/j.ress.2016.11.014.

[17] Zhang K, Duan M, Luo X, Hou G. A fuzzy risk matrix method and its application to the installation operation of subsea collet connector. J Loss Prev Process Ind 2017;45:147–59. https://doi.org/10.1016/j.jlp.2016.11.014.

[18] Li X, Chen G, Khan F, Xu C. Dynamic risk assessment of subsea pipelines leak using precursor data. Ocean Eng 2019;178:156–69. https://doi.org/10.1016/j.oceaneng.2019.02.009.

[19] Yuanjiang C, Xiangfei W, Changshuai Z, Guoming C, Xiuquan L, Jiayi L, et al. Dynamic Bayesian networks based approach for risk analysis of subsea wellhead fatigue failure during service life. Reliab Eng Syst Saf 2019;188:454–62. https://doi.org/10.1016/j.ress.2019.03.040.

[20] Wu W, Li Y, Cheng G, Zhang H, Kang J. Dynamic safety assessment of oil and gas pipeline containing internal corrosion defect using probability theory and possibility theory. Eng Fail

Anal 2019;98:156–66. https://doi.org/10.1016/j.engfailanal.2019.01.080.

[21] Cai B, Xie M, Liu Y, Liu Y, Feng Q. Availability-based engineering resilience metric and its corresponding evaluation methodology. Reliab Eng Syst Saf 2018;172:216–24. https://doi.org/10.1016/j.ress.2017.12.021.

[22] Mi J, Li YF, Yang YJ, Peng W, Huang HZ. Reliability assessment of complex electromechanical systems under epistemic uncertainty. Reliab Eng Syst Saf 2016;152:1–15. https://doi.org/10.1016/j.ress.2016.02.003.

[23] Cai B, Liu Y, Liu Z, Tian X, Dong X, Yu S. Using Bayesian networks in reliability evaluation for subsea blowout preventer control system. Reliab Eng Syst Saf 2012;108:32–41. https://doi.org/10.1016/j.ress.2012.07.006.

[24] Bensi M, Kiureghian A Der, Straub D. Efficient Bayesian network modeling of systems. Reliab Eng Syst Saf 2013;112:200–13. https://doi.org/10.1016/j.ress.2012.11.017.

[25] Mamudu A, Khan F, Zendehboudi S, Adedigba S. Dynamic risk assessment of reservoir production using data-driven probabilistic approach. J Pet Sci Eng 2020;184. https://doi.org/10.1016/j.petrol.2019.106486.

[26] Adumene S, Adedigba S, Khan F, Zendehboudi S. An integrated dynamic failure assessment model for offshore components under microbiologically influenced corrosion. Ocean Eng 2020;218. https://doi.org/10.1016/j.oceaneng.2020.108082.

[27] Kannan P, Kotu SP, Pasman H, Vaddiraju S, Jayaraman A, Mannan MS. A systems-based approach for modeling of microbiologically influenced corrosion implemented using static and dynamic Bayesian networks. J Loss Prev Process Ind 2020;65:104108. https://doi.org/10.1016/j.jlp.2020.104108.

[28] Cai B, Shao X, Liu Y, Kong X, Wang H, Xu H, et al. Remaining Useful Life Estimation of Structure Systems under the Influence of Multiple Causes: Subsea Pipelines as a Case Study. IEEE Trans Ind Electron 2020;67:5737–47. https://doi.org/10.1109/TIE.2019.2931491.

[29] Kammouh O, Gardoni P, Cimellaro GP. Probabilistic framework to evaluate the resilience of engineering systems using Bayesian and dynamic Bayesian networks. Reliab Eng Syst

Saf 2020;198:106813. https://doi.org/10.1016/j.ress.2020.106813.

[30] Mamudu A, Khan F, Zendehboudi S, Adedigba S. A hybrid intelligent model for reservoir production and associated dynamic risks. J Nat Gas Sci Eng 2020;83. https://doi.org/10.1016/j.jngse.2020.103512.

[31] Cai B, Liu Y, Liu Z, Chang Y, Jiang L. Bayesian Networks for Reliability Engineering. 1st Editio. Springer Nature Singapore Pte Ltd; 2020. https://doi.org/10.1007/978-981-13-6516-4.

[32] Marsili E, Kjelleberg S, Rice SA. Mixed community biofilms and microbially influenced corrosion. Focus Microbiol Aust 2018:152–7. https://doi.org/10.1071/MA18046.

[33] Khan F, Hashemi SJ, Paltrinieri N, Amyotte P, Cozzani V, Reniers G. Dynamic risk management: a contemporary approach to process safety management. Curr Opin Chem Eng 2016;14:9–17. https://doi.org/10.1016/j.coche.2016.07.006.

[34] Wu PPY, Julian Caley M, Kendrick GA, McMahon K, Mengersen K. Dynamic Bayesian network inferencing for non-homogeneous complex systems. J R Stat Soc Ser C Appl Stat 2018;67:417–34. https://doi.org/10.1111/rssc.12228.

[35] Khan F, Yang M, Veitch B, Ehlers S, Chai S. Transportation Risk Analysis Framework for Arctic Waters. Vol 10 Polar Arct Sci Technol 2014:V010T07A018. https://doi.org/10.1115/OMAE2014-23421.

[36] Wang YF, Li YL, Zhang B, Yan PN, Zhang L. Quantitative Risk Analysis of Offshore Fire and Explosion Based on the Analysis of Human and Organizational Factors. Math Probl Eng 2017;2015:537362. https://doi.org/10.1155/2015/537362.

[37] Abaei MM, Arzaghi E, Abbassi R, Garaniya V, Chai S, Khan F. A robust risk assessment methodology for safety analysis of marine structures under storm conditions. Ocean Eng 2018;156:167–78. https://doi.org/10.1016/j.oceaneng.2018.02.016.

[38] Abimbola M, Khan F, Khakzad N. Dynamic safety risk analysis of offshore drilling. J Loss Prev Process Ind 2014;30:74–85. https://doi.org/10.1016/j.jlp.2014.05.002.

[39] Cai B, Kong X, Liu Y, Lin J, Yuan X, Xu H, et al. Application of Bayesian Networks in

Reliability Evaluation. IEEE Trans Ind Informatics 2019;15:2146–57. https://doi.org/10.1109/TII.2018.2858281.

[40] Amin MT, Khan F, Imtiaz S. Dynamic availability assessment of safety critical systems using a dynamic Bayesian network. Reliab Eng Syst Saf 2018;178:108–17. https://doi.org/10.1016/j.ress.2018.05.017.

[41] Palencia OG, Teixeira AP, Soares CG. Safety of Pipelines Subjected to Deterioration Processes Modeled Through Dynamic Bayesian Networks. J Offshore Mech Arct Eng 2019;141:1–11. https://doi.org/10.1115/1.4040573.

[42] Kim J, Shah AUA, Kang HG. Dynamic risk assessment with bayesian network and clustering analysis. Reliab Eng Syst Saf 2020;201:106959. https://doi.org/10.1016/j.ress.2020.106959.

[43] Weber P, Munteanu P, Jouffe L. Dynamic Bayesian Networks Modelling the Dependability of Systems with Degradations and Exogenous Constraints. IFAC Proc Vol 2004;37:207–12. https://doi.org/10.1016/s1474-6670(17)36120-7.

[44] Murphy KP. Dynamic Bayesian Networks: Representation, Inference and Learning. University of California Berkeley, 2002.

[45] Adumene S, Khan F, Adedigba S. Operational safety assessment of offshore pipeline with multiple MIC defects. Comput Chem Eng 2020;138. https://doi.org/10.1016/j.compchemeng.2020.106819.

[46] Aljaroudi A, Khan F, Akinturk A, Haddara M. Risk assessment of offshore crude oil pipeline failure. J Loss Prev Process Ind 2015;37:101–9. https://doi.org/10.1016/j.jlp.2015.07.004.

[47] Hashemi SJ, Ahmed S, Khan FI. Loss scenario analysis and loss aggregation for process facilities. Chem Eng Sci 2015;128:119–29. https://doi.org/10.1016/j.ces.2015.01.061.

[48] Kaiser MJ. Offshore pipeline construction cost in the U.S. Gulf of Mexico. Mar Policy 2017;82:147–66. https://doi.org/10.1016/j.marpol.2017.05.003.

[49] Thodi P, Khan F, Haddara M. Risk based integrity modeling of offshore process

components suffering stochastic degradation. J Qual Maint Eng 2013;19:157–80. https://doi.org/10.1108/13552511311315968.

[50] Khakzad N, Khan F, Amyotte P. Dynamic safety analysis of process systems by mapping bow-tie into Bayesian network. Process Saf Environ Prot 2013;91:46–53. https://doi.org/10.1016/j.psep.2012.01.005.

[51] Javaherdashti R. Microbiologically Influenced Corrosion. 2nd Editio. Springer International Publishing Switzerland; 2017.

[52] Ibrahim A, Hawboldt K, Bottaro C, Khan F. Review and analysis of microbiologically influenced corrosion: the chemical environment in oil and gas facilities. Corros Eng Sci Technol 2018:1–15. https://doi.org/10.1080/1478422X.2018.1511326.

[53] Papavinasam S, Doiron A, Revie RW. Model to Predict Internal Pitting Corrosion of Oil and Gas Pipelines. Corrosion 2010;66:1–11.

[54] Xiao Q, Chaoqin C, Li Z. Time series prediction using dynamic Bayesian network. Optik (Stuttg) 2017;135:98–103. https://doi.org/10.1016/j.ijleo.2017.01.073.

[55] NACE-RP0775. Recommended Practice Preparation, Installation, Analysis, and Interpretation of Corrosion Coupons in Oilfield Operations. NACE Int Houston, TX USA, 2005.

[56] Haile T, Teevens P, Zhu Z. Sulphate-reducing bacteria growth kinetics-based microbiologically influenced corrosion predictive models. J Pipeline Eng 2015;14:259–67.

[57] Uusitalo L. Advantages and challenges of Bayesian networks in environmental modelling. Ecol Modell 2007;203:312–8. https://doi.org/10.1016/j.ecolmodel.2006.11.033.

[58] Saltelli A, Annoni P, Azzini I, Campolongo F, Ratto M, Tarantola S. Variance based sensitivity analysis of model output. Design and estimator for the total sensitivity index. Comput Phys Commun 2010;181:259–70. https://doi.org/10.1016/j.cpc.2009.09.018.

[59] Afenyo M, Khan F, Veitch B, Yang M. Arctic shipping accident scenario analysis using Bayesian Network approach. Ocean Eng 2017;133:224–30. https://doi.org/10.1016/j.oceaneng.2017.02.002.

[60] Srivastava SK, Katarki M V., Cherian V. Failure analysis of a 30-in subsea oil pipeline. Mater Perform 2008;47:52–6.

[61] Genome Canada. Managing Microbial Corrosion in Canadian Offshore and Onshore Oil Production; Project Database 2019. 2019.

[62] Bhandari J, Khan F, Abbassi R, Garaniya V. Pitting Degradation Modeling of Ocean Steel Structures Using Bayesian Network. J Offshore Mech Arct Eng 2017;139:1–11. https://doi.org/10.1115/1.4036832.

[63] Mehrafrooz B, Edalat P, Dyanati M. Cost consequence-based reliability analysis of bursting and buckling failure modes in subsea pipelines. J Ocean Eng Sci 2019;4:64–76. https://doi.org/10.1016/j.joes.2019.01.001.

[64] Al-Darbi MM, Agha K, Islam MR. Comprehensive Modelling of the Pitting Biocorrosion of Steel. Can J Chem Eng 2005;83:872–81. https://doi.org/10.1002/cjce.5450830509.

[65] Bai H, Wang Y, Ma Y, Zhang Q, Zhang N. Effect of CO2 partial pressure on the corrosion behavior of J55 carbon steel in 30% crude oil/brine mixture. Materials (Basel) 2018;11. https://doi.org/10.3390/ma11091765.

[66] Renpu W. Oil and gas well corrosion and corrosion prevention,. Adv. Well Complet. Eng. 3rd Editio, Gulf professional publishing, Boston; 2011, p. 619–39.

[67] Xu D, Li Y, Gu T. Mechanistic modeling of biocorrosion caused by biofilms of sulfate reducing bacteria and acid producing bacteria. Bioelectrochemistry 2016;110:52–8. https://doi.org/10.1016/j.bioelechem.2016.03.003.

[68] Melchers RE. Effect of temperature on the marine immersion corrosion of carbon steels. Corrosion 2002;58:768–82. https://doi.org/10.5006/1.3277660.

Chapter 8

Summary, Conclusions and Recommendations

8.1. Summary

This study demonstrates the novel application of the Bayesian network structure, Markovian stochastic process, Monte Carlo Simulation, Markovian mixture structure, Copula-based Monte Carlo algorithm, dynamic Bayesian network, and loss aggregation technique for dynamic risk-based integrity assessment of corroding marine and offshore systems. The existing mechanistic models for microbial corrosion susceptibility assessment are not dynamically structured, unable to capture the unstable, dynamic, and non-linear interactions among MIC influential factors for failure predictions. Dynamic risk-based assessment techniques for microbial corrosion induced failures are developed to capture the significant factors' non-linear interactions; they address the knowledge gaps and aid integrity management of the corroding systems.

This thesis presents an integrated and dynamic probabilistic model to assess the integrity of marine and offshore systems suffering microbiologically influenced corrosion. The model accounts for the contributory parameters' interdependency and their effects on the pipeline's corrosion rate and failure probability. The stochasticity in the microbial metabolism and its impact on the failure behavior of the corroding pipeline are captured. Also, the random response variables variability and the multiple defects interactions effects on the corroding system survivability are predicted for optimum integrity management strategy. The Copula-based Monte Carlo algorithm captures the likely microbial induced failure modes and the response parameters spatial dependencies for the system reliability prediction. The analysis results suggest a reliable reliability-based integrity management strategy under multispecies microbial biofilm architectures. Furthermore, an

integrated dynamic Bayesian network - loss aggregation technique is developed to forecast the associated risk of microbial induced failures. The results provide prognostic risk-based tools that could aid operational decision making by engineers and integrity managers.

8.2. Conclusions

The major conclusions drawn from the current research is summarized as follows:

8.2.1 Development of an innovative failure predictive model

This research presents a new failure assessment model for corroding offshore systems, emphasizing the non-linear interactions among influential parameters. The BN structure is adopted to model the dependencies among the monitoring operating parameters (e.g., temperature, fluid flow rate, salinity, CO_2, and pH) and the bacteria (e.g., SRB) for microbial corrosion rate predictions. The BN structure's input parameters are the prior probabilities and conditional probability of the monitoring operating parameters. The prior probabilities are assessed from the parameters' sample data based on the partitioning approach, while the conditional probability is estimated from corrosion models and subject matter expert opinions. Given the prior and conditional probabilities, the BN structure is simulated to predict the MIC rate. The predicted corrosion rate is used in the Markovian stochastic formulation as the transition intensity for the failure probability prediction. The Markovian process utilizes a four states pit depth formulation to characterize the corrosion deterioration process for the corroding system. The fourth state, which is the critical failure state (i.e., at pit depth > 75%), is used for the failure prediction based on the probability distribution at any time step. The failure time of the corroding system is then predicted based on the safety class regulation. Subsequently, the future pit depth distribution is forecasted. The proposed model's effectiveness is validated through the application of the model on the

corroding subsea pipeline. The probabilistic predictive model's application provides an early warning guide for a timely intervention to prevent the corroding subsea pipeline's total failure.

8.2.2 Development of an integrated operational safety model

The current study presents an operational safety assessment model for offshore systems with multiple MIC defects. The model integrates the BN-Markovian mixture structure with the Monte Carlo algorithm to explore the evolving effects of non-linear interaction among operating parameters and the defects interaction on the corroding system's survivability. The emphasis is placed on the non-linearity in the dependencies among the influential critical factors, defect interaction, and the complex multispecies characteristics of the microbial biofilm structure. BN is more appropriate for representing complex dependencies among microbial corrosion influential parameters and capturing the uncertainty in modeling. The BN shows a high capability of abductive reasoning and the ability to capture multivariate interactions. The stochastic nature of the propagation and interactions among the defects is considered for an effective growth rate prediction using the Markovian mixture formulation. The Monte Carlo algorithm stochastically predicts the remaining strength of the corroding system. The model is demonstrated with an in-service corroding offshore pipeline. The results analysis shows the evolving effects of the defects' interaction and the multispecies biofilm characteristics on the asset's survival likelihood. The model provides a parametric-based condition monitoring tool for effective integrity management of corroding offshore pipelines.

8.2.3 Development of dynamic reliability model considering multiple failure modes

This study has developed a dynamic methodology for reliability prediction of corroding offshore systems considering multi-failure modes dependencies. The BN-CMC model offers a technique

for predicting the effects of complex parametric dependencies and non-linear correlation on offshore systems' reliability. The CMC utilizes the concordance measure (i.e., the Kendall tau) to predict the correlation effects of corrosion response parameters and their failure modes on the system performance. The model is validated with a subsea pipeline with different defects depth under multispecies biofilm architecture. The research outputs show that the system's failure probability differs diversely with the degree of correlation among the random corrosion response parameters. The model predicts the failure indexes that could aid integrity management of corroding offshore systems considering spatial interdependencies..

8.2.4 Development of a probabilistic integrity assessment model

This phase of the study develops a probabilistic model for integrity assessment of corroding pipeline structures. The integrated model utilizes different susceptibility models for the pipeline's degradation rate and defects growth prediction in a mixed corrosive environment. The Monte Carlo simulation is used to capture the random response parameters and the microstructural variability for failure probability prediction. The model is demonstrated on three different steel grade pipelines with corrosion defects. The model explores the effects of heterogeneities characteristics and mixed corrosive environment on the steel pipelines' failure behaviors. The model offers a systematic framework for an appropriate material selection and risk-based integrity management strategy for corroding offshore structures.

8.2.5 Development of dynamic risk assessment model

The current research phase introduces a dynamic risk analysis methodology for offshore systems suffering microbial induced stochastic degradation. A novel DBN structure is applied to model the influential corrosion factors' evolving characteristics and the time-evolution effects of the

degradation process for failure assessment. The loss aggregation function is used to forecast the expected economic loss value associated with different loss scenarios due to system failures. The model is tested on a subsea pipeline. The integrated model utilizes a probabilistic formalism that captures the safety barriers' soft and hard failure on the investment's overall financial losses. The model offers a dynamic framework for the prediction of the expected economic losses (value at risk) due to microbial corrosion induced failures and for integrity-based decision making.

8.3. Recommendations

This study was intended to develop effective models for dynamic risk-based integrity assessment of corroding marine and offshore systems. Based on completed objectives, the following areas are recommended for further investigation:

- The development of a hybrid dynamic risk and uncertainty modeling technique for integrity assessment of corroding offshore systems should be vigorously explored. This can enable us to adequately separate the epistemic and aleatory uncertainties, considering the sources of data for reliable system integrity decision making.
- The development of an advanced data acquisition and process digitalization framework for microbial corrosion related information should be further investigated. This will help to thoroughly gather, share, and analyze relevant information for a reliable integrity management plan.
- The integration of the time-nonhomogeneous Markovian process with the dynamic model can be conducted. This will explore the significance of time-variant defect growth on failure probability prediction and future pit depth distribution under multispecies microbial biofilm structure.

- The development of an integrated Copula-based stochastic dominance framework should be explored for microbial corrosion risk minimization decision making under uncertainty.
- The development of a dynamic cost-based integrity management optimization framework for offshore systems under microbial induced stochastic degradation can be a promising research work.

Supplementary Material

SA: An illustrative example to facilitate understanding of the hybrid dynamic failure assessment methodology

A simple hypothetical illustrative example with an assumed dataset is shown below to demonstrate how the hybrid connectionist model can be used to predict the MIC rate and the failure probability for an offshore pipeline. A 6mm wall thickness offshore pipeline under microbially influenced corrosion is examined, and the following procedure summarizes the application of the integrated dynamic model. The detailed calculation for each step for the MIC rate and the time step's failure probability prediction is shown.

Step1: Collect monitoring operating parameters data log for the period of 3 years together with inspection data; identify the bacteria characteristic associated with the corrosion and establish their counts; partition the data into set bounds (high, moderate, and low) for the monitoring operating parameters and the environmental factors that influence the corrosion given the data range; from the partitioned data, estimate the parameters' prior probabilities based on the data counts within the range. The literature [6,68] shows that the monitoring operating parameters (temperature, pH, CO_2 partial pressure, salinity, flow velocity) play key roles in the corrosion mechanism in offshore/marine systems. Consequently, the presented data is associated to the different defect growth rates. The estimated probabilities based on the data range is shown in Table SA1.

For this phase, the following assumptions hold:

a) The data bounds as shown in Table SA1 depict the range in which the operating parameters fall under the prevailing environmental conditions for the period under consideration.

b) The future defect growth is predicted based on the corrosion defect rate and is constant for the period under consideration.

c) The Markov process is defined based on the assumption that the asset was at an initial state with no defects.

d) The future defect growth prediction is assumed linearly propagated for the period under consideration.

Table SA1: Hypothetical corrosion influencing parameters & their probabilities for long-term MIC rate prediction

Variables (Node)	Range	State /Probability
pH	Min 4 Max 10.67	Acidic ~ 0.4411 Neutral ~ 0.3105 Basic ~0.2484
Temperature (degree C)	Min 15 Max 50	High ~ 0.4193 Moderate ~ 0.3321 Low ~ 0.2486
Fluid velocity (m/s)	Min 0.06 Max 3.04	High ~ 0.0132 Moderate ~ 0.3312 Low ~ 0.6556
Salinity		Present ~ 0.67 Absent ~ 0.33
Steel composition		Present > 0.5% ~ 0.6 Absent < 0.5% ~ 0.4
Exposure period		Max. > 3.5yrs ~ 0.6121 Mean 2.5-3.5yrs ~0.2813 Min < 2.5yrs ~ 0.1066
SRB	Low < 10000cfu/ml	

10000 < Moderate <100000
High> 100000 cfu/ml

Step 2: The probabilistic data from step 1 is used as input data for the BN model. The BN model is developed for MIC rate prediction based on the relationship among the monitoring operating parameters, environmental factors, mechanical properties, and the corrosion mechanism. The structure depicts the interdependency and interaction among these factors to probabilistically predict the MIC rate under the prevailing operating conditions. To determine the operating parameter effects on the MIC rate, this important rate is categorized into four states (severe, high, moderate, and low) according to the NACE-RP0775 [75] recommendation. The dependency among these MIC influencing parameters is defined by their conditional probability. The conditional probabilities for the child node are created by studying the dynamic relationship that exists among microbial corrosion influencing factors. The theoretical and experimental corrosion model proposed by the scholars [6,69] is adopted for additional information for conditional probability. In the case of incomplete information, data from subject matter expert opinion and literature [56] is adopted for the analysis.

Step 3: The prior probabilities obtained from Table SA1 for the monitoring operating parameters and material properties (temperature, pH, CO_2, salinity, alloy effect) are incorporated into the developed cause-effect BN structure (see Figure SA1). The MIC rate is probabilistically predicted with these monitoring operating parameters' prior probabilities and conditional probabilities, as shown in Figure SA1. The prediction describes the parametric learning of the BN structure, which captures the characteristic non-linear dependency. The result of the simulation is shown in Figure SA1, with the predicted MIC rate of 0.0103mm/year, 0.2301mm/year, 0.3124mm/year, and 0.4523mm/year for the low, moderate, high, and severe corrosion rate category, respectively.

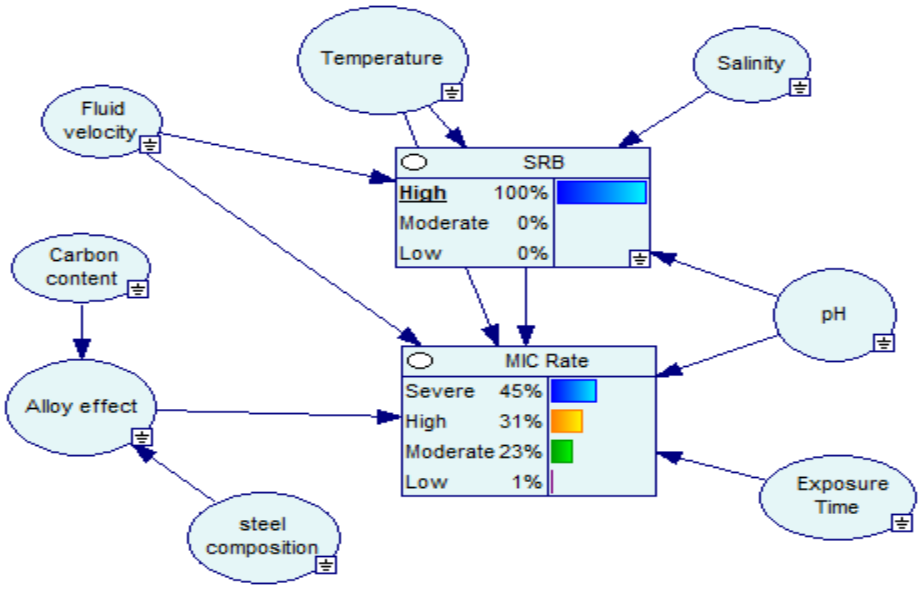

Figure SA1: BN for MIC rate prediction using the upper bound probability of corrosion influencing factors

Step 5: Once the MIC rate is predicted by the BN, as shown in Figure SA1, the predicted MIC rate is integrated into the Markov process as transition intensity for component failure probability prediction. To predict the failure probability, the pipeline wall thickness is first discretized into four corrosion pit depth states, as demonstrated in Figure SA2, which represent different percentages of corrosion pit depth of the pipe wall thickness (see Table SA2). Pit depth state IV refers to the critical failure state of the pipeline based on the criteria in the literature [70].

Assuming a corrosion pit depth of 0.87 mm is identified, which falls within pit depth state I (see Table SA2). The prior pit depth state's probability distribution is then defined by $\pi_i = [1 \quad 0 \quad 0 \quad 0]$ based on the identified pit depth. π_i describes the prior state of the pipeline, which shows an initial state of no defects at the commencement of operation. For the application of the predicted MIC rate in the Markovian process, the low, high, and severe corrosion rate categories

are used for $\mu_{12}(t), \mu_{23}(t), and\ \mu_{34}(t)$, respectively. This is used to form the transition intensity matrix (generator matrix), as shown by Equation (SA1) based on the predefined pit states.

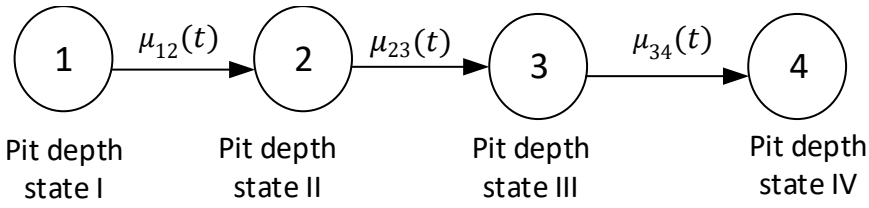

Figure SA2: Discretization of the pipe wall thickness into MIC pit depth states

$$\text{Generator matrix} = \mathrm{Q} = \begin{Vmatrix} -\mu_{12}(t) & \mu_{12}(t) & 0 & 0 & \cdots \\ 0 & -\mu_{23}(t) & \mu_{23}(t) & 0 & \cdots \\ 0 & 0 & -\mu_{34}(t) & \mu_{34}(t) & \cdots \\ \vdots & \vdots & \vdots & \vdots & \cdots \\ \vdots & \vdots & \vdots & \vdots & \ddots \end{Vmatrix} \qquad (SA1)$$

Table SA2. Pipe wall thickness for different pit depth states

	Pit depth state 1	Pit depth state II	Pit depth state III	Pit depth State IV
Pit depth states (pipe wall thickness discretization)	0-1.5mm	1.5-3.0mm	3.0-4.5mm	4.5-6mm
% pipe wall thickness discretization	0%-25%	25%-50%	50%-75%	>75%
Pipe wall thickness (6mm)				

Step 6: Given the transition intensity, as shown in steps 4 and 5, the state's transition probabilities can be estimated by the set of Kolmogorov forward differential equations (KFE) (see Equation (SA2)). The set of differential equations developed to estimate the pit depth state transition probability is solved using the Laplace-Stieltjes transform and its inverse (see Equation (SA3)). The output is used to form the transition probability matrix, as shown by Equation (SA4).

$$\begin{cases} \frac{dP_{11}(t)}{dt} = -\mu_{12}P_{11}(t) \\ \frac{dP_{12}(t)}{dt} = \mu_{12}\,P_{11}(t) - \mu_{23}P_{12}(t) \\ \frac{dP_{13}(t)}{dt} = \mu_{23}P_{12}(t) - \mu_{34}P_{13}(t) \\ \frac{dP_{14}(t)}{dt} = \mu_{34}P_{14}(t) \end{cases} \qquad (SA2)$$

Step 7: The states' probabilities at different time steps are estimated by Equation (SA3) to form the state transition probability matrix and the row vector (π), representing the prior probability. The dynamics of the state's probabilities are dependent on the MIC rate for failure probability prediction.

Step 8: All the steps in the procedure can be repeated for different scenarios and with different corrosion pit depth states.

For the four-state pit depth interval as shown in Figure SA2, the developed differential equations can be solved by applying the Laplace-Stieltjes transform and its inverse to the KFE, which gives:

$$P_{11}(t) = e^{-\mu_{12}t}$$

$$P_{12}(t) = \frac{\mu_{12}}{\mu_{12}-\mu_{23}}(e^{-\mu_{23}t} - e^{-\mu_{12}t}) \qquad (SA3)$$

$$P_{13}(t) = \frac{-\mu_{23}\mu_{12}[(\mu_{12}-\mu_{23})e^{-\mu_{34}t} + (\mu_{34}-\mu_{12})e^{-\mu_{23}t} + (\mu_{23}-\mu_{34})e^{-\mu_{12}t}]}{(\mu_{12}-\mu_{23})(\mu_{34}-\mu_{12})(\mu_{23}-\mu_{34})}$$

$$P_{14}(t) = 1 - P_{11} - P_{12} - P_{13}$$

Inputting the MIC rate from Figure SA1, step 3 (i.e., taking $\mu_{12} = 0.0103$; $\mu_{23} = 0.3124$; $\mu_{34} = 0.4523$) into Equation (SA3) gives:

$$P_{11}(t) = e^{-\mu_{12}t} = e^{-0.0103} = 0.9898$$

$$P_{12}(t) = \frac{\mu_{12}}{\mu_{12} - \mu_{23}}(e^{-\mu_{23}t} - e^{-\mu_{12}t}) = \frac{0.0103}{0.0103 - 0.3124}(e^{-0.3124} - e^{-0.0103}) = 0.0088$$

$$P_{13}(t) = \frac{-\mu_{23}\mu_{12}[(\mu_{12} - \mu_{23})e^{-\mu_{34}t} + (\mu_{34} - \mu_{12})e^{-\mu_{23}t} + (\mu_{23} - \mu_{34})e^{-\mu_{12}t}]}{(\mu_{12} - \mu_{23})(\mu_{34} - \mu_{12})(\mu_{23} - \mu_{34})} =$$

$$= \frac{-0.0103(0.3124)[(0.0103 - 0.3124)e^{-0.4523} + (0.4523 - 0.0103)e^{-0.3124} + (0.3124 - 0.4523)e^{-0.0103}]}{(0.0103 - 0.3124)(0.4523 - 0.0103)(0.3124 - 0.4523)}$$

$$P_{13}(t) = 0.0013$$

$$P_{14}(t) = 1 - P_{11} - P_{12} - P_{13} = 0.0001$$

The result is used to form the state transition probability matrix as shown below:

$$\text{Transition probability matrix P} = \{p_{ij}\} = \begin{Vmatrix} 0.9898 & 0.0088 & 0.0013 & 0.0001 \\ 0 & 1 & 0 & 0 \\ 0 & 0 & 1 & 0 \\ 0 & 0 & 0 & 1 \end{Vmatrix} \qquad (SA4)$$

Substitute SA4 and $\pi_i = [1 \quad 0 \quad 0 \quad 0]$ and their transpose into Equation (SA5) for the failure probability distribution prediction for a t- step transition.

$$\mathbb{P}(X_t = j) = \sum_{i=1}^{N} \mathbb{P}(X_t = j | X_{t-1} = i)\mathbb{P}(X_{t-1} = i) = \sum_{i=1}^{N} (P^t)_{ij}\pi_i = (\pi^T P^t)_j \qquad (SA5)$$

The probability function (SA5) is used to predict the failure probability distribution at each t-step transition based on the defined pit depth states in the MATLAB environment. The result from the critical pit depth states' probabilities for the period under consideration is used to characterize the failure profile for the microbial influenced corroded offshore pipeline under the prevailing environmental conditions, as shown in Figure SA3.

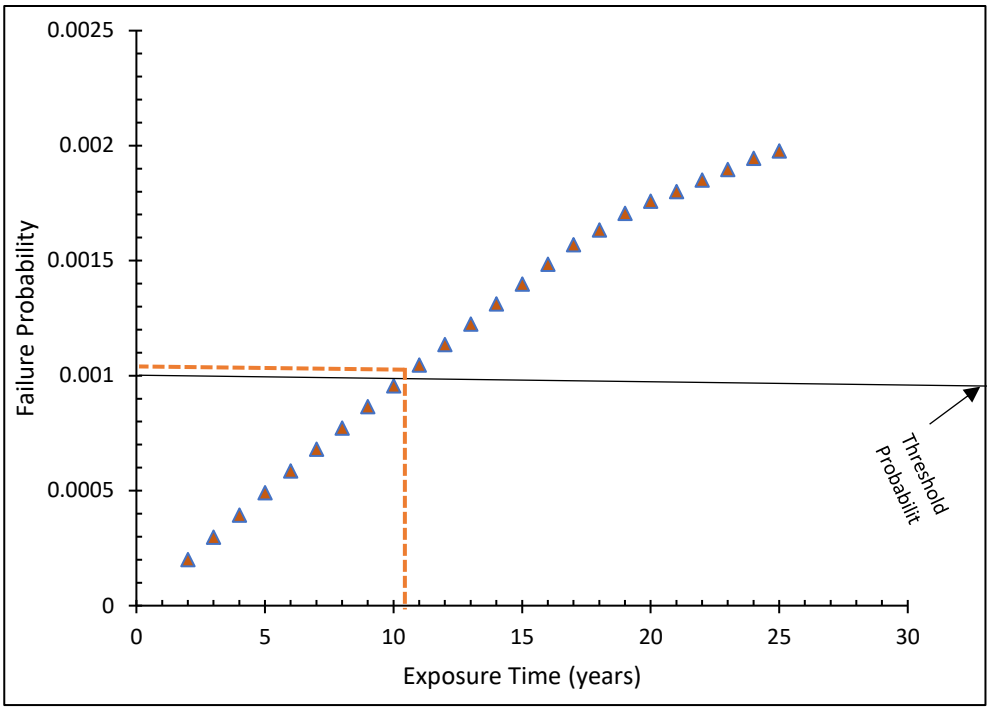

Figure SA3: Predicted failure probability for microbial influenced corroded pipeline

Operational and integrity management decision-making can be inferred from the developed failure characteristic profile for an offshore pipeline under microbial influenced corrosion. For instance, the result in Figure SA3 shows that at the threshold of 1.00×10^{-3}, the likely critical failure probability of the offshore pipeline is 1.046×10^{-3}, while the critical failure time occurs at 10.5 years of exposure.

SB: An illustrative example to facilitate understanding of the hybrid operational safety assessment methodology

A simple illustrative example is shown below to demonstrate how the hybrid model can be used to predict the MIC rate, time variant strength loss, and the survival lifetime of corroded offshore pipeline under multiple defects interaction. A 762 mm diameter offshore pipeline under microbial influenced multiple defects interaction is examined and the following procedure summarizes the application of the hybrid methodology:

1. Collect monitoring operating parameters and inspection data, identify the bacteria and their counts; establish set bounds, estimate their probability, and categorize the state into low, moderate, high or severe, where applicable, depending on the degree of influence, as shown in Table SB1.
2. The second step is to develop a model for the prediction of an initial individual MIC pits growth rate from inspection data and monitoring operating parameters. Identify interacting pits based on the criteria and clusterize them into a single or group of pits. Discretize the pipe wall thickness into pits depth state to represent the overlapping and interacting pits depth.
3. Furthermore, the effect of pits interaction on the MIC rate is predicted using Markov Mixture Model (MMM). The effect of the interaction on pit depth and length based on the interaction criteria is also captured.
4. The residual strength model is formulated to be MIC growth rate dependent for estimating the effect of pits interaction on the corroded system residual strength over time. Further

analysis is presented considering residual strength, safe operating pressure based on the mixture model MIC growth rate, and survival likelihood prediction.

Illustrative Example:

Step 1

Assuming that from a single inspection data and operating parameters, the following data ranges are selected including the microbial counts that support the corrosion mechanism. The probability is evaluated from the available data, literature, and SME.

Table SB1: Monitoring operating parameters for MIC growth rate prediction

Variables (Node)	Range	State /Probability
pH	2.8 ~ 10.67	Acidic ~ 0.4481 Neutral ~ 0.3105 Basic ~0.2414
Temperature (degree C)	10 ~ 50	High ~ 0.4193 Moderate ~ 0.3321 Low ~ 0.2486
Fluid velocity (m/s)	0.06 ~ 3.04	High ~ 0.0132 Moderate ~ 0.3312 Low ~ 0.6556
Salinity		Present ~ 0.67 Absent ~ 0.33
Steel composition		Present > 0.5% ~ 0.6 Absent < 0.5% ~ 0.4
Exposure period		Max. > 3.5yrs ~ 0.6121 Mean 2.5-3.5yrs ~0.2813 Min < 2.5yrs ~ 0.1066
SRB	Low < 10000cfu/ml 10000 < Moderate <50000	APB: Low < 1000cfu/ml 1000 < Moderate <10000

Step 2

Assumed from the BN, the predicted MIC rates under the prevailing condition are 0.3683 mm/yr., 0.2466 mm/yr., 0.2198 mm/yr., and 0.1654 mm/yr., for severe, high, moderate, and low corrosion rate categories, respectively.

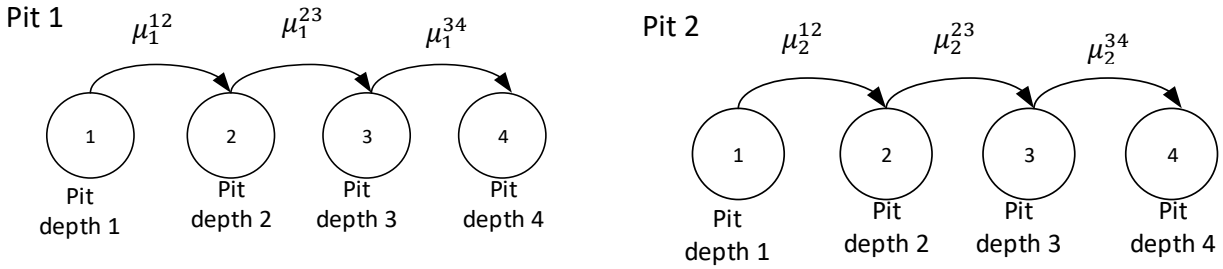

Figure SB1: Pit depth states

Also given that $\mu_1^{12} = 0.1654, \mu_1^{23} = 0.2466, \mu_1^{34} = 0.3683$ *and* $\mu_2^{12} = 0.0827, \mu_2^{23} = 0.1233, \mu_2^{34} = 0.2198$

Considering interaction among adjacent pits and overlapping pits, the following conditions must hold:

$$l_{12} \leq 2.0\sqrt{D.wt} \qquad (SB1)$$

$$w_{12} \leq \pi\sqrt{D.wt} \qquad (SB2)$$

where D is the outer diameter of the pipeline; and wt is the pipe web thickness

Assuming that the longitudinal and transverse distance between the pits met the above criteria and their exist interaction among the pits; a mixture model is proposed for the effective merged defect growth rate prediction.

Step 3:

The Markov mixture concept is formulated from Actuarial Science [48] with the transition intensity (MIC growth rate) equivalent to the force of mortality: This is an acyclic model with transient states and the last sate being the absorbing. It is represented as a phase type distribution with convolution of exponential distribution.

Let the random variable M determines the Markov chains. The Mixing probabilities are $P(M = 1)$ and $P(M = 2)$ for the two identified defects. The transition for the two Markov chains are $\{\mu_1^{ij}; i: j\epsilon\{1,2,3,4\}, i \neq j\}$ and $\{\mu_2^{ij}; i; j\epsilon\{1,2,3,4\}, i \neq j\}$ respectively and are evaluated in Step 1

The mixture of the two pits Markov chains leads to a process that depends on the individual pit depth state history, because the intensities of observable transitions are function of a history that contains the information about duration and the state of the pit for an individual pits up to the current time.

Let the history of the pits state up to time t be denoted by $\mathcal{H}_t$; using similar notation by Aalen [48], for a mixture model, the mixture transition intensity gives

$$\lambda^{ij}(t|\mathcal{H}_t) = \mu_1^{ij} P(M = 1|\mathcal{H}_t) + \mu_2^{ij} P(M = 2|\mathcal{H}_t) \qquad \textit{(SB4)}$$

Thus, $\lambda^{ij}(t|\mathcal{H}_t)$; the transition intensity of the mixture model is dependent on the history of the process through the conditional probabilities on the right-hand side of Equation (SB4):

In general, the multi-state Markov Mixture Model transition intensity gives [49,51]:

$$\lambda^{ij}\left(t\middle|\mathcal{H}_t^k\right) = \frac{\sum_{m=1}^{n} \mu_m^{ij} P\left(\mathcal{H}_t^k\middle|M = m\right) P(M = m)}{\sum_{m=1}^{n} P\left(\mathcal{H}_t^k\middle|M = m\right) P(M = m)} \qquad (SB5)$$

So, for a two set of interacting pits, we have

$$\lambda^{ij}\left(t\middle|\mathcal{H}_t^k\right)=\frac{\mu_1^{ij}P\left(\mathcal{H}_t^k\middle|M=1\right)P(M=1)+\mu_2^{ij}P(\mathcal{H}_t^k|M=2)P(M=2)}{P\left(\mathcal{H}_t^k\middle|M=1\right)P(M=1)+P\left(\mathcal{H}_t^k\middle|M=2\right)P(M=2)} \quad (SB6)$$

where $P(M=m)$ is an assumed probability of mixture of the pits; for the two pits let $P(M=1)=0.6$ and $P(M=2)=0.4$.

For the history-based conditional probability of the Pit**,** it is assumed that the condition probability $P\left(\mathcal{H}_t^k\middle|M=m\right)$ follow the transition probability formulation across the states based on the pit depth state history. Using the Laplace Stieltjes transformation gives:

$$P(\mathcal{H}_t^1|M=1)=\exp(-\mu_1^{12})=e^{-0.1654t}$$

$$P(\mathcal{H}_t^2|M=1)=\frac{\mu_1^{12}}{\mu_1^{12}-\mu_1^{23}}\left(e^{-\mu_1^{23}t}-e^{-\mu_1^{12}t}\right)=\frac{0.1654}{(0.1654-0.2466)}(e^{-0.2466t}-e^{-0.1654t})$$

$$P(\mathcal{H}_t^3|M=1)=\frac{-\mu_1^{23}\mu_1^{12}[(\mu_1^{12}-\mu_1^{23})e^{-\mu_1^{34}t}+(\mu_1^{34}-\mu_1^{12})e^{-\mu_1^{23}t}+(\mu_1^{23}-\mu_1^{34})e^{-\mu_1^{12}t}]}{(\mu_1^{12}-\mu_1^{23})(\mu_1^{34}-\mu_1^{12})(\mu_1^{23}-\mu_1^{34})}$$

$$-\mu_1^{23}\mu_1^{12}=-0.04079$$

$$\mu_1^{12}-\mu_1^{23}=-0.0812; \qquad e^{-\mu_1^{34}t}=e^{-0.3683t}$$

$$\mu_1^{34}-\mu_1^{12}=0.2029; \qquad e^{-\mu_1^{23}t}=e^{-0.2466t}$$

$$\mu_1^{23}-\mu_1^{34}=-0.1217; \qquad e^{-\mu_1^{12}t}=e^{-0.1654t}$$

$$P(\mathcal{H}_t^3|M=1)=0.0599e^{-0.2466t}-0.02395e^{-0.3683t}-0.0359e^{-0.1654t}$$

$$P(\mathcal{H}_t^4|M=1)=1-P(\mathcal{H}_t^1|M=1)-P(\mathcal{H}_t^2|M=1)-P(\mathcal{H}_t^3|M=1)$$

$$=1-3.001e^{-0.1654t}+1.977e^{-0.2466t}+0.02395e^{-0.3683t}$$

Similarly, the history-based conditional probability for Pit 2 is obtained as follows**:**

$$P(\mathcal{H}_t^1|M=2) = \exp(-\mu_2^{12}) = e^{-0.0827t}$$

$$P(\mathcal{H}_t^2|M=2) = \frac{\mu_2^{12}}{\mu_2^{12}-\mu_2^{23}}\left(e^{-\mu_2^{23}t} - e^{-\mu_2^{12}t}\right) = \frac{0.0827}{(0.0827-0.1233)}(e^{-0.1233t} - e^{-0.0827t})$$

$$P(\mathcal{H}_t^3|M=2) = \frac{-\mu_2^{23}\mu_2^{12}[(\mu_2^{12}-\mu_2^{23})e^{-\mu_2^{34}t} + (\mu_2^{34}-\mu_2^{12})e^{-\mu_2^{23}t} + (\mu_2^{23}-\mu_2^{34})e^{-\mu_2^{12}t}]}{(\mu_2^{12}-\mu_2^{23})(\mu_2^{34}-\mu_2^{12})(\mu_2^{23}-\mu_2^{34})}$$

$$-\mu_2^{23}\mu_2^{12} = -0.0102$$

$$\mu_2^{12}-\mu_2^{23} = -0.0406; \qquad e^{-\mu_2^{34}t} = e^{-0.2198t}$$

$$\mu_2^{34}-\mu_2^{12} = 0.1371; \qquad e^{-\mu_2^{23}t} = e^{-0.1233t}$$

$$\mu_2^{23}-\mu_2^{34} = -0.0965; \qquad e^{-\mu_2^{12}t} = e^{-0.0827t}$$

$$P(\mathcal{H}_t^4|M=2) = 1 - P(\mathcal{H}_t^1|M=2) - P(\mathcal{H}_t^2|M=2) - P(\mathcal{H}_t^3|M=2)$$

$$= 1 - 1.204e^{-0.0827t} + 4.383e^{-0.1233t} - 0.771e^{-0.2198t}$$

Note that the mixture model intensity is represented as a phase type distribution with convolution of exponential distribution. Assume that Pit 1 and Pit 2 was at pit depth states 1 & 2 at the point of inspection (see Figure. SB1) and their exist interaction between the pits, the clustered MIC pit (mixture model) growth rate gives the following relationships:

$$\lambda^{12}(t|\mathcal{H}_t^1) = \frac{\mu_1^{12}P(\mathcal{H}_t^2|M=1)P(M=1) + \mu_2^{23}P(\mathcal{H}_t^3|M=2)P(M=2)}{P(\mathcal{H}_t^2|M=1)P(M=1) + P(\mathcal{H}_t^3|M=2)P(M=2)}$$

$$\lambda^{12}(t|\mathcal{H}_t^1)$$

$$= \frac{0.2022e^{-0.1654t} - 0.2022e^{-0.2466t} + 0.038e^{-0.2198t} + 0.1157e^{-0.1233t} - 0.0904e^{-0.0827t}}{0.7333e^{-0.1654t} - 0.7333e^{-0.2466t} + 0.3034e^{-0.2198t} - 0.9384e^{-0.1283t} + 0.7332e^{-0.0827t}}$$

$$\lambda^{23}(t|\mathcal{H}_t^2)$$

$$= \frac{0.00354e^{-0.3683t} - 0.0089e^{-0.2466t} + 0.0053e^{-0.1654t} + 0.0879e^{-0.0827t} + 0.3853e^{-0.1233t} - 0.0678e^{-0.2198t}}{0.01441e^{-0.3683t} - 0.03594e^{-0.2466t} + 0.0359e^{-0.1654t} + 0.4 - 0.4816e^{-0.0827t} + 1.7532e^{-0.1233t} - 0.3084e^{-0.0827t}}$$

$$\lambda^{34}(t|\mathcal{H}_t^3)$$

$$= \frac{0.221 - 0.6632e^{-0.1654t} + 0.4369e^{-0.2466t} + 0.00529e^{-0.3683t} + 0.0879 - 0.1058e^{-0.0827t} + 0.3853e^{-0.1233t} - 0.0678e^{-0.2198tt}}{0.6 - 1.806e^{-0.1654t} + 1.1862e^{-0.2466t} + 0.0144e^{-0.3683t} + 0.4 - 0.4816e^{-0.0827t} + 1.7532e^{-0.0827t} - 0.3084e^{-0.2198t}}$$

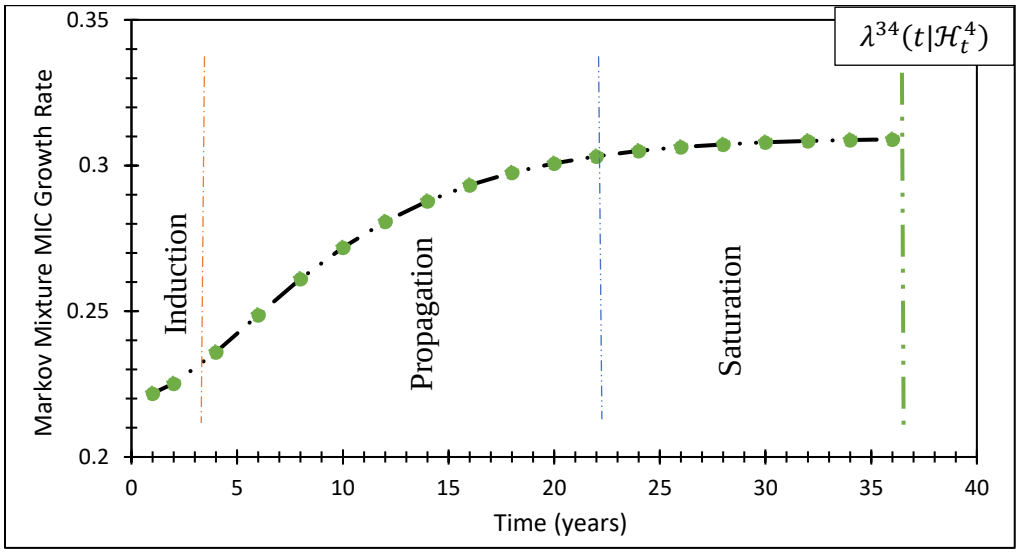

Figure SB2. The mixture MIC pit growth rate under pits interaction (State 3)

The effects of pits overlapping and interactions on the MIC rate is shown in Figure SB2. It is observed that the interaction (mixture) effects gradually increase the predicted MIC rate with exposed time. Also, the empirical mixture `MIC rate increase from the point of pit induction through the propagation (sustainable nutrients) stage to the saturation point were constant rate (asymptotic limit) is reached.

Step 4

The corroded offshore pipeline practically fails when the residual strength falls below the operating pressure. For a time-variant failure analysis, the strength loss can be stochastically expressed and is estimated using the Monte Carlos Simulation (MCS).

The time variant strength loss model for the corroded offshore pipeline was formulated with reference to the literature [14]. The mixture MIC defect rate (see Step 2) predicted based on the pits interaction criteria is used in the linear corrosion growth model by [57], to gives

$$d_{max}(T) = d_{max}(0) + \lambda^{ij}\left(t\middle|\mathcal{H}_t^k\right) \cdot t \qquad (SB7)$$

$$L_{eff}(T) = L_{eff}(0) + \lambda^{ij}\left(t\middle|\mathcal{H}_t^k\right) \cdot t \qquad (SB8)$$

where $\lambda^{ij}\left(t\middle|\mathcal{H}_t^k\right)$ is the time-dependent transition intensity (Mixture (merged) pit growth rate).

and

$$P_{nm}(t) = \frac{2\sigma_u wt}{(D - wt)}\left[\frac{1 - \left(\frac{d_{nm}(0) + \lambda^{ij}(t|\mathcal{H}_t^k) \cdot t}{wt}\right)}{1 - \left(\frac{d_{nm}(0) + \lambda^{ij}(t|\mathcal{H}_t^k) \cdot t}{Q_{nm} wt}\right)}\right] \qquad (SB9)$$

Thus, the residual strength can be stochastically model in term of the basic random variables as the primary contribution factors if their distribution is known. That is

$$P_{nm}(t) = f\left(l_{eff}(0), \sigma_y, d_{max}(0), D_0, wt, \lambda^{ij}\left(t\middle|\mathcal{H}_t^k\right), t\right) \qquad (SB10)$$

The value in Table SB2 gives probabilistic properties of the corrosion parameters and is used as input parameters for Equation (SB9) and model using Monte Carlos Simulation. The results of

the time-variant simulation for the strength loss over the lifecycle of the pipeline is shown in Figure SB3.

Table SB2. Assumed data from single inspection for a mid-strength pipeline as worked example

Symbol	Variable	Unit	Distribution	Mean	Std. Dev
D_o	outer diameter	mm	Normal	762	0
wt	pipe wall thickness	mm	Normal	7.92	0.077
σ_y	yield strength	Mpa	Normal	461	16.13
l_{eff}	mixture pit length	mm	Normal	95	32
d_{max}	mixture pit depth(max)	mm	Normal	2.2	0.81
σ_u	tensile strength	MPa	Normal	517	19.23

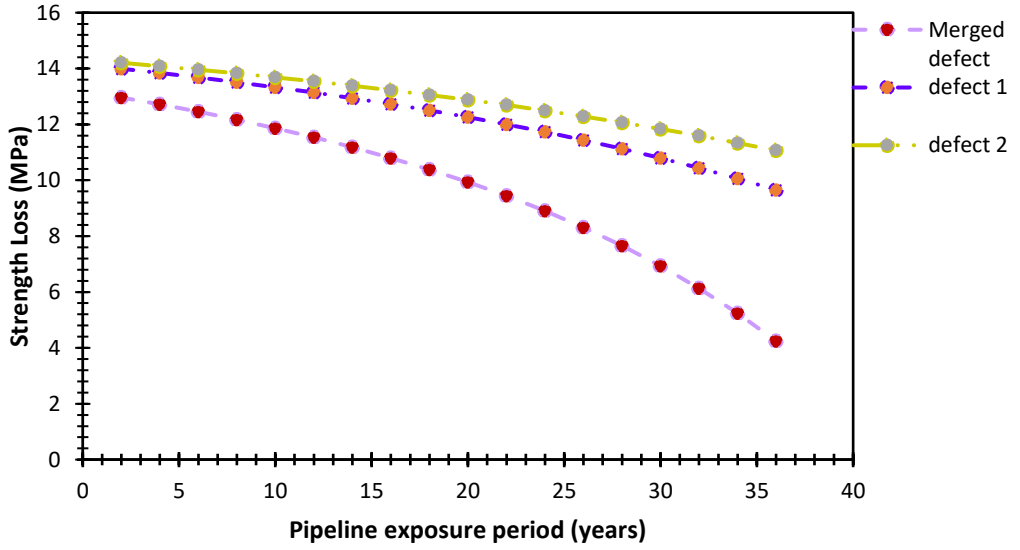

Figure SB3. Time-variant strength loss for corroded offshore system under single and multiple defects interaction effects

The result shows the percentage reduction in the residual strength under single pit and merged pit growth rate with time, which can be estimated accordingly.

The maximum safe operating pressure for the corroded offshore pipeline is influenced by the acceptable defect depth and the corroded length. For an amalgamated pit (mixture), the maximum allowable operating pressure can be predicted by the expression [14]:

$$P_{MAOP}(t) = \frac{2wt\sigma_u F}{(D_0 - wt)}\left(\frac{1 - \frac{d_{max}(T)}{wt}}{1 - \frac{d_{max}(T)}{wtQ_{eff}}}\right) \quad (SB11)$$

where $Q_{eff} = \text{length correction factor} = 1 + 0.31\left(\frac{l_{eff(T)}}{\sqrt{D_0 wt}}\right)^2$ and F is the design factor, which is normally 0.72

From the analysis under the given pipeline operating condition and MIC defects interaction, the time variant safe operating pressures (MSOP) gives 9.879MPa and 5.9904MPa as the mean upper bound and lower bound operating pressure respectively under high MIC rate category.

The survival characteristic for the pipeline can be estimated from the strength loss and the phase type distribution series model (acyclic Markov) using the mixture (merged) MIC defect rate, which gives

$$S(t)$$

$$= \frac{\lambda^{23}(t|\mathcal{H}_t^k)\lambda^{34}(t|\mathcal{H}_t^k)}{(\lambda^{12}(t|\mathcal{H}_t^k) - \lambda^{23}(t|\mathcal{H}_t^k)(\lambda^{12}(t|\mathcal{H}_t^k) - \lambda^{34}(t|\mathcal{H}_t^k))} exp(-\lambda^{12}(t|\mathcal{H}_t^k)t)$$

$$- \frac{\lambda^{12}(t|\mathcal{H}_t^k)\lambda^{34}(t|\mathcal{H}_t^k)}{(\lambda^{12}(t|\mathcal{H}_t^k) - \lambda^{23}(t|\mathcal{H}_t^k)\left(\lambda^{23}(t|\mathcal{H}_t^k) - \lambda^{34}(t|\mathcal{H}_t^k)\right)} \exp(-\lambda^{23}(t|\mathcal{H}_t^k)t)$$

$$+ \frac{\lambda^{12}(t|\mathcal{H}_t^k)\lambda^{23}(t|\mathcal{H}_t^k)}{(\lambda^{12}(t|\mathcal{H}_t^k) - \lambda^{34}(t|\mathcal{H}_t^k)\left(\lambda^{23}(t|\mathcal{H}_t^k) - \lambda^{34}(t|\mathcal{H}_t^k)\right)} exp(-\lambda^{34}(t|\mathcal{H}_t^k)t) \quad (SB12)$$

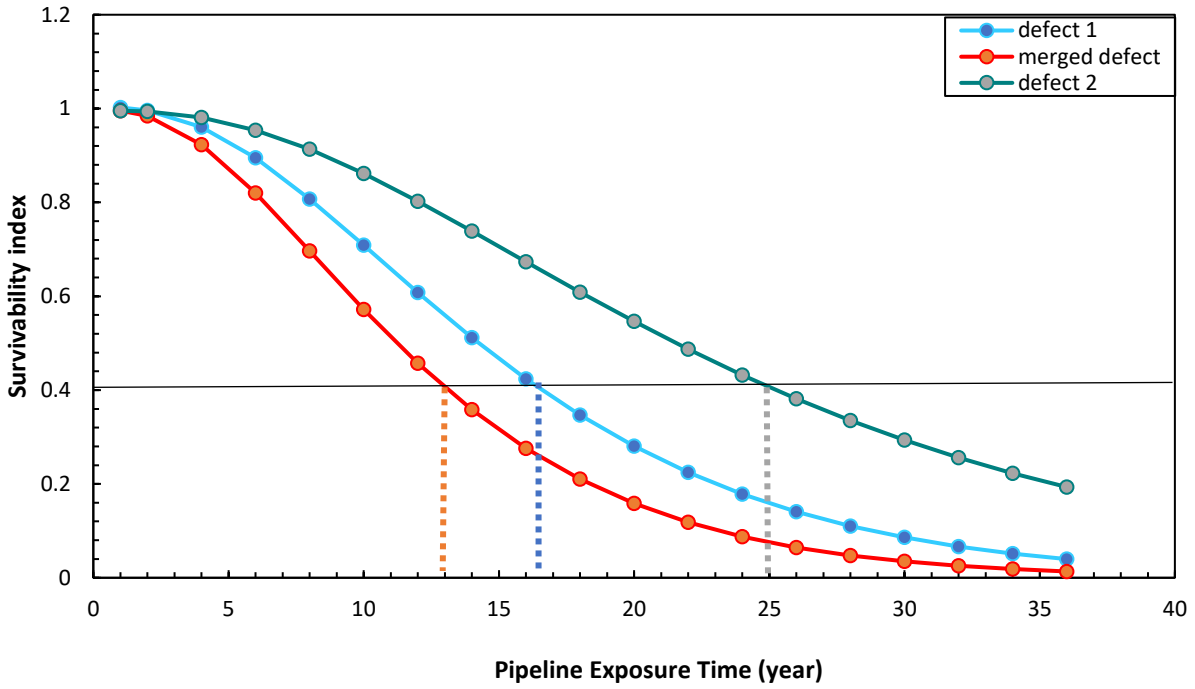

Figure SB4. Survival probability curve of the pipeline estimated with MIC rate for the merged(mixture) pit and the individual pits.

By assuming a minimum survival index (criteria) of 0.4 (which represent over 60% pipe wall penetration) as shown in Figure SB4 under the predefined operating conditions, the predicted maximum critical survival time of the pipeline for the MIC (merged) pit and individual pits gives 13years, 16.5 years and 25 years respectively. Hence, the pipeline is likely to be unserviceable at the predicted exposed year based on the survivability index. This result will aid intervention and decision-making plans for integrity management of the corroding offshore pipeline.